Journal of the National Academy of Forensic Engineers®

http://www.nafe.org
ISSN: 2379-3252
DOI: 10.51501/jotnafe.v38i1

Vol. 38 No. 1 June 2021

National Academy of Forensic Engineers®

Journal Staff

Technical Review Process

The Technical Review Committee Chair chooses the reviewers for each Journal manuscript from amongst the members and affiliates of the NAFE according to their competence and the subject of the paper, and then arbitrates (as necessary) during the review process. External reviewers may also be utilized when necessary. This confidential process concludes with the acceptance of the finished paper for publication or its rejection/withdrawal. The name(s) of authors are included with their published works. However, unpublished drafts together with the names and comments of reviewers are entirely confidential during the review process and are excised upon publication of the finished paper.

National Academy of Forensic Engineers®

Board of Directors

President
Liberty Janson, PE, DFE
Senior Member

President-Elect
Samuel Sudler, PE, DFE
Senior Member

Senior Vice President
Joseph Leane, PE, DFE
Fellow

Vice President
Steven Pietropaolo, PE, DFE
Senior Member

Treasurer
Bruce Wiers, PE, DFE
Senior Member

Secretary
Richard Rice, PE, DFE
Fellow

Past Presidents
James Petersen, PE, DFE
Fellow

John Certuse, PE, DFE
Fellow

Martin Gordon, PE, DFE
Fellow

Directors at Large
Daniel Couture, PEng, DFE
Member

Robert Peruzzi, PhD, PE, DFE
Member

Executive Director
Rebecca Bowman, PE, Esq.

Journal of the National Academy of Forensic Engineers®

Editorial Board

Submitting Proposed Papers to NAFE for Consideration

Please visit the Journal's author page at
http://journal.nafe.org/ojs/index.php/nafe/information/authors for submission details.

We are looking for NAFE members who are interested in giving presentations on technical topics that will further the advancement and understanding of forensic engineering at one of the academy's biannual meetings and then developing those presentations into written manuscripts/papers, which will go through a single-blind peer review process before publication. Only papers presented at a NAFE regular technical seminar and have received oral critique at the seminar will be accepted for review and publication. We recommend that you review the About the Journal page for the journal's section policies, as well as the Author Guidelines listed on the Submissions page. Authors need to register with the journal prior to submitting or, if already registered, can simply log in and begin the process. The first step is for potential authors to submit a 100- to 150-word maximum abstract for consideration at an upcoming conference into the online journal management system.

Copies of the Journal

The Journal of the National Academy of Forensic Engineers® contains papers that have been accepted by NAFE. Members and Affiliates receive a PDF download of the Journal as part of their annual dues. All Journal papers may be individually downloaded from the NAFE website. There is no charge to NAFE Members & Affiliates. A limited supply of Volume 33 and earlier hardcopy Journals (black & white) are available. The costs are as follows: $15.00 for NAFE Members and Affiliates; $30.00 for members of the NSPE not included in NAFE membership; $45.00 for all others. Requests should be sent to Mary Ann Cannon, NAFE, 1420 King St., Alexandria, VA 22314-2794.

Comments by Readers

Comments by readers are invited, and, if deemed appropriate, will be published. Send to: Ellen Parson, Journal Editor, 3780 SW Boulder Dr, Lee's Summit, MO 64082. Comments can also be sent via email to journal@nafe.org.

Material published in this Journal, including all interpretations and conclusions contained in papers, articles, and presentations, are those of the specific author or authors and do not necessarily represent the view of the National Academy of Forensic Engineers® (NAFE) or its members.

 ISSN: 2379-3252

Table of Contents

‡ Paper presented at the NAFE seminar held in January 2018 in Phoenix.

+ Paper presented at the NAFE seminar held in January 2019 in Orlando.

* Paper presented at the NAFE seminar held in July 2018 in Buffalo.

† Paper presented at the NAFE seminar held in July 2019 in Denver.

Table of Contents

* Paper presented at the NAFE seminar held in July 2018 in Buffalo.

† Paper presented at the NAFE seminar held in July 2019 in Denver.

§ Paper presented at the NAFE seminar held in January 2020 in San Diego.

The Applications of Matchmoving for Forensic Video Analysis of a Fatal Sprint Car Accident: Part I

By Richard M. Ziernicki, PhD, PE, (NAFE 308F), Martin E. Gordon, PE (NAFE 699F), Steve Knapp, PE (NAFE 819S), and Angelos G. Leiloglou, M. Arch. (NAFE 956C)

Abstract

The methodology used for the reconstruction of a high-profile Sprint Car accident that was captured by at least three different video recording devices is presented in two parts. Part I discusses a classical method of an accident reconstruction, and Part II discusses matchmoving technique to accurately analyze the video footage of the accident. Accidents captured on video are unlike most simple car collision evaluations and require expert knowledge from experienced professionals. Understanding the race car vehicle dynamics as it relates to recorded video footage allows a proper methodology to be followed in order to gather and process the evidence needed to provide meaningful data to the trier of fact. This paper discusses the classical process to reconstruct the accident as well as the currently acceptable scientific methodologies that were used to collect and interpolate the available scientific evidence. A visualization of the vehicles involved, Sprint Car #13 (SC#13) and Sprint Car #14 (SC#14), is shown in ***Figure 1****.*

Keywords

Race car, Sprint Car, crash reconstruction, matchmoving, high-definition scanning, camera match

In, 2014, a fatal incident occurred where the decedent was participating in a Sprint Car Race (SC#13) on a low-banked dirt oval track with the straights running south-west and northeast. The grandstands are positioned on the north side of the track. The track corners are divided into quadrants (1 to 4) with the cars racing counterclockwise. Turn 1 is the first turn after passing the grandstands on the main straightaway (as shown in **Figure 2**).

Figure 1
Visualization of SC#13 and SC#14 entering turn 1.

During the race, the decedent driver in SC#13 and a driver in SC#14 entered Turn 1 at approximately the same time as the driver of SC#14 attempted to overtake SC#13. During the overtake, the driver of SC#13 lost control of his vehicle and contacted the west edge track barrier where his vehicle came to a stop near the end of Turn 2.

Figure 2
Google image illustration of the racetrack where the incident occurred.

Richard M. Ziernicki, PhD, PE, 7185 S. Tucson Way, Centennial, CO 80112, (303) 925-1900, rziernicki@knottlab.com

After impacting the barrier, the driver of SC#13 exited his vehicle, and the remaining Sprint Car racers went under a "yellow flag" alert. (During a yellow flag, racers are alerted by track officials to exercise caution and reduce speed for a hazard on the racetrack.) A caution announcement was also broadcast over the drivers' helmet headsets with instructions to stay low (toward the infield of the racetrack). As the Sprint Cars slowed for the "yellow flag," they were observed in the video footage passing the wrecked SC#13 on the inside of Turn 2 (as the driver of SC#13 was walking behind the rear of his Sprint Car). As the driver of SC#13 began to walk toward the middle of the track, he was passed by a total of six Sprint Cars traveling on the inside of the track.

Unlike the first six Sprint cars to pass the driver of SC#13, SC#14 failed to acknowledge the yellow flag and radio call to stay low on the track. As SC#14 approached the driver of SC#13 in Turn 2, its right rear wheel impacted SC#13 driver, causing fatal injuries. Witnesses reported that the rear of SC#14 was sliding ("drifting") into the driver of SC#13, and video footage/witness testimony confirmed that the SC#14 had revved its engine prior to impact with the driver of SC#1. The SC#13 driver was thrown a distance of approximately 91 feet after being impacted by the SC#14.

Data Review and Analysis

Witness Statements

Statements from the driver of the SC#14, track officials, spectators in the stands, Safety Truck attendants, and other Sprint Car drivers were taken at the time of the incident. The statements assisted in organizing a sequence of events, but failed to provide the details necessary to accurately reconstruct the accident itself. The statements described drivers hearing the warning for a caution lap. However, there were inconsistencies in the statements regarding whether the driver accelerated or revved his engine prior to the incident. There were also inconsistencies relating to whether the driver of SC#13 walked into the right rear tire — or if SC#14 went sideways — before impacting the decedent (driver SC#13).

A critical component to these inconsistencies was the varying perspectives of the witnesses who gave statements. These witnesses varied in their viewing location, knowledge of the sport, and relationship to the Sprint Car drivers. A summary of the witness statements is presented as follows:

Track Official: Located on the back stretch (south side of the track), a track official testified that he observed the driver of SC#13 get out of his Sprint Car and come down closer to the cars that were on the caution lap. The track official also testified that the driver of SC#13 walked into the right rear of the SC#14 — and that he did not hear any acceleration or revving of SC#14 prior to the incident.

Racer in SC#45: The racer in SC#45 testified that he was racing his Sprint Car in front of SC#14 and witnessed the driver of SC#13 getting out of his Sprint Car as he came back around the track on the caution lap. The driver of SC#45 reported that the driver of SC#13 came toward his car, and he swerved away from him toward the inside of the track.

Racer in SC#1: The racer in SC#1 testified that he was in his Sprint Car directly behind SC#14 at the time of the incident. The SC#1 racer also witnessed the driver of SC#13 walking down the track as he entered into Turn 1. Before the impact, he witnessed the impacting SC#14 rear tires grow tall and skinny with dust rolling off of them. He indicated that the rear of SC#14 kicked out a little bit with "power going to the rear tires."

Racer in SC#00: The racer in SC#00 testified that she was also racing directly behind SC#14. She testified that she heard the caution broadcast on her radio by the time she was in Turn 3 (two corners before the incident occurred). She indicated that she heard on the radio that the officials were instructing all Sprint Cars to stay low on the track. As they approached the driver of SC#13, she witnessed SC#14's left front wheel turn to the right to direct the Sprint Car closer in the direction of where the driver of SC#13 was standing. Just prior to impact, she saw the rear of #SC14 stand up with dust coming off the rear tires as the driver of SC#14 hit the throttle. The witness reported that the application of the throttle caused the rear of SC#14 to come around with the front end of the car pointing to the left. She testified that as SC#14 began traveling sideways, it struck the decedent driver of SC#13.

Spectator Witness: A spectator located in the grandstands near Turn 1 was a witness that was deposed regarding the subject incident. He testified that he witnessed SC#14 enter low into Turn 1 and drift up the track toward the driver of SC#13. He testified that he heard the SC#14 engine rev and witnessed its rear end begin to slide sideways to the right. He saw the driver of SC#13 "stutter step," as if he were attempting to avoid being hit by SC#14. In his opinion, the spectator witness testified that had SC#14 not moved up the track toward the decedent driver of SC#13, the incident would not have occurred.

Safety Official 1 (SO1): The SO1 was positioned in the truck bed of the track Safety Truck that was positioned at Turn 1 at the time of the incident. SO1 testified that he witnessed cars slowing for the caution and going through Turn 1 in single and double file — and that he saw one Sprint Car moving out and an engine rev somewhere on the track. The SO1 testified that he witnessed SC#14 make what appeared to be an intentional "out and in" movement during the incident and reported that SC#14 moved up the track prior to impact.

Safety Official 2 (SO2): The SO2 was positioned in the truck bed of the track Safety Truck that was positioned at Turn 4 at the time of the incident. The SO2 testified that they were in route to SC#13 before Turn 1 when he witnessed SC#14 go up the track, "gas it," and come back down as the right rear tire "collected" the driver of SC#13. The SO2 reported that the vehicle in front of SC#14 was able to steer away to the low side of the track to avoid the driver of SC#13 and indicated that the driver of SC#13 came down and stopped at the mid-section of the track before the impact occurred with SC#14.

Racer in SC#14: The racer in the impacting SC#14 testified that he was made aware of the caution lap through radio communication and from the flagman and yellow flag that was observed on the main straightaway. The driver of SC#14 testified that he attempted to change direction to the left to go down the track by applying throttle to the car.

Imaging of SC#13 and Exemplar Sprint Car

The Sprint Car being driven by the decedent on the night of the subject incident was examined and photographed, as shown in **Figure 3**. The right rear tire of the car is flat and had not been repaired since the incident.

An exemplar Sprint Car was scanned in 2016. The Sprint Car was being prepared for sale and did not have an engine at the time of inspection. Additionally, the wing actuators (device used to move the large wing on the Sprint Car) had been removed. Otherwise, the vehicle had the same dimensions as both SC#13 and SC#14 at the time of the subject collision. The 3D scan collected approximately 390 million data points. An image of the scanned exemplar Sprint Car is presented in **Figure 4**.

Inspection and Testing with Exemplar Sprint Car

Another exemplar Sprint Car was inspected and test driven during the course of this investigation. The physical dimensions, weight, tire sizes, engine, and transfer box were all similar to the Sprint Cars being driven during the subject incident.

After driving and inspecting the exemplar Sprint Car, testing was conducted to determine the effect of avoidance maneuvers relative to the dirt-banked track conditions that were present at the time of the accident. An exemplar track with a similar low-banked dirt construction was utilized for testing. The Sprint Car setup suspension and tire setup were the same for racing at the track where the incident occurred. Prior to testing, the track had been raked and was very dry, making the exemplar track slicker and thus more difficult to drive on than during the subject incident.

A cone was placed at Turn 2 in the vicinity of where the decedent driver was standing when he was struck and killed by SC#14. The exemplar Sprint Car was driven for approximately 10 laps using caution lap pace as well as race driving pace. During the testing, it was concluded that the cone was easily visible coming out of Turn 1, and very

Figure 3
Image of decedent's Sprint Car.

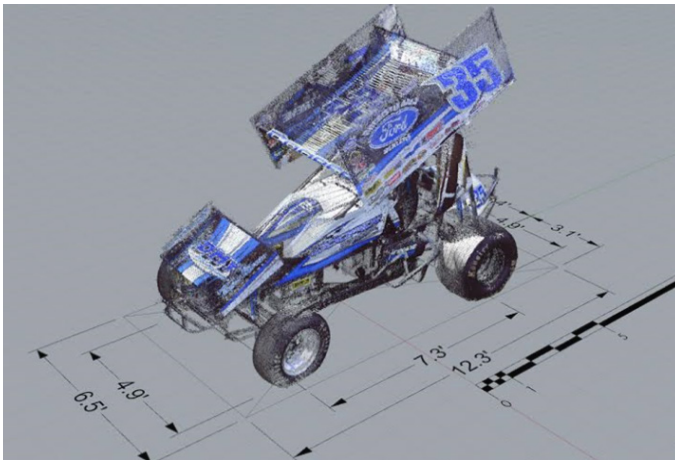

Figure 4
Scanned exemplar Sprint Car with dimensions.

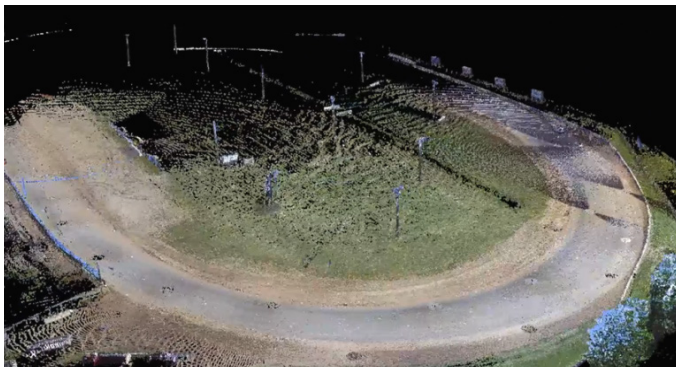

Figure 5
Aerial view of the scanned Sprint Car track.

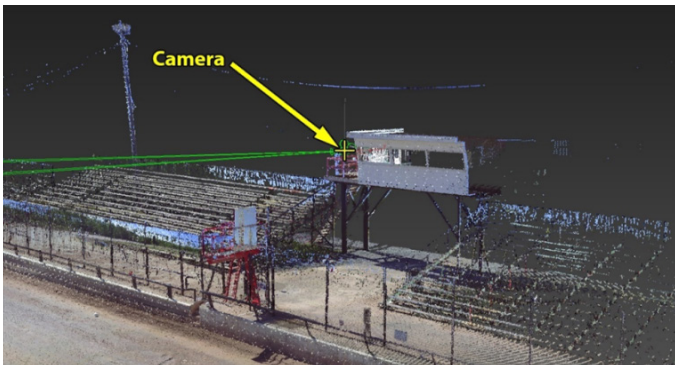

Figure 6
Perspective view of grandstands showing the location of the camera that captured video of the incident.

minor steering input was required to prevent hitting the cone during the testing exercise.

Inspection of Accident Site

The racetrack venue where the incident occurred was scanned for the purpose of documenting relevant areas of the track and grandstands. 3D scanning during the inspection produced approximately 860 million data points. The scans were captured using a Faro Focus 3D X330 Laser scanner and registered together to produce a 3D "point cloud" of the racetrack. Each data point in the point clouds is defined by its three-dimensional coordinates (x, y, z) and is accurate to within a few millimeters. Neither the track geometry nor the grandstand geometry appeared to have changed since the date of the incident. An image of the scanned subject Sprint Car track is presented in **Figure 5**.

By the time the opposition's experts visited the site at a later date, the track had been altered into a different configuration. Visual landmarks and track dimension had changed significantly and became critical factors in the precise reconstruction of the incident. The change of the racetrack landmarks is discussed in Part II of this paper.

Video

The subject incident was captured by three video cameras. Two of the available videos were captured by spectators with cellular phones located in the grandstands. The third video camera was positioned on the east side of the announcer's box, as shown in yellow in **Figure 6**. The camera captured the incident event with video footage recorded at 29.970 frames per second.

Limitations of Reconstruction Based on Physical Evidence

When reconstructing motor vehicle accidents, causes and contributing factors are analyzed to determine how and why an accident occurred. In forensic engineering, after analyzing physics of the accident, understanding how an accident occurs becomes apparent with the speed, direction, acceleration, and motion of the vehicle. Forensic engineering provides the factual basis of the case and the sequence of events that led up to and followed the accident.

In the subject incident, witnesses provided conflicting testimony regarding the SC#14 movement at the time of the impact with the decedent driver of SC#13. In one scenario, the driver of SC#14 is moving down the track in an attempt to avoid the driver of SC#13. In the other scenario, SC#14 is being driven up the track to drift his Sprint Car closer to the driver of SC#13. The second scenario potentially suggests a reckless disregard for the driver of SC#13 that must be carefully evaluated.

There is an engineering limit in determining the cause of an accident, specifically when it comes to analyzing the intent of a driver. It was hypothesized that the second scenario (where SC#14 is going up the track) was an attempt to perform a technique known in the racing community as "stoning" your competitor. This occurs when a racer applies significant throttle to spin the rear driven tires to kick up dirt and rocks onto another competitor. While this is a possible intent of the SC#14 driver, the physics and vehicle motion were the factors that were analyzed and considered by the authors.

What could be deducted from the analysis and witness statements was that it was likely that SC#14 was moving in such a manner that it traveled up the track and struck the decedent driver that was stationary at the time of the impact. Witness reported observing the motion of SC#14 in addition to hearing the car's engine revving and tires spinning prior to impact with the decedent. Regardless of the intent, the observed vehicle dynamics and witness

accounts are, in fact, consistent with one attempting to stone a competitor.

Video Processing

Since the accident scene is constructed of dirt and contains multiple tire paths — and debris existed on the track — no meaningful evidence was available or documented for the purpose of reconstructing the accident. Therefore, video footage that captured the incident became the single most important factor in analyzing the vehicle motions and determining which scenario of the accident, as presented by the drivers and witnesses, was probable.

Unlike the witness statements that offered conflicting scenarios of the accident, the video footage that was a record of the incident could be analyzed and compared to data that was collected at the accident scene. The analyzed video footage of the incident panned rapidly across the racetrack, moving left and right as it began to focus and zoom in on the decedent driver walking toward the middle of the track. Due to camera angle and significant distance between the video camera and the location of the incident (approximately 550 feet), analyzing the Sprint Cars' exact distance from the camera source becomes a highly sensitive analysis and outside the realm of a typical vehicle reconstruction. In order to properly analyze and understand the vehicle dynamics captured in the video of the incident, videogrammetry and matchmoving process was the only viable scientific option. The methodology of utilizing videogrammetry and matchmoving technique to reconstruct this accident is presented in Part II of this paper.

Conclusion

Proper documentation and collection of time-sensitive scene data was conducted in order to perform analysis of the incident that was captured with video footage. Conflicting witness statements indicated two scenarios of the accident. In one scenario, the driver of SC#14 is moving down the track in an attempt to avoid the driver of SC#13. In the other scenario, SC#14 is being driven up the track to drift his Sprint Car closer to the driver of SC#13. Due to the orientation of video camera relative to the incident location, videogrammetry and matchmoving analysis utilizing the data collected from this investigation was employed to determine accurate vehicle location, speed, and heading angle of each Sprint Car. Understanding the relative motion of each Sprint Car and the decedent driver would lay down scientific foundation to understand how the subject accident occurred.

The Applications of Matchmoving for Forensic Video Analysis of a Fatal Sprint Car Accident: Part II

By Richard M. Ziernicki, PhD, PE (NAFE 308F), Martin E. Gordon, PE (NAFE 699F), Steve Knapp, PE (NAFE 819S), and Angelos G. Leiloglou, M. Arch. (NAFE 956C)

Abstract

This paper presents the application of the photogrammetric process known as matchmoving to analyze a racetrack video and reconstruction of a fatal Sprint Car race accident. The use of high-definition 3D laser scanning technology made it possible to accurately perform the matchmoving process on racetrack video footage to determine the path, heading, speed, and acceleration of the involved Sprint Cars. In addition to the accident racetrack, another video of a Sprint Car race on a similar racetrack, taken by a drone, was also analyzed using the same matchmoving method to evaluate the speed and yaw angle of a drifting Sprint Car.

Keywords

Matchmoving, photogrammetry, high-definition scanning, video analysis, drone video footage, accident reconstruction, lens distortion correction, SynthEyes, forensic engineering, Sprint Cars

Introduction

Cameras surround us in our everyday lives. Today, more accidents and shootings are being captured on video, whether it be by surveillance cameras, police body-worn cameras, air units, dash cameras, or by witnesses using smart phones. With this widespread use of cameras, one of the first things that is done after an accident/catastrophic event is to secure any video footage that may have captured the accident. The proper scientific analysis of these videos is vitally important in reconstructing these accidents.

In recent years, with the advances of technologies like high-definition 3D laser scanning (also known as Light Detection and Ranging or LiDAR) and drones — as well as advancements in software — it is now possible to apply matchmoving to video footage, extract accurate information, and use it to reconstruct what happened.

Matchmoving is a process based on the science of photogrammetry that is used to solve for or "calibrate" a virtual camera to "match" the "movement" and lens characteristics of the real-world camera used to capture a given video. After calibrating the virtual camera, the motion of objects depicted in the video, such as vehicles, pedestrians, or other objects can be determined through the process of object tracking or object matching.

The second in a two-part series, this paper presents the application of matchmoving to a 13.8-second video clip of a racetrack video (**Figure 1**) to reconstruct the accident and determine the path, heading, speed, and acceleration of seven race cars and the movement of the pedestrian who was struck and killed.

Background

The accident occurred at a motorsports park with a

Figure 1
Still frame from track video moments before the fatal impact.

Richard M. Ziernicki, PhD, PE, 7185 S. Tucson Way, Centennial, CO 80112, (303) 925-1900, rziernicki@knottlab.com

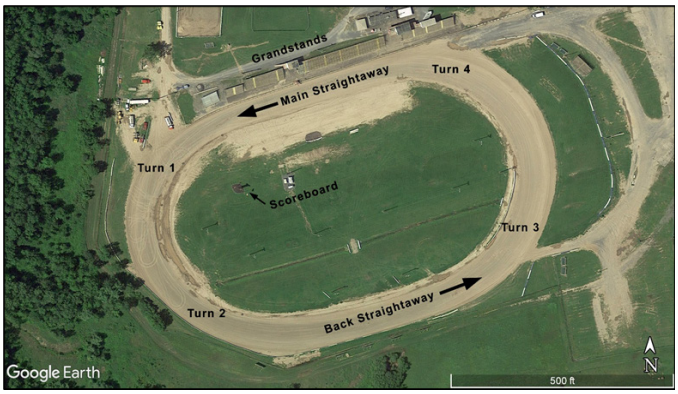

Figure 2
Google aerial imagery of the motorsports park with annotations added by authors.

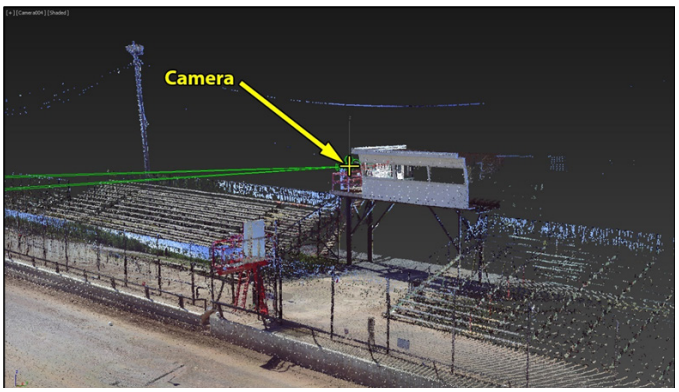

Figure 3
Photo of motorsports park grandstands showing the location of the camera that recorded the video of the accident.

low-banked dirt oval track with the straights running southwest and northeast and the grandstands positioned on the north side of the track. The track corners were divided into quadrants (1 to 4) with the cars racing counter-clockwise. Turn 1 was the first turn after passing the grandstands on the main straightaway as shown in **Figure 2**.

The driver in Sprint Car #13 (SC#13) and another driver in SC#14 were both competing with their Sprint Cars and entering into Turn 1 at approximately the same time when the driver in SC#14 attempted to overtake the driver in SC#13. The driver in SC#13 lost control of his Sprint Car during the maneuver and made contact with the outer edge track barrier where his Sprint Car came to a stop near the end of Turn 2.

After impacting the barrier, the driver in SC#13 immediately exited his Sprint Car. Because of this incident, the remaining Sprint Car drivers went under a "yellow flag." (During a yellow flag, drivers are alerted to exercise caution, and reduce speed for a hazard on the racetrack.) Also, a caution announcement was broadcast over the drivers' helmet headsets with instructions to stay low (toward the infield of the racetrack).

As the Sprint Cars slowed for the "yellow flag," SC#2, SC#20, and SC#28 passed SC#13, which was stopped on the inside corner Turn 2 of the track as the driver of SC#13 was walking behind the rear of his Sprint Car. SC#19 passed the driver of SC#13 at the mid to lower portion of the track. As the driver of SC#13 began to walk toward the middle of the track, he was passed by SC#10 and SC#45 on the inside corner of the track. As the driver in SC#14 approached the driver of SC#13 in Turn 2, the right rear of the SC#14 impacted the driver of SC#13, causing fatal injuries.

Motorsports Park Camera Video Footage

The motorsports park was recording the Sprint Car racing event with a video camera that was mounted on a tripod and positioned on the east side of the announcer's box located in the middle of the grandstands (**Figure 3**). The camera captured video of the event at 29.97 frames per second in full high-definition (FHD) resolution.

Despite being recorded from a tripod and having relatively high resolution, the video footage was a challenge to analyze for a number of reasons. First, the camera man was panning and zooming in and out throughout the video, which means the orientation and field of view (FOV) of the camera was constantly changing. Secondly, the accident occurred in Turn 2, which was approximately 550 feet away from the camera (**Figure 4**). Finally, because the race was at night, the low light and combination of the camera's shutter speed and aperture, vehicle speed, and the movement of the camera (panning and zooming) produced some motion blur in parts of the video.

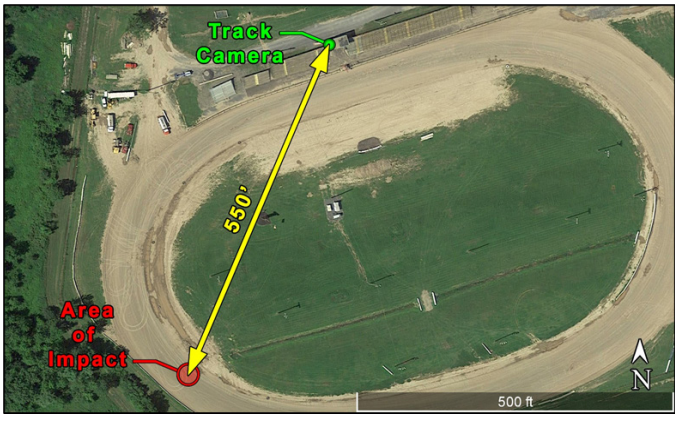

Figure 4
Aerial view of racetrack, depicting the distance between the track camera and the area of impact.

Rudimentary speeds of the vehicles could have been determined using the traditional method of using landmarks or sight lines to measure the distance a vehicle traveled between two points and dividing that distance by the time it took for the vehicle to travel between the two points. However, the lack of lane lines and the relatively low angle and far distance the camera was relative to the incident would make it practically impossible to yield reliable results regarding the vehicles' and pedestrian's lateral position on the track using typical analytical methods.

For this reason, the authors used an established photogrammetric method called "matchmoving" to reconstruct the speeds and paths of the vehicles and pedestrian. The matchmoving method is outlined in a paper titled, "Forensic Engineering Application of the Matchmoving Process." The matchmoving method has been used for decades for visualization purposes, but has only in recent years been able to be used for video analysis and accident reconstruction — thanks to the advancements of matchmoving software and the now established technology of high-definition 3D laser scanning[1].

High-Definition 3D Laser Scanning

In order to ensure the matchmoving process yielded accurate results, high-definition 3D laser scanning was used to capture three-dimensional point clouds of an exemplar Sprint Car vehicle, which was similar in shape and size to SC#13 and SC#14, and the motorsports park racetrack. Before scanning of the track, it was noted that neither the track geometry nor the grandstand geometry was changed since the date of the incident.

The point clouds were captured using a Faro Focus 3D X330 Laser Scanner and consisted of approximately 860 million data points for the racetrack and approximately 390 million data points for the exemplar Sprint Car (**Figure 5**). Each data point in the point clouds is defined by its three-dimensional coordinates (x, y, z) and is accurate to within a few millimeters. The point cloud models of the racetrack and the exemplar Sprint Car were used by the authors to perform videogrammetry analysis on the provided racetrack video footage.

Videogrammetry

The authors performed videogrammetric analysis on the provided racetrack video footage to determine the spatial movement of SC#14, the preceding six Sprint Cars and the decedent driver of SC#13, as depicted in the video.

The videogrammetric analysis involved first using the established scientific process called matchmoving[2,3] to define a virtual camera that "matches" the location, orientation, focal length, and lens distortion of the camera used to record the provided racetrack video footage. Further, a process called object matching was used to determine where objects (seven Sprint Car vehicles and a decedent driver) were physically located on the racetrack in each frame of the video.

Figure 5
Point cloud model of the racetrack (left) and the exemplar Sprint Car vehicle model (right.)

Matchmoving

The authors used a well-known software called "SynthEyes" to perform the matchmoving process. First, two-dimensional points (features) were identified and tracked through multiple frames of the video. Each feature represents a specific point on the surface of some fixed object on the racetrack (i.e., fence post, concrete barrier, scoreboard, etc.). Each tracked feature was then assigned and constrained to the feature's corresponding three-dimensional coordinates (x, y, z) as defined by the racetrack point cloud (**Figure 6** and **Figure 7**).

Using the 2D trackers and their given 3D XYZ coordinate constraints, SynthEyes was then used to mathematically solve for (or "calibrate") a virtual camera (relative to the racetrack point cloud) that emulated the lens characteristics and movement (panning and zooming) of the real-world camera that was used to record the racetrack footage.

The virtual camera's solution was determined to a high degree of scientific certainty. **Figure 8** shows the error rate between the constrained or "locked to" position of each 3D (xyz) tracker, and the 3D "solved position." The average error rate of all the constrained 3D trackers was 0.0017 feet (approximately 0.5 mm).

As further verification, the solved virtual camera's location in the racetrack point cloud, matched with the location where the real-world racetrack video camera was located in the stands at the time of the incident (**Figure 9**).

Figure 10 shows match of image by virtual camera

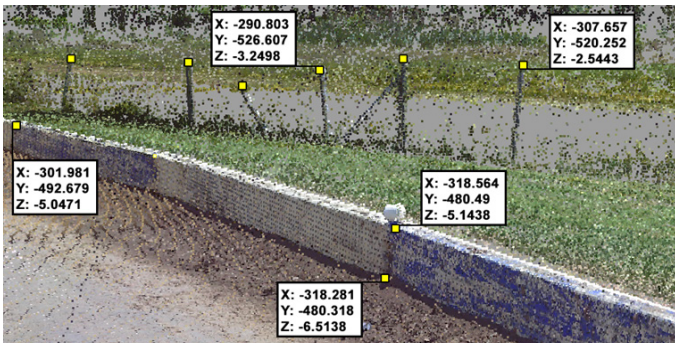

Figure 7
Sample of the 3D (XYZ) coordinates data (extracted from the author's 3D racetrack point cloud) used to constrain the corresponding 2D trackers.

Axes	Tracker	Locked To	Distance	Solved Position	Error
XYZ	#2	x=-323.542 y=-515.667 z=-3.0515		-323.541 -515.668 -3.049	0.003
XYZ	#4	x=-184.255 y=-195.603 z=9.078		-184.258 -195.602 9.074	0.005
XYZ	#6	x=-182.215 y=-197.105 z=5.894		-182.210 -197.107 5.892	0.005
XYZ	#7	x=-182.704 y=-196.79 z=8.92		-182.702 -196.791 8.917	0.003
XYZ	#8	x=-318.564 y=-480.49 z=-5.1438		-318.562 -480.491 -5.145	0.002
XYZ	#10	x=-185.536 y=-194.669 z=7.385		-185.538 -194.668 7.393	0.008
XYZ	#12	x=-185.526 y=-194.671 z=4.3866		-185.525 -194.672 4.388	0.002
XYZ	#28	x=-231.584 y=-529.991 z=-5.0209		-231.584 -529.991 -5.021	0.000
XYZ	#151	x=-255.4 y=-447.8 z=-11.1		-255.401 -447.800 -11.099	0.001
XYZ	#153	x=-250.112 y=-521.951 z=-5.0859		-250.112 -521.951 -5.085	0.000
XYZ	#282	x=-251.73 y=-448.4 z=-11		-251.731 -448.400 -11.000	0.001
XYZ	#283	x=-262.059 y=-536.37 z=-2.9811		-262.059 -536.370 -2.981	0.000
XYZ	#291	x=-345.719 y=-457.953 z=-5.5006		-345.719 -457.953 -5.501	0.000
XYZ	#292	x=-328.921 y=-514.48 z=-2.9217		-328.924 -514.479 -2.922	0.003
XYZ	#298	x=-182.176 y=-197.102 z=11.001		-182.172 -197.103 10.999	0.004
XYZ	#299	x=-333.945 y=-468.48 z=-5.3998		-333.945 -468.480 -5.398	0.002
XYZ	#300	x=-285.121 y=-503.865 z=-4.95		-285.121 -503.865 -4.950	0.000
XYZ	#302	x=-302.276 y=-492.26 z=-4.9496		-302.278 -492.259 -4.950	0.002
XYZ	#304	x=-239.618 y=-542.924 z=-2.7346		-239.618 -542.924 -2.735	0.000
XYZ	#305	x=-226.718 y=-547.141 z=-3.0185		-226.718 -547.141 -3.019	0.000
XYZ	#326	x=-235.676 y=-528.2 z=-5.092		-235.675 -528.200 -5.092	0.001
XYZ	#331	x=-267.628 y=-513.8 z=-5.12		-267.628 -513.800 -5.120	0.001
XYZ	#332	x=-355.724 y=-513.394 z=-3.9003		-355.724 -513.394 -3.902	0.002
XYZ	#336	x=-233.857 y=-408.773 z=-8.7813		-233.857 -408.773 -8.781	0.000
XYZ	#338	x=-211.284 y=-410.795 z=-8.875		-211.284 -410.795 -8.875	0.000
XYZ	#341	x=-212.867 y=-537.255 z=-4.848		-212.867 -537.255 -4.848	0.000

Figure 8
Table of the constrained trackers used to calibrate the virtual racetrack camera. The far-right column (highlighted by the authors in yellow) shows the error rate between the constrained or "locked to" position of each 3D (xyz) tracker and the 3D "solved position" in feet.

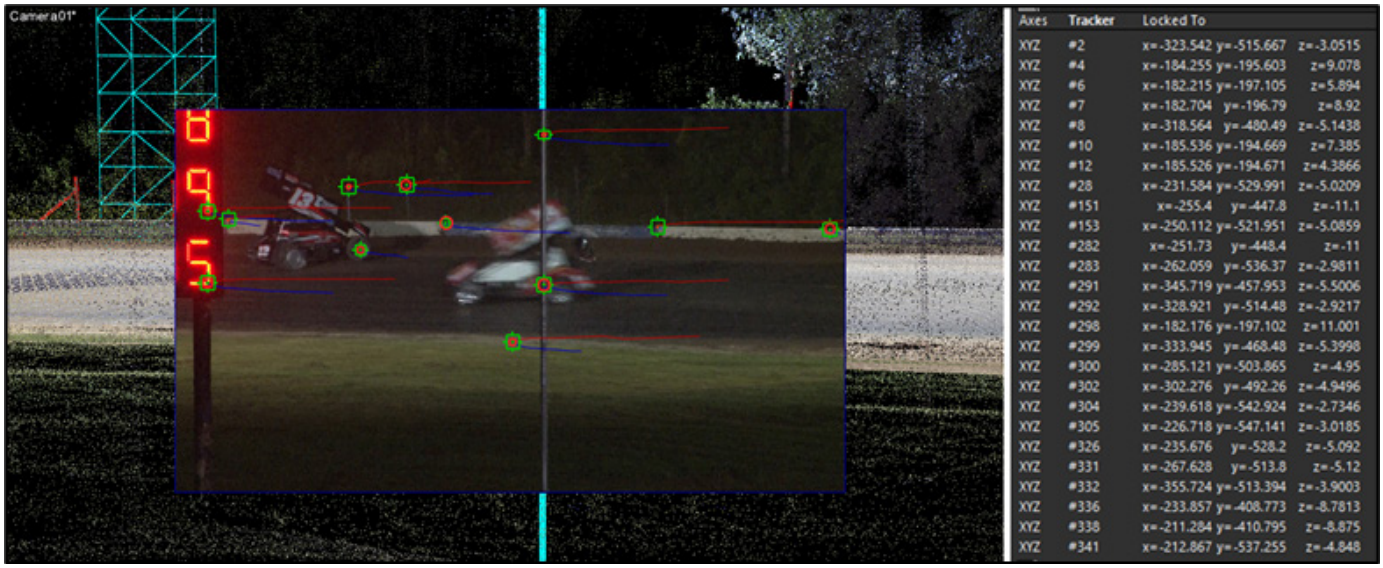

Figure 6
Tracked 2D points (in green, left) constrained to 3D x,y,z coordinates (right).

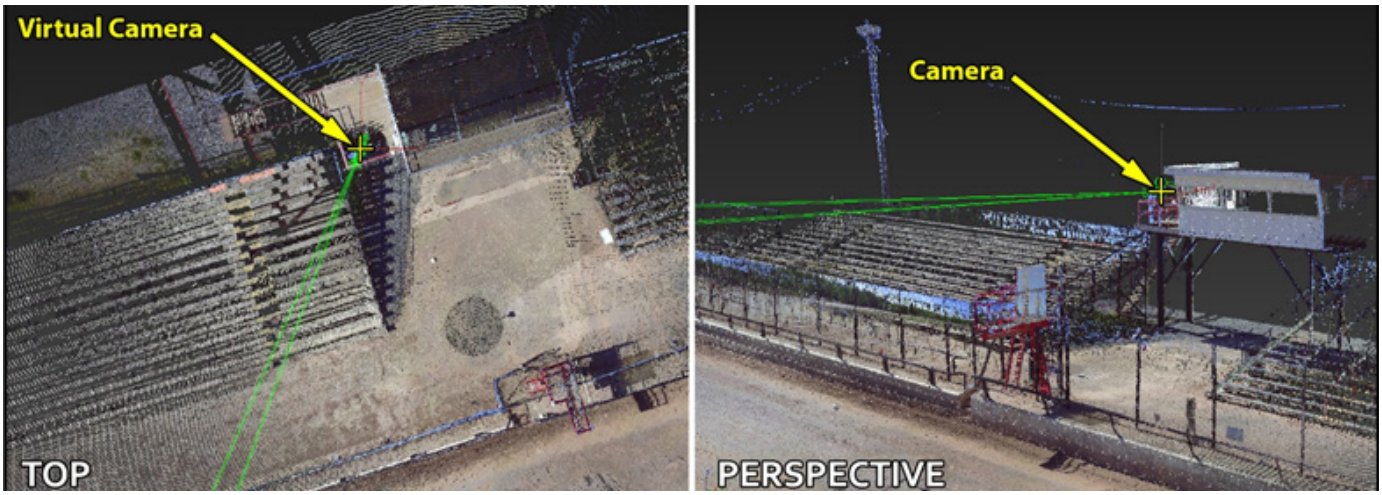

Figure 9
Top view (left) and perspective view (right) of the motorsports park grandstands showing the location of the virtual camera solved by matchmoving.

and the point cloud. Once the calibration of the virtual camera was confirmed to be accurate, the next step in the videogrammetric process was to use a process called "object matching" to determine the three-dimensional position of the vehicles and pedestrian in every video frame to determine their paths, speed, and acceleration.

Vehicle and Pedestrian Matching/Tracking

The calibrated virtual camera and the racetrack point cloud model were brought into a virtual scene in 3D Studio Max. In the virtual scene, a three-dimensional virtual model of a Sprint Car, which was based on the point cloud of the exemplar Sprint Car (SC#35), as shown in **Figure 11**, was positioned on the surface of the race track in the point cloud to match the location of SC#14 in each frame of the video, as viewed through the virtual camera (**Figure 12**).

It is important to note that when positioning the virtual Sprint Car model, the main constraint is that the bottom of the wheels of the model must be in contact with the surface of the racetrack. The virtual model is then moved laterally along the racetrack super elevation (toward or

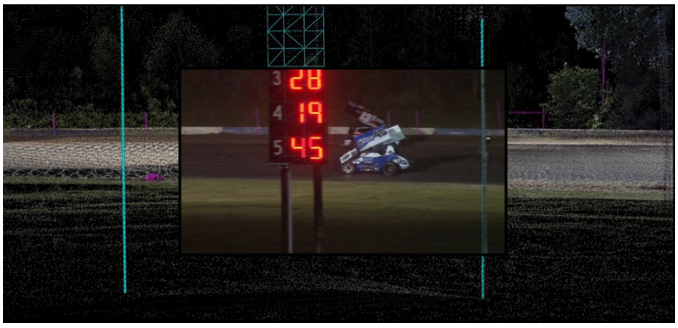

Figure 10
Matchmove "virtual" camera view verifying a correct solve.

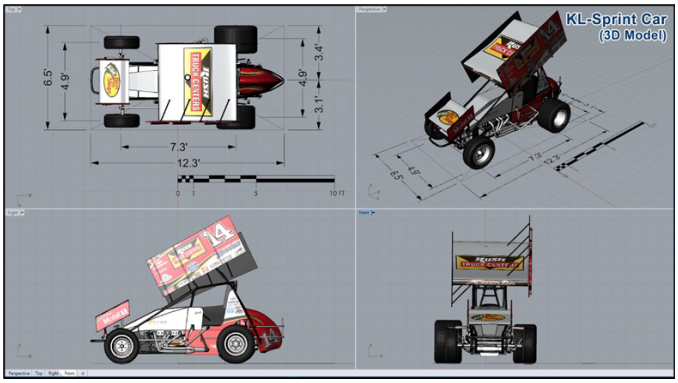

Figure 11
3D virtual model of Sprint Car based on point cloud of exemplar Sprint Car.

Figure 12
Frame by frame matching of SC#14. Left column: video frames. Right column: virtual Sprint Car model matched to position of Sprint Car seen in video.

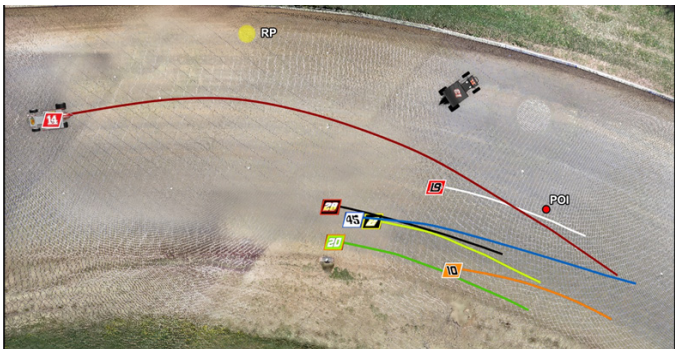

Figure 13
Seven Sprint Car paths resulting from videogrammetric analysis.

away from the camera) and oriented (heading) on the track surface until the model matched in size to the Sprint Car depicted in the video frame.

The authors also performed the same matching process for the six Sprint Cars that passed the decedent driver prior to SC#14. Once the vehicles had been tracked/matched, the 3D translation (x, y, z) and orientation angles (roll, pitch, yaw) data of each vehicle, for each video frame, was exported directly from 3D Studio Max program and imported into an Excel spreadsheet where the object's motion data (i.e., speed, acceleration, heading angle, etc.) was calculated and graphed. The vehicles' motion data was then evaluated to confirm that they were in line with the laws of physics. The resulting paths (**Figure 13**), yaw angles (**Figure 14**), speeds, and accelerations were plotted and graphed.

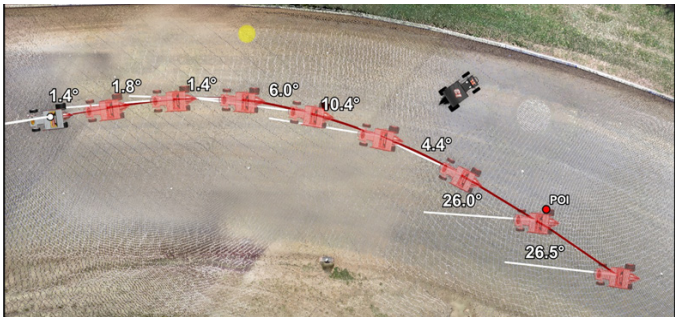

Figure 14
SC #14 yaw angle along path.

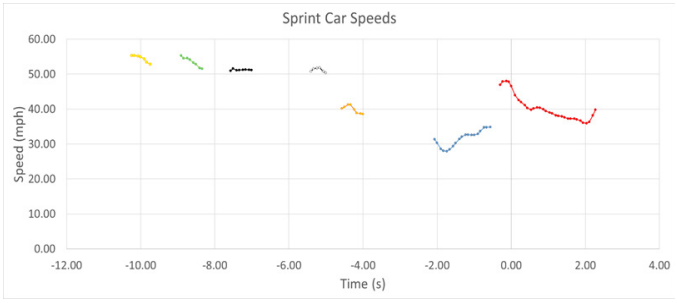

Figure 15
Speed data resulting from videogrammetric analysis.

Note: The Sprint Cars' paths shown are only those that could be seen in the track video. Plots of speed and acceleration are shown in **Figure 15** and **Figure 16**, respectively. The pedestrian and his path are shown in **Figure 17** and **Figure 18**.

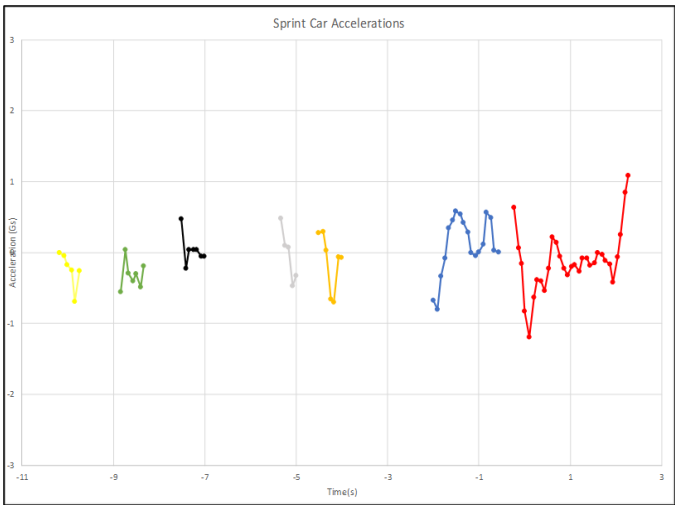

Figure 16
Acceleration data resulting from videogrammetry analysis.

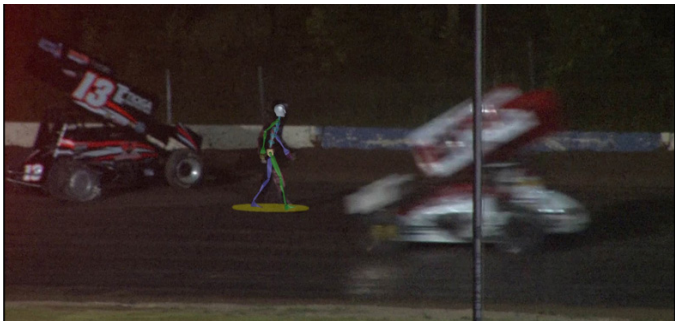

Figure 17
Virtual surrogate bi-ped model used to match the motion of the driver of SC#13.

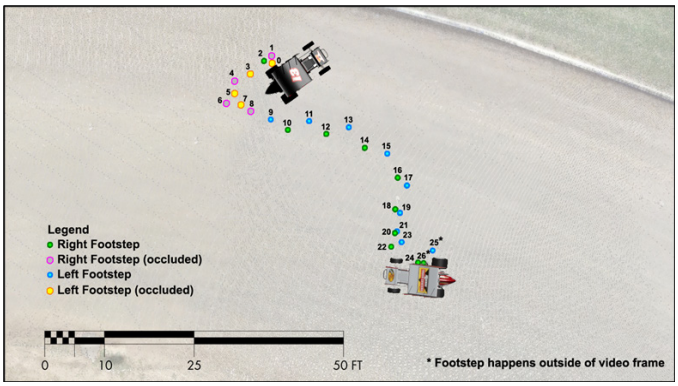

Figure 18
The footsteps of driver SC#13 determined through videogrammetry. Red and yellow circles denote steps that were occluded by the scoreboard in racetrack video.

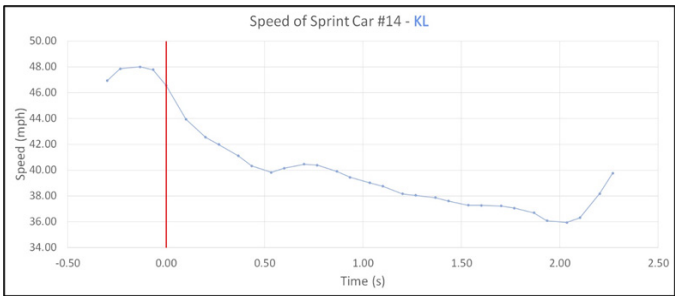

Figure 19
Graph of SC#14 speed data.

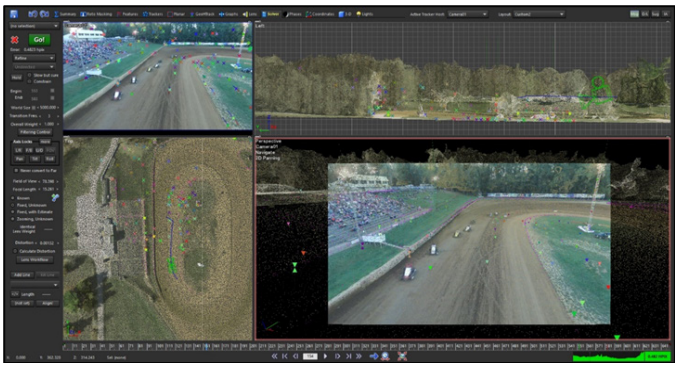

Figure 20
USGS LIDAR data used as constraint to accurately matchmove drone video footage during Sprint Car race.

Based on the review of the vehicle position, speeds, accelerations, and heading angle, resulting from the vehicle motion analysis performed by the authors, it was confirmed that the vehicle motions were valid and within the limits of a physics-based model of the subject event. Typically, accelerations would be expected to be in the vicinity of +/- 1G for Sprint Cars operating at low to moderate speeds and under caution. The vehicle motions, calculated speeds, accelerations, and heading angle were all based on frame-by-frame computations of the Sprint Cars' positions, which resulted in realistic and reliable data to analyze the incident sequence by these engineers.

The analysis of each car's movement started when the car comes into the frame of the video. All seven cars' positions, time, and speeds were analyzed at a frequency of 30 frames per second, resulting in 1,050 data points for each second of car motion from entering video frame until passing area of impact. Sprint Car #14 speed data is shown in **Figure 19**.

The position of SC#13 at rest position was also matched to the video. Additionally, the authors matched the SC#13 driver's walking motion by using a virtual biped surrogate model to match (track) the driver's body parts (legs, arms, head, etc.) relative to the racetrack surface in each frame where he was viewable in the video and not occluded by the scoreboard or passing Sprint Cars.

Results

Based on the videogrammetric analysis, the authors were able to conclude that driver SC#14's speed, acceleration, heading angle, and vehicle path toward driver SC#13 was different than the six Sprint Cars that passed the driver SC#13's location without incident. In fact, driver SC#14 was drifting sideways up the track when it struck driver SC#13, resulting in his death.

Supplemental Video Analysis (Another Case Study)

One of the claims was that driver SC#14 could not have been drifting up track at 50 mph. The authors utilized the same matchmoving method as described above on a video captured by a drone of a Sprint Car race in Lincoln Park raceway, on a similar dirt track to determine if a Sprint Car was capable of drifting up-track at lower speeds (40 to 55 mph).

Aerial Imagery and LiDAR data attained from the United States Geological Survey (USGS)[4] were used to accurately matchmove the video footage (**Figure 20**). Using object matching, the authors were able to match an exemplar Sprint Car model to one of the Sprint Cars depicted in the video (**Figure 21**). The position and rotational data of the Sprint Car were analyzed and showed that the Sprint Car was drifting at speeds below 50 mph (**Figure 22**). As demonstrated on **Figure 21**, the angle between the car heading and car velocity is called yaw angle and was found to be 26.8 degrees.

Matchmoving Done Wrong

It is important to understand that in order for the

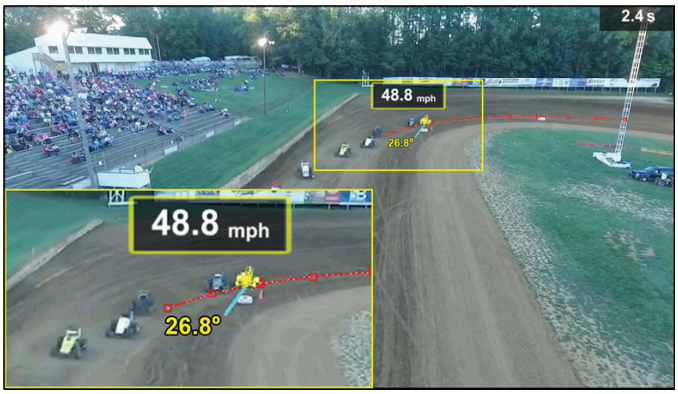

Figure 21
3D virtual model of Sprint Car matched to Sprint Car depicted in the video (yaw: a= 26.8°).

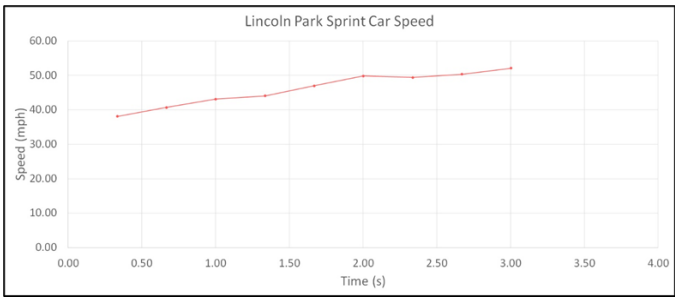

Figure 22
Speed plot of the matched Sprint Car.

matchmoving method to yield accurate results, there must be sufficient accurate 3D data points to use as constraints to calibrate the camera. The location of those 3D points must be the same as they were at the time the video was recorded.

For example, in the previously discussed motorsports park fatal incident, the concrete barriers that were around the outer perimeter of the track at the time of the incident are vital 3D features that were tracked in order to calibrate the virtual track video camera. Those barriers had not been moved between the incident and the time the authors scanned the racetrack. However, when the opposing expert scanned the racetrack, the barriers around the area of the incident had already been removed (**Figure 23**).

Since the opposing expert failed to scientifically calibrate the racetrack camera, they had to estimate the location of the missing barriers resulting in error (**Figure 24** and **Figure 25**).

The insufficiency or inaccuracy of the 3D point data did result in an inaccurate camera calibration, if a calibration can be solved at all. If the camera calibration is inaccurate (i.e., not in the correct place, panning and zooming), then the analysis will be fundamentally flawed — and any resulting analysis or conclusions derived are simply unreliable and without scientific merit. An example

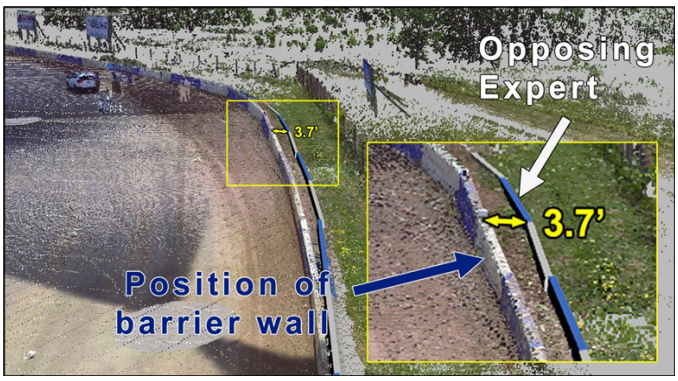

Figure 24
The barriers modeled by the opposing expert (white arrow) compared to the barriers (point cloud) documented by the authors.

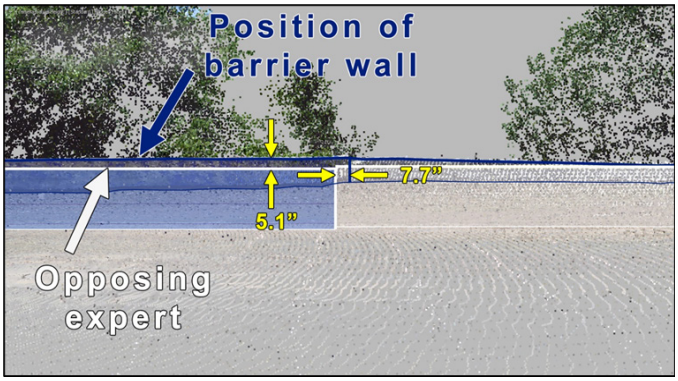

Figure 25
The barriers modeled by opposing expert (white arrow) compared to the barriers (point cloud) documented by the authors. Orthographic side view.

Figure 23
Left: Point cloud of the portion of the track where incident occurred (barrier wall highlighted in yellow);
Right: Barrier wall had been removed/moved when the opposing expert scanned the racetrack.

of faulty analysis is discussed below.

A flawed or inaccurate calibration becomes evident when viewing the virtual scene through the virtual camera, and the tracked 3D features do not accurately match with those same features depicted in the video (**Figure 26**).

The error in the flawed camera calibration and analysis is further highlighted when attempting to match/track the position of the objects like the vehicles in the video frames. Physical constraints (i.e., the bottom of the wheels of the Sprint Car must rest directly on top of the surface of the racetrack) cannot be satisfied. The result is that the Sprint Cars are often "floating" above the surface of the racetrack or traveling below the racetrack level as shown in **Figure 27** and **Figure 28**. The inaccurate vehicle motion is shown in red in **Figure 29**.

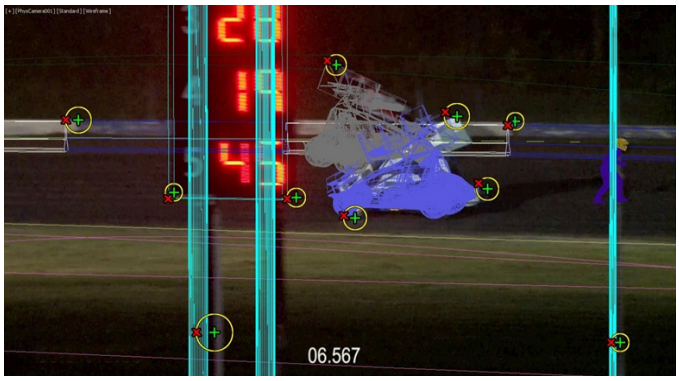

Figure 26
Sample frame from opposing expert's analysis illustrating the inaccuracy of their camera calibration and vehicle matching. Green plus signs mark where the point on an object (i.e., edge of barriers, scoreboard corners, vehicle wheels, etc.) are depicted in the video. Red "X"s mark where those points are projected when viewed through the virtual camera in the opposing expert's 3D scene.

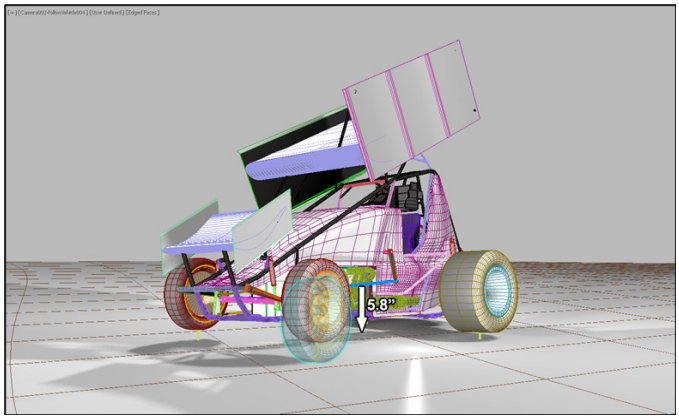

Figure 27
Opposition's Sprint Car floating above the surface due to poor calibration.

In the end, the ultimate evidence of a flawed and erroneous video analysis is that the resulting vehicle dynamics were not only inconsistent with the actual video, but they also violated real-world physics. The opposing expert's analysis of the Sprint Car speeds and accelerations shown in **Figure 30** and **Figure 31** violated real-world physics.

Conclusion

With advancements in matchmoving software programs, high-definition laser scanning, and other related technologies, the matchmoving technique has become very effective in forensic engineering investigations/accident reconstruction to accurately determine and analyze

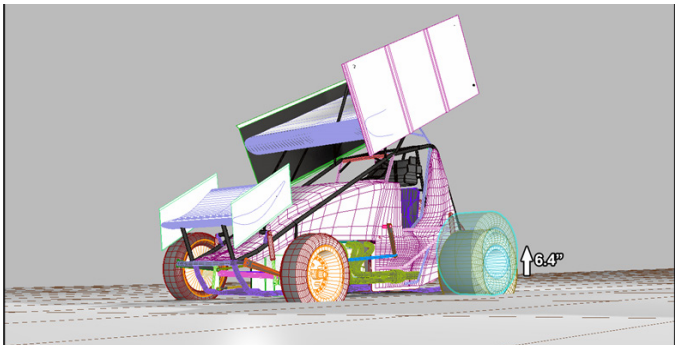

Figure 28
Opposition's Sprint Car traveling below the surface due to poor calibration.

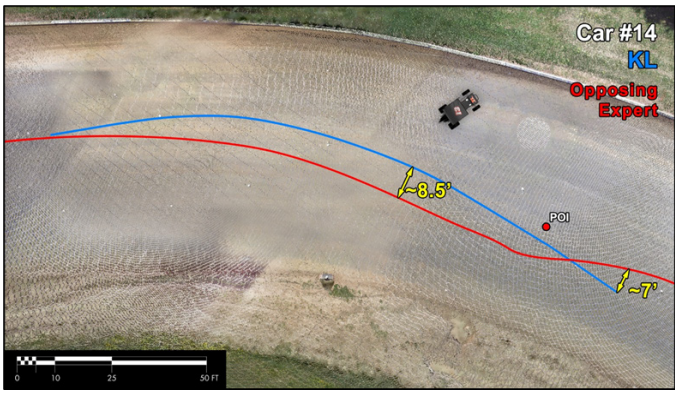

Figure 29
Opposition's inaccurate vehicle motion shown in red color.

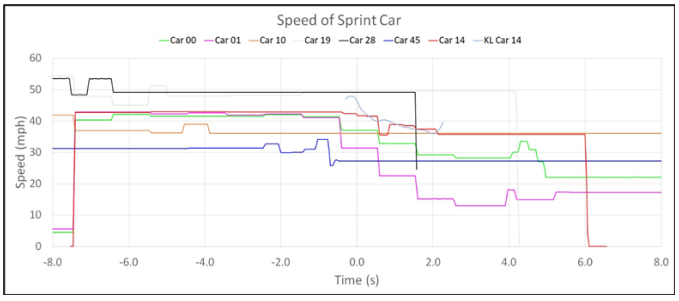

Figure 30
Opposing expert animated Sprint Car speeds.

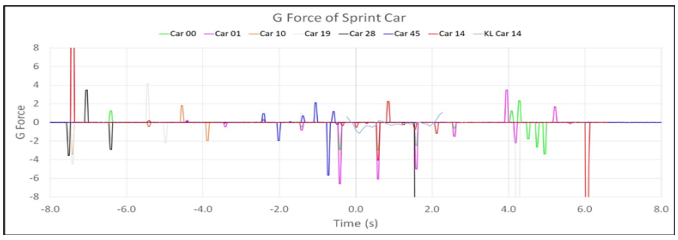

Figure 31
Opposing expert animated Sprint Car accelerations.

the orientation, translation, velocity, and acceleration of vehicles, pedestrians, or other objects depicted in video footage captured by moving cameras.

When an incident is depicted in a video, the match-moving method can yield much more precise, accurate, and reliable data than the traditional landmark or line-of-sight method. It is important to recognize that the matchmoving process has to be done correctly to yield accurate results. The simplest verification, whether or not the matchmoving process was done correctly, is to look through the virtual camera and evaluate the alignment between the 2D tracked features with the 3D (calibrated) markers or features. In a good calibration, the 3D markers should be aligned with the feature they represent in the image.

Most matchmoving software programs conveniently feature the ability to visually evaluate the error of each 3D markers position versus the 2D tracker position in each frame of the video and also report the matchmoving overall error. Finally, the matchmoving method described in this paper has been accepted and used by the authors in both state and federal court — and has passed Daubert challenges.

References

1. D. Tandy, C. Coleman, J. Colborn, T. Hoover, et al., “Benefits and Methodology for Dimensioning a Vehicle Using a 3D Scanner for Accident Reconstruction Purposes,” SAE Technical Paper 2012-01-0617, 2012.

2. R. M. Ziernicki, A. G. Leiloglou, T. Spiegelberg, and K. Twigg, “Forensic Engineering Application of the Matchmoving Process,” JotNAFE, vol. 35, no. 2, Jan. 2018.

3. R. M. Ziernicki and A. G.. Leiloglou, “Advanced Technologies Utilized in the Reconstruction of an Officer-Involved Shooting Incident,” JotNAFE, vol. 34, no. 2, Jan. 2017.

4. U.G. Survey, “Apps,” 13 July 2019. [Online]. Available: https://apps.nationalmap.gov.

Ergonomics and Forensic Engineering

By GM Samaras, PhD, DSc, PE (NAFE 966S), and EA Samaras, DNP, RN

Abstract

In disputes, forensic engineers routinely investigate available hardware and software and may examine other engineering attributes and activities. Human factors and ergonomic (HF&E) aspects may be considered, but these tend to be more limited or overlooked. This paper discusses an HF&E framework for forensic analysis, including its four major subdisciplines (micro-, meso-, macro-, and mega-ergonomics), the role each plays throughout the product life cycle, and examines their relationship to known and foreseeable use and misuse of a product or system. A taxonomy of errors, including distinguishing features of individual user errors versus system use errors, is presented and then used in a diagnostic rubric developed for forensic engineers to help identify HF&E issues as part of a forensic analysis. A health care setting case study is offered to demonstrate rubric use, but the rubric is generalizable to other domains.

Keywords

Human factors, ergonomics, forensic engineering, rubric, use error, user error

Introduction

Today, the terms "human factors" and "ergonomics" are used either interchangeably or in combination: human factors and ergonomics (HF&E). Historically, ergonomics was a term originating in Europe, whereas the term human factors originated in North America. HF&E spans the biological sciences and social sciences; ergonomics engineering is one of four industrial engineering subdisciplines.

The central objective of HF&E is to fit tools to the available humans in contrast to historical efforts to fit humans to whatever tools were available. This human-centered approach has been demonstrated repeatedly to reduce the probability of errors and increase safety[1]. Conversely, improper, defective, or nonexistent HF&E arguably increases the probability of errors and occurrence of incidents in all settings where humans engage in individual and team efforts.

In disputes, forensic engineers routinely examine available hardware, software, and other attributes and activities, such as quality engineering (e.g., design control, risk management). HF&E aspects may be considered, but this tends to be limited in scope (e.g., biomechanics only) or overlooked. The intent of this paper is to provide forensic engineers with a diagnostic rubric designed to detect the presence of HF&E flaws, defects, or concerns. The rubric consists first of classifying an identified human error proximate to the failure either as a system use error or an individual user error. Based upon that classification, the rubric leads the user through steps that facilitate analyzing the circumstances surrounding individual user(s) and associated organizations throughout the device or system life cycle in search of both enabling and root cause(s). A simple illustrative example will be offered from the health care technology setting to demonstrate the rubric's use, but the basic principles are generalizable to other domains. Other case studies are readily available[2,3], which may be used for additional insight and/or practice employing the rubric.

This paper seeks to provide HF&E-related theoretical perspectives and diagrammatic tools so that the forensic engineers from other disciplines may better consider additional potential causes of failure in the case under analysis and help determine when specialized HF&E expertise in the root cause analyses may be warranted. When searching for HF&E experts, forensic engineers should consider the Board of Certification in Professional Ergonomics (www.bcpe.org), an internationally recognized, U.S.-based, non-profit organization analogous to the National Academy of Forensic Engineers (www.nafe.org).

Theoretical Perspectives

Human-Centered System Complexity Spectrum

HF&E engineering is a subdiscipline of industrial engineering, but is also practiced by biologists, psychologists, sociologists, and others. The concept of "tools" is

GM Samaras, 7755 Soda Creek Road, Pueblo, CO 81005, (719) 485-3751, george@samaras-assoc.com

broadly construed to include just about any job aid. The HF&E system complexity spectrum[4] extends from using simple hand tools (physical ergonomics) to operating within a specific culture or subculture (e.g., nurses working with engineers within a hospital). The basic science disciplines involved range from biology to psychology to social psychology to sociology and political science. The spectrum encompasses four levels of complexity:

1) Micro-ergonomics (physical ergonomics) — involves human(s) operating with tools and considers anthropometry, biomechanical and sensory processes;

2) Meso-ergonomics (information ergonomics) — involves human(s) operating tools with automation and considers verbal and non-verbal, affective, cognitive, and physiological behaviors;

3) Macro-ergonomics (social ergonomics) — involves human(s) operating within organizations and considers communication, coordination, conventions, and expectations; and

4) Mega-ergonomics (cultural ergonomics) — involves human(s) operating within (sub-) cultures and considers language, artifacts, beliefs, customs, and morals.

Overt and Covert Phenomenon

At each of the four levels identified above, there are both overt and covert phenomena. "Overt" in this context means detectable with one or more of our five senses; "covert" means additional instrumentation is required for detection. For example, at the micro-ergonomic level, the overt attribute is the range of physical dimensions of humans of differing ages, gender, ethnicity, etc.; the covert attributes include biomechanical and sensory attributes (including sensory-motor integration) of humans of varying genders, ages, etc.

These overt and covert human attributes underpin the Needs, Wants, and Desires (NWDs)[5,6] of tool users, ranging, for example, from size of display fonts to ensure enhanced readability for most users (micro-ergonomic) to language of instruction manuals that corresponds with users own preferences (mega-ergonomic). They can also elucidate sources (root causes) of potential problems, if these and other user NWDs are not adequately addressed. **Figure 1** (adapted from Reference #5) summarizes examples

Ergonomics	Factor	Example(s)
Micro-	Overt:	Static size & fit of an individual (range of adjustment of operating table)
	Covert:	Biomechanical – weight & balance of individual surgical tools Sensory – multiple alarms interfering with high priority alarm recognition. Sensory-motor Integration – hand/eye coordination fidelity
Meso-	Overt:	Verbal/Non-verbal information management behaviors – verbalization & trackball operations while using computerized system
	Covert:	Affective – frustration with simultaneous alarms Cognitive – difficulty recognizing highest priority alarm. Physiological - ↑ Heart rate/respiration rate due to time pressure & alarm recognition issues
Macro-	Overt:	Communication – 2 nurses verifying drug & dosage setting for device. Coordination – equipment buyer not coordinating with nurse end users
	Covert:	Conventions – buyer ignores nurse users' preference; buyer uses "preferred" vendors. Expectations – buyer expects clinicians will "safely & effectively" use any device
Mega-	Overt:	Language – clinicians & engineers do not use/understand same language. Artifacts – devices familiar to clinicians unfamiliar to engineers & vice-versa
	Covert:	Shared values, such as beliefs, customs, ethics, & morals, differ between clinicians and others (engineer, legal, business, etc.)

Figure 1
Examples of factors (overt and covert) by ergonomic level.

of overt and covert factors by ergonomic level that warrant consideration by the forensic engineer.

At the physical (micro-) ergonomic level, the overt factors relate to anthropometry issues, such as the size of an individual's hand (e.g., to grasp a tool), a comfortable working height of a task surface (e.g., the adjustment range of an operating table), and easily accessible placement of operating controls (e.g., the distance required to reach a knob or switch). The covert micro-ergonomic factors include biomechanical issues (e.g., expected grip strength), sensory issues (e.g., expected visual, auditory, or tactile acuity), and the related sensory-motor integration capabilities expected of humans of differing ages, gender, ethnicity, (dis)abilities, etc.

At the information management (meso-) ergonomic level, the overt factors are both verbal and nonverbal (e.g., gesture) behaviors required to interact with automated or partially automated tools (e.g., voice-controlled devices, swiping on a screen, etc.). The degree to which those overt factors are non-intuitive, difficult to understand, or poorly designed or implemented, engenders user difficulties that engage the covert meso-ergonomic factors, such as affective (e.g., feelings and emotions) behaviors, cognitive behaviors, and psychophysiological behaviors.

At the social (macro-) ergonomic level described above, the overt factors are communication and coordination among team members or other stakeholders (e.g., end-users, manufacturers, clients, or any individual or entity with a "stake" in the device or system) working toward a putatively agreed-upon objective. The covert macro-ergonomic factors are conventions (e.g., roles and norms, especially among individuals with varying gender, age, education, organizational position, etc.) and expectations, which are often misplaced or unreasonable[5].

Finally, at the cultural (mega-) ergonomic level, the overt factors are linguistics and tangible artifacts. These include jargon and use of tools familiar to members of one subculture, but foreign to another (e.g., a stethoscope and a multimeter for nurses and engineers, respectively). Additionally, broader cultural issues may be at work, such as overall workplace "safety" culture (or lack of), perception/reality of fairness, diversity, and the like. Underlying — and intimately connected to — these overt factors are the mega-ergonomic covert factors: beliefs, customs, ethics, and morals, many of which vary by training, profession, upbringing, and other human attributes.

While these four discrete ergonomic levels may appear, at first, to be disparate and unrelated, this is incorrect. Generally, there is significant interconnectivity and interaction between discrete levels. For example, consider a simple set of operating instructions (i.e., the ubiquitous "user manual"). The correct choice of wording and sentence construction to yield acceptable domestic readability statistics (e.g., English language, >70% reading ease, and <8th grade reading level) are overt mega-ergonomic factors. Typography (e.g., font size, etc.) and graphics (e.g., size, contrast, complexity, etc.) manifest overtly, but involve covert elements of micro-ergonomic factors (i.e., required visual acuity and contrast sensitivity). The medium on which the manual is presented (i.e., hardcopy or electronic) has elements of both micro- and meso-ergonomic overt factors. The presentation and subsequent evaluation of comprehension of the user manual include both overt and covert macro-ergonomic factors. This reflects merely a partial analysis of a simple user manual when considered across the full range of human-centered system complexity.

Taxonomy of Errors

HF&E is ubiquitously relevant to forensic engineering analyses because human users are invariably involved in all human-built systems (with their concomitant flaws). Even in completely autonomous systems, we have developers and manufacturers prior to system installation, installers prior to deployment, and service personnel after deployment.

Root causes of incidents are human errors insofar as, at some point, somewhere, a human took or omitted an action that initiated the chain of events. But, unlike attempts to always blame the operator (often cited as a proximal "cause"), HF&E recognizes that human work occurs within one or more socio-technical systems. Socio-technical systems can be understood to be systems resulting from the intersection of tangible infrastructure (hardware and software) and human social systems (strengths and limitations). These socio-technical systems directly impact the probability of human error; depending upon the system design, it can increase or decrease the frequency of human errors. **Figure 2** provides a taxonomy of human error[4]; errors are jointly dependent on error type and error category.

Figure 2 illustrates the four basic types of error behavior: expected, unexpected, misguided, and malicious. But the underlying source also depends on the primary error category — is it a system use error, or is it an individual user error? System use errors are the result of the actions and decisions of the development, deployment, maintenance, or disposal organizations. Individual user

ERROR TYPE	ERROR CATEGORY: SYSTEM USE ERROR	ERROR CATEGORY: INDIVIDUAL USER ERROR
EXPECTED BEHAVIOR	ACTIVE (KNOWN BUGS)	ROUTINE USE
UNEXPECTED Behavior	LATENT (UNKNOWN BUGS)	NOVEL USE
MISGUIDED Behavior	DRIFT (BEYOND DESIGN ENVELOPE)	MISUSE
MALICIOUS Behavior	SABOTAGE	ABUSE
	LOCUS OF CONTROL: *DEVELOPMENT, DEPLOYMENT,& MAINTENANCE ORGANIZATIONS*	**LOCUS OF CONTROL:** *INDIVIDUAL HUMAN(S)*

Figure 2
Human error taxonomy.

errors are the result of actions and decisions of individual users, who may be end-users or members of the stakeholder organizations. These two primary error categories can exist at every phase of the product life cycle (e.g., pre-launch, deployment, end-user, and/or service and disposal). System use errors involve organizational issues of engineering design, development, deployment, maintenance, and disposal (referred to as 3DMD), which are ultimately traceable to the organization's personnel and management errors, including internally codified standard operating procedures (SOPs).

Unlike identifying operator errors, system use errors can be more subtle and difficult to diagnose. Products and systems are the resultant of processes; defective products and systems are the resultant of defective processes. The system use error types are active ("known bugs or operation") and latent ("unknown bugs or operation")[7], drift ("operation beyond the design envelope")[8], and sabotage. So, the forensic analysis of system use errors requires an investigation of the organizational 3DMD processes. The best starting point for this analysis is the life cycle design/deployment control and risk management processes. It is virtually guaranteed that a defective product or system may be traced back to a defective design or deployment control or a defective risk management process. That defective process then adversely impacts personnel selection and training — and the proper user focus[9]). Combined with the above, these distinctions form the basis for organizing data collected for inclusion in the proposed diagnostic HF&E rubric.

The Human Factors & Ergonomics Rubric

The proposed diagnostic rubric, entitled "Human Factors and Ergonomics Rubric," is comprised of **Figures 3, 4,** and **5**. **Figure 3** provides the "big picture." It describes the life cycle phases that the investigator selects from (all that apply) of: 1) pre-launch (or pre-market); 2) deployment; 3) end-user; and 4) service and disposal phases. This is followed by a diagrammatic prompt to "Go To B: Individual User Errors" (**Figure 4**) and then to "Go To C: System Use Errors" (**Figure 5**) for further illumination of those respective errors by phase. Finally, it guides the investigator to report on the categories and types of HF&E issues uncovered. **Figure 4** is essentially an inset of **Figure 3**, which expands upon on the primary, secondary, and tertiary individual user errors that the investigator may encounter. **Figure 5** is a companion inset expanding upon the primary, secondary, and tertiary system use errors.

To navigate the rubric:

- Start in **Figure 3** by recognizing which of the following users may be involved: e.g., pre-launch, deployment, end-user, and/or service and disposal.

- Next categorize and elucidate the error category

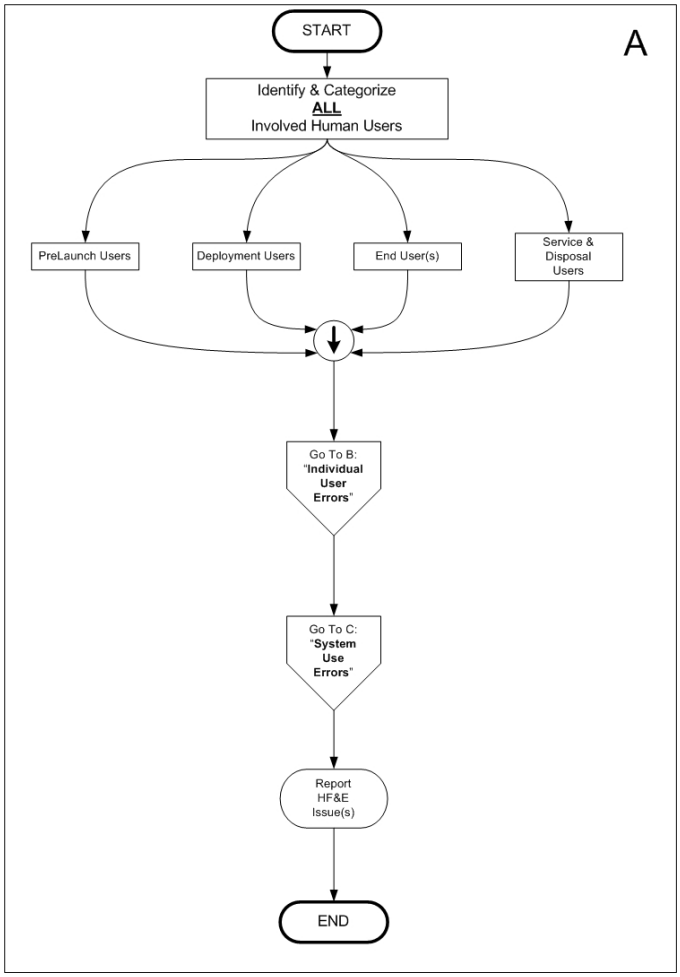

Figure 3
Human factors and ergonomic rubric.

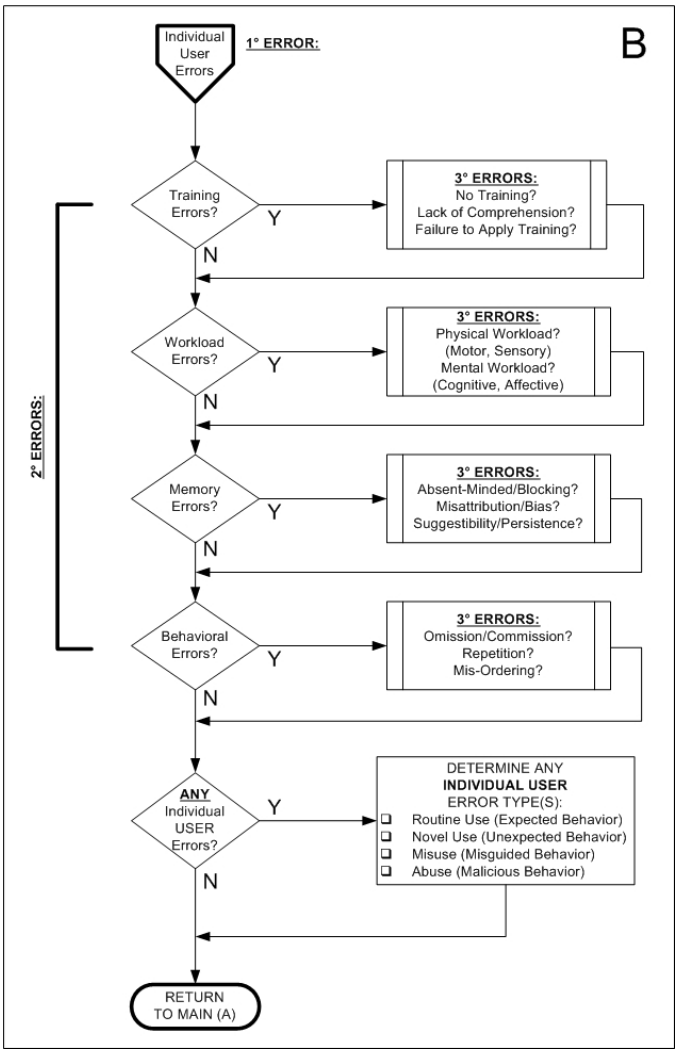

Figure 4
Human factors and ergonomic rubric.

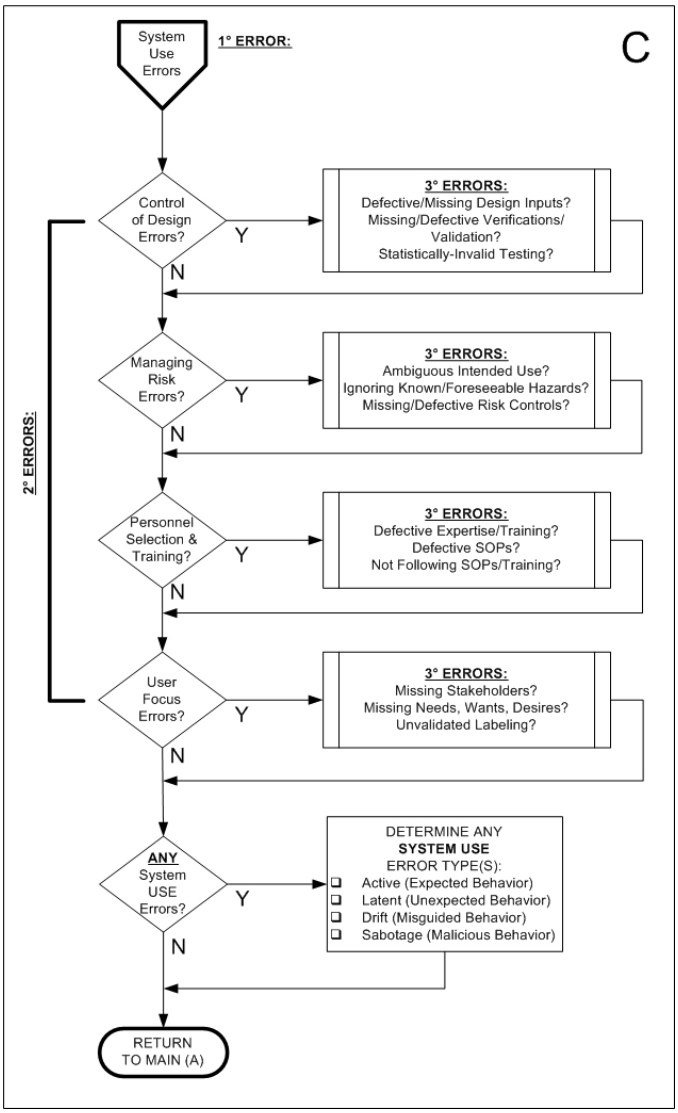

Figure 5
Human factors and ergonomic rubric.

for each user group selected above. If individual user errors are recognized as potential factors, go to **Figure 4**. Then choose which secondary individual user errors of training/expertise, workload (both physical and mental), memory, and the objective behaviors of the individual(s) may be involved in the incident (e.g., the operator) and identify their associated tertiary errors. If system use errors are likely factors, as well, proceed to **Figure 5** and identify which of the secondary errors in control of design, managing risk, personnel selection and training, and user focus may be factors; subsequently, identify which of their associated tertiary errors may be contributory.

- Next determine the respective associated error type. In the case of a system use error, the error type will be identified as either active or latent[7], drift[8], or sabotage; in the case of an individual user error, the error type will be identified as routine use, novel use, misuse, or abuse (as described earlier in **Figure 2**).

- Finally, return to **Figure 3,** and report all the HF&E issue(s) uncovered by the rubric in the forensic analysis.

A practical example will illustrate this is neither complex nor onerous, until you get down deep into the HF&E details, at which point you should consult an expert in one of the specific subdisciplines of HF&E, if needed.

Practical Application: Case Study

Consider the following scenario. A gastroenterologist

(a physician specializing in digestive tract illness) is about to do a procedure on a patient in the hospital. The patient is anaesthetized and prepared for the procedure. The physician arrives in the operating room where the patient and an endoscope system await him.

Because his iPhone battery is nearly depleted, the physician plugs the iPhone into the USB port on the endoscope equipment rack front panel, so that the battery will charge while he is treating his patient. Unfortunately, the endoscope refuses to operate, even though it was working properly for the previous procedure just 30 minutes ago. Fortunately, neither the patient nor the iPhone were injured. This is colloquially known as a near miss, although it is more correctly termed a near hit; missing is not always the case and such events, in slightly different circumstances, may result in serious injuries or even deaths.

A forensic engineer is asked to conduct an analysis by hospital management and to report on the problem and possible solutions. The investigator uses the steps and information diagrammed on the "Human Factors and Ergonomic Rubric" as demonstrated in **Figures 3, 4**, and **5,** to organize the inquiry and categorize and report on the findings. Following the first task diagrammed in the rubric in **Figure 3**, the investigator identifies all involved human users and subsequently categorizes them as: Prelaunch Users (e.g., manufacturer personnel); Deployment Users (hospital personnel); and End-User (gastroenterologist). The Service & Disposal Users were not considered to be factors in this case study investigation and are not discussed.

In this case, the forensic engineering investigator initially visits the deploying organization (the site of the reported incident), and conducts interviews with the physician, surgical staff, risk managers, and others. The investigator also requests production of various documents from the endoscope manufacturer and the hospital. Following the diagnostic rubric, the forensic investigator uncovered multiple HF&E failures and documented errors made by the various categories of identified human users. The following narratives (with corresponding summary tables) illustrate many, but not all, of the reported findings:

A. End-User(s) (Gastroenterologist)

The gastroenterologist committed several individual user errors. These were recognized as secondary errors of training, workload, memory, and behavior. The physician denied receiving any training regarding the fact that the USB port was solely for use by service personnel and would automatically force the equipment into a system diagnostic mode. This error type was unexpected and constituted a novel use of the endoscope system.

The investigator determined the physician had made a behavioral error because the USB port was positioned in the surgical room at chest height, easily seen and readily accessible; using a USB port for iPhone charging is a normal and customary activity, so it was deemed a routine type error for iPhone users.

Workload errors were also considered factors as the user was a highly trained, busy physician under constant time pressure focused on the specifics of the patient; this was noted by the investigator as increased mental workload. The physician user plugged the iPhone into the port without taking the time to consider whether that action was appropriate, which constituted misuse. Workload issues may have further contributed to memory errors, which manifested in the tertiary error of absent-mindedness, when plugging his personal iPhone into a readily accessible USB port. This was consistent with secondary behavioral and tertiary repetitive errors identified in the rubric and frequently emitted in other settings.

The physician's action (plugging his iPhone into the endoscopy system) was deemed the proximate cause of the equipment failure; it was not the root cause. In summary, the investigation uncovered primary, secondary, and tertiary error categories and types found among End-User(s) as follows in **Figure 6**:

1° ERROR CATEGORY	2° Error Category	3° Error Category	ERROR TYPE
Individual User(S)Errors	***Training***	No Training	Novel Use (Unexpected)
	Workload	Mental Workload	Misuse (Misguided)
	Memory	Absent-Minded	Misuse (Misguided)
	Behavior	Repetition	Routine Use (Expected)

Figure 6
Summary of end-user(s) category errors and types.

B. Deployment User(s) (Hospital Personnel)

Hospital staff were found to be involved in system use errors, which were exacerbated by individual user errors (that have some systems features). A deployment user error occurred as one of the surgical technicians was aware of the problem with use of the prominent USB port (having made the error previously, but not having reported it). This was deemed a behavioral error of omission and a failure to apply training; it was a misuse error type.

That same technician was working during the case procedure but had a family emergency the previous night and was sleep deprived. This resulted in secondary user

errors, such as elevated workload (both mental and physical) and memory errors (failure to remember problem with port) as well as not noticing the physician plugging into the USB port, as the technician was properly focused on attending to their specific duties. This was deemed a novel use error type, in that staff were not expected to operate under those conditions.

There were also system use errors, uncovered by employing the rubric, specifically those associated with managing risk. The hospital risk manager had not identified the prominent, front-facing USB port as a potential hazard and, therefore, had not engaged in effectively managing risk errors by ignoring known/foreseeable hazards. This resulted in missing/defective risk controls, such as a failure to block the port or train clinicians (including surgical staff) on the risk of unauthorized use. These were considered latent error types. The biomedical equipment personnel were equally unaware of the potential hazard, even though they were aware of the purpose of the device's diagnostic port. The system use error is associated with an unexpected, latent error type insofar as it involved an equipment defect (identified as a control of design secondary error) that the hospital organization was generally unaware, even though it was known by the manufacturer, but not recognized as a "defect."

The errors identified above further indicated defects in proper user identification, defects in communication and coordination within the hospital organization, and a need to alter conventions and expectations among different subgroups (biomedical equipment technicians, surgical staff, hospital management, and potentially attending physicians). This evidenced secondary system use errors involving user focus errors insofar as there were missing stakeholders and invalidated (or missing) labeling. These were also deemed latent error types from the hospital's perspective, even though they were (or should have been) known from the manufacturer's perspective.

The hospital organization's socio-technical system design and management was reported as an intermediate and enabling cause, not the proximate cause or the root cause. In summary, the investigation uncovered primary, secondary, and tertiary error categories and types found among Deployment User(s) as follows in **Figure 7**:

1° ERROR CATEGORY	2° Error Category	3° Error Category	ERROR TYPE
Individual User(S) Errors	***Training***	Failure to Apply Training	Misuse
	Workload	Mental & Physical Workload	Novel Use
	Memory	Absent-Minded	Novel Use
	Behavior	Omission	Misuse
System Use Errors	***Managing Risk***	Ignoring Known/Foreseeable Hazards Missing/Defective Risk Controls	Latent
	User Focus Errors	Missing Stakeholders Unvalidated Labeling	Latent

Figure 7
Summary of deployment user(s) category errors and types.

C. Pre-Launch User(s) (Manufacturer Personnel)

Pre-Launch users (manufacturer personnel) were involved in both individual use errors and system use errors; only the system user errors are identified here.

The investigator reviewed the documented risk analysis and discovered the front panel USB port was identified as a "hazard," but only from the perspective of the service personnel not being able to work with the equipment if the port malfunctioned. This was deemed an active error type insofar as the equipment defect was a known "feature," but not recognized as a use hazard; this is in contrast to it being deemed a latent error for the hospital. There were also secondary errors associated with user focus. The investigator discovered that there was virtually no user focus — all foreseeable users were not identified, no effort was made to determine their NWDs, and use hazards were not (and could not be) systematically identified; this was deemed a latent error type.

The risk analysis falsely reduced the estimated risk priority by including detectability[10]. Once the equipment leaves the plant, the manufacturer has no control over whether users will: (a) detect a specific risk; (b) attend to that risk, if they detect it; (c) remember what action to take for that specific risk, if they attend to it; and (d) have the time or other resources necessary to implement an effective risk mitigation strategy. As a result, managing risk secondary errors also occurred as the use hazard was not understood, the resultant risk control(s), such as blocking or labeling, could not be incorporated in the equipment product design requirements, and no verification or validation[11] could be executed to address the hazard to users.

Examination of post market complaint documentation indicated that the problem had occurred prior to this incident. However, given the failure to identify it as a use hazard in the risk management process, it was not recognized as a problem requiring corrective or preventive action. These missing/defective risk controls constitute latent error types, as the users were unaware of the defects in their internal processes.

Secondary system use errors in personnel selection and training were also found. Examination of the manufacturer's standard operating procedures (SOPs) indicated they were generic and not specifically tailored to the unique

products being manufactured (defective SOPs). Therefore, these were not adequate to inform the employees of their specific duties and responsibilities. No documented evidence was found of personnel training that mitigated these shortcomings and that was supported by the engineering flaws identified in risk management and control of product design (defective training). These were deemed drift error types, as the SOPs and expertise/training were outside the design envelope required for the organization's product development efforts.

The management of the manufacturer's organization was identified as the root cause of the incident. In summary, the investigation uncovered primary, secondary, and tertiary error categories and types found among Pre-Launch User(s) as follows in **Figure 8**:

1° ERROR CATEGORY	2° Error Category	3° Error Category	ERROR TYPE
System Use Errors	***Managing Risk***	Ignoring Known/Foreseeable Hazards Missing/Defective Risk Controls	Active Latent
	User Focus Errors	Missing Stakeholders Missing, Needs Wants, Desires	Latent Latent
	Personnel Selection & Training	Defective SOPs Defective Expertise/Training	Drift Drift

Figure 8
Summary of pre-launch user(s) category errors and types.

Conclusion

Forensic engineering in disputes routinely examines available hardware engineering, software engineering, and quality engineering (e.g., design controls and pre- and post-market risk management) attributes and activities. HF&E expertise should no longer be relegated to an afterthought or footnote, but rather must become an integral element in forensic investigations. Use of the Human Factors and Ergonomics Rubric, within the context of some of the underlying HF&E theoretical perspective presented here, offers forensic engineers, regardless of discipline, a structured, systematic approach to analyzing and exposing a wider breath of HF&E failures and human errors related to an ongoing incident investigation.

Even though reasonable investigators may make different judgements and thus arrive at different conclusions, the use of this diagnostic rubric promotes identification of both individual and organizational errors that provide a more balanced explanation of the underlying causation. Approaching forensic investigations using these tools also arguably fosters better mitigation efforts aimed at problems found at all levels. While beyond the scope of this paper, "closing the loop" by reporting identified problems to relevant regulatory agencies may be indicated. Rigorously validating interventions aimed at resolving problems identified during these HF&E-oriented forensic investigations will likely do much to forward the goal of prevention of future adverse events.

Acknowledgements

The authors would like to acknowledge the three reviewers for their constructive comments.

References

1. G. Salvendy, Handbook of Human Factors and Ergonomics, 4th Edition, Hoboken, NJ: John Wiley & Sons, inc., 2012.

2. S. M. Casey, Set Phasers on Stun: and Other True Tales of Design, Technology and Human Error, 2nd edition, Santa Barbara: Aegean, 1998.

3. S. M. Casey, The Atomic Chef: and Other True Tales of Design, Technology and Human Error, Santa Barbara: Aegean, 2006.

4. G. M. Samaras, "Reducing latent errors, drift errors, and stakeholder dissonance," WORK: A Journal of Assessment, Prevention, and Rehabilitation, 41(s1):1948-1955, 2012., vol. 41, no. s1, pp. 1948-1955, 2012.

5. E. A. Samaras and G. M. Samaras, "Using Human-Centered Systems Engineering to Reduce Nurse Stakeholder Dissonance," Biomed Instrum & Technol, vol. 44, no. (s1), pp. 25-32, 2010.

6. G. M. Samaras, "Human-Centered Systems Engineering: Managing Dissonance in Healthcare Delivery," in Management Engineering for Effective Healthcare Delivery: Principles and Practices, Kolker, A. & Story, (Eds), Philadelphia, IGI Global, 2011, pp. 148-171.

7. J. Reason, Human Error, Cambridge: Cambridge University Press, 1990.

8. S. W. Dekker, Ten Questions about Human Error: A New View of Human Factors and System Safety, New Jersey: Lawrence Erlbaum Associates, 2005.

9. G. M. Samaras, "Medical Device Life Cycle Risk Management," ASQ Biomedical Division Biofeedback Newsletter, Volume 43 (2), August 2015.

10. G. M. Samaras, "Misuse, and Abuse of the Device Failure Modes Effects Analysis," MD+DI Online, 2013.

11. G. M. Samaras, "An Approach to Human Factors Validation," Journal of Validation Technology, vol. 12, no. 3, pp. 190-201, 2006.

Forensic Identification and Root Causes of Hot Socket Problems Found in Electrical Meters

By David J. Icove, PhD, PE, DFE (NAFE 899F) and Thomas A. Lawton, BSME

Abstract

Electric meters play a critical role in electric utility distribution systems, especially for residential customers. Because it occurs so infrequently, forensic engineers may not recognize a dangerous condition within these meters known as a "hot socket." This condition exists where the meter blades make insufficient electrical contact with the socket jaws. This paper reviews methods for forensically examining, diagnosing, and explaining the hot socket phenomenon while exploring smart meters' incident trends.

Keywords

Electrical utility distribution systems, hot sockets, smart meters, forensic engineering

Introduction

Electric meters play a critical role in electric utility distribution systems, especially for residential customers. Because it occurs so infrequently, forensic engineers may not be fully aware of a condition within these meters known as a "hot socket." This condition occurs where the meter blades make inadequate electrical contact with the meter's socket jaws[1]. This inadequate contact can be caused by many things, but the leading culprits are corrosion, vibration, metal fatigue, and mechanical assault. These poor connections can lead to high-resistance heating, fires, and risk of injury to individuals accessing these meters.

In this paper, the authors will review forensic engineering[2] methods for examining, diagnosing, and explaining the hot socket phenomenon while exploring incident trends involving smart meters. They will also provide recommended engineering guidelines to reduce the risk of spoliation while investigating meter box fires.

The professional standards on which the authors base this analysis include, but are not limited to, the National Fire Protection Association (NFPA) *Guide for Fire and Explosion Investigations* (NFPA 921)[3], the *Standard for Professional Qualifications for Fire Investigator* (NFPA 1033)[4], various related ASTM International forensic standards, and expert treatises in the field of fire and explosion investigations. The ASTM International publications form the foundation for the standards of care for the investigative and engineering fields, particularly those overseen by the ASTM Committees on Fire Testing (E05), Forensic Sciences (E30), and Forensic Engineering (E58).

Both NFPA 921 and NFPA 1033, which are approved American National Standards Institute (ANSI) standards, mandate that the science of fire investigation involves determining both the fire's origin and cause[5]. Making these determinations requires a "systematic approach" with the scientific method[6]. The basic concepts of the scientific method are: observe, hypothesize, test, and conclude using reliable and reproducible scientific principles and methodologies.

Residential Metered Electrical Power

Most homes in the United States have a 120/240V, single-phase, three-wire system for the meter center. Two of these wires, called "main service entrance conductors," are ungrounded and energized ("hot"); the third wire is the "neutral." If a voltmeter reading is taken between the two hot conductors (line to line), it will measure 240VAC. If a reading is taken between a hot conductor and the neutral (line to neutral), it will measure 120VAC.

Utility companies usually do not allow unmetered power, so virtually every residence has what is called a "service entrance." This entrance (for electrical power) contains a separate meter for measuring power consumption.

The device used to measure the power consumption is

David Icove, PhD, PE, DFE, PO Box 1348, Knoxville, TN 37901-1348, (865) 693-4361, icove@utk.edu

called a "watt-hour meter."

The watt-hour meter is typically supplied by the utility company; the property owner supplies the meter socket cabinet. The meter socket is the receptacle and structural support for the meter. Historically, utility companies provided both the meter and the meter "box" for the first 80 years or so of the power grid (~1890 to 1970). As they're known today, socket meters were first introduced in the late 1920s, but did not become popular until the post-WWII building boom, which began in the late 1940s. From 1970 to 1990, most utilities and state utility commissions transitioned ownership of the meter socket to the homeowner, including those already in place.

A homeowner today that is upgrading an electrical service or building a new residence has a contractor purchase and install the meter box; the utility company inspects the socket installation and installs an electric meter. The meter socket must be approved by Underwriters Laboratories (UL) and the local utility[7].

Within the socket are four clamps, commonly referred to as "jaws." On the back of the typical meter face are four matching prongs known as "blades." The jaws, which are similar to leaf springs, must have sufficient force between the blades and the surface of the jaws to maintain proper contact and minimize electrical resistance. The greater the gripping force of the jaws that come into contact with the meter blades, the lower the contact resistance.

When the meter is correctly plugged into its designated socket, the blades on the rear of the meter are inserted directly into the gripping jaws of the socket (**Figure 1**). The unit is locked in place by a retaining ring or by the meter socket cover, neither of which can be secured unless the blades are inserted into the jaws completely[8].

Loss Histories of Electrical Meter Center Fires

National fire statistics[9] show that electrically caused fires within residential meter centers are rare. For example, NFPA statistics on residential electrical fires in data from the National Fire Incident Reporting System (NFIRS) and the NFPA's annual fire department experience survey show that approximately 45,210 electrical fires occurred in home structures between 2010 and 2014 per year. Approximately 39,650 of these fires involved an electrical equipment malfunction as the leading factor contributing to the ignition (**Figure 2**). Of those 39,650 fires associated with electrical equipment malfunctions, the NFPA statistics show that, on average, 760 fires are involved with meters or meter boxes (1.9%). Consequently, even forensic experts who analyze electrical fires regularly may investigate very few fires originating in residential meter centers.

The Issue with "Hot Sockets"

The electrical components of the residential meter center should outlast the structures they serve under normal conditions. But there are conditions that can lead to their deformation, which, if left unchecked, can cause fires.

Overheating of electrical connections such as those in meter service panels are complex and can involve a

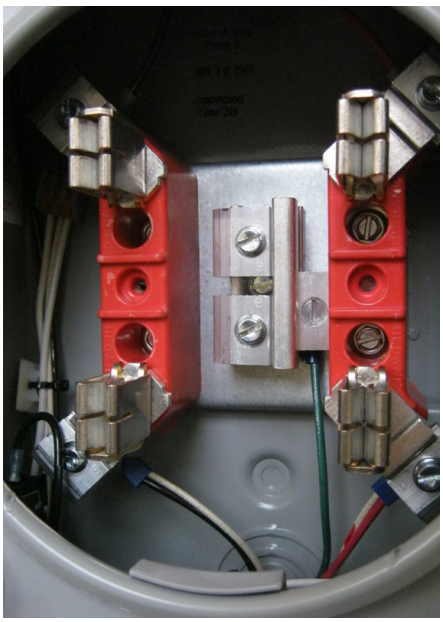

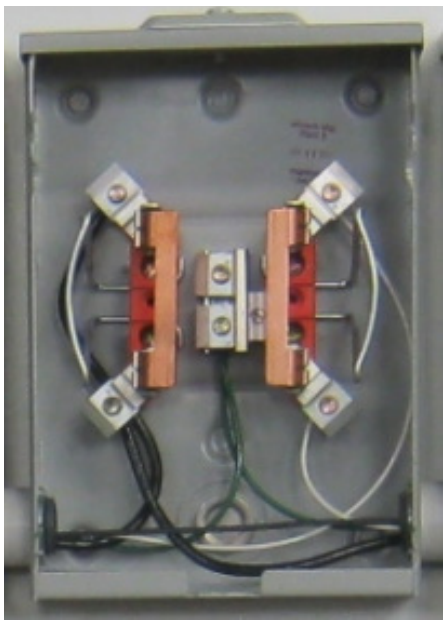

Figure 1
Typical meter socket base, meter socket, and jaws (left to right). Source: TESCO – The Eastern Specialty Company, Bristol, Pa; reprinted with permission.

Equipment Involved	Fires	%
Electrical distribution, lighting, and power transfer	22,510	57
Unclassified electrical wiring	7,880	20
Electrical receptacle or outlet	3,090	8
Electrical branch circuit	2,230	6
Panelboard, switchboard, or circuit breaker panel	1,180	3
Extension cord	1,180	3
Electrical service supply wires from utility	820	2
Electrical meter or meter box	*760*	*2*
Wiring from meter box to circuit breaker panel	590	1
Unclassified lamp or lighting	560	1
Electrical power service cables (utility)	560	1
Incandescence lighting fixture	530	1
Surge protector	460	1
Unclassified electrical cord or plug	390	1
Tabletop, floor or desk lamp	290	1
Detachable electrical power cord or plug	270	1
Permanently attached electrical power cord or plug	260	1
Wall switch	250	1
Fluorescent lighting fixture or ballast	220	1
Battery charger or rectifier	210	1
Other known electrical distribution or lighting equipment	780	2

Figure 2
Breakdown of 39,670 U.S. residential fires involving electrical equipment failures or malfunctions as a leading factor contributing to the ignition (2010 to 2014 averages); Source: Campbell, R. 2017. Electrical Fires. Research, Data and Analytics Division. Quincy, Mass., National Fire Protection Association.

number of variables. Some of the reported conditions contributing to hot sockets include, but are not limited to, the:

- Introduction of moisture into the electric meter enclosure.
- Localized resistive heating in electrical connections.
- Corrosion of the electrical meter socket jaws.
- Improper insertion of electrical meters into the meter sockets.
- Vibration.
- Deep electrical cycling.
- Unbalanced electrical loads.
- Tampering of or electrical power theft[10].
- Failure of the initial installer of the meter base enclosure to apply sufficient torque to the screws holding down the electrical cables to the meter mount (NFPA 70, 2017, Section 110.14(D) requires proper torque at cable terminations).

The failure of the electrical meter center components through localized heating of the jaws of the meter socket is well-documented in forensic engineering literature[11]. The engineering sciences behind localized heating of the electrical meter center connections can be complex in nature[12]. Many inter- and intra-related problems include copper oxide formation, increased contact resistance connection, creep and relaxation, vibration, electric arc erosion, and arcing through char.

- Typical conditions that result from localized heating associated with hot socket cases include, but are not limited to, pitted and discolored meter blades.
- Melted plastic around one or more of the meter stabs (typically the plastic around one stab is where the deformation starts).
- Pitted and discolored socket jaws.
- Loss of spring tension in the socket jaws[13].

Figures 3, 4, and **5** show typical jaw and blade damages that can lead to hot socket conditions and blade abnormalities.

Removing and reinserting the electric meter into the jaws, particularly those with overheated connections, can also lessen the spring tension. The reasons for the removal of an electric meter from its sockets can vary, such as: termination of electric service to a customer, routine service, or calibration of meters due to tampering of electric service of theft[14]. Each provides an opportunity for the damage needed to create a hot socket.

Studies by The Eastern Specialty Company (TESCO) have shown that the normal insertion force for an electric meter to its jaws can be as high as 50 lb. If an electric meter is removed and re-inserted into its socket eight times, the insertion force can drop to approximately 15 lb[15]. Several additional removals and insertions of the electric meter can drop the force to approximately 5 lb[16] or less. If the compromised electric meter connection is subject to localized heating at 700°F (370°C) for 5 minutes, this results in the potential for a hot socket condition.

The hot socket condition can also extend to the cables

connecting the electric meter to the jaws of the socket through the jaw screws or when the electric meter blades do not make a good electrical contact with the jaws. This condition occurs due to the jaw blades spreading, corrosion, insulating effect within the meter socket, or the failure to tighten the bolted terminal connections of the jaws properly.

Under-torqueing the main electrical service entrance cables and the load cable connections to the meter centers is also an underlying issue associated when terminals attached to the jaws are not tightened sufficiently to ensure a sound connection. This also applies to the torque standard for the terminals connected to both the supply and load cables affixed to the meter socket. Although there is no set standard, the typical maximum temperature rating of a connector is 158°F (70°C)[17].

This torquing problem was recently addressed in the 2017 Edition of the *National Electrical Code* (NFPA 70, 2017)[18]. If conductors are not properly torqued (tightened), a high-resistance connection can occur. These connections can lead to arcing, which, in turn, increases the heating effect. This increased heating can lead to a short circuit or ground fault, fire, or arc flash.

Forensic engineers are responsible for being aware of potential product liability issues and to report them to their clients, interested parties, and, when appropriate, to the U.S. Consumer Product Safety Commission (CPSC). Electric meter centers exist that have inherent manufacturing weaknesses. One example occurred in 2009: the CPSC in cooperation with the Milbank Manufacturing Company

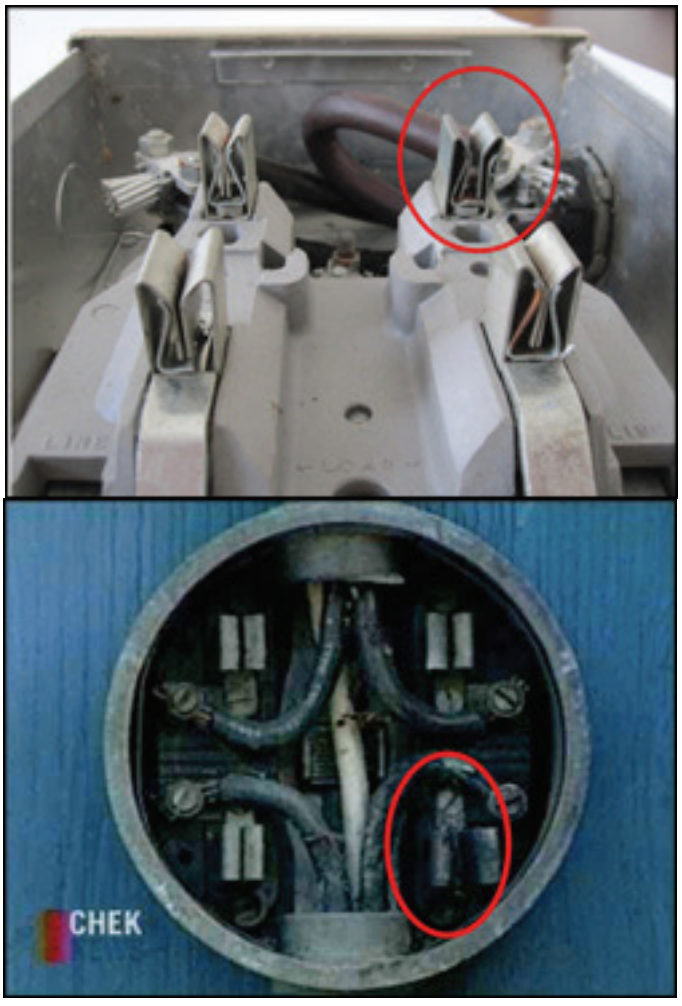

Figure 3
Typical trademark damage features for hot socket conditions showing pitted and discolored jaw sockets. Source: Lawton & Schamber (2017).

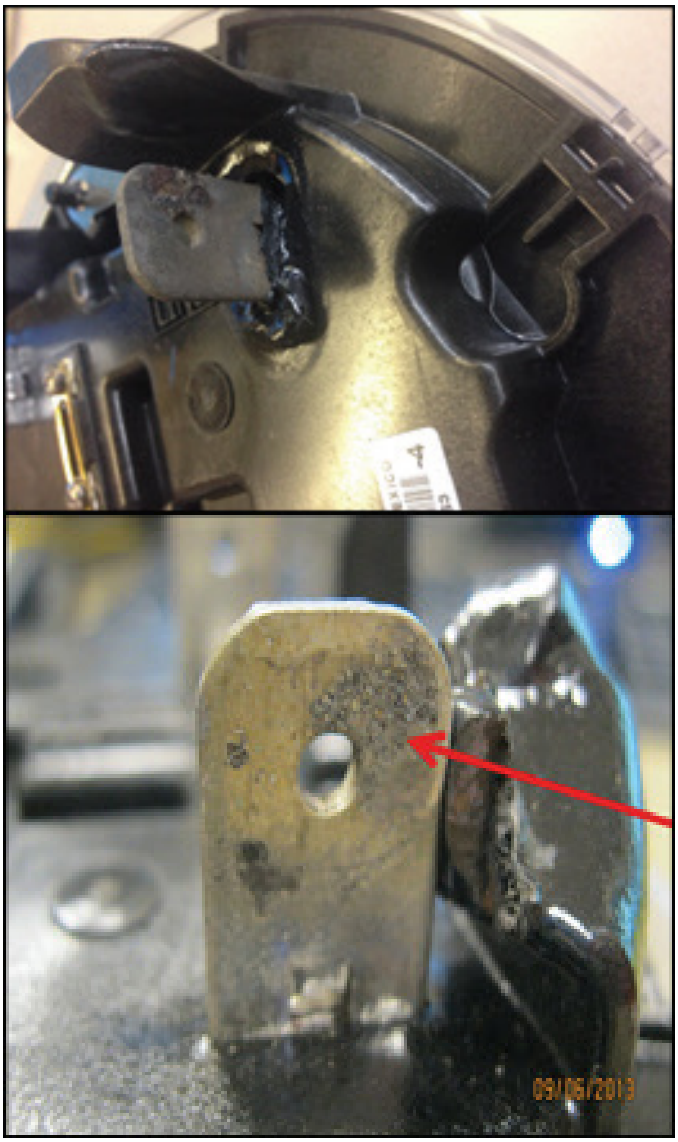

Figure 4
Typical trademark damage features for hot socket conditions showing signs of incipient jaw-to-blade arcing. Source: Lawton & Schamber (2017).

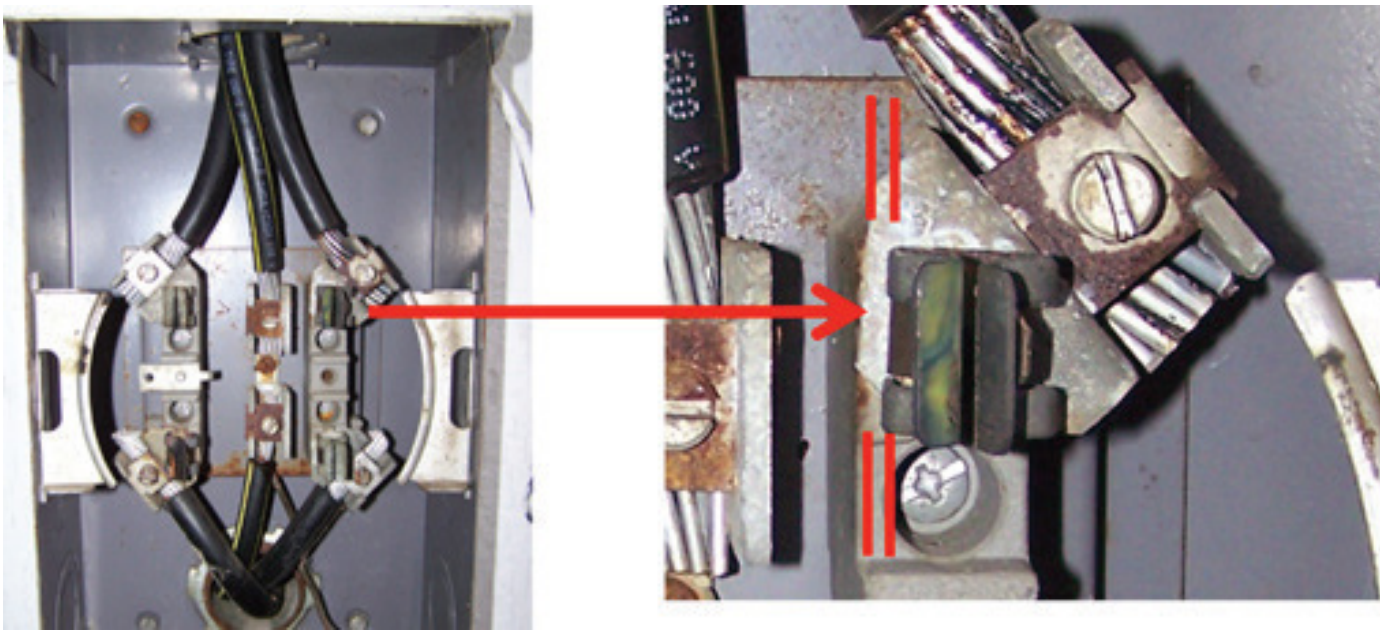

Figure 5
Example of a deformed jaw that results in evidence of localized heating and discoloration due to a poor electrical connection. Source: Lawton & Schamber (2017).

of Kansas City, Missouri[19]. The recall stated that certain electric meter sockets in a single meter center may short while energized due to an incorrect bridge, which was attached to the meter jaws. If a manufacturing defect exists, all metal parts of the electric meter could create an electric shock hazard. Burns could occur to personnel if the cover is off, and the meter socket is energized. Fortunately, of the three incidents reported to the CPSC of the unit shorting, none caused an injury.

Forensic Engineering Analysis of Hot Socket Cases

A forensic engineer should address a wide range of areas as part of regular field service, inspections, and failure investigations of electrical meter centers. Following are recommended areas of inspecting electric meter centers and associated equipment, and, if possible, the subject electric meter:

- Gaps in the electric meter socket jaws.
- Unique or inconsistent discoloration in any of the jaw blades.
- Signs of melted or deformed plastic on the meter base.
- Pitting of either the meter blades or socket jaws.
- Loss of tension in the meter socket jaws.
- Condition of the cable insulation and connections to meter jaws.
- Overall condition of the box, socket, electric meter, how they attach to each other and to the building.
- Signs of tampering.
- Signs of corrosion.
- Signs of water or debris inside of the electric meter can or box.

Once a potential hot socket or related condition is discovered by the forensic engineer during an investigation, a higher level of professional responsibility is triggered. This responsibility includes notice to the responsible agencies of the potentially unsafe conditions, the client, and other interested parties[20]. This is not necessarily true. The forensic investigation may discover a not properly torqued cable connection.

When there are signs of damaged jaws or electric meter blades, the engineer should not conduct any field repairs. Forensic investigations do not involve repairs. This repair is the responsibility of the property owner. These conditions, along with other indicators, should be documented per guidelines outlined in the appropriate NFPA

and ASTM standards. In cases where the entire electric meter center should be secured as evidence, the forensic engineer has a responsibility to immediately notify the client, property owner and occupant, and other interested parties. Again, this paper deals with forensic investigations, not repairs. To do a forensic investigation implies that the forensic engineer was called to investigate the electric meter. The electric meter was removed in order to do the investigation, or meter tampering was suspected.

The forensic engineer should be careful around energized electric meter centers. This applies to working with all energized electrical equipment. For example, measurement of voltages with non-commercial metering equipment may cause hazardous or life-threatening arc flash conditions. These events are of grave concern when handling energized electrical equipment and circuits. Individuals exposed to arc flash conditions can be seriously injured or killed, particularly if they are not wearing appropriate personal protective equipment.

Emerging Areas of Hot Sockets Involving Smart Meters

Since the late 1980s, the standard baseline electromechanical meters and electronic meters have been steadily replaced with a new generation of electronic solid-state meters known as "smart meters," defined as meters with two-way communication capability. Deployment of them began in North America in 2007. Loss histories suggest that the new smart meters should be designed with hot socket detection components in mind.

Over the past two or three years, smart meter manufacturers have started designing meters to withstand hot sockets. Improvements include placing temperature sensors closer to the meter blades (instead of only on the metrology boards), specifying heat-resistant components within the meter itself, increasing the mass of plastic at the meter base to better insulate the inside of the meter. Historically, meter bases used glass and phenolic and then moved to thermoplastics. One smart meter maker is now using high-temperature base plate plastic.

One innovative design for early detection of hot socket conditions is the use of a specialized field detector embedded within the meter that makes use of the smart meter's two-way communication capacity "to send an alarm back to the utility." Since arcing emits broadband energy in the form of radio waves sometimes referred to as "pink noise," the intensity of this falls off with increasing frequency. Sensors couple through the air with the nearfield electric and magnetic fields, which induce a detectable signal. Advantages of this approach include no direct connection, and the communication method is resistant to interference from other radio frequency emitting devices such as cell phones and power lines.

Analytical Tools

NFPA 921 outlines a range of tools and analytical approaches for the investigator's use in analyzing the cause of the failure of a component or system involved in a fire or explosion. These tools can assist in organizing information and help an investigator comply with the scientific method. Such tools suggested by NPPA 921's Chapter 22 on "Failure Analysis and Analytical Tools" include, but are not limited to, timelines (pt. 22.2), systems analysis (pt. 22.3), mathematical modeling (pt. 22.4), fire testing (pt. 22.5), and specialized data collection (22.6).

These approaches include the use of timelines (pt. 22.2.1), which NFPA 921 considers "a graphic or narrative representation of events related to the fire incident, arranged in chronological order." A timeline can show event relationships, gaps, or inconsistencies of data — and is a logical approach to complex cases. Shown previously in Table 1 is the representational timeline for this case as suggested by NFPA 921.

• Identified by NFPA 921, Failure Mode and Effects Analysis (FMEA) is an appropriate technique for identifying the basic sources and consequences of failure within electric meter centers. Factors used when applying FMEA can include the component, failure mode and frequency, direct effect, potential hazard, and corrective actions. The results of the FMEA assists in identifying the item (or action) being analyzed.

• Basic fault (failure) or error that created the hazard.

• The consequence of the failure.

An action is said to have "foreseeable consequences" if it can be reasonably assumed that it will cause a certain direct effect or harm based upon a reasonable person's actions. The benefit of these analytical tools as recommended by NFPA 921 is that they can assist in organizing information and help the forensic engineer comply with the scientific method.

Responsibilities of the Forensic Engineering Expert

The expert treatise, Kirk's Fire Investigation, makes

clear that the fire scene is often the most important piece of evidence in forensic analysis and reconstruction, particularly when the fire could result in criminal or civil litigation. Therefore, a major concern of fire investigators is the preservation of evidence before it is submitted for examination and analysis. Failure to prevent spoliation can result in the damaging disallowance of testimony, sanctions, or other civil or criminal remedies[21].

Both NFPA 921 (pt. 12.3.5.1) and ASTM E860 caution that spoliation may occur during fire scene processing, particularly when the movement or the alteration of debris impairs the ability of other interested parties to obtain the same evidentiary value from the evidence as did any prior investigator. The act of spoliation is also a violation of professional standards of conduct for the forensic fire investigation and engineering fields. These standards include NFPA 921, NFPA 1033, and various related ASTM International forensic standards.

Forensic engineers, fire investigators, insurance claims personnel, and attorneys must be well informed on their responsibilities to alert interested parties, collect, and preserve evidence, and share the appropriate information. They are routinely taught at continuing education seminars and in textbooks to correct methods for avoiding spoliation[22]. They are instructed that breaches of professional conduct in the documentation, collection, analysis, and preservation of evidence may undermine their legal case, whether it be civil or criminal (NFPA 921, pt. 11.3.5.3). Remedies for spoliation may include monetary sanctions, application of evidentiary inferences, exclusion of evidence and expert testimony, dismissal of the claim or defense, tort actions for the intentional or negligent destruction of evidence, and potential prosecution under criminal statutes relating the obstruction of justice (NFPA 921, pt. 12.3.5.3).

The cited reference[23] by Dean entitled "Legal Issues Involved in Failure Analysis" sets forth clear guidance to investigators, particularly engineers.

There can be missed opportunities during the preliminary and follow-up investigations of meter center fires. It is important that forensic engineers be cognizant that evidence in hot socket fires are often fleeting, and the engineer may not get a second chance to later document, preserve, and collect critical evidence.

When confronted with potential hot socket cases, the forensic engineer should:

- Per NFPA 921 (NFPA 921, pt. 12.3.5) and ASTM E860 (ASTM E860, pt. 5.2, et seq.), recognize, secure, preserve essential evidence, and notify interested parties.
- Perform non-destructive and destructive testing of the meter, meter center, jaws, and associated equipment to document the hot socket condition as well as any signs of tampering or vandalism.
- With destructive testing of the jaws, determine whether there is still sufficient jaw tension to preclude a hot socket from being the cause. Here, it is important to recognize that the fire itself could have dramatically reduced the jaw tension.
- Look for signs of pitting on the jaw and the blade, which is usually a result of prolonged meter arcing (a series of intermittent events that occurred in ever increasing durations over a prolonged period).
- Conduct scanning electron microscopy and, where possible, x-ray computed tomography, and focused ion beam of the electrical equipment.
- Determine the difference between arcing and melting of components.
- Inspect neighboring meters and meter centers to determine if there existed similar conditions.
- Notify other interested parties of their existence and, if necessary, file the appropriate disclosures to the U.S. Consumer Product Safety Commission if potential product defects were found.

Summary and Conclusions

Hot sockets start with a loss of tension in at least one of the meter socket jaws. This loss of tension can be from a variety of sources. These may start as early as improper installation or even "tight sockets." Loss of tension is one factor necessary to create the initial micro-arcing conditions. Sockets with repeated electric meter exchanges observed to have higher incidence of hot socket issues, and "booting" a meter may loosen a meter's jaws even more. Hot socket repair kits are not available that contain all the tools and parts for servicing meters[24].

Vibration appears to be the most common catalyst for the micro-arcing that creates the initial heat in a "hot

socket." The meter must be energized, but current is not a significant factor in how quickly or dramatically a hot socket occurs. The effects of vibration and weakened jaws can reinforce each other.

Electric meter manufacturers have been working on the design of their meters to better withstand a hot socket. These new electric meters have better baseline performance than even the older electromechanical meters, though the heat from a hot socket will eventually consume even the most robust meter.

When replacing an electric meter, the installer should conduct tension inspection tests for all the jaws. A non-invasive check that the minimum safe holding force or greater is present in all socket jaws should be performed[25]. Advanced forensic engineering testing equipment is also available to evaluate the health of the meter socket.

References

1. Bao, Z., & Li, Z. 2016, July. Identifying Hot Socket Problem in Smart Meters. In Power and Energy Society General Meeting (PESGM), 2016 (pp. 1-5). IEEE.

2. Per the National Academy of Forensic Engineers (www.nafe.org), Forensic Engineering is defined as "the application of the art and science of engineering in matters that are in, or may possibly relate to, the jurisprudence system, inclusive of alternative dispute resolution."

3. NFPA 921 (2021 Edition). NFPA 921 – Guide for Fire and Explosion Investigations, National Fire Protection Association, Quincy, MA. All references to NFPA 921 are to the current 2021 edition unless otherwise noted.

4. NFPA 1033 (2014 Edition). NFPA 1033 – Professional Qualifications for Fire Investigator, National Fire Protection Association, Quincy, MA. All references to NFPA 1033 are to the current 2014 edition unless otherwise noted.

5. NFPA 921, 2021 Edition, Ch. 3.3.76 defines fire investigation as "The process of determining the origin, cause, and development of a fire or explosion."

   NFPA 921, 2021 Edition, Ch. 3.3.140 defines a fire's origin as "The general location where a fire or explosion began."

   NFPA 921, 2021 Edition, Ch. 3.3.71 defines a fire's cause as "The circumstances, conditions, or agencies that brought about or resulted in the fire or explosion incident, damage to property resulting from the fire or explosion incident, or bodily injury or loss of life resulting from the fire or explosion incident."

6. NFPA 921, 2021 Edition, Ch. 3.3.167 defines the Scientific Method as "The systematic pursuit of knowledge involving the recognition and definition of a problem; the collection of data through observation and experimentation; analysis of the data; the formulation, evaluation and testing of hypotheses; and, when possible, the selection of a final hypothesis."

7. See for example: Southern Company. 2017. Georgia Power BlueBook for Electrical Service. In S. Company (Ed.).

8. Cutler-Hammer. 1999. 101 Basic Series: Metering. edited by Eaton. Milwaukee, Wisconsin U.S.A.: Eaton and Cutler-Hammer University.

9. Campbell, R. 2017. Electrical Fires. Research, Data and Analytics Division. Quincy, MA, National Fire Protection Association.

10. K.A. Seger and D.J. Icove. 1988. "Power Theft: The Silent Crime," FBI Law Enforcement Bulletin. (U.S. Department of Justice, Washington, D.C., March 1988.)

11. Lawton, T. and S. Schamber. 2017. Hot Socket Issues: Causes and Best Practices. Mid-South Electric Metering Association Conference, Gatlinburg, TN, TESCO - The Eastern Specialty Company.

12. Babrauskas, V. 2003. "Fires Due to Electrical Arcing: Can 'Cause' Beads Be Distinguished from 'Victim' Beads by Physical or Chemical Testing?" in Proceedings Fire and Materials 2003, (London: Interscience Communications), 189–201.

13. Hot Socket Issues - TechAdvantage. https://www.techadvantage.org/wp-content/uploads/2015/03/

LL1C_Tom_Lawton.pdf.

14. Seger, K.A. and Icove, D. J. 1988. "Power Theft: The Silent Crime," FBI Law Enforcement Bulletin. (U.S. Department of Justice, Washington, D.C., March 1988.)

15. Lawton, T. and S. Schamber. 2017. Hot Socket Issues: Causes and Best Practices. Mid-South Electric Metering Association Conference, Gatlinburg, TN, TESCO - The Eastern Specialty Company.

16. Id.

17. Hattangadi, A.A. 2000. Electrical Fires and Failures: A Prevention and Troubleshooting Guide. McGraw-Hill Companies, p. 128.

18. Per NFPA 70, 2017 Edition, the National Electrical Code, pt. 110.14(D) states "Where a tightening torque is indicated as a numeric value on equipment or in installation instructions provided by the manufacturer, a calibrated torque tool shall be used to achieve the indicated torque value, unless the equipment manufacturer has provided installation instructions for an alternative method of achieving the required torque."

19. CPSC. 2009. Single Meter Sockets Recalled by Milbank Manufacturing Due to Fire and Electrocution Hazards. (Release # 10-012). Washington, DC: Office of Information and Public Affairs Retrieved from http://www.cpsc.gov/cpscpub/prerel/prhtml10/10012.html.

20. NFPA 921 (2021, pt. 3.3.123) defines an interested party as: Any person, entity, or organization, including their representatives, with statutory obligations or whose legal rights or interests may be affected by the investigation of a specific incident.

21. Burnette, G. E. 2012. Spoliation of Evidence. Tallahassee, FL: Guy E. Burnette, Jr, P.A.

22. Examples include the Annual Training Conference and Seminar of the Insurance Committee for Arson Control (ICAC) in which present and former representatives from State Farm Insurance are frequent participants and attendees.

23. Dean, R. A. 2004. Legal Issues Involved in Failure Analysis. Journal of Failure Analysis and Prevention, 4(2), 7-16. Doi:1547702041876.

24. Lawton, T. 2021. Hot Socket Repair Kit. TESCO-The Eastern Specialty Company. Retrieved from https://www.tescometering.com/.

25. Lawton, T. 2021. Hot Socket Gap Indicator. TESCO - The Eastern Specialty Company. Retrieved from https://www.tescometering.com/.

Chemical Incident Analysis Involving Storage of Fertilizer Product

By Rogerio de Medeiros Tocantins, H. J. C. Júnior, S. Pericolo, G. Parabocz, R. S. Oliveira, and B.T. Heckert

Abstract

A forensic engineering analyses of a chemical incident is presented that was classified as a self-sustaining decomposition (SSD) event, which occurred in a load of 10,000 tons of NK 21-00-21 fertilizer bulk stored inside a warehouse in the city of São Francisco do Sul in Brazil. The chemical reaction developed within the fertilizer mass and took several days to be controlled, resulting in the evacuation of thousands of residents. The water used to fight against the reaction, after having contact with the load of fertilizer material, promoted changes in adjacent water bodies, causing the death of animals (fish, crustaceans, and amphibians). The smoke from the chemical reaction products damaged the incident's surrounding vegetation. Large SSD events are rare, with an average worldwide frequency of one every three years. Therefore, in addition to presenting a case study of this type of phenomenon, the main objective of this work is to discuss the causes that led to SSD reaction at this event, evaluate its consequences, and motivate future studies. Fire and external heat sources — factors that usually trigger the SSD — were ruled out as determinant factors of this SSD event. Small-scale experiments carried out concluded that a combination of an acidic condition, the presence of catalytic substance, and the occurrence of the "caking" phenomenon acted as primary triggers of the chemical incident.

Keywords

Self-sustaining decomposition, fertilizer, ammonium nitrate, forensic engineering, exothermic reaction, self-heating

Introduction

The city of São Francisco do Sul has a population of approximately 47,500 inhabitants, the majority of which had to be evacuated due to a chemical incident and the release of toxic gases. The event aroused chaotic situations in the city, such as lack of fuels and supplies, various thefts, and environmental damage to the surrounding fauna and flora. Several public security agencies were involved in evacuating the population, fighting and controlling the chemical incident, as well as investigating its causes in order to provide forensic evidence to courts of law.

A multidisciplinary staff of forensic officers (engineers, chemists, and environmentalists) was nominated by the state government to register, collect, and analyze evidence as well as find the causes of the chemical incident and evaluate its consequences. The forensic officers' investigations led to a hypothesis related to a self-sustaining decomposition (SSD) event that involved ammonium nitrate-based fertilizer. Published scientific studies show that events of this nature are most probably caused by an external heat source[3,4,5,6,7,8,9,10]. However, there was no such evidence at the scene, making the forensic analysis a challenge.

Ammonium nitrate (NH_4NO_3) is a product that has two main commercial uses worldwide: one as a key ingredient for blasting agents or high explosives (e.g., manufacture of ANFO - Ammonium Nitrate/Fuel Oil); the other as a plant nutrient in the manufacture of ammonium nitrate-based fertilizers[1,2]. Ammonium nitrate-based fertilizers in the widest sense refer to a variety of commercial products, roughly classified according to their application into two types: straight nitrogen fertilizers, where the element nitrogen is the principal plant nutrient; and compound (complex or blend) fertilizers, NPK/NP/NK products that contain at least one other nutrient, such as phosphate (P) or potash (K)[2], in addition to nitrogen (N).

Hazardous Properties

All fertilizers based on ammonium nitrate, under normal conditions, are stable materials, which in themselves present no risk. However, under abnormal conditions, they

Rogerio de Medeiros Tocantins, IGP-SC-Brazil, +55-48-988273650, rogerio_tocantins@yahoo.com

can give rise to hazards, including intensification of pre-existing fires, self-heating, thermal decomposition (including self-sustaining decomposition), and, under extreme conditions, explosion[3,4].

Fire Hazard

Fertilizers based on ammonium nitrate are not combustible. Although not all ammonium nitrate-based fertilizers are classified as oxidizers, they are oxidizing in nature. When heated sufficiently, they can decompose, giving off oxygen or nitrogen oxides that can assist other materials to burn (even if air is excluded)[3,4,5].

Experience shows that fires in fertilizer stores usually start outside the fertilizer stacks or heaps in combustible materials inappropriately stored near the fertilizer or in associated equipment, such as trucks or belt conveyors. Therefore, the risk of fire depends on other general combustible materials that may be stored together with the fertilizer (heated parts, flammable substances, or combustible materials)[3,4,5].

Self-Heating

Self-heating is the phenomenon in which the temperature within a body of material rises due to the heat being generated by some process taking place within the material[10]. Ammonium nitrate-based fertilizers are thermally stable and are not prone to self-heat in normal conditions of storage (i.e., without moisture absorption or presence of contaminants)[3]. However, when stored under abnormal conditions that result in an acidic mixture, they can produce a self-heating due to the exothermic chemical reactions between the fertilizer's components. If the heat produced by these reactions has difficulty dispersing to the atmosphere, then it can lead to a thermal decomposition of the fertilizer with the release of gases that contain toxic compounds[4,5].

Thermal Decomposition

When heated above 210°C, ammonium nitrate-based fertilizers decompose and release toxic fumes. The decomposition gives off a mixture of gases, such as water vapor, nitrogen, nitrous oxide, nitric oxide, ammonia, chlorine, hydrogen chloride, and others gases, including oxide vapors of nitrous oxide (NO_2), and carbon (CO, CO_2), resulting from a series of reactions. Therefore, ammonium nitrate-based fertilizers will suffer decomposition if involved in a fire or exposed to external heat[1,2,3,4,5,11].

The thermal decomposition process is complex. First, decomposition develops endothermically; afterward, a complex set of exothermic reactions happens[1,3].

When these fertilizers are acidic and/or contain materials that have a catalytic effect, such as chlorides, copper, and/or zinc, thermal decomposition can take a different course — and be initiated when the fertilizers are in the solid state, and toxic oxides of nitrogen (together with hydrochloric acid vapor and chlorine gas) can be evolved. It is worth mentioning that it is important to look at the potential risk that compound fertilizers based on ammonium nitrate containing chloride in their composition might have (e.g., compounds with ammonium nitrate and potassium chloride), as extremely low chloride contents may be sufficient to produce a significant effect on thermal decomposition[1,3,4,5].

Self-Sustaining Decomposition

In many cases, the decomposition (initiated by an external heat source) will stop when the external source is removed. With some fertilizers, however, the decomposition will continue and spread deep within the mass of material — even when the heat source is removed. This is the phenomenon of self-sustaining decomposition, sometimes referred to as "cigar burning" or "fuse-type decomposition," where the decomposition propagates through the mass of the material. No flames are produced unless paper, oil, or other organic material is present. The decomposing material does not usually get hot enough to glow. Fume off conditions are the most dangerous of situations due to the large mass being involved in such a short time[2,3,4,5,6,7,8,9,10].

In addition to external sources of heat, there are other factors that can trigger self-sustaining decomposition. Fertilizers based on ammonium nitrate under acidic conditions and/or containing materials that have catalytic effects, such as chlorides or copper, can also trigger it. Ammonium nitrate-based fertilizers whose formulation contains the presence of chloride (e.g., potassium chloride) have a greater susceptibility to self-sustaining decomposition[2.3,4,5,6,7,10].

Hadden, Jervis, and Rein[9] report that incidents of self-sustaining decomposition can be initiated by self-heating if the heat generated by it cannot be lost to the surroundings at the rate greater than it is generated, thus providing a thermal runaway, which allows heat to accumulate in the mass of the fertilizer material. Hadden and Rein[10] (qtd. in Babrauskas[16]) highlight that this will occur when large quantities of fertilizer material remain undisturbed for long periods of time (e.g., in bulk storage

or transportation), when the room temperature is high, and/or if there is contamination with organic material with which the ammonium nitrate begins to react directly at approximately 100°C.

According to Hadden and Rein[10] (qtd. in Kiiski[17]), large self-sustaining decomposition events are rare with an average worldwide frequency of one every three years. For Kiiski[8], the demand for more concentrated compound fertilizers from the 1950s led to a group of compound fertilizers whose concentration enabled emergence of the hazard of self-sustaining decomposition.

The incidents experienced in fertilizer warehouses and in maritime transport cargoes in the past motivated a number of studies on the factors that govern self-sustaining decomposition. In addition, international standards were developed for transportation and storage of fertilizers[1,8,9,10].

Explosion Hazard

The risk of explosion of ammonium nitrate-based fertilizers from past major accidents is obviously a bigger threat in terms of the extent of immediate potential consequences. Indeed, a number of these tragedies have killed hundreds of people, injured many more, and led to massive destruction, as in Oppau (Germany, 1921), Texas City (United States, 1947), Brest (France, 1947)[2,3], and recently in Beirut (Lebanon, 2020).

The high nitrogen content in the product was identified years ago as a key factor in the detonation ability. This is the reason why most current regulations and codes differentiate ammonium nitrate-based fertilizers according to the concentration of nitrogen content[2].

The two main mechanisms that can potentially cause an explosion in an ammonium nitrate fertilizer heap are the development of rapid decomposition (deflagration) in a fire situation and the initiation by a shock produced by an adjacent high-energy explosion[3]. When heated strongly under confined conditions (in a fire, for example), ammonium nitrate-based fertilizers can decompose violently, causing an explosion[3,6,11,14].

Currently, fertilizers based on ammonium nitrate are difficult to detonate, as such fertilizers are produced to have high resistance to detonation and thus require very energetic shocks. However, if fertilizers of these kinds are not treated properly, a number of factors can decrease this resistance, including prolonged heating, limited ventilation, presence of contaminants, strongly acidic conditions, particle size reduction, and thermal cycling[2,3,6].

Contamination of fertilizer with combustible and other reactive substances increases this risk. The explosion hazard is increased by the presence of organic materials such as oil, sulfur, grease, charcoal, and combustible dusts near the fertilizer[3,6,14].

Thermal Cycling

Among the crystalline transitions to which ammonium nitrate is subject, one of particular interest to the fertilizer industry is the transition to 32°C. This crystalline transition is accompanied by a substantial volume increase or decrease (approximately 3.6%) as the temperature is raised or lowered, respectively. Thus, temperature fluctuations across 32°C in storage situations of ammonium nitrate-based fertilizers produce effects of expansion, and contraction of the material volume can cause the product to break down into fine dust by thermal fatigue[3,4,5,7]. Therefore, physical disaggregation of the fertilizer can be promoted while stored in direct sunlight or under conditions where fluctuations between high and low temperatures can occur, particularly if they are inadequately stabilized or have picked up moisture. The transition at 32°C is particularly harmful in climates where ambient temperature is often close to this temperature[3,4,5,7].

Humidity

Ammonium nitrate-based fertilizers, like many other fertilizers, are hygroscopic. Therefore, they tend to absorb moisture from the atmosphere to which they are exposed, depending on the relative humidity of the air. In general, unwanted moisture absorption causes product deterioration as caking and/or physical breakdown[3,12].

Caking is the formation of a solid mass or lumps of fertilizer from individual particles. The amount of free water remaining in the fertilizer after manufacture or absorbed during storage has a huge impact on a fertilizer's tendency to cake (form lumps)[13]. NK fertilizers are made from ammonium nitrate and potassium chloride, and are subject to hard caking. Breakdown can also occur in wet conditions. Under such conditions, the material may disintegrate into dust or wet powder[7].

The more hygroscopic a fertilizer is, the more problems you can expect during storage and handling. The Critical Relative Humidity (CRH) is the property that is used as an indicator of the degree of likely interaction with atmospheric moisture. It is the value of the relative humidity of the surrounding air, above which the material

absorbs moisture and below which it does not[3,7,12,13]. According to Clayton[12] and Rutland[13], the CRH for commercial fertilizers compounds of ammonium nitrate and potassium chloride mixtures is between 55% and 67.9%.

Contaminants

Numerous incompatibilities have been identified with ammonium nitrate that may significantly increase the fire and explosion risk at both manufacturing and storage facilities — and lower the decomposition onset temperature in many cases. The determination of the sensitizing degree of the various potential contaminants (organics, chlorides, metals, metallic salts, urea, etc.) would also contribute to scientific analysis of the hazardous processes. However, due to its complexity (and despite the scientific interest aroused), the decomposition mechanisms influenced by contaminants are not yet defined[1,2,11].

Regarding ammonium nitrate-based fertilizers, as the solution becomes more acidic, its stability decreases, and it may be more likely to decompose and/or explode[3,4,5,7].

In cases where potassium chloride is part of the ammonium nitrate fertilizer mixture, consideration should be given to the possibility of self-sustaining decomposition and the overall level of the coating. Potassium chloride is the main potassium source in fertilizers; however, it is readily dissolved in water-forming chloride ions, which are catalysts of the thermal decomposition reaction[3,4,5,6,7,8,9,10].

São Francisco do Sul Self-Sustaining Decomposition Incident

This case study refers to a chemical incident classified as a self-sustaining decomposition event that took place in 10,000 tons of NK type 21-00-21 fertilizer cargo stored in bulk form in a warehouse. The chemical incident, shown in **Figure 1**, took place in the city of São Francisco do Sul of Santa Catarina (SC) State in Brazil. The reaction developed inside the mass of fertilizer for several days until controlled, resulting in the evacuation of thousands of inhabitants.

Forensic Exams

Field and laboratory data were collected. The field examinations were divided into two parts: the environmental impact assessment and the warehouse analysis. There was substantial environmental impact on the surrounding vegetation and adjacent water bodies. At the warehouse, the layout patterns of reacted material in the structure and the morphological features of the reacted material allowed the identification of the origin of the

Figure 1
Chemical incident (second day).
Courtesy of the City Hall of São Francisco do Sul[18].

reaction. Search, registration, and collection of traces that could be related to the incident were performed by the forensic team of six scientists and engineers. Virgin and reacted fertilizer material samples for the accomplishment of comparative forensic analyses in the laboratory were collected. Laboratory analyses included granulation and acidity exams. In addition, flammability and temperature tests were also performed (**Figure 2**).

Environmental Impact

The water used by the firefighters to suppress and control the chemical reaction, after contacting the load of fertilizer material, became contaminated with ions (NH_4^+, NO_3^-, K^+ and Cl^-), and was absorbed by the adjacent soil and water bodies. Measurements of the surrounding water bodies' conditions showed high values of acidity (low pH), salinity, and nitrogen in the form of ammonium (NH_4^+) and nitrate (NO_3^-) ions. The contaminated water promoted changes in the soil and adjacent water bodies and resulted in the death of animal species (fish, as shown in **Figure 3**, crustaceans in **Figure 4**, and amphibians in **Figure 5**). It was also established that the smoke from the products of the chemical reaction promoted damage to the vegetation around the incident area. The surrounding vegetation was composed of native (Atlantic Forest) and exotic species (**Figure 6**).

parameter	Measurement
pH	2.15
NH_4^+ (mg/L-N)	99.59
NO_3^- (mg/L-N)	> 100
Salinity (ppt)	58.35
Temperature (°C)	18.28

Figure 2
Measurements at 450 m from origin on September 26, 2013.

The Warehouse

The warehouse that stored the fertilizer load had damages produced by the firefighters' combat in order to extinguish the reaction of the incident. The chemical reaction's origin occurred in the right posterior portion of the warehouse. It was identified by the presence of reaction by-products on the exterior face of the building wall (**Figure 7**) as well as by the intensified state of corrosion of metallic parts in this region, as a result of the oxidizing gases actions produced by the chemical reaction (**Figure 8**).

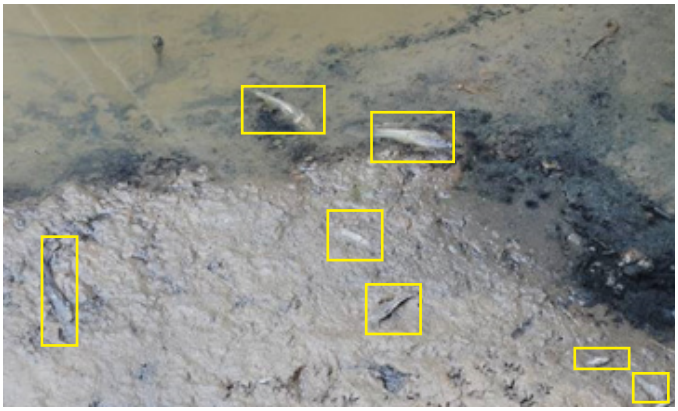

Figure 3
Dead fish in the surrounding water bodies.

Figure 4
Dead crustacean in the surrounding mangrove area.

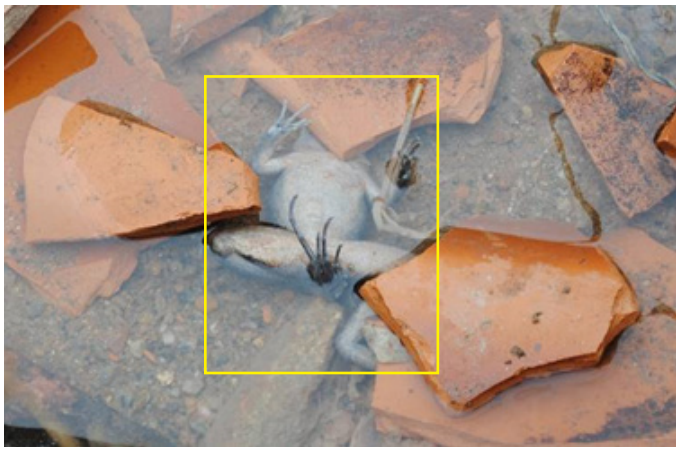

Figure 5
Dead amphibian in the surrounding water bodies.

The fertilizer material stored in the warehouse had several macroscopic aspects, varying among solidified formations of alveolar-like deposits of the substance in the unchanged conformation (**Figure 9**). These characteristics were similar to those observed by Hadden and Rein[10] in small-scale experiments with a diverse fertilizer composition and using a heat source (**Figure 10**).

Based on the EFMA manual[3], the levels of ammonium nitrate and potassium chloride in fertilizers of type NK 21-00-21 were calculated, obtaining, respectively, 60% and

Figure 6
Vegetation damaged: north (red ellipse)
and northeast (yellow ellipse) of the warehouse.

Figure 7
By-products of the reaction on the outer face of the warehouse wall.

40%. According to experimental data from FM Global[6], this type of fertilizer will undergo self-sustaining decomposition (**Figure 11**).

Despite being the most common cause of thermal decomposition, the hypothesis of the incident having started by an external source of heat was ruled out. Besides the absence of traces of charring, there was no evidence of the presence of combustible materials (wood, straw, hay, gasoline, etc.), flammable substances, heated parts, or electrical equipment near the reaction's origin area that might start a fire close to the fertilizer and trigger the chemical reaction by heat transfer. The analysis of the electrical system and the certification of their protective circuit breakers also did not corroborate the occurrence of an electrical fault or defect to support such a hypothesis.

Figure 8
Metal gate (internal surface) — intense corrosion.

Figure 9
Macroscopic aspect of the reacted fertilizer material.

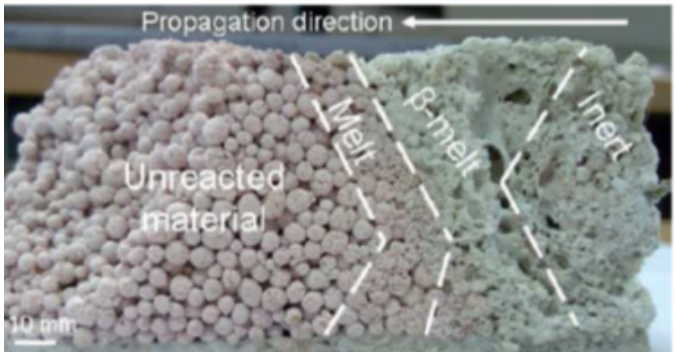

Figure 10
Cross section showing partially reacted sample with four phases visible in a small-scale experiment conducted by Hadden and Rein[10].

It was not possible to state the storage conditions of the material prior to the chemical incident (height of the fertilizer material stack, distance from the walls, presence of contaminants, etc.) due to the necessary actions of the firefighters to combat the incident. However, there was a load of 4,000 tons of the same batch of fertilizers from the same ship stored in the warehouse of another company in the same city about four kilometers away from the origin area. This material was analyzed because it was the same type fertilizer, transported in the same ship, stored nearby under similar ambient conditions, and was caked (**Figure 12**). Caking results with some bulk materials when it absorbs moisture.

The city's closest weather station's meteorological data reported an average of 82% of the relative humidity between the beginning of the fertilizer material's storage (August 30, 2013) and the date of the incident (September 16, 2013).

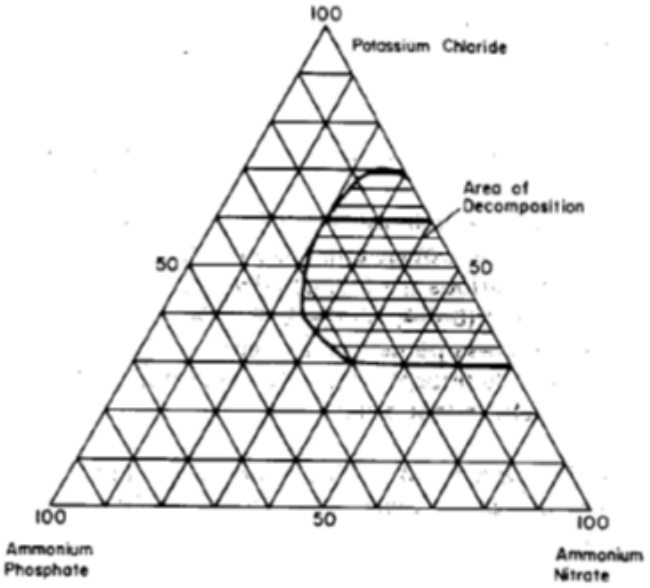

Figure 11
Area of self-sustaining decomposition in mixtures of ammonium nitrate, ammonium phosphate, and potassium chloride[6].

Figure 12
Fertilizers' caking.

Figure 13
Fertilizer material, in acid medium, with oven at 150ºC.

Flammability Tests

Samples of virgin fertilizer material were subjected to flammability tests with a flame source, flammable fuel source (ethanol) associated with the flame, and an electric current source. Exposure to the flame (about 30 seconds of exposure with a flame height of 20 mm) did not lead to ignition, but to a thermal decomposition of the material that stopped whenever the flame source was removed. Applying absolute (99% to 100%) ethanol on the fertilizer associated with a flame reached the same result — no ignition. The thermal decomposition remained as long as there was ethanol to burn, and stopped when it finished. Electric current sparks applied on the fertilizer also did not produce ignition of the fertilizer. The samples are self-extinguishing materials after the source is removed (i.e., doesn't support the fire).

Granulation, Acidity, and Temperature Tests

The virgin fertilizer material presented granulation characteristics in the form of spheres, which were brittle and easily sprayed powder when handled by applying small pressure with the fingers.

To evaluate the behavior of the substance in acidic medium, aliquots of 5g of fertilizer material were used in both granulated and pulverized form (eight samples for each granulated and pulverized form). These samples were tested with and without addition of acidic substance. In those tested in acid medium (four samples for each granulated and pulverized form), 1 ml of 5M hydrochloric acid was added. The samples were submitted to increasing temperature in the range of 30ºC to 265ºC in a programmable electric oven with timer drying control.

It was observed that the samples submitted to acidic medium developed yellowish coloration with temperature above 50°C and evolved to pink-whitish after 150ºC when the material acquired an alveolar appearance similar to that observed at the event origin (**Figure 13**). Non-acidified samples retained the original (orange) coloration until the temperature of 210°C, when they evolved to pink-whitish and alveolar appearance. No significant differences were observed between the results obtained with the samples of granulated and pulverized material.

The results show that in an acidic medium, the decomposition reaction is catalyzed by the presence of chloride ions, according to Kiiski[7,8] and with Hadden and Rein[10], which demonstrate that the chloride catalyzed decomposition reaction is the main mechanism involved in self-sustaining decomposition.

External Heat Source

In the adjacent area to the storage of the fertilizer material, there was no presence of combustible materials or flammable substances (wood, gasoline, oils, grease, etc.) — neither of heated parts nor electrical equipment as well as no trace of carbonization. The warehouse where the fertilizer was stored had overhead electrical wiring that did not have any traces of electrical failure. During the combat to the chemical reaction, the firefighters reported no detection of flames. Thus, fire or external heat sources as the cause of the thermal decomposition were ruled out.

Physical Breakdown

Temperature fluctuations above and below 32°C were common during the days and nights in the subtropical climate region of the incident site. This caused successive crystalline transitions and its effects of expansion and contraction of the material volume, which, as well as the verified moisture absorption, facilitated product breakdown into fine dust. In the form of dust, the contact

surface of the material is higher — the higher surface area of the reagents, the higher the rate of a reaction.

Caking

The moisture absorption also promoted the "caking" phenomenon. The hardening of the outer layer of the fertilizer pile imprisoned air among the fertilizers' pellets, acting as a thermal insulation (hampering the heat exchange between the interior of the heap and the environment).

Dissociation of Salts, Acid Mixture, and Catalyzer

The fertilizer compound (NK 21-00-21) was a mixture of two salts: ammonium nitrate (NH_4NO_3) and potassium chloride (KCl). The absorption of moisture (water) by these salts led to the dissociation of salts into ions (NH_4^+, NO_3^-, K^+ and Cl^-) generating an acidic mixture (low pH). Additionally, the chloride ion (Cl^-) generated in the dissociation consists of a catalyst for the thermal decomposition reaction. The exams performed showed that the samples of the material, in an acid medium, developed thermal decomposition reactions (yellowish color) with temperatures around 50°C.

Conclusions

Based upon the scene examination, laboratory tests/analysis, and reviewed literature, the hypothesis that an external heat source (mechanical, electrical, fire) caused the self-sustaining decomposition was eliminated.

The most probable cause was the combination of the known air thermal cycling, the observed moisture absorption, as well as the influence of chloride ions on the acid medium. This hypothesis was supported and validated by:

a. The physical breakdown of the fertilizer promoted by thermal cycling, which, together with the absorption of moisture (water), becomes susceptible to the dissociation of salts of potassium chloride (KC1) from its own composition, forming chloride ions;

b. The fertilizer, in the presence of moisture (water), starts to present acidic conditions;

c. The acidic condition associated with the presence of chloride and/or other contaminants are characteristics that lead to a self-heating reaction; and

d. The long period that the material remained inert, combined with the low thermal conductivity of the fertilizer, aggravated by the caking phenomenon that formed a thermally insulating layer. This caking made it difficult to dissipate the heat generated inside the fertilizer pile to the environment. Considering that the heat generated by the chemical reaction was greater than that dissipated to the environment, the consequent evolution to a chloride (Cl^-) catalyzed thermal decomposition reaction — and, afterward, to a situation of self-sustaining decomposition — is the most probable cause.

The rarity of self-sustaining decomposition events — especially those that are not triggered by the action of external heat sources — require further studies on the subject.

Acknowledgements

The author would like to sincerely thank his family members for their unconditional support, to all public security professionals involved in combating the chemical incident, especially Colonel Vanderlei Vanderlino Vidal and Colonel Charles Fabiano Acordi, both Officers of the Military Fire Brigade of Santa Catarina (CBMSC), for the support and support to expert work. Thanks to the National Institute of Criminalistics (INC), the Technical-Scientific Office (DITEC) of the Federal Police Department, for the characterization tests of the fertilizer material and to the General Institute of Forensic Science of Santa Catarina (IGP/SC) by the administrative support. Deep thanks to Prof. Dr. Guillermo Rein, PhD, Professor of Mechanical Engineering at Imperial College London - London-UK, for sending scientific articles related to the chemical phenomenon. Special thanks to Prof. Guy Marlair, MsEng, researcher and scientist of the Division of Accidental Hazards of the Institut National de l'Environnementindustriel et des Risques (INERIS) – Verneuil-en Halatte-França, for sending scientific articles related to the chemical phenomenon and the scientific contributions inherent to this work. Thanks to Prof. Dr. David J. Icove, PhD, PE, FSFPE, of the Department of Electrical Engineering and Computer Science of the University of Tennessee, for encouraging me to write this paper.

References

1. G. Marlair, M.A. Kordek, C. Michot, "High Challenge Warehousing: Ammonium Nitrate as a Typical Case Study," Extended abstract - Sup-Det 2010 Symposium, Orlando, FL USA, 2010.

2. G. Marlair, M. A. Kordek, "Safety and Security Issues Relating to Low Capacity Storage of AN-based Fertilizers," Journal of Hazardous Materials, vol. A123, pp.13-28, 2005.

3. EFMA, "Guidance for the Storage, Handling and Transportation of Solid Mineral Fertilizers," Belgium: European Fertilizer Manufacturers' Association, 2007.

4. ANDA, "Guia Técnico para Armazenagem, Manuseio e Transporte Seguro do Nitrato de Amônio Fertilizante," São Paulo-SP, Brazil: Associação Nacional para Difusão de Adubos, 2013 [Online]. Available: http://www.anda.org.br/multimidia/guia_de_armazenagem_manuseio_e_transporte_seguro_do_nitrato_de_amonio.pdf. Accessed on: Sep., 30, 2013.

5. IFA, International Fertilizer Industry Association, EFMA, European Fertilizer Manufacturers Association, "Handbook for the Safe Storage of Ammonium Nitrate Based Fertilizers," 1992 [Online]. Available: http://www.euexcert.it/wp-content/uploads/2011/10/HANDBOOK-AN-STORAGE-1992.pdf. Accessed on: Nov., 3, 2013.

6. FM Global, "Property Loss Prevention Data Sheets: Ammonium Nitrate and Mixed Fertilizers Containing Ammonium Nitrate," USA, 2013.

7. H. Kiiski, "Properties of Ammonium Nitrate Based Fertilisers," Finland, 2009. Available: https://helda.helsinki.fi/bitstream/handle/10138/21085/properti.pdf?sequence=1. Accessed on: Nov., 2, 2013.

8. H. Kiiski, "Self Sustaining Decomposition of Ammonium Nitrate Containing Fertilisers," IAF Technical Conference, USA, 2000.

9. R. Hadden, F. X. Jervis, G. Rein, "Investigation of the Fertilizer Fire aboard the Ostedijk," Fire Safety Science – Proceedings of the Ninth International Symposium, pp. 1091-1102, UK, 2008.

10. R. M. Hadden, G. Rein, "Small-scale experiments of self-sustaining decomposition of NPK fertilizer and application to events aboard the Ostedijk in 2007," Journal of Hazardous Materials, vol. 186, p. 731-737, 2011.

11. S. Cagnina, P. Rotureau, C. Adamo, "Study of Incompatibility of Ammonium Nitrate and its Mechanism of Decomposition by Theoretical Approach," Chemical Engineering Transactions, vol. 31, Italy: AIDIC (The Italian Association of Chemical Engineering), 2013 [Online]. Available: http://www.aidic.it/lp2013/webpapers/141cagnina.pdf. Accessed on: Nov., 2, 2013.

12. W.E. Clayton, "Humidity Factors Affecting Storage and Handling of Fertilizers," International Fertilizer Development Center (IFDC), USA, 1984 [Online]. Available: http://pdf.usaid.gov/pdf_docs/pnaaq558.pdf. Accessed on: Nov., 9, 2013.

13. D. Rutland, J. Polo, "Fertilizer Dealer Handbook: Products, Storage, and Handling," International Fertilizer Development Center (IFDC), USA, 2005 [Online]. Available: http://www.amitsa.org/wp-content/uploads/bsk-pdf-manager/222_IFDC_FERTILIZER_DEALER_HANDBOOK.PDF. Accessed on: Nov., 9, 2013.

14. NFPA 490, "Code for the Storage of Ammonium Nitrate," National Fire Protection Association, MA, USA: Quincy, 1993 [Online]. Available: http://inferno4.spffa.com/pdf/nfpacodes/nfpa_490.pdf. Accessed on: Dec., 5, 2013.

15. P. C. Bowes, "Self-heating: Evaluating and Controlling the Hazards," Her Majesty's Stationary Office, London, 1984.

16. V. Babrauskas, "Ignition Handbook," WA, USA: Fire Science Publishers, 2003.

17. H. Kiiski, "Self sustaining decomposition of ammonium nitrate containing fertilisers," Presented at 70th International Fertiliser Association Conference, Paris, 2002.

18. City Hall of São Francisco do Sul-SC-Brazil.

Pinched Power Cord is Latent Defect Causing Fire When Appliance Is Not in Use

By Michael D. Leshner, PE (NAFE 559F)

Abstract

After a fatal residential fire, witness statements and burn patterns pointed investigators toward an electrically powered upholstered reclining chair as the origin. A search for exemplar recliners identified slightly different designs of the power supply, which converts house current to low-voltage direct current for driving the motor. Although the fire left no direct evidence of its cause, analysis of unburned exemplars uncovered a design defect in the power supply electrical enclosure design, causing damage to the power cord during assembly. The transformer was found to press against the two-conductor power cord, in a location inside the unit that was concealed after assembly. The newer units did not have this design defect. Investigators developed the hypothesis that over time, the sustained force of the transformer against the cord enabled the insulation to deform such that a short circuit occurred in the power cord and caused the fire — even when the recliner was not in use and if the house wiring circuit had been protected by a circuit breaker. This paper details the investigation, testing, and findings, including dissenting expert opinions. More importantly, it shows how forensic engineers conduct detective work and apply scientific principles to achieve useful results.

Keywords

Fire, electrical, ignition, causation, products, defect, NFPA 921

The Fire

A fire occurred in a residence during the night while three occupants were asleep. One of the residents was awakened by the sound of the fire, and witnessed an upholstered recliner in flames as he ran past it toward an exit. The witness saw flames enveloping the chair and on curtains behind — but nowhere else. The fact that the general origin of the fire was witnessed permitted the exclusion of other electrical appliances in the room of origin. The witness survived with severe burns, and the other two occupants perished in the fire. The chair's electrical power system included an AC power cord, DC power supply, and DC motorized actuator to adjust its position.

Scene Inspection and Evidence Collection

The fire occurred on one of the coldest nights of the winter, and firefighters took a long time to suppress the fire with water. In the morning, the burned building and evidence inside were covered with ice. When fire cause and origin investigators attempted to document the scene and collect evidence, the ice was a significant obstacle — and evidence collection and identification were less than optimal.

Investigators on the scene concluded that the fire originated in a downstairs room where the powered recliner was located. The evidence collected included the remains of the recliner, a nearby power strip, and every electrical item in the room where the fire was observed. The nearby light switches, outlets, and associated wiring and junction boxes were collected. Each bit of evidence was examined carefully using x-ray and destructive examination by experts from all interested parties. The steel articulating frame of the burned recliner remained, with burned remains of the actuator and power supply below. The power actuator for the recliner was damaged, and the nearby power supply and its electrical enclosure were heavily damaged by fire. The power supply cord was found plugged into a receptacle on an adjacent wall.

Considering all the electrical devices in the burned evidence, only one device — the recliner's power supply — remained powered with its circuitry "hot" whenever the power cord was plugged in. All the other electrical devices recovered were examined by all parties, none of which were suggested as points of origin. The power strip located near the chair was generally intact, and damage to

Michael D. Leshner, PE, 47 N. Lockwood Road, Elkton, MD 21921, (410) 964-0311, mike@leshner.com

the strip and wiring was consistent with external heating. The power strip was ruled out as well, based on absence of any electrical activity.

Scope of the Assignment

Based on the witness's observations and the plaintiff's Fire Cause and Origin Investigator's report, this author was engaged to look more closely at the recliner and consider whether the evidence might help to determine the cause of the fire.

Investigation

The first assignment for this author involved identification of the recliner's manufacturer. Based on information from the dealer where it was purchased, there were three manufacturers who supplied such products to the store. A new exemplar from each of the three manufacturers was obtained and examined. The steel frame from the fire-damaged evidence was nearly a perfect match with one of the exemplars — with the exception of two weld details.

Since the manufacturer refused to acknowledge the product was theirs, additional exemplars were obtained with manufacturing dates before and after the fire evidence, in order to find an exact match with the welding details on the frame. Two such exemplars were obtained, and their power supply enclosures were different from the new exemplar. Examination of new and old exemplars revealed two critically important results:

- The chair's manufacturer was positively identified (although never admitted), and;
- The design of the power cord and power supply enclosure were revised after the subject product was manufactured.

Exemplar power supplies representing both new and old designs were compared. The significant differences:

	Old Power Supply	Revised Power Supply
Length of AC Power Cord	9 feet	2 feet
Length of DC Cord to Actuator	2 feet	9 feet
Power Supply Location	Under recliner	Outside Recliner

Electrical Inspection

Together with a forensic electrical engineer, the old and new versions of the power supply were examined. It was determined that the product in the burned evidence was of the older design, based on the length of the power cord. The timing of the original purchase was also consistent with the older design.

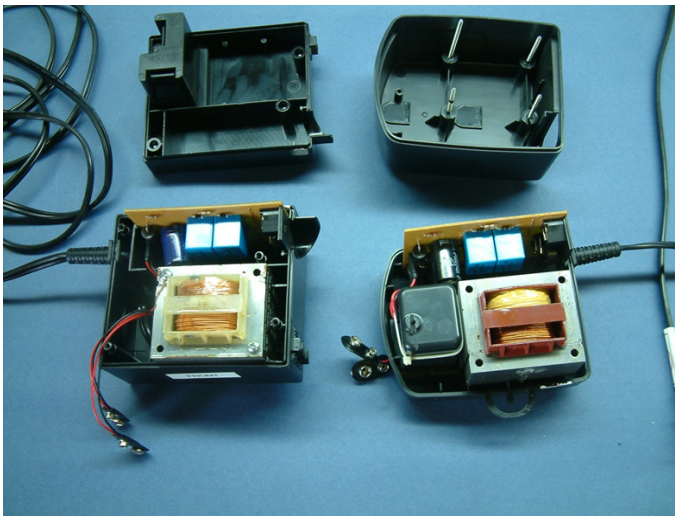

Figure 1
Power supply designs — old (left) and new (right).

Both designs were functionally equivalent, having the same transformer, circuit board, and connections. Revisions in the plastic enclosure provided more space for the wiring and a more direct path for the power cord. The short AC power cord and long DC cord reflected the altered location of the power supply. In the former design, the power supply was permanently mounted under the recliner. In the new design, the short AC power cord made it unlikely that the power supply could find its way under the recliner.

Corrective Actions?

The power supply design changes raised a suspicion that the revisions were corrective actions in response to a recognized problem. Although the discovery record did not indicate any similar incidents, the nature of the design revisions suggested corrective action. Was there something about the older design power supply enclosure and wiring that was problematic? To investigate further, exemplars of both old and new power supply designs were disassembled. In the older design, once the cover was removed, screws securing the transformer prevented inspection of the wiring without removing those screws. **Figure 1** shows the new and older design enclosures with the plastic covers removed. Connections between the power cord and transformer are hidden under the transformer.

In the revised design, the same internal components are used. No screws secure the transformer, and the power

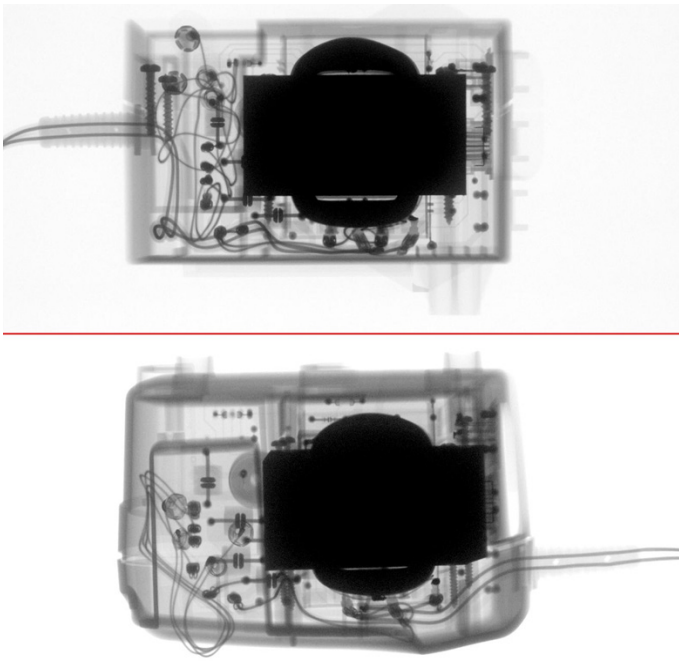

Figure 2
X-ray images of the old design (top) and new (bottom).

cord enters at a different location. All wiring is inspectable as the housing is assembled. **Figure 2** shows x-ray images of the power cord paths and the space between the transformer terminals and the side of the enclosure.

In the older design, the power cord took a tortuous path to the transformer and became compressed against the inside of the enclosure. In the revised design (lower image), the power cord took a direct path to the transformer and has adequate clearance to the inside of the enclosure.

Figure 3 shows the wiring connections under the transformer. While attempting to carefully re-assemble the power supply, the transformer did not fully "nest" into position before the screws were tightened against the transformer. It felt like the wiring was in the way. To prevent damaging the wiring under the transformer by tightening the screws, the transformer was carefully removed again for a closer look at the wiring. **Figure 4** shows significant damage to the power cord insulation from being compressed against the transformer frame and terminals.

Measurement of the enclosure's internal spaces revealed that there was insufficient space to accommodate the wiring connections without compressing and damaging the power cord insulation as the transformer screws are tightened during assembly. **Figure 5** shows the back of the power cord where it was flattened by compression against

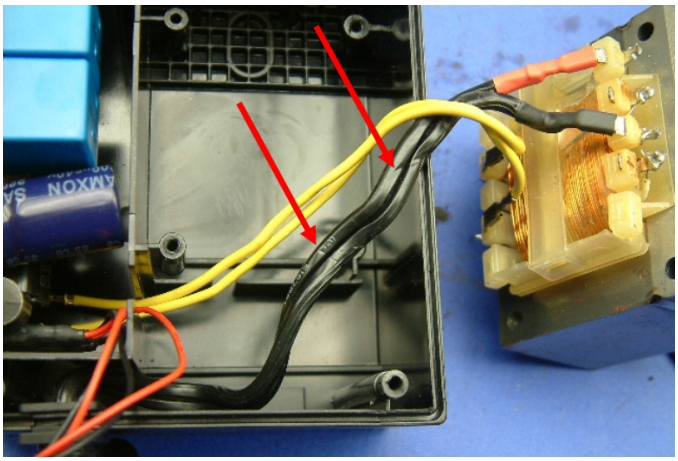

Figure 3
Wiring connections in the older design show evidence of external force (red arrows).

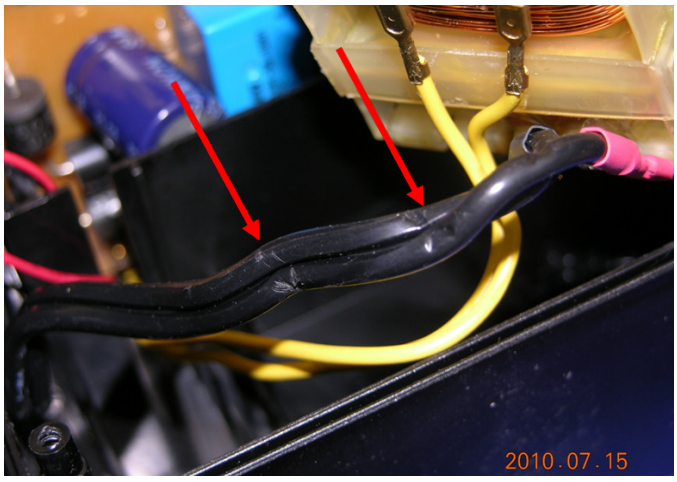

Figure 4
Damaged power cord within enclosure shows evidence of pinching against the transformer terminals (red arrows).

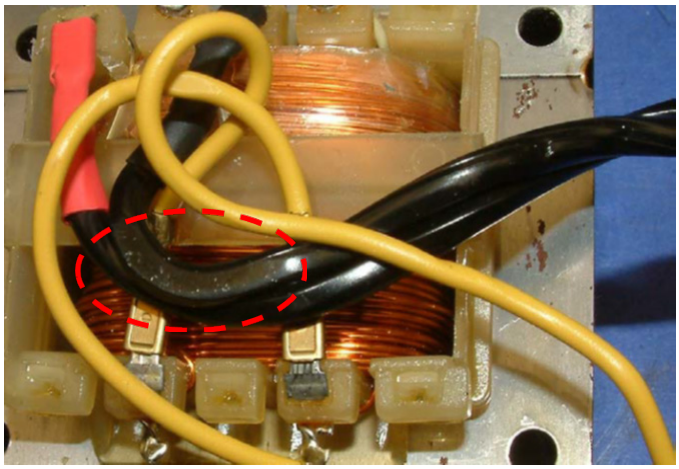

Figure 5
The portion of the power cord inside the ellipse has been flattened from continuous pressure against the inside of the enclosure in a warm environment.

the inside of the enclosure.

Based on the finding of a pinched AC power cord in a single exemplar power supply, another older exemplar was obtained. Another pinched power cord was found as shown in **Figure 6**. This result was expected because the older design electrical enclosure cannot be assembled without applying an external force the power cord, deforming the insulation.

Defect Theory and Hypothesis of Fire Causation

In the older power supply design, the power cord becomes compressed between the transformer and plastic enclosure as screws are tightened to install the transformer during assembly. The enclosure deforms, acting like a spring. The spring force is applied continuously throughout the life of the product.

The power supply is energized continuously, and gets warm. Temperatures within the power supply enclosure were measured at 135°F while powered on the bench, and may become even warmer when located under the chair. The power supply remains warm when the product is plugged into a power source, keeping the power cord insulation warm and soft and enhancing its ability to deform where an external force is applied.

The working theory was that the AC power cord on the product became damaged during assembly, due to a design defect in the electrical enclosure. Over time, insulation on the pinched cord experienced material deformation and allowed some current to flow between the line and neutral conductors of the cord within the enclosure. Such an unintended electrical path tended to begin at a low level of current and develop into an overcurrent (in excess of the current an 18 gauge power cord was intended to carry). The overcurrent caused the power cord to become extremely hot before the cord melted and separated or the circuit breaker tripped. In this case, the circuit breaker tripped, preserving the power cord conductors and plug blades. The hypothesis: An overheated power cord ignited nearby combustible material, initiating the fire.

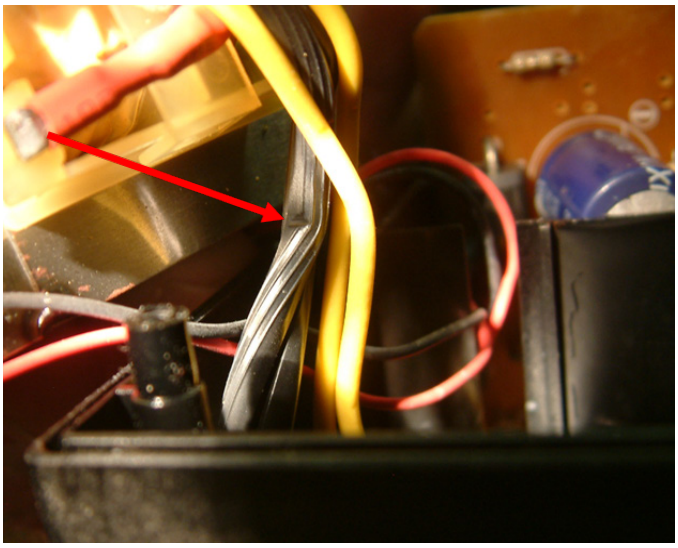

Figure 6
Another exemplar shows evidence of a pinched power cord (red arrow).

Testing the Hypothesis

The hypothesis was tested by subjecting representative two-conductor plastic power cords (“lamp cord”) to intentional overcurrent. Under five to 10 times rated current, some shorted cords became hot enough for their insulation to melt and briefly burn before a typical circuit breaker tripped. One exemplar cord failed in a near-replication of the incident, and its burning insulation did ignite the upholstery of its exemplar recliner.

As shown in **Figures 7** and **8**, an exemplar power cord was positioned under the product and energized with 60 amps. The cord glowed orange and ignited the fabric within about 20 seconds.

Circuit Breakers

The circuit breaker on the branch circuit supplying the chair was a 20-amp breaker, and it was found to be tripped after the fire. It was not removed from the panel, and its specific model is unknown. However, the typical trip characteristics for a circuit breaker are shown in **Figure 9**. The typical trip curve indicates that a circuit breaker can sustain multiples of its rated current for 10 to 20 seconds or

Figure 7
Ignition of fabric by glowing power cord.

Figure 8
Propagation of fire to fabric.

longer. **Figure 9** represents the performance of a typical circuit breaker.

Circuit breakers are designed to protect wiring in the building, and can tolerate many times their rated capacity for a short time. For example, as shown in **Figure 9**, a typical 20-amp circuit breaker can handle 100 amps for up to 5 seconds, or 40 amps for up to 30 seconds, before tripping. The specific performance curve for the 20-amp circuit breaker model supplying the branch circuit connected to the power supply was not available in the record. However, the fact that a circuit breaker was in the line cannot prevent a short-lived overcurrent in the power cord before

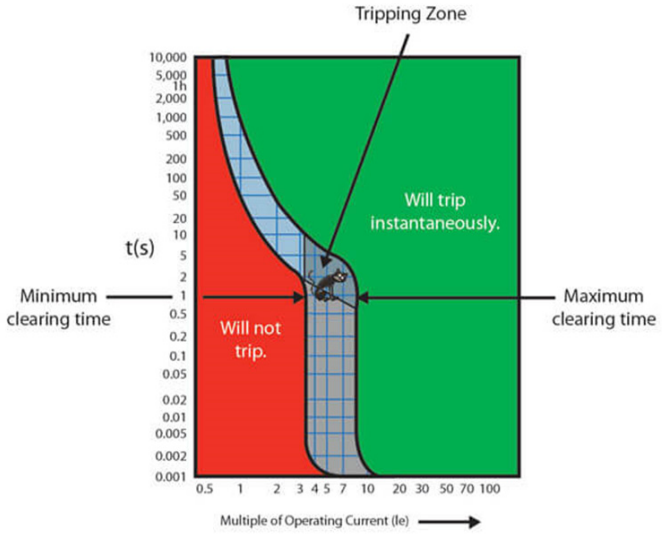

Figure 9
Representative circuit breaker trip curve indicating the time it will take to trip at multiples of its rated operating current[2]. Image reprinted with permission from c3controls, Beaver, Pa.

the circuit breaker trips. The circuit breaker on the branch circuit feeding the chair was, in fact, tripped.

Observations during exemplar testing revealed that as current in the power cord was increased, the insulation melted, burned, and turned to char as the copper conductors glowed orange, radiating intensely in all directions. In some tests, the copper conductors melted and separated, stopping the current. At a current of about 50 to 60 amps, the copper conductors glowed brightly but remained energized. As observed in the tests described above, there was a period when the copper can become a radiant source of ignition in quasi-steady equilibrium. With power input nearly equal to the radiant power loss, the cord can glow like the inside of a toaster until the circuit breaker trips or the copper conductors melt.

Connecting the Dots

When the burned evidence and exemplar evidence for this fire were evaluated in concert, the theory of a design defect as the cause of the fire was well supported. The older design power supply was present in the product determined to be the origin of the fire by the plaintiff's fire cause and origin investigator. A design defect was found in both exemplar power supplies of the same design, pinching and damaging the power cord within the enclosure as the product was assembled. Accordingly, it was reasonable to conclude that the same defect was present in the fire evidence. In the normal use of this product, the power cord lay on the floor and came very close to the furniture's fabric. Testing confirmed that an overheated power cord was capable of igniting the fabric.

There was a solid basis to prove that a design defect existed in the product, damaging the power cord. Such damage was capable of causing a fire. Even without any direct evidence of the fire's cause, sufficient evidence existed for the plaintiff's forensic engineering experts to support their opinion that the design defect caused the fire.

Subsequent Remedial Measures

While subsequent remedial measures are not evidence of a defect[3], the design changes that occurred in this product were precisely what a prudent manufacturer would have done to correct a problem after becoming aware of the problem. The manufacturer never admitted that the design was revised to correct a problem, or that they were the manufacturer of the subject chair. However, the "subsequent remedial measures" effectively moved the power supply out from under the product and eliminated the pinch-points on the power cord within the power supply

enclosure. Together with the rest of the evidence, the design revisions provided a clue that led to further investigation and a theory of causation.

Dissenting Opinions

Defense experts correctly pointed out that evidence from the fire was not collected according to best practices for evidence recovery, due to the heavy ice at the scene. All that remained of the power supply was the transformer, bare wires, and a bit of the printed circuit board, making identification of the point of failure remote or impossible, due to the extent of fire damage.

Since no specific evidence of electrical activity was found, defense experts labeled the cause as undetermined. It was argued that if the cause was within the power supply enclosure, there should be some evidence of electrical activity in the recovered debris. It was also argued that because the condition of the recovered evidence was poor, some other electrical devices in the area could not be ruled out conclusively. The defense experts did not propose any alternative theory of fire causation and performed no testing.

Afterthoughts

Fires tend to destroy or obscure evidence of their cause, and often leave few clues, aside from burn patterns. In this case, the evidence supporting a cause determination did not rely on the fire evidence. The investigation of unburned exemplars revealed critical evidence of the fire's cause.

NFPA 921 *Guide for Fire & Explosion Investigations*[1] does suggest that investigators may obtain historical exemplars for suspect products. In this case, the exemplars were obtained to inspect details of the steel frame. The recognition of a design change in the power supply was serendipitous.

Once revisions in the power supply and its change in placement to outside the product were recognized, a theory of causation began to take shape. Hands-on inspection of the older design power supply added substantial weight to the theory, exposing the design defect. Without the recognition of a defect in the exemplars, no reasonable explanation for the fire would have been found, based on the fire evidence alone.

The investigative path in this case was initially directed toward proof of the product manufacturer's identity. After collection of several exemplar chairs, the plaintiff's experts noted the design changes to the chair's power supply that occurred after the subject chair was manufactured. NFPA 921[3] advised inspection of unburned exemplars to understand the operation more fully and explore ignition scenarios. Hands-on internal inspection of the old and new power supply exemplars uncovered the design defect.

NFPA 921[3] describes retaining specialized experts such as mechanical or electrical engineers when the origin and cause investigator does not have the expertise for the investigation. In this case, the inspection of exemplars led the forensic engineers in an unexpected direction. Recognition of the defect and resulting theory of causation evolved as a result of "getting to know the product."

References

1. *Guide for Fire and Explosion Investigations*, NFPA 921-2014, National Fire Protection Association, Quincy, MA, 2014.

2. c3controls, Beaver, PA. *Understanding Trip Curves*. Accessed: July 4, 2021. [Online]. Available: https://img.c3controls.com/image/upload/resources/c3controls-Understanding-Trip-Curves.pdf.

3. U.S. House. 115th Congress, 51st Session (2017, Dec. 1. *Federal Rules of Evidence, Rule 407. Subsequent Remedial Measures*. [Online]. Available: https://www.uscourts.gov/sites/default/files/evidence-rules-procedure-dec2017_0.pdf.

Interdisciplinary Forensic Engineering As a Result of Substantial Completion Request: A Case Study

By Edward L. Fronapfel, PE (NAFE 675F)

Abstract

A project owner commonly relies on the contractor and design professional to determine substantial completion of a construction project. If the need arises, the owner may engage independent reviewers. The potential for forensic consulting arises when the contractor fails to provide construction in conformance with the contract documents or when the designer errantly designs, observes, approves, or omits work during the process. If a forensic consultant is engaged near or at completion of the work and reports substantial deviation from the contract documents, the owner must determine how to handle the need for corrective action. The deviations must be categorized and allocated to the responsible parties, and a means and cost to cure such defects are necessary. This paper provides a case study of the forensic review process under Colorado Rules of Evidence, although the rules are substantially similar in other states and on the federal level.

Keywords

Forensic, investigation, inspection, substantial completion, punch list, building code, NFPA, testimony, cost

Background

In 2016, approximately one year from the beginning of the construction of a dormitory addition and renovation to a private school in Colorado, the project owner engaged an engineer to perform a preliminary observation to verify substantial completion and authorize final disbursal of payment to the contractor. The site is a 25,000-square-foot school and residential dormitory for private use.

During the site observation, the engineer identified a number of details in the construction of the building that did not comply with code or industry standards. Review of the owner-provided punch list verified that not only were items beyond simple cleanup, but these items would also require substantial modification to cure the multitude of non-conforming work related to the construction of the building and site development. The discovery of issues gradually increased the magnitude of the original scope, leading to the need for additional information gathering about the design and construction of the project. The nature of the discoveries triggered additional document analysis, code reviews, and site investigations, including intrusive examination, all of which were necessary to provide the owner and litigants a complete understanding of the issues noted on the property.

Analysis

Forensic engineering requires a thorough understanding of the local, state, and federal laws regarding construction defects to provide proper analysis and reporting in the event that the substantial completion reporting begins the process of construction defect litigation. Also, since the scope of work could ultimately become a basis of action under the provisions of the contract, the forensic engineering process must include a review of the agreements, modifications, and addenda between the owner and contractor in order to evaluate the claims and their impact on the standards of work as set forth within the contract. In the project profiled herein, uncompleted work that was accepted by the owner via the owner's architect, or other third party, created a number of potential issues surrounding the determination and allocation of the damages, the costs to cure the work, and, in some cases, the acceptance of the work despite the damages.

Two-Prong Approach

In order for the engineer to evaluate the work against the contract documents and determine if such work

Edward Fronapfel, PE, 5926 McIntyre Street, Golden, CO 80403, (303) 425-7272, efronapfel@callsbsa.com

resulted in either a non-conformance or a construction defect, a methodology has to be utilized in order to more clearly and consistently position opinions within the subjective field of forensic analysis. Understanding of the forensic engineer's long-standing and consistent position with respect to the origination and evolution of construction defects, as well as the resultant damage, is necessary for building and site analysis. This position is ultimately developed out of the forensic engineer's experience, education, and training specific to the design, construction, and validation of compliance. This position has become known as the "two-prong approach" and is the foundation for the findings and opinions utilized in the case study presented herein. The two-prong approach is founded on the following precepts:

- The first prong of damage is the inability of a product, component, or system to perform its intended function. If the constructed condition cannot perform its intended function throughout its expected useful life, then it is first-prong damage. Thus, it satisfies the definition of damage commonly used within the legal framework of construction. The first prong of damage analysis, the ability of the system or element to perform the intended function, is defined by the code requirements, site-specific construction documents, manufacturer product information, and relevant industry standards.

- The second prong of damage is defined as the resultant manifestation of physical damage or distress that stems from the first prong. The observable distress or loss of use resulting from the inability of the system to function as intended is a result of the original inability of the product or system to perform. The manifestation of damage may create further resultant damages to the product, component, system, or adjoining systems that would otherwise be undamaged.

First- and second-prong damage may be readily observable, latent, or expected and depends on a combination of the forensic engineer's education and experience, as well as access to the first- and second-prong damage via visual or intrusive examination. **Figure 1** graphically displays the relationship of damage characteristics of the two prongs and also introduces a causal relationship into the overall process using water intrusion as an example.

First-prong damage initially occurs near substantial completion when the non-compliant construction is

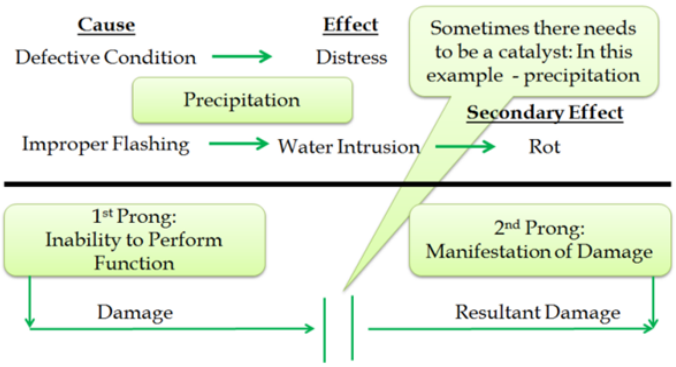

Figure 1
Damage manifestation timeline.

installed and/or becomes a part of the completed system. The result is a system that cannot function as it was intended. The first-prong damage, standing alone and absent a causal event, yields no resultant manifestation of damage. However, the current condition also does not necessarily result in loss of use, voidance of product warranties, or apparent damage to the property. Simply stated, improperly assembled construction, despite lack of physical damage, does not (and will not) work in its constructed state. Any conditions that include this first-prong damage should, therefore, be repaired so that the product, component, or system can function as intended.

The second prong, as discussed above, is the actual resultant manifestation of damage. This is when first-prong damage becomes observable. In **Figure 1**, the manifestation may not be observable until such items as visible biological growth are noticed by an owner. Here, it is important to emphasize the distinction of observations by an expert trained to recognize construction defects compared to a less sophisticated person without the education, experience, and knowledge of an expert in the field.

To further explain the **Figure 1** graphic, the defective first-prong condition (improper flashing) results in the second-prong water intrusion damage. After repeated rain events, the moisture builds up in the underlying products causing material deterioration to occur. Further, resultant damage will typically occur after substantial completion of a project.

During construction, the developer and contractor have the ability to remedy any discovered defective conditions. For example, an exterior cladding drainage system may be installed in a manner that directs water inward toward moisture-sensitive materials. This is a prong one condition that, with a high degree of engineering certainty, results in second-prong damage. However, if that damaged

condition (first-prong damage) is identified and corrected prior to completion of the project, then the condition is no longer at risk of resultant loss of use. In theory, the developer and contractor are able to correct any deficient conditions until the end of the construction warranty terms of the project. The forensic services should include communication with the owner's counsel to verify whether the defective construction is a breach of contract versus a claim of defective construction.

During the design and construction process, the owner may make choices based upon the acceptance of risk. The substantial completion request does not fully address the entirety of the design and construction process. The forensic engineer could inherently question the use of products or systems without the knowledge of predetermined decisions. This information should be provided to the forensic engineer to ensure that previous decisions that modified the construction were properly and thoroughly documented and entered into the files.

For example, with the case study herein, one of the issues in the punch list that had been provided by the owner and developed with the architect in August 2016 included isolation of the door trim from the concrete slabs. Review of the file found that while the original geotechnical report was provided for the site in July 2014, after the first site reporting, a second geotechnical report was issued in August 2014. This second report allowed a change of the foundation system and altered the bidding as part of the guaranteed maximum price (GMP) contract in February 2015.

This request to modify the foundation and floor systems was made with the design team and builder's input with the sole intent of reducing the cost of construction. In review of the structural engineering documents and architectural finishes, this change in the foundation system resulted in substantial risk acceptance, detailing changes and architectural impacts on the property that required substantial modification to the fire walls and finishes, and owner acceptance of the risks associated with slab-on-ground and expansive soils. This decision had to be connected to the understanding of the change from a cost-savings issue to one of building damage and associated repairs due to the expansive soils on the site.

Review Format According to Discipline

In order to comprehensively review the project for final compliance, engineers must employ a methodology based on organized engineering disciplines. Following such a review structure also aids in allocating and attributing responsibility for defects to the various trades involved with the construction. With this project, engineers analyzed substantial completion based on the following general interdisciplinary fields:

- Geotechnical
- Structural
- Civil
- Building envelope
- MEP systems
- Accessibility
- Acoustics
- Fire protection

After initial observation of the subject project and identification of non-conforming construction, this review structure was customized to the specifics of the project. The following list of non-conformances was used over one year of proceedings in negotiations with the owner's attorneys:

- Geotechnical
  - – Geotechnical report review
- Structural
  - – Foundation system – spread footings
  - – Floor system – slab-on-ground
  - – Superstructure – conventional wood frame
- Civil
  - – Grading and drainage
  - – Streets and roadways
  - – Concrete flatwork
- Building envelope
  - – Façade (exterior cladding and sealants) Type 1
  - – exterior insulation and finish system (EIFS)

– Façade (exterior cladding and sealants) Type 2 – adhered brick veneer

– Moisture-management system (barriers, flashings, drainage, etc.)

– Fenestrations (windows, doors, curtain walls, etc.)

- Workmanship issues
- Owner noted items
- Fire-resistance rated construction

Applicable Codes, Contracts, and File Disclosure Challenges

All parties involved in the construction project are bound by the contract documents. This contract should be the main focus of the substantial completion request. The contract documents are comprised of the legal agreements between the various construction parties, design drawings, specifications, and construction communications, such as requests for information, change orders, meeting minutes, and correspondence with the authorities having jurisdiction (AHJ) over the project. The contract documents form the fundamental minimum requirements set forth for the project. Since the contract documents evolve during construction with the inclusion of ongoing clarifications and change orders, the forensic engineering review must include a review of the current set of contract documents, including all changes to or clarifications of the contract, drawings, and specifications, as well as reviewing as-built drawings prepared by the contractor. The construction process requires that changes to the contract documents be carefully recorded and preserved.

Because of varying recordkeeping practices, the gathering of contract documents can be a lengthy, disorganized, and incomplete ordeal. The primary way to acquire contract documents is through voluntary tender or subpoena of the involved parties.

Forensic engineers should exercise their best ability to gather the information, compare changes from original work, and validate that such changes were properly submitted to the design team, owner, and AHJ. Establishing the applicable codes involves contacting the local AHJs and verifying the codes used in the review, inspection, and design of the project in order to accurately review the contract documents and construction.

Local AHJs often store physical copies or scans of submittal documents and are a secondary source of AHJ-approved construction drawings and approval communications; however, contract provisions can require the on-site parties to maintain these records. Owners usually desire to have an as-built set of the drawings and specifications (including operation and maintenance manuals) at the completion of the work.

On some projects, the disarray of documents can reduce the forensic engineer's ability to comprehensively review a file within the necessary timelines of the project. The expert's need to review the disclosed files in a timely manner can be impacted by the failure of the parties to provide full disclosure. When this doesn't occur, seeking legal remedy through retaining counsel is likely necessary to gain access to the entirety of the records. Corrections, updates, and supplemental reporting due to an incomplete file can result in the need for additional discovery, which can drastically lengthen the resolution process and ultimately increase the cost of the legal proceedings.

In the case of the subject private school project, the builder's file of documents was provided in a haphazard manner. In addition, the engineer noted within the reviewed contract documents numerous drawing revisions that, unfortunately, were not provided at the beginning of the engagement. This lack of provided information resulted in additional numerous report revisions and increased testimony time. Ultimately, the file in this case required an arduous forensic re-creation. Thus, information that was provided in late disclosure resulted in correction of claims against the design and construction of the property.

Four sets of disclosed documents were ultimately produced during the scope of work. The owner had 10,094 pages in the initial disclosure and 2,597 pages in the supplemental disclosure, in comparison to the builder, who disclosed 13,283 documents originally. The owner had provided a punch list developed with the architect in August 2016 and a field observation report from a third party that was dated one month after the punch list. After completion of the first engineering report, and even during the first arbitration period, the builder continued to produce documents. This late discovery further hampered the forensic engineer's ability to provide timely reporting. The second and third round of disclosed documents from the builder in early December 2017 included an additional 13,065 and 6,191 documents, respectively.

Ultimately, more than 50,000 pages of disclosures were produced. These disclosures were done with little to no means to identify fully all parts of the construction process. Documents were undated, misplaced, or generally out of order. During review of the documents, the engineer ultimately determined there were no less than eight drawing revisions. Having multiple designs ultimately became an underlying issue specific to the fire separation construction that involved many noted deficiencies.

Had the builder, as required per contract, created and provided an as-built set, the file review process, reporting, testimony, and overall clarity of the proceedings would have been substantially improved — both with reduced time and efficiency of efforts. Even in the final arbitration, the defense expert (who replaced the original defense expert used in the first hearing) relied on the incorrect drawings, which showed an assembly that was never actually constructed.

The main references that were used in the evaluation of the work for the substantial completion — and ultimately for both the breach of contract and construction claims — were drawn from the American Institute of Architects standard A102 documents[1], including the use of the general requirements set forth in A201. The architect was contracted under standard B101 forms and engaged the mechanical, electrical, plumbing, fire suppression, civil, and structural sub-designers. The owner independently contracted with the geotechnical firm. The selection of the contractor was made after for GMP agreements, with four addenda being incorporated during the bidding process. The forensic engineer had to carefully review the entirety of the contracts, modifications, and associated documents. Following are the specific non-conformances that were discovered by the engineer during review of substantial completion organized by the engineering disciplines outlined above and the consequent repairs that were proposed.

Geotechnical Review

The original foundation system at the subject site (as shown in **Figure 2**) originally included deep-drilled cast-in-place concrete piers. The uplift of the expansive soils in the active zone required that the lower concrete shafts be keyed into the claystone bedrock. This is not a typical design for two-story buildings and likely did not match the original building, which was founded on spread footings. During the cost review, a decision was made to change the foundation system to spread footings and a slab supported on ground. This change clearly reduced the cost of the project; however, the costs associated with the upkeep

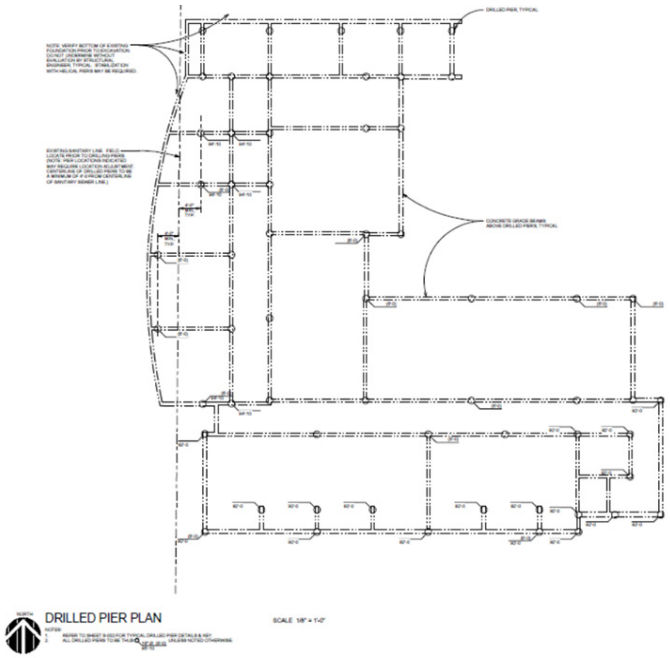

Figure 2
The original project documents included a foundation design using shear ring piers, which was consistent with the geotechnical report. An addendum changed the foundation to spread footings. No documentation exists evidencing the owner was apprised of the change in risk tolerance to the finish materials and structure due to the change in foundation type.

of a building that is more prone to movement would have to be absorbed by the owner. The change in the design and construction would require the contractor, designer, and owner to review, acknowledge, and accept the risks versus the cost savings. Unlike value engineering, this change would not provide similar functions to the deep-seated foundation systems, including the inability to maintain below slab MEP systems.

An updated geotechnical report was provided to relay the relevant information to the structural and architectural designers with respect to the foundation change; structural and architectural plans were updated to reflect the reduced foundation. As described above, the use of a two-prong analysis is important in properly analyzing the building and performance. The updated geotechnical report indicated that the movement of the soils could result in upwards of 3 inches of vertical rise. It is important to analyze this movement on the foundation- and slab-supported elements of the building and below grade non-accessible MEP systems. The interior demising walls, which are explored further in this paper, do not have the ability to absorb this type of movement. The structural engineer passed the information to the architect via a general note on the structural drawings. The architect created

slip-jointed fire separations in order to handle the anticipated movement. This fire wall, as described in this report, has inherent maintenance issues as the floors move. The architect, however, omitted any special detailing needed to accommodate the additional floor-to-foundation wall movement or better protect brittle surfaces, door frames, wall-to-wall connections, plumbing below the slab, or any other movement-sensitive areas. In addition, this decision contradicted opinions from the geotechnical report, which stated and illustrated: "In our opinion, a straight shaft pier (caisson) foundation should be used for the proposed building structure at the site. The piers should be drilled at least 6 feet into the bedrock. Shallow foundations are a riskier option for non-occupied features."

During observations, the forensic engineer noted several issues throughout the building. First floor dormitory room door frames were separating from the hallway drywall, and cracks had developed in the brick veneers and flooring. These manifestations of physical damage, or second-prong damages, occurred because the building systems were not constructed with tolerance or ability for movement that was expected in the secondary selection of the slab-on-ground and footing systems.

The inability of the foundation system to perform under the known movement parameters was the first-prong damage. Rather than suggesting a reconstruction of the building to provide a system that could perform on the expansive soils, a systematic means for maintenance was established and a capital expenditure account set up for the anticipated damages. Repair recommendations developed by the engineer after the forensic evaluation included implementation of a capital expenditure program that would deal with damages to the floor, walls, appurtenances, and fire assemblies. Ultimately, a knowledgeable contractor and design team should have informed the owner that movement issues may surface as part of switching to a more movement-prone foundation system.

Structural Review

Since the forensic work had to include both review of the construction as well as the potential breach of contract issues, not only did the engineer consider the change of the foundation system and its effect on the architectural and MEP systems but also found that the rebar had been wet-stabbed into the footings (as shown in **Figure 3**). This method of placing reinforcement after the concrete pour is improper and was not provided in accordance with the specifications. The structural notes in the documents issued for permit for the project stated, "All reinforcing shall be accurately placed and adequately supported prior to concrete placement (no wet stabbing) per IBC Section 1907.5."[2] Since there is not sufficient lateral load issues on this foundation system, it would be expected that no second-prong damages associated with this poor workmanship were observed or expected, thus no costs to cure this issue were assigned to the claim. The issue was used, however, in establishing an opinion of the overall quality of work provided by the general contractor.

Figure 3
Owner-provided photograph (Nov. 6, 2015), showing concrete placement for footings. Note that the dowels necessary to connect the footing to the foundation walls are not in place prior to the pour. The stabbing of dowels is a violation of the code, and was strictly forbidden by the structural engineer of record.

The foundation system change was not the only indicator of the unusual construction. The educational building was being constructed as an R-2, Type V building[3]. Although wood framing is allowed in the R-2 setting, it is much more common to see fire-resistant materials (such as masonry or steel) in the construction of educational buildings. Making the decision to sidestep more commonly accepted building materials presents additional coordination challenges to the design team.

The structural engineer required both horizontal and vertical slip joints to allow for the movement of the structure independent of the slab system. However, the architect omitted such detailing for vertical connections, and the contractor constructed the walls improperly at both vertical ends. Upon discovery of the non-conforming issues by a jurisdictional fire inspector, the contractor deconstructed the work and reconstructed the room demising walls to allow movement at the top of the walls with a floating connection, also known as a site-fabricated deflection track.

The design and construction team had originally sought a metal deflection track system manufacturer for incorporation of wood-frame walls with floated assemblies while the construction continued. The jurisdiction would not accept this metal track as a means to provide one-hour assembly to the demising walls.

With a constructed wood-floated track, no tested assembly of this construction exists, and the contractor sought an engineering decision from a proprietary group to establish the construction of the joint. Although that decision was not provided, the walls nonetheless were constructed. Upon the issuance of the engineering letter, the contractor moved the item to the resolved list even though no inspection, verification, or other work was done to validate the already completed work.

As the issue was tabled, it ultimately resurfaced through meeting minutes. None of this was noted in the disclosed file for over a year, and once it was determined, had to be carefully admitted during the arbitration hearings to lay foundation to each element. Had this been provided in the as-built, resubmitted set of drawings, it would have provided a clear means to the analysis necessary to determine the substantial completion of the building. The investigation showed that the wall had been constructed in general conformance with the Engineering Judgment Letter. But in review of the floating connection, other floor/ceiling assembly fire-resistance rating issues were found to be improperly constructed. It should be noted that the plan revisions indicated ultimately a callout to the Engineering Judgment Letter; however, those plans and modifications were not disclosed until very late in the case.

In consideration of the movement of the floor that was cost shared between the owner and contractor, and the foundation-supported frame walls, the floor will move independent of the foundation, and this float connection will require ongoing drywall seam repair each time the slab-on-ground floor system moves. This would include door tracks on the slabs and foundations, the vertical joint between the slab-supported demising wall and the foundation-supported corridor wall, and all ceiling float joints that are above the ceiling lid and thus non-observable.

Lastly, another issue came to light in review of the Engineering Judgment Letter and the comments from the original plan review of the fire department. The fire department noted that the engineered wood joists would require proper installation of the drywall to comply with one-hour assemblies. As is typical, that included either two layers of Type X drywall or a single layer of Type C drywall[4]. However, it was discovered that only a single layer of Type X drywall was used in the construction of the floor-ceiling assembly that attached to the one-hour demising and corridor walls; thus, the contractor failed to provide a rated assembly for the Type V construction. The substantial completion observation could not have determined this condition as it was latent and not accessible without intrusive testing.

Civil Review

The use of a slab-on-ground on expansive soils, as well as site appurtenances, requires that the builder provide proper drainage in accordance with the site-specific geotechnical report. In addition to the need for proper grade, the increased risk of building damages due to the foundation change and connection of the slab-on-ground to existing foundation-supported elements presents the likelihood of future damages and higher maintenance obligations. The builder and designers should have provided clear direction to reduce the likelihood that the soil movement would damage the building. Grading on sites that will move should consider not just the minimum standards, but increased standards that will allow discrete maintenance, such as additional fall in the backfill zone, structural landings and walks near the building, and drainage conveyance that can be easily manipulated to provide discrete repairs, such as inlets and storm drainage in bounding areas. Failure to consider maintenance in the design and construction does not allow owners a reasonable means to ensure their site is functioning as necessary to avoid first-prong damages that will ultimately result in second-prong damages.

The site drainage plan was provided by a civil engineer under contract through the architect. The builder, architect, and engineer all had the opportunity to understand the potential associated effects that are the result of poor drainage around the building, and the change of foundation and floor types increased those associated risks. The site observations conducted during the substantial completion revealed two primary conditions with the grade: the first was the lack of effective slope within the backfill zone, also referred to as the “protective zone;” the second condition was ponding water near the building’s foundation (as shown in **Figure 4** and **Figure 5**).

During construction, the builder attempted to remediate bad work where ponding was occurring by adding a small yard inlet located in the east courtyard. This modification to the contract documents would require that the

Figure 4
Substantial completion observation (July 24, 2018) showing storm drainage water accumulation at the backfill zone of the foundation.

Figure 5
Substantial completion observation (July 24, 2018) showing storm drainage water accumulation at the backfill zone of the foundation.

owner be willing to accept deficient, non-conforming work without cost reduction in the GMP and that the owner be willing to accept additional risks associated with water migration toward the structure and site. Building code and the geotechnical report both required that 5 percent minimum grading be maintained for 10 feet from the foundation perimeter[5]. This slope is visually apparent as 6 inches of fall in 10 horizontal feet, and the use of a perforated landscape edge is easily recognizable.

The original reporting for substantial completion included this visual assessment of the failure to provide code- or contract-compliant grading. During the arbitration, the argument from the builder's expert was that the forensic evaluation did not include a topographical survey and that an assessment of grading could not be provided without a surveyor's information. In defense of the visual approach to observation, the report included photographs showing ponding water; hence, a survey would not be needed to show this failure to meet the requirements of the plans, codes, or specifications. The contract required as-built plans. Had the contract been adhered to, the survey would have been provided by the contractor prior to the request for substantial completion.

Building Envelope Review

As constructed, the cladding system at the subject site incorporated an expanded polystyrene rigid insulation board (XPS) that was clad with adhered brick, a modified stucco system, and metal panels, depending on location. In all cases, the construction of the system provided no provisions for drainage of moisture that would accumulate behind the claddings.

Other non-compliant items were also observed during the substantial completion observations, such as the failure to provide proper joints at dissimilar materials, no separation of the claddings at water table systems, and the failure to provide for changes in façade based on the backup systems such as the foundation and framing elements. The construction attempted to create a barrier exterior insulation and finish system (EIFS). The code clearly does not allow barrier EIFS on Type V construction[6] and, thus, both the contractor's substitution and the architect's silence resulted in a non-compliant assembly.

The only viable means to cure the first-prong condition (the defective moisture-management system) and provide a tested fire protective assembly was to de-clad the structure back to the exterior wall sheathing, allowing the proper creation of the fire and moisture systems. Although the substantial completion scope identified missing components, the forensic investigation required intrusive examination of the building envelope. This intrusive examination revealed numerous flaws even in the constructed assembly, such as fastening, lapping, and coverage of materials. As constructed, in no instance could the building perform its intended function regarding drainage behind the architectural veneers. Based on the age of the building at substantial completion, observation of second-prong damages would not be expected, and the opposing side used that as its argument — since no damage had been found on the less than one-year-old building, it must in fact be performing. The first-prong argument states that

the expectation of failure of performance — hence, the loss of the intended use — is, in fact, damage.

Fire Protection Review

Ultimately, what became one of the most contested matters in the case arose during the first substantial completion observation. Per the project documents, the building was to be constructed with an NFPA 285-compliant cladding system, and this was clearly specified in the project manual. NFPA 285 requires that the cladding system be subjected to testing to determine its resistance characteristics to fire[7].

As discussed above, a decision was reached during the design phase to construct the addition out of wood framing, or Type V construction, in lieu of a safer and more typical application in this building's use of a Type III construction. The Type III would include non-combustible exterior walls as part of the inherent passive strategy. NFPA 285 testing is not specifically considered as part of Type V wood-framed construction. However, the question remains that if NFPA 285 was, in fact, considered in Type I to Type IV construction, there is no reason the veneer assembly could not comply with the standards.

The use of a more combustible product on combustible construction is allowed within the parameters of the code because combustible construction is typically not associated with institutional construction. The allowed classification of the dormitory renovation as occupancy type R-2 instead of the arguably more appropriate educational or institutional occupancy type is, in part, to blame for the exclusion of NFPA 285 requirements and the allowance of Type V construction in this setting.

The decision to construct the dormitory out of combustible materials did not result in the elimination of the NFPA 285 requirements in the specifications. However, two items must be investigated in the substantial completion of the project and in the review of the specifications in light of the GMP contract.

The contractor provided the GMP bid based on the drawings and specifications, which required components that complied with the NFPA 285 rating. During construction, the contractor submitted a hybridized system consisting of NFPA 285-compliant and non-compliant materials. Although the architect, via specifications, demanded a verifiably safer system, the architect did not exercise the diligence to reject the proposed materials and thus construction continued. No deductive change order was provided to the owner for the lack of compliance with the drawings and specifications. The owner was not informed about the reduction in the protective class of the building, its components, or its assembly.

Upon discovery of these issues, it was noted that the plans indicated specific areas for fire-retardant treated plywood (FRT). These requirements were in the bid set of construction documents and thus should have been incorporated into the construction cost prior to the contract award. During the substantial completion observations, no FRT was found on the building, and this was later confirmed in the testimony of the contractor's agents. Contractor construction photos showing the various layers of the building were only produced after intrusive testing confirmed the lack of FRT on the building, contrary to assertions from the other side's experts. Earlier disclosure of the construction photos could have significantly reduced the need for intrusive testing.

The FRT would have provided additional protection in the lobby, parapets, and stair areas on the Type V building; it would be logical that such increased level of protection would be advised in a dormitory setting, and inclusion of this material was understood as an essential component in the fire-protection scheme for a higher-risk residential dormitory. Ultimately, the architect testified that the specification in the manual and on the drawings was likely a mistake. However, this issue is complicated for two reasons. The first is the cost deduction for not installing the FRT should have been reflected in the GMP bid. The second is that the permit set, as required by the AHJ (local building department), requires documentation of any detail changes, especially those concerning life-safety features. Omission of the FRT should have been submitted via an RFI, a cost deduction, and a resubmittal of the plans to the AHJ for review and incorporation into the file.

Lastly, coordination with the sprinkler system design for NFPA 13 or 13R compliance would require such information to be reviewed in the determination of the layout and selection of the appropriate sprinkling systems for the building. None of these necessary tasks were completed in this project, leaving the issue open for the arbitration and requiring substantial time and testimony to determine a proper resolution. The original architect's conclusion is compromised by the fact that on-site construction observations were provided, and this framing would have been open and obvious during the observation. The architect failed to note that the framing systems were not in compliance with the architectural plans, and admission of this

issue could indicate fault on the architect's behalf.

Design of the dormitory, lobby, education areas, recreation areas, library, storage, retail, and other areas requires that the designers review the applicable construction type, the allowable areas for each use, and the restrictions associated with the prescriptive code for each of the occupancy groups. The fire provisions included appropriate egress considerations, active and passive fire protection features, and many other design aspects that are related to the safety and well-being of the building occupants. According to the plans, a one-hour fire separation was to be constructed between the old educational wing and the new lobby, between renovated assembly areas and the old educational wing, between the residential dorm room wing and the lobby, and, albeit not required as a one-hour separation because of the sprinkler, between each individual residential dorm room and the adjacent hallway. Because the dormitory wing consists of two floors, floor/ceiling separations also required review.

At first review, the architectural plans indicated adequate separation between identified occupancy groups. However, concerns arose due to unconventional combining of non-residential uses as part of a gross residential area. These areas included the bookstore, conference rooms, student lounges, commercial-style laundry, and utility and maintenance rooms — all of these spaces were combined within the gross student residential occupancy group. Inclusion of spaces that are an accessory to the host occupancy group is generally allowed; however, the size and use must fall within allowed parameters defined within the code and industry[8].

During substantial completion observations, area calculations determined that the amount of accessory spaces included in the residential occupancy was approximately twice the allowed limit, included non-residential equipment and uses, and exceeded occupant loads expected under the residential category. The building codes establish required fire separation ratings according to generally understood uses, elevating separation requirements where the risk of fire increases. Interpretation of the building code through a formal International Code Council review was sought, specifically to address the overstepping of non-residential functions and risks that were included within the residential occupancy designation.

The life-safety protection features in the codes are primarily founded on failure-based precedence and are matters that should always be carefully considered in any project — not taken advantage of or misinterpreted for the sake of reducing material costs by a comparatively insignificant amount. The difficulty in the interpretation included non-utilized space for normal activity, such as closets. The forensic review should anticipate the ambiguous portions of the code in relation to the industry knowledge and acceptance of how these spaces are considered in area calculations.

Repair Recommendations

Arbitration- and trial-based rulings rely on carefully composed cost estimates provided from both plaintiff and defendant to arrive at accurate damage valuations based on the acceptance of the arguments. In this case, the repairs for curing the non-conforming, non-accepted work were prepared by an outside estimating firm that based its work on the forensic reporting.

For most items, a scope of work was prepared that would provide resolution. In some instances, no costs were provided because although the work was non-conforming, no repair scope was provided. The costs included both correction to poor workmanship as well as defective work. This cost analysis, with multiple repair scopes encompassing the litany of damages, would allow the arbiter to review the case under both legal claims: one of breach of contract and one of defective construction. The cost analysis provided to the client in some cases must take into account independent repair costs to each potential party, thus needing to be separate and distinct for each party.

These scenarios must include separate costs for rip and tear items. An example is if the stucco was placed over a non-flashed window, the costs associated to remove the necessary components to get to the missing head flashing and the costs to replace the removed components have to be separated from the cost of the missing flashing. The policy language may not include coverage for that missed component but would include coverage for the costs to resolve the damage. A similar point can be made if there are two trades that share a cost to repair. The repair estimate may include a cost for each trade separately, as though the dual work never existed. The job-specific understanding and communication with the legal team are essential in developing appropriate segregated repair costs.

Summary

In summary, interdisciplinary forensic engineering can provide the necessary tools to help finalize outstanding contractual obligations. However, as noted in this report, lack of documentation and other challenges can

derail a smooth substantial completion process. The forensic expert should have knowledge both via education and experience to provide an understanding of the various engineering disciplines or engage others to review the multitude of potential issues. The engineer must weigh the building use, construction types, foundation types, occupancy types, and impact of each design and construction decision against the adjoining work, areas, and impact on other trades. Review of the provided documentation must be thorough and completed with meticulous attention. It must be fully separated by each trade and trade interface. Job file communications, such as the RFI responses, change orders, supplemental instructions, field directives, and even emails, should be reviewed to determine who, when, and where such needs impact work product.

References

1. American Institute of Architects (AIA), A102 "Standard Form of Agreement Between Owner and Contractor" A201 "General Conditions of the Contract for Construction," and B101 "Standard Form of Agreement Between Owner and Architect," 2007.

2. International Code Council, Inc. (ICC), "International Building Code" (IBC), 2009, Chapter 19 "Concrete," Section 1907 "Details of Reinforcement," subsection 1907.5 "Placing reinforcement."

3. International Code Council, Inc. (ICC), "International Building Code" (IBC), 2009, Chapter 6 "Types of Construction," Section 602 "Construction Classification," subsection 602.5 "Type V."

4. Gypsum Association, Underwriter Laboratories Rated Assemblies.

5. International Code Council, Inc. (ICC), "International Building Code (IBC)," 2009, Chapter 18 "Soils and Foundations," Section 1804 "Excavation, Grading and Fill," subsection 1804.3 "Site Grading."

6. International Code Council, Inc. (ICC), "International Building Code" (IBC), 2009, Chapter 14 "Exterior Walls."

7. National Fire Protection Association, NFPA 285 "Standard Fire Test Method for Evaluation of Fire Propagation Characteristics of Exterior Non-Load-Bearing Wall Assemblies Containing Combustible Components," 2012.

8. International Code Council, Inc. (ICC), "International Building Code (IBC)," 2009, Chapter 5 "General Building Heights and Areas."

State of the Arc (Mapping)

By David J. Icove, PhD, PE, DFE (NAFE 899F), Elizabeth C. Buc, PhD, PE, Mark E. Goodson, PE, and Thomas R. May, JD, Esq.

Abstract

NFPA 921 Guide for Fire and Explosion Investigations *considers the technique arc mapping to be one of the methodologies used in isolating a fire's origin and spread. Provided the technique is used properly and understanding its limitations, it is a tool for investigators. Synthesized here is the latest peer-reviewed research and discussions on the implications of increased use of ground- and arc-fault circuit interrupters on arc mapping analysis. Incorporated are case studies and evaluations of recent legal decisions. The goal is to arm investigators with what's needed to maximize the arc mapping's efficacy and best present its use and results.*

Keywords

Fire investigation, arc mapping, *Daubert*, fire origin, metallurgy, computed tomography, forensic engineering

Introduction

The standard of care for fire investigations is the National Fire Protection Association's NFPA 921 — *Guide for Fire and Explosion Investigations*, currently in its 2021 Edition[1]. If possible, fire investigators are tasked to reliably establish a room or area of origin for subsequent cause determination. When conducting a thorough fire scene examination, the fire investigator examines the structure, specific parts of the structure, and the geographic location within a fire scene to determine and identify the three-dimensional area of fire origin where it is reasonably believed to be located. NFPA 921 Par. 3.3.13 defines the area of origin as "[a] structure, part of a structure, or general geographic location within a fire scene, in which the 'point of origin' of a fire or explosion is reasonably believed to be located[1]."

This process is of paramount importance and must precede efforts to determine the fire cause, as defined by NFPA 921 Par. 3.3.27 as "[t] circumstances, conditions, or agencies that brought about or resulted in the fire or explosion incident, damage to property, bodily injury, or loss of life[1]." If the area of origin cannot be established, it is difficult to identify the fire's cause. Basic fire science, experience, surveillance camera footage, witness statements, and other tools or techniques, such as burn pattern analysis, are used to identify as small as possible an area wherein a fuel encounters a competent ignition source. Par. 18.1.2 of NFPA 921 states that the determination of a fire's origin relies on the interpretation of one or more of the following[1]:

(1) Witness Accounts and/or Electronic Data. The analysis of observations reported by persons who witnessed the fire or were aware of conditions present at the time of the fire as well as the analysis of electronic data including but not limited to security camera footage, alarm system activation, or other such data recorded in and around the time of the fire event.

(2) Fire Patterns. The analysis of effects and patterns left by the fire, which may include patterns involving electrical conductors.

(3) Fire Dynamics. The analysis of the fire dynamics [i.e., the physics and chemistry of fire initiation and growth and the interaction between the fire and the building's systems].

Fire origin determination can be complex when considering one, many, or all of these factors. In some cases, credible witness information may not be available. (Of course, witness information must be corroborated.) In other cases, fire patterns may be obscured or not useful, especially after full-room involvement. The weight of arc mapping to establish an area of origin must be based on data, including agreement or verification of each arc site, and include a survey and documentation of the room of origin and nearby circuits and devices.

Reliability of Arc Mapping

The definition of arc mapping according NFPA 921 Par. 3.3.9 is[1]:

David Icove, PhD, PE, DFE, PO Box 1348, Knoxville, TN 37901-1348, (865) 693-4361, icove@utk.edu

"Identifying and documenting a fire pattern derived from the identification of arc sites used to aid in determining the **area of fire origin or spread**." (emphasis added)

This process utilizes the evaluation of electrical arc sites' spatial location found during a systematic examination of the electrical circuit configuration, including devices. The investigative technique continues to be taught as one of the factors used to establish a fire's area origin per NFPA 921[1].

The principle of arc mapping has seen widespread utilization within the fire investigation community, but the quality of arc mapping varies. The presumed basis for mapping is that it correlates with the area of origin of an emerging fire as it damages the insulation on electrical wiring in its path. The developing fire creates short circuits and visible arcs in that damaged wiring, often before circuit breakers and other protection equipment shut down the electrical circuits in those areas. However, the presence of ground-fault and arc-fault current interrupters (AFCIs and GFCIs) may de-energize circuits and therefore prevent arcing conditions. Where this occurs, the absence of arcs does not always mean that the origin area of the fire is elsewhere.

Fire investigators have used arc mapping for decades. A succession of scientific and engineering articles as far back as that of Delplace and Vos in 1983[2] to a doctoral dissertation by Carey in 2009[3] and his follow-up study in 2010[4] described the usefulness of arc mapping to identify the fire origin and trace the fire's development. In Carey's 42 fully furnished repetitive room configurations, he determined through the analysis of the post-fire three-dimensional data that a high probability exists that arcing damage observed on electrical conductors occurred in close proximity to the fire's origin area.

Whether arc mapping can be considered a pillar of origin determination or merely a tool (such as burn pattern analysis) is the subject of recent debate. Assuming confirmation of arc sites, the ability of the fire investigator or engineer to properly infer an area of origin from the available data was identified as an important factor in the arc mapping process. In other words, it is crucial that the investigator have skill in performing and interpreting arc damage patterns. The skillset is a combination of background, training, and experience. Although an electrical engineer may not be required to perform arc mapping, electrical engineers are keenly qualified to calculate and evaluate the levels of available short-circuit current or circuit tracing activities that produce an arc. Metallurgists may be consulted to confirm or differentiate between fire melting, arc sites, and eutectic melting, though additional testing may be needed to verify and validate these observations.

Like fire test methods, investigation tools such as arc mapping have limitations. **Figure 1** provides lists of circumstances where arc mapping might or might not be useful.

The question is whether an arc site identified by an investigator can be scientifically relied upon in conjunction with other available information in confirming the area of fire origin. For that question to be answered, the fire investigator must have sufficient knowledge, training, and experience in correctly recognizing, collecting, and preserving this evidence and be able to demonstrate to meet or exceed the standards of care in performing these tasks.

For example, the following is a hypothetical situation involving the documentation of an arc site during a routine fire investigation:

> *A woman was in the basement doing laundry when she reported a light bulb above a table of stored goods failed. She cleaned up glass remains and went upstairs. Moments later, she was alerted to smoke and fire in the basement and vacated the structure. A v-pattern originated from table of stored goods. A severing arc site was found on the exposed Romex wiring directly above the location of the broken bulb; glass fragments were found in the basement trash receptacle.*

The methodology assumes that the fire attacks an energized wire causing degradation of the insulation and that a fault occurs between the hot conductor and one at

When arc mapping is useful	When arc mapping is not useful
• Incipient stage fires • Limited damage • Clearly defined arc site • On power cords to devices and appliances • Open fuses • Notches in metal appliance housing • Exposed Romex (e.g., basements) • Older structures • Vehicles with limited fire damage	• Copper thieving • Explosions (ignition of fugitive gasses) • Extensive, widespread fire damage • Fires with temperatures exceeding the melting temperature of copper • Circuits with AFCIs, GFCIs, other forms of RCDs • Aluminum conductors • New construction (due to the wide presence of RCDs) • Motor vehicles with extensive fire damage

Figure 1
When arc mapping is and is not useful.

a different potential. The arcing that occurs damages the conductor. Ideally, the circuit breaker will trip, and the arcing will cease. Arc site damage is not limited to conductors; it can also affect other elements in a circuit, including fuses.

This paper considers other scenarios that are not ideal. In some room configurations, arc sites may be more prolific adjacent to exposed areas of heavy fuel concentration or significant ventilation patterns. Such areas do not always correspond to the area of fire origin.

In some cases, wires may be completely transected or a partial collapse of part of a structure has occurred. In other instances, a breaker may trip before the arcing has severed the wiring. Other times, the breaker never trips, but bare wires fly apart, stopping the arcing. However, in any event, the arc damage indicates the first-place heat flux was sufficient to damage the insulation of energized cabling. As such, the arc site may tell something about the development of the fire's progression or origin area. The weight placed on one or more arc sites in establishing an origin area rests with the practitioner.

This paper assumes an investigator has the minimum NFPA 1033 (*Standard for Professional Qualifications for Fire Investigators*)[5] understanding of electricity and is capable of distinguishing arc sites from other forms of conductor damage. Any question regarding the cause of damage to conductors should be resolved, or the area of origin expanded.

A recent paper by Babrauskas, *Arc Mapping: A Critical Review*[6], has shown that arc mapping may not be as instructive as previously believed. In his article, Dr. Babrauskas shows that the published research does not support the notion that arc mapping can reliably indicate an area of origin under most circumstances. Also, there seems to be a basic misunderstanding as to what arc mapping shows. Fire investigators can be unaware that arcing artifacts more often correspond to areas of heavy fuel or areas of significant ventilation than a fire's origin area. Coupled with this misunderstanding is a lack of basic electrical knowledge by some practitioners. Finally, a series of electrical components that is being used in new construction such that arc mapping (and the resultant lab work and analysis) will look very different in newer structures than in older ones that lack these devices.

So, the questions emerge as to whether arc mapping is dead, and how useful is it as an investigative tool? The authors are resolute in stating that arc mapping can be a viable technique if used in the right circumstances and with an understanding of its limitations.

For directional patterns, this requires a severing arc and another arc downstream of that, in which case the local direction of fire propagation may be inferred. For intensity patterns, it requires that effects of local fuel load concentrations and local ventilation patterns be correctly accounted for. The latter task may be difficult or impossible in many cases.

Only if the work is done by a competent professional who has analyzed the fire scene from this point of view — and has been able to demonstrate that ventilation or fuel load would not have dominated the arcing propensity — will the data gathered be useful. But it has been the authors' experience that too often investigators have not shown such care. When this happens, arc mapping is likely to be misused, and misleading conclusions are likely to be drawn. The misuse of arc mapping can result in the wrong area of origin and, therefore, the wrong cause. Fire investigation reports should address arc mapping's reliability and limitations, and the author(s) must be prepared to explain both.

Electrical faults can also act as ignition sources. It is generally accepted that arcs can ignite low-density lightweight combustible fuels, dust, gases, and vapors, but an arc in a 120V branch circuit may not ignite solid fuels such as wood 2×4s. Also, there are no valid laboratory techniques to distinguish between an arc site that caused a fire or was the victim of a fire. Furthermore, absent video recordings, no one can say when a particular arc occurred.

For the investigator, the question becomes whether arc mapping can, or cannot, be validly used in a given fire.

Arc Mapping at the Site

Site processing techniques and data collection applied post-fire event should follow NFPA 921 Chapter 9, Electricity and Fire[1]. The process involves systematically examining circuits and wire remains for localized damage to conductors or plug blades. Colored tape or a flag is used to mark arc site locations. Damage requiring additional examination may be flagged with a different color. The arc sites are typically indicated on a map or plan drawing or annotated photograph. The entire length or sections of wiring with arc sites may be preserved. At a minimum, the arc site damage should be photographed using some form of magnification (e.g., macro lens,

cameras with microscope feature, portable microscopes). Fire investigators must be capable of distinguishing arc sites from other forms of damage (e.g., mechanical damage, eutectic melting).

To demonstrate proficiency, the fire investigator or engineer needs to confirm and defend the arc site(s) and understand factors influencing the response of circuit breakers and residual current devices at those sites. The following summarizes the significance of laboratory data and the inferences that can be made based on the circuits and their protection devices to support or negate fire origin and spread hypotheses. It is recommended that the fire investigator or electrical engineer examine electrical wiring and devices in rooms adjacent to the area of origin until they are satisfied that their analysis is sufficient to support their findings.

Applicable Laboratory Techniques to Confirm Arc Sites

Damage mechanisms to conductors from fire scenes may be mechanical, chemical, thermal, or electrical. The appearance of melting distinguishes electrical and thermal from mechanical damage. Examples of mechanical damage include gouging from twist-on wire connectors and fractured ends. The only form of chemical damage with physical evidence of melt is eutectic melting, typically aluminum or solder contacting a conductor, which can occur even if the conductors are not energized. Questionable damage to conductors should be subject to additional examination, if not confirmation in a laboratory.

Most arc sites have characteristic, macroscopic physical indicators on the exterior of the wire: that is, smooth melt in the shape of a round globule(s) with a distinct area of demarcation between the arc damage and conductor and notches. Buc and Reiter et al pointed out that not all arc sites are discernible with the naked eye; some sites are so small that the area requires magnification[8].

In the laboratory, there are four techniques used to further study localized damage to conductors and other electronic devices and appliance subcomponents. These analytical techniques include: 1) cleaning by ultrasonic and/or plasma etching; 2) imaging by stereomicroscopy and/or radiography; 3) chemical analysis by Energy Dispersive X-ray Spectroscopy; and 4) examination of microstructure by metallography[8]. The various techniques and their ability to distinguish between the various causes of damage to conductors is illustrated in **Figure 2**.

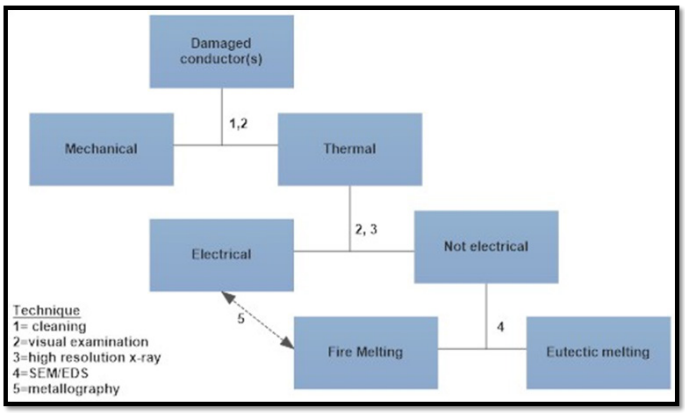

Figure 2
Protocol for the examination of damage to copper conductors from fire scenes.

Cleaning with an abrasive, such as glass fiber pens, can damage finer features on the surface. The best method for examining arc damage is an ultrasonic cleaner and mild detergent in hot water. For this, more time may be required to remove stubborn surface debris. Microscopy, using a stereomicroscope or equipped camera, preserves the arc site's appearance and should include the area of clear demarcation and the condition of the conductor away from the arc site. A second distinguishing feature of an arc site is internal porosity. High resolution, two-dimensional radiography is capable of distinguishing voids in the otherwise solid melt. X-ray is a non-destructive option to confirm the presence or absence of porosity compared to metallography.

A number of authors have investigated arc sites in detail using one or more of the above techniques. Laboratory-created arc sites are analyzed and compared with arc sites and fire melting from the field to establish the list of arc site characteristic attributes. Photographs of arc sites and fire melting are contained in NFPA 921 Chapter 9, Pt. 9.10, entitled *Interpreting Damage to Electrical Systems*[1]. Additional examples of arc sites are shown in **Figure 3**.

Fire investigators must be aware that arc sites to or involving brass and other alloys may have different characteristic physical attributes.

Circuit Breaker Basics

Identifying beads, marks, and other indicators of electrical arc activity is only one-half of the task. Information that is also needed is the determination of circuit breaker status, circuit breaker characteristics, how that would affect the arc fault duration, and (given the indications and duration) was the arc activity in close proximity to combustible material(s).

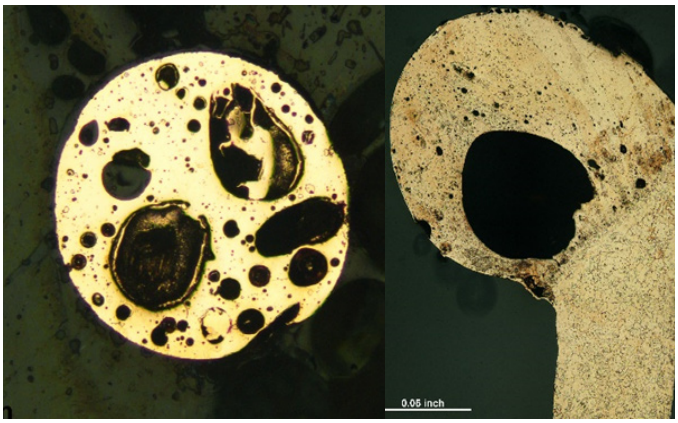

Figure 3
Arc sites to copper conductors.

What causes an arc event to stop? One scenario is the tripping of a breaker or the opening of a fuse. A circuit protected by a ground fault circuit interrupter (GFCI) or similar type device may also activate, causing the cessation of current flow. Moreover, finally, the magnetic forces associated with arcing (as well as expansive thermal forces associated with spatter) may cause the conductors to repel and current flow to stop. These interruptions of current are key to arc mapping. If the current flow does not timely cease, the sharp melt transition lines viewed microscopically become blurred; arc sites start to appear as melt sites.

UL 489 *Standard for Molded Case Circuit Breakers* (MCCBs) is often referenced[9]. OCP (overcurrent protection) is normally in the form of an MCCB or a fuse. An OCP is designed to protect house wiring and permanently installed appliances only. **Figure 4** shows the ratings of MCCBs and their design load:

1. MCCBs follow an inverse time-current relationship: the larger the overcurrent, the shorter the time allowed to trip.

2. There are two salient trip points – 135% of handle and 200 % of handle. At 135%, a 20-ampere breaker must trip in less than 1 hour at a load of 27 amperes. At 40 amperes, the same breaker must trip in less than 120 seconds. At breaker sizes of 40 and 50 amperes, 240 seconds are allowed for a trip time at 200% handle rating.

3. Overcurrent or overload situations cause heat to generate in a breaker, causing the tripping. This is referred to as the "thermal" mechanism of the breaker.

4. The thermal part of the breaker is also affected by ambient temperature. It will trip faster in hot weather and be slow to trip (or may not trip at all) in cold temperatures.

5. Short circuits cause the magnetic portion of the breaker to trip. While this depends upon the breaker size and manufacturer, typical short circuit trip-levels are from 5X to 12X the handle rating. A 20-ampere breaker would instantaneously trip at levels between 100 and 240 amperes, depending on how the manufacturer has designed and made the breaker.

6. Magnetic trip times are not affected by heat.

MCCB Ampere	AWG
15	14
20	12
30	10
40	8
50	6

Figure 4
MCCB ampere-AWG ratings.

Some forensic engineers and investigators neglect the notation from above regarding OCP being designed for protecting permanent wiring and appliances. For example, assume that an 18 AWG line cord is connected to an appliance and is plugged into an outlet with a 20-amp breaker protecting the circuit. The appliance malfunctions and starts to draw 25 amperes. A 20-ampere breaker is not required to trip until a sustained current of 27 amperes (135%) exists for an hour. The appliance can overheat and cause a fire, and the breaker is of little use in preventing the problem. Similarly, the 18 AWG line cord will overheat and could well catch fire.

Residual Current Devices

On occasion, the investigator may encounter a true Residual Current Device (RCD) as utilized in Europe. This original RCD trips at a fault current of ~30 mA. This device, unlike its American counterparts, is strictly a mechanical device. The 30 mA level is the "trip" level, unlike the 6 mA sensitivity used in the United States.

This difference in operation is brought in by the fact that 30 mA is deemed (by the IEC) not to cause electrical deaths; obviously, there are differing opinions on this. This European model uses a magnetic field to cause a mechanical relay to open and stay latched. The 30 mA trip level is instantaneous; there is no delay time in the breaker tripping. On the other hand, at 30 mA, the GFCI is allowed up to 56 seconds to trip.

In Europe, a common type name for one type of circuit protection is the RCD. In general, these are the GFCIs and their various permutations. One type of device that is truly not an RCD is an AFCI. This device looks for the signature of a repetitive arc (such as with a loose connection). In many devices sold in the U.S., the AFCI also contains ground fault protection. For this paper, the AFCI will be considered an RCD.

The common forms of RCDs include:

- Ground fault circuit interrupter breaker
- Ground fault circuit interrupter receptacle
- Ground fault equipment protector
- Leakage current detection interrupter
- Appliance leakage circuit interrupter
- Immersion detection circuit interrupter
- Arc fault circuit interrupter

These devices affect the conclusions that can be drawn from arc mapping. For example:

> *A fire breaks out in a bathroom. Arc mapping of the structure reveals that there was bare type NM wiring, but no arc beads on any of the bathroom wiring; similarly, the circuit breaker serving the bathroom wiring was not tripped. Arc mapping would lead one to state that the fire did NOT start in the bathroom. Continued work processing the scene showed that there was a GFCI in another bathroom but protecting this bathroom. This GFCI was tripped. During the fire, the Hot and Ground leaked to one another at a level of 6 mA or more, or the neutral and ground faulted to each other during the fire. Either condition would be brought on by invasive thermal heat, degrading the type NM insulation. Similarly, these conditions cause the GFCI to trip, taking away power from the downstream bathroom.*

Goodson brought the impact of RCD devices to the fire investigation community in 1999[10]. He addressed the issue again at ISFI in 2016. Nevertheless, the authors collectively run into many fire investigators who are unable to see why the RCDs and their properties are important.

GFCI Breaker — GFCI breakers reside in a breaker panel. The breaker portion of the device is a conventional 15- or 20-amp T-M (thermal magnetic), per UL 489. In addition, this MCCB contains ground fault protection. The output hot and neutral is run in opposing directions through an internal toroid. Should the currents differ from the other by about 6 mA, the circuit is interrupted — BOTH poles are removed from the load. It is further noted that this device does not need a working ground to cause tripping when the ~ 6 mA differential is exceeded. The allowed time to trip follows (per UL 943)[11]:

$$T = \left(\frac{20}{I}\right)^{1.43}$$

Where I is the current in mA, and T is the time in seconds allowed for the device to respond. However, the actual response time is much less. Testing by Goodson of several GFCIs (not GFCI breakers) made by Cooper Industries showed an average trip time of 31 mS when a 10 mA fault is created between the line and ground. Per the formula, 2.7 seconds is allowed.

This device also responds to a downstream ground to neutral fault; should they touch — both output poles (hot and neutral) are removed from the load. Testing of several GFCI breakers made by Square D showed that with a 2-ohm resistor placed between the load side neutral and the ground of the GFCI, the GFCI would never trip. At a 1 ohm short between output neutral and ground, the N G fault was immediately detected, and the GFCI shut down in less than 100 mS.

GFCI Receptacle — This has the same operation as the GFCI portion of the GFCI breaker, only it is mounted and installed as part of a duplex outlet receptacle. The GFCI protects loads plugged in the receptacle and downstream loads. It does not respond to overloads. It will sense a hot to ground fault (short circuit) but will not respond to a hot to neutral fault (short circuit).

Ground Fault Equipment Protector — This device works like a GFCI, but trips at higher levels, such as a 30 or 50 mA differential. It is not reliable in protecting against electric shock injury, because of its higher trip level (relative to the 6 mA GFCI trip level). Rather, it is designed to protect equipment from catastrophic destruction.

Leakage Current Detection Interrupter — LCDIs are permitted as an alternative to AFCIs in accordance with Section 440.65 of the *National Electrical Code* (NEC)[12]. LCDI power supply cord assemblies use a special cord employing a shield around the individual conductors and are designed to interrupt the circuit when a leakage current occurs between a conductor and the shield. The LCDI is often found on cord sets for window air conditioning units and contains the male blades.

> ***440.65*** *— Single-phase cord- and plug-connected air conditioners shall be provided with one the of the following factory-installed devices:*
>
> 1. Leakage current detector-interrupter (LCDI)
>
> 2. Arc-fault circuit interrupter (AFCI)
>
> 3. Heat detecting circuit interrupter (HDCI).

Appliance Leakage Current Interrupter — ALCI is an appliance leakage current interrupter. The main difference between the GFCI and ALCI is that GFCI not only senses current imbalance, but it also has the ability to identify improper wiring. The ALCI does not have that feature. Having either an open neutral or a neutral-ground short will trip GFCI right away, whereas an ALCI will not detect these hazards. ALCIs are used as components on appliances, where these wiring conditions can be guaranteed. Typical applications for ALCI are portable appliances such as bathroom heaters, carpet cleaners, power washers, and hair dryers. ALCI devices are used to protect customers from immersion electrocution. The ALCI will trip if the portable appliance is immersed in grounded water (i.e., sink, tub, etc.).

Immersion Detection Circuit Interrupter — An IDCI is a component device that interrupts the supply circuit to an immersed appliance. When a conductive liquid enters the appliance and contacts both a live part and an internal sensor, the device trips when current flow between the live part and the sensor exceeds the trip current value. The trip current may be any value below 6 mA sufficient to detect immersion of the connected appliance. The function of an IDCI is not dependent on the presence of a grounded object, in applications in accordance with Section 422.41 of the NEC.

422.41 — Cord- and plug-connected, free-standing appliances subject to immersion. Cord- and plug-connected, free-standing appliances and hand-held hair dryers shall be constructed to protect personnel against electrocution when immersed while in the "on" or "off" position.

Arc Fault Circuit Interrupter — An arc fault circuit interrupter is a device that analyzes current flow to a load and determines whether or not abnormal arcing is taking place. We first define "normal" arcing, the kind of arcing that occurs during the usual operation of a load or appliance. For example: arcing at a switch when a light is turned off or on; arcing between brushes and a commutator in a drill motor or small appliance; and arcing internally to a fluorescent light bulb. These are examples of normal arcing that do not start fires (we specifically exclude fires caused by spark ignition of fugitive vapors here).

An example of abnormal occurring is that associated with a loose connection. Current increases and decreases are analyzed by the AFCI, and a "signature" is developed; i.e., what do the changes in current look like? The signature is then classified as to its mode — normal or abnormal. The AFCI then removes power from the load. The AFCI is mentioned with the RCD devices because some AFCIs installed in the United States also have GFCI protection built in.

Field Case Studies

Below are representative field case studies that have relied on some of the principles of arc mapping. It is worth noting that absence of arcing is sometimes just as important as finding arc beads.

Field Case Study No. 1

A 6-foot length of bare 16 AWG 2 SJT (Junior Service) cable was found on an outdoor porch, plugged into an exterior GFCI receptacle mounted on the wall of a residence. The SJT was found with both conductors fractured distally. The GFCI had not tripped. The upstream OCP was provided by a 20-amp T/M breaker found in the tripped position. The temperature in the utility closet where the load center was located had not singed or discolored the paper calibration tags on the circuit breaker body. The NM cable from the circuit breaker to the GFCI

had no arc damage; the NM cable was examined both grossly and microscopically. Downstream type NM wiring protected by the GFCI was found to be completely bare in places but without arc damage. No loads were present on the circuit, except for whatever the Junior Service cord was feeding.

The question is why something tripped the breaker. No physical cause, however, was noted; there were no indications of arcing or overloading on the type NM on this branch circuit. Breakers can trip from heat, but the breaker was not abnormally hot. This would indicate that the SJT was not all recovered (also indicated by fractured ends), and one would expect that the additional missing wiring (and possibly load) would explain why the breaker would have tripped.

Field Case Study No. 2

A large (30,000-square-foot) three-story mansion caught fire. The fire department responded twice to the fire, having to receive alarms from the smoke detection system. Seeing no smoke or flame, the firefighters twice departed the house. On the third visit of the fire department, the house was seen to be well engulfed in flame. The mansion was a total loss.

Many of the fire investigators determined the area of origin to be in a utility closet. This was the area of lowest burn, and the area immediately outside the closet had no fire damage. Examination of a type NM cable in this room showed that it was bare but with no arcing. The cable fed a set of lighting sconces located at the front door.

During the investigation, the interview of a neighbor showed that the neighbor had taken numerous photos of the mansion during the fire. One of the photos showed that the sconces were illuminated well into the fire. This illumination (obviously) could not have happened if the fire began in the utility closet.

Field Case Study No. 3

A fairly new window AC unit was seen catching on fire in a security video. Examination of the window unit showed a motor with good windings, wiring that in no instance had arcing, a good capacitor, and an intact line cord with an intact LCDI. We could not tell whether the LCDI had tripped, as the unit had been handled after the fire.

A product's liability lawsuit was undertaken. The video was clear as to both the fire's cause and origin. The defense position was that any AC unit that caught fire would have to arc internally on the wiring — a very valid point, in that most of the wiring inside the AC unit was bare.

Testing of the same brand LCDI showed that when a fire starts in the AC unit, the generated plasma causes the LCDI to trip. More particularly, the line cord terminates in the AC unit such that an internal fire will be detected and cause the plasma to bridge between the conducive pieces on the LCDI triggering circuit, causing a cessation of power. The cause of the fire was a leaked refrigerant line. The refrigerant oil, dispersed as an atomized mist, caught fire, and the ion-rich plasma tripped the LCDI.

Field Case Study No. 4

A decorated soldier from the Iraq war lived with his family in an apartment complex in Kentucky. The family paid increased rent such that they had access to a private locking "closet" to store bicycles, sporting goods, and the like. A fire occurred at the apartment complex, and its origin was determined to be the unlocked storage closet rented by the family. The soldier was charged with arson.

Several lengths of type NM cable passed through the closet. They were never made available for examination, but the pictures showed them to be bare secondary to heat damage. The prosecution maintained that because the cables were protected upstream by AFCIs, the cables could never arc.

AFCIs detect arcing by developing a signature. This signature takes several cycles of data (minimum) to be analyzed. During that time, a hot to ground fault (arc) can occur and ignite combustibles. The point of this case scenario is that AFCIs detect and respond to repetitive arcs — a single arc event will not cause the AFCI to trip. Likewise, the single arc event can occur without the AFCI tripping.

Field Case Study No. 5

The fire involved an older residence. Wiring was of type NM, and (as best as could be traced out) every circuit had one or more instances of arcing present. Some of the conductors were severed by arcing, and some did not sever the wiring. The unusual feature of this fire was that the load center had a large number of breakers, but only a few of that number tripped.

This fire demonstrates one of the underlying assumptions of arc mapping — arc events are short-lived because a breaker trips or wires repel (or sever), and continuity is lost; these short lives of the arc events result in the rapid

Figure 5
Federal Pacific Electric (FPE) panel.

transition in the copper from the melt to non-melt regions. When a breaker is slow to trip, this can result in multiple arc sites being present or in the wiring having the appearance of the melt. A typical FPE breaker panel is shown in **Figure 5**.

Field Case Study No. 6

A fire occurred in a large room. The local authorities first thought it was an incendiary fire. However, they could not rule out a fire of electrical origin. An engineer was hired. He examined the evidence, with his report reading as follows:

> *No signs of electrical overheating were found in the evidence analyzed, based upon the scene examination, within a degree of scientific probability. Damage to the circuits found to date is consistent with fire attack to the circuits.*

Based on the engineering report, the fire was ruled arson. There was a suspect, and he was convicted and sent to prison. The defendant was later exonerated of the crime and filed suit against the electrical engineer for generation of a misleading report.

At one end of the large room, there was an open load center. At least five instances of arcing were found in the load center. These instances of arcing were all attributed to external fire attack (the word consistent was used). The problem with the word consistent is that the investigators are not looking for facts that are consistent; they are looking for uniqueness. It is well known that an arc site that started a fire cannot, in and of itself, be distinguished from an arc site that resulted from an external heat attack of an energized conductor.

In this case, a wrongful arson conviction occurred and demonstrated the issue of *reliability*. Arc mapping was utilized and was deemed to have eliminated electricity as a cause of the fire. In this case, the origin and cause personnel examined a report. The report eliminated electrical causes. With the elimination of electrical, the arson case could be filed. The problem, though, was a lack of communication between the engineer and the investigator. For the engineering opinion to be reliable, the engineer had to be aware of the circumstances associated with the fire; that is, the fire originated within, attacked, and caused arcing within the load center. Without the two investigators talking to one another, reliability was sacrificed.

Discussion

Arc mapping is a scientific tool. Its use is based on scientific and engineering principles. The underlying premise is sound: *An energized cable will allow arcing to develop between two conductors carrying different potentials when then the insulation is sufficiently damaged (compromised), and further, that the arc damage will occur where the breech of insulation was sufficient to allow conduction between conductors at two different potentials.*

In considering the reliability of arc mapping, guidance can be sought from NFPA 921[1], which includes laboratory verification, similar to confirming canine hits for possible ignitable liquids.

With arc mapping, the location of the arc sites is just as important as the lack of arcing in other areas. The Buc and Reiter paper et al, noted earlier, clarifies that some arc sites could only be found microscopically. With this being the case, one has to ask if it's necessary to retain all wiring for a laboratory exam and confirm every arc site with lab work. If one cannot see all arcs without using a microscope, is it possible that arcs in the field may be missed? This answer is, obviously, "yes." This factor alone immediately indicates that arc mapping has reliability issues unless *all* wiring is examined in the laboratory.

The 16 areas of competency of NFPA 1033[5] dictate that the fire investigator should have an understanding of electrical systems in a building, and the introduction of new wiring devices requires the investigator remain current in their knowledge and training. NFPA 921[1] also indicates that a fire investigator should be able to perform arc mapping. The quality of the work performed is highly dependent upon the skills and training of the person who is carrying out the task. This is where the authors have concerns with the use of arc mapping when carried out by someone other than a forensic engineer, especially if other circuit devices are not considered, or the absence of arcing directs a fire investigator to another area that is not the true area of origin. The fire investigator may be able to map out and locate arc damage on an older structure but may have difficulty on a newer structure fire. The various nuances of how each device operates are likely beyond the training of many investigators. Moreover, there are times when a laboratory examination will yield details contrary to what was deduced at the fire site. To wit,

> *A residential fire occurs. In the area of origin, there is found a "home run" length of type NM (14/2 AWG w/ ground). The type NM is bare for about 6 feet in this area of origin. The breaker serving the NM has tripped. Examination of the bare conductors by way of palpation revealed no nodules or discontinuities (i.e., no arc damage). The load center is in a closet which did not suffer elevated temperatures. There are no downstream loads present.*

How does one analyze this situation? Possible explanations are:

1. The circuit breaker had tripped for some other reason before the fire.

2. The cable was unpowered during the fire.

3. The area of origin is wrong.

However, there is also a fourth explanation: the research by Reiter et al has shown that some instances of arcing were so small in his testing that they could only be identified with microscopy[8]. Another possibility is an arcing event may occur that leaves no identifiable marks, even to the microscopist. The lesson to be learned here is that the absence of arcing (as noted in the field) should be at least verified by microscopy in the lab.

Finally, fire investigators and electrical engineers benefit from open communication and working together in the field when arc mapping is performed. Coordination of efforts and understanding circuits, circuit breakers, and residual current devices is best performed on-site.

Legal Cases and Expert Testimony Involving the Use of Arc Mapping

For arc mapping evidence and testimony to be admissible, the data must meet the Daubert and a federal rule of evidence governing admission of expert testimony. *Daubert v. Merrell Dow Pharm., Inc.*, 509 U.S. 579, 113 S. Ct. 2786 (1993). Factors that may be considered in determining the soundness of the scientific methodology include, but are not limited to:

1. Testing — Whether the theory or technique can be and has been tested;

2. Peer Review and Publication — Whether the theory or technique has been subjected to peer review and publication;

3. Error Rates and Standards — What is the known or potential rate of error and the existence and maintenance of standards; and

4. General Acceptance — Whether the theory or technique used has been generally accepted.

Rule 702 simply requires that: (1) the expert be qualified; (2) the testimony address a subject matter on which the fact finder can be assisted by an expert; (3) the testimony be reliable; and (4) the testimony "fit" the facts of the case (quoting Fed.R.Evid. 702 advisory committee's note).

The advantages and limitations of arc mapping as a principal indicator of fire origin are well known by forensic fire investigative expert practitioners. Nevertheless, an increase in criticisms concerning the limitations of arc mapping methodology as a fire investigation tool for the accurate inference of area of fire origin conclusions are on the rise in the relevant scientific community. Several of the criticisms cited in court cases that fire investigators should be prepared to both address and include:

1. Overpromises on the technique's precision,

2. Exaggerated inferences from the available data,

3. Failure to adequately account for potential methodological flaws,

4. Deficient scientific rigor in establishing evidentiary fire origin-related reliability,

5. Errors due to deficient practitioner training and experience, and

6. Indeterminate findings based upon subjective visual analysis.

In *Glassman v. Home Depot USA, Inc.*, 2018 WL 3569344 (C.D. Cal.), an experienced electrical engineer performed an arc map survey and thereafter confirmed the fire investigator's area of origin was "on the top of a workbench in the garage." The arc mapping expert then surveyed the designated area of fire origin for ignition sources and formed an "initial hypothesis was that a [defendant] Ryobi charger or battery sitting in the charger [on the workbench] was the cause of the fire." After a laboratory CT scan of the benchtop battery revealed that it was not manufactured by defendant Ryobi and was not the hypothesized ignition source, the expert's ignition scenario and area of origin morphed into a "Ryobi batter[y] that investigators recovered *from the floor of the garage*." (emphasis added). The court subsequently stated: "[t]o say this raises an eyebrow is an understatement," but irrespective of the arc mapping expert's "serendipitous changes of heart," ultimately ruled that his "opinions were shaky but admissible."

In P*owell v. State Farm Fire & Casualty*, Case No. 2:15-cv-13342 (E.D. MI 2016), after a basement fire occurred, the fire investigator initially determined that "[a] n electrical issue caused the fire. It started above the circuit breaker panel involving the service conductor where it comes into the house." The defendant insurance company thereafter transferred the fire claim to its large loss team and retained an electrical engineer to perform an arc mapping analysis to "rule out electrical." The arc mapping expert performed a single visual on-scene examination and determined that "the branch circuit conductors and associated electrical components located in the area of interest were not causal elements of the fire." Armed with this conclusion, the fire investigator's area of origin mutated into "in the ceiling space, ["on top of a suspended ceiling tile in the basement bathroom"] approximately 21 inches east of the west wall and east of the circuit breaker panel." The fire expert's rehabilitated fire classification opinion metamorphosed into incendiary due to "the introduction of combustible material on top of a lay-in-ceiling and ignited with an open flame."

Clearly, the fluctuating hypotheses in the above cases resulted from the misapplication of validated methods or deficiencies in qualitative analysis. Fire investigators continue to be reminded that in *Gen. Elec. Co. v. Joiner*, 522 U.S. 136, 146, 118 S. Ct. 512, 519 (1997), the Court noted that:

> *conclusions and methodology are not entirely distinct from one another. Trained experts commonly extrapolate from existing data. But nothing in either Daubert or the Federal Rules of Evidence requires a district court to admit opinion evidence that is connected to existing data only by the ipse dixit of the expert. A court may conclude that there is simply too great an analytical gap between the data and the opinion proffered.*

The above cases exemplify potentials for analytical gaps between the available data and the opinions reached.

The jury is still out where arc mapping methodologies are concerned. According to Novak "[A]rc mapping is a continuing topic of debate within the fire investigation community[14]." "The (ATF) Fire Research Laboratory (FRL) also recommends further training and research on the principles and use of arc mapping in fire investigation[15]."

Additional legal cases involving arc mapping are listed under References.

Conclusions

Arc sites have to be carefully identified, characterized. They should be laboratory verified where questionable, and their location in a compartment and within a circuit documented and described, including the type, presence, and absence of various circuit and appliance protection devices. Because arc mapping may support an area of origin — the most essential first step of fire investigation — the results should be based on a transparent and scientific methodology with careful consideration of its limitations[16]. The weight or reliability of the arc mapping depends on a thorough investigation and understanding of electrical and circuit protection basics. Fire investigators should be aware of and prepared to address limitations, current criticisms, and legal issues, including the *Daubert* criterion[17].

Cited and Related Legal Cases

Argonaut Ins. Co. v. Samsung Heavy Industries Co. Ltd., 929 F. Supp. 2d 159 (N.D. N.Y. 2013)

Burgett v. Troy-Bilt LLC, No. CIV. 12-25-ART, 2013 WL 3566355 (E.D. Ky. July 11, 2013)

Carroll v. Otis Elevator Co., 896 F.2d 210, 212 (7th Cir.1990)

Cole's Tool Works v. Am. Power Conversion Corp., 2009 WL 1298236 (N.D. Miss. 2009)

Connecticut Nat. Bank v. Germain, 503 U.S. 249 (1992)

Daubert v. Merrell Dow Pharm., Inc., 509 U.S. 579, 113 S. Ct. 2786 (1993)

Deherrera v. Decker Truck Line, Inc., 820 F.3d 1147, 1160 (10th Cir. 2016)

Derienzo v. Trek Bicycle Corp., 376 F. Supp. 2d 537 (S.D.N.Y. 2005)

Diet Drugs (Phentermine/ Fenfluramine/Dexfenfluramine) Product Liability Litigation, 706 F.3d 217 (3d Cir. 2013)

Gen. Elec. Co. v. Joiner, 522 U.S. 136, 146, 118 S. Ct. 512, 519 (1997)

Gladden v. Solis, 2011 WL 2274179 (E.D. Pa. 2011).

Glassman v. Home Depot USA, Inc., 2018 WL 3569344 (C.D. Cal.)

Hayes v. Carroll, 314 S.W.3d 494, 504 (Tex. App. 2010)

Kumho Tire Co. v. Carmichael, 526 U.S. 137 (1999)

Locklear v. Colvin, 2014 WL 6606572 (E.D.N.C. 2014)

Meemic Ins. Co. v. Hewlett-Packard Co., 717 F. Supp. 2d 752 (E.D. Mich. 2010)

Mirena Ius Levonorgestrel-Related Prod. Liab. Litig. (No. II), 2018 WL 5276431 (S.D.N.Y. 2018)

Occidental Fire & Cas. of North Carolina v. Intermatic Inc., 2013 WL 4458769 (D. Nev.)

Paoli R.R. Yard PCB Litigation, 35 F.3d 717 (C.A.3 (Pa.) 1994)

People v. Leahy, 8 Cal. 4th 587, 612, 882 P.2d 321 (1994)

Powell v. State Farm Fire & Casualty, Case No. 2:15-cv-13342 (E.D. MI 2016)

Primrose Operating Co. v. Nat'l Am. Ins. Co., 382 F.3d 546, 562 (5th Cir. 2004)

Pyramid Techs., Inc. v. Hartford Cas. Ins. Co., 752 F.3d 807 (9th Cir. 2014)

Ruiz-Troche v. Pepsi Cola of Puerto Rico Bottling Co., 161 F.3d 77 (1st Cir. 1998)

Scottsdale Ins. Co. v. Deere & Co., 115 F. Supp. 3d 1298 (D. Kan. 2015)

Stagl v. Delta Air Lines, Inc., 117 F.3d 76 (2d Cir. 1997)

State v. Montalbo, 73 Haw. 130, 138, 828 P.2d 1274 (1992)

State v. Sharp, 928 A.2d 165 (Law. Div. 2006)

Trimboli v. State, 817 S.W.2d 785, 790 (Tex. App. 1991)

United States v. Bonds, 12 F.3d 540, 560 (6th Cir. 1993)

United States v. Crabbe, 556 F. Supp. 2d 1217 (D. Colo. 2008)

United States v. Palo, 168 F.3d 503 (9th Cir. 1999)

U.S. ex rel. M.L. Young Const. Corp. v. Austin Co., 2005 WL 6000505 (W.D. Okla. Sept. 29, 2005).

Walters v. S & F Holdings LLC, 2015 WL 5081689 (D. Colo. 2015)

Wal-Mart Stores, Inc. v. Merrell, 313 S.W.3d 837, 840 (Tex. 2010)

Whiting v. Boston Edison Co., 891 F. Supp. 12, 24 (D.Mass.1995)

Wilson v. Petroleum Wholesale, Inc., 904 F. Supp. 1188, 1190 (D. Colo. 1995)

Cited References

1. National Fire Protection Association. 2021. NFPA 921: Guide for Fire & Explosion Investigations. Technical Committee on Fire Investigations.

2. Delplace, M., & Vos, E. 1983. Electric short circuits help the investigator determine where the fire started. Fire Technology, 19(3), 185-191.

3. Carey, N.J. PhD thesis, 2009. Developing a reliable systematic analysis for arc fault mapping. Centre for Forensic Science - Pure & Applied Chemistry. 2009, University of Strathclyde, Glasgow.

4. Carey, N., & Daeid, N.N. 2010. Arc mapping. Fire and Arson Investigator, 61(2), 34-37.

5. National Fire Protection Association. 2014. NFPA 1033, Standard for Professional Qualifications for Fire Investigator. National Fire Protection Association, Quincy, MA.

6. Babrauskas, V. 2018. Arc Mapping: A Critcal Review, Fire Technology 54, 749-780 (2018).

7. West, L., & Reiter, D.A. 2005. Full-Scale Arc Mapping Tests, Fire & Materials Conference, San Francisco.

8. Buc, E., Reiter, D., Battley, J. Sing, T.M., & Sing, T.M. 2013. Method to Characterize Damage to Conductors from Fire Scenes Proc. Fire and Materials.

9. UL 489 Standard for Molded Case Circuit Breakers (MCCBs), Underwriters Laboratories..

10. Goodson, M.E.1999. GFIs and Fire Investigation, Fire & Arson investigator, January 1999.

11. Goodson, M.E. & Davis, K.R. 2016. Arc mapping in the advent f AFCI, GFCI and GFEP Circuit Protection Devices, ISFI Proceedings, ISFI 2016.

12. National Fire Protection Association, Section 440.65 of the National Electrical Code.

13. Atlass Insurance Group, 1300 South East 17th Street, Suite 220, Fort Lauderdale, FL 33316, https://goatlassinsurance.com/560/homeowners-insurance/electrical-panels-may-prevent-getting-insurance Last downloaded November 25, 2018.

14. Novak, C. 2018. ATF Fire Research Laboratory, Letter to the Editor in Response to 'Arc Mapping: A Critical Review', Fire Technology Vol. 54, Number 5, September 2018.

15. Arc Mapping as a Tool for Fire Investigation (ATFFRL-TB-170001 March 17, 2017).

16. Icove, D.J. & Haynes, G.A. 2018. Kirk's Fire Investigation, 8th Edition. Pearson, New York, NY.

17. May, T.R & Icove, D.J. 2020. Arc Mapping Methodologies & the Pursuit of Magical Globules, Notches & Beads: A Bridge Too Far to Establish Fire Origin? Lincoln Memorial University UL Rev., 7, p. 37.

Computer Fire Modeling and the Law: Application to Forensic Fire Engineering Investigations

By David J. Icove, PhD, PE, DFE (NAFE 899F) and Thomas R. May, MS, JD

Abstract

Computer fire modeling can be a two-edged tool in forensic fire engineering investigations. Professional standards of care recommend that fire modeling's primary use is in examining multiple hypotheses for a fire as opposed to determining its origin. This paper covers the current acceptable benefits of computer fire models, historical and pending legal case law, and methods to use modeling results within expert reports and testimony. Particular issues reviewed are the use of animations versus simulations, evidentiary guidelines, and authentication using verification and validation studies.

Keywords

Fire modeling, forensic fire engineering investigation, Frye and Daubert challenge, animations, simulations, verification and validation (V&V), admissibility of evidence, expert reports, expert testimony

Introduction

Computer fire modeling is now commonplace in support of complex forensic fire and explosion investigations involving fatalities and significant monetary losses, although models have existed since the 1960s[1]. Fire modeling initially centered on explaining, verifying, and validating the physical phenomena of fires.

Fire scientists and forensic engineers are using open source programs developed by the National Institute of Standards and Technology (NIST), which have undergone verification and validation (V&V) by the U.S. Nuclear Regulatory Commission (NRC). These scientists and engineers have pushed the acceptability and application of fire modeling out of laboratory conditions and into the world of forensic fire scene reconstruction[2-9]. Early successes of fire modeling in the field of fire litigation and reconstruction led the way to define its usefulness[10-12]. In addition, selected peer-reviewed references further underscore its application[12-14].

Computer fire models constitute independent scientific evidence (e.g., scientific tests) under legal rules to simulate or reconstruct a fire event, draw inferences from existing information, and analyze complex mathematically driven theories. Therefore, the evidentiary standards and rules of admissibility for scientific computer-generated displays ultimately determine whether increasingly complex expert testimony and visual illustrations will be presented to fact finders. Although the rules in state and federal courts do not specifically address computer-generated displays' admissibility, the existing rules are adequately flexible to provide sufficient management of the ever-developing cases and controversies.

It is imperative for any advocate of computer fire modeling to comprehend and remain current regarding the legal rules implicated in the admission or exclusion of scientific evidence at administrative hearings and trials. After all, an unfavorable evidentiary ruling involving essential case facts is a lost opportunity to narrate a hypothesis at a minimum and could potentially have the adverse effect of changing the case result in its entirety.

Selection/Application of Computer Fire Models

Computer fire modeling (particularly of structures) can render a wide range of acceptable uses — mainly when used in forensic fire scene reconstructions. However, in choosing the "right tool for the job," the user must have insight into the model's purpose and bounded conditions[15].

Fire models are not limited solely to forensic engineering applications. Early work at NIST[16] defined the various broader areas that fire modeling can be applied,

David Icove, PhD, PE, DFE, PO Box 1348, Knoxville, TN 37901-1348, (865) 693-4361, icove@utk.edu

which include, but are not limited to:

- Avoiding repetitious full-scale fire testing;
- Establishing flammability of materials;
- Helping designers and architects increase the flexibility and reliability of performance-based fire codes;
- Identifying needed fire research;
- Assisting in fire investigations and litigation.

Fire modeling in forensic cases can assist in extending the interpretation of existing data, incorporating peer-reviewed historical findings, and evaluating the incapacitating impact of byproducts of combustion on humans[14,17]. However, the proper fire model's selection and use is the decision of the forensic engineer or investigator[15]. The following available classes of fire models are recognized for use by fire investigators[1] who perform a wide range of calculations:

- *Spreadsheet* — Calculates mathematical solutions for interpretations of actual case data[5,18-20];
- *Zone* — Calculates the fire environment through two homogeneous zones[7,21-25];
- *Field* — Calculates the fire environment by solving conservation equations, usually using finite-element mathematics[9,14,26-36];
- *Post-flashover* — Calculates time-temperature history for energy, mass, and species and is useful in evaluating structural integrity in fire exposure[37-39];
- *Fire protection performance* — Calculates sprinkler and detector response times for specific fire exposures based on the response time index[34,40-44];
- *Thermal and structural response* — Calculates the structural fire endurance of a building using finite-element calculations[45-57];
- *Smoke movement* — Calculates the dispersion of smoke and gaseous species[21,58-70];
- *Egress* — Calculates the evacuation times using stochastic modeling using smoke conditions, occupants, and egress variables[71-76].

The atypical/uncommon use of two or more computer fire models by an investigator, such as a first-order calculation followed by a more accurate model, may help the expert self-peer-review the bounds of a fire scenario. This methodology can be accomplished by first approaching the fire scenario using a spreadsheet calculation of first-order relationships followed by a zone and even a field model.

Peer-reviewed findings[77] show that when applying the multiple model approach in three different apartment fire scenarios, the reported results were in relatively good agreement, particularly in the early stages of the fire. Using simpler models is cost-effective, less time-consuming, and can confirm the order of magnitude of the results from more complex models.

Finally, engineering guidelines and standards exist for selecting, applying, and determining computer fire models' accuracy through exhaustive reviews and testing. The Society of Fire Protection Engineers publishes guidelines[78-80] along with ASTM International[81-84]. The National Fire Protection Association NFPA 921's *Guide to Fire and Explosion Investigations*[85] Chapter 22 on "Failure Analysis and Analytical Tools" devotes an entire section to the guidance for the use of fire models along with their limitations in forensic fire investigations. Understanding, applying, and referencing these standards enhance the benefits derived from the investigator's application to forensic cases, support their conclusions, and subsequently can be upheld during scrutiny in expert challenges in court.

Challenges to the Use of Computer Fire Modeling in Forensic Fire Investigations

V&V is a formal process of establishing acceptable uses, suitability, and limitations of fire models. Verification determines that a model correctly represents the developer's conceptual description. Validation determines that a model is a suitable representation consistent with scientific evidence of the real world and is capable of reproducing phenomena of interest[3].

What concerns both expert witnesses and the courts is the reliability of computer fire models to predict the fires' common features accurately. These features include upper-layer temperatures and heat fluxes, generation of toxic byproducts of combustion, and activation of smoke alarms, heat detectors, and sprinkler systems. For example, NRC's V&V studies compare actual fire test results

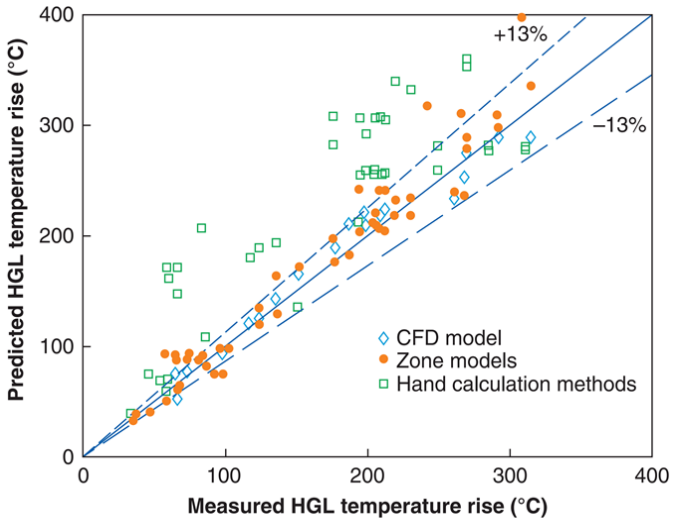

Figure 1
NRC verification and validation studies showing the comparison of hot gas layer (HGL) temperatures measured in full-scale tests compared with predictions of hand calculations, zone models, and FDS models. A predicted +/-13% variability range is included. Note that the hand calculations tended to overpredict layer temperatures, whereas both zone and field model predictions were generally within variability limits.

and predictions of hand calculations, zone models, and field models. As shown in **Figure 1**, when the models are applied correctly to fires that are in their incipient stage of development and pre-flashover, there is general agreement among them and the variability of real-world fires.

Mathematical, experimental, physical, structural, computational, and input/output uncertainties are an unfortunate reality when choosing which computer fire models to apply. To maintain the trustworthiness of computer fire modeling, the users of this technology are challenged to: (a) mitigate error by ensuring the use of quality input data; (b) quantify and articulate uncertainties that can inherently plague the underlying calculations; and (c) ensure that quality expert judgment is used when introducing and utilizing computer fire modeling as evidence during testimony and trials.

The United States Nuclear Regulatory Commission (NRC) has written a 2,000+ page series of V&V manuals to analyze various computer fire models. These documents contain voluminous materials on computer fire modeling uncertainties that are inherent in the models. Also, manuals accompanying the computer software contain disclaimers that can be used to attack even the most attentive practitioner.

Use of Animations Vs. Simulations

Anytime computer-generated materials are entered into evidence, whether in an expert report, a hearing, or a courtroom proceeding, the report's admission will likely be scrutinized. Computer-generated exhibits typically fall into two general categories: animations or simulations. An animation is an artificially created continuation of events, while a simulation determines the missing components or data that led up to the event[86].

Animations

Reconstructions using fire modeling often involve the computer-generated approach. Suggested definitions by Morande[87] propose that animation should be viewed as merely a computer-generated set of snapshots used to guide and illustrate a witness's testimony. The key here is that animations are precisely that — interpretations of what a witness perceives to be an incident's outcome.

It is important to note that the animation alone needs a qualified expert to draw conclusions and generate opinions derived from this computer-generated animation. For example, an experienced radiologist would interpret x-rays or computed tomography (C.T.) scans. Although an animation is not substantive evidence, its use at trial is governed by the Rules of Evidence.

Animations are demonstrative aids that are used to illustrate and support a witness's testimony and opinion. Testimony is utilized to recreate the event; an animation has secondary relevance to the issues and does not depend on the proper use of scientific rules. Animations are admissible in a court of law if they supplement a witness's verbal description of the transpired event, clarify some issue in the case, and are more probative than prejudicial.

Simulations

Morande[87] defines that a simulation is computer-generated substantive evidence. A simulation creates a series of scaled diagrams strung together to produce what appears to be a moving image. For example, NIST's CFAST and FDS computer models generate data interpreted by a program known as Smokeview[88]. This visual data consists of a combined series of frames that (in rapid sequence) produce a movie.

However, the Smokeview visualization of each data frame is associated with a specific predicted time by FDS in the fire event. The data frames can be played back at a single rapid, real-time, or slow-motion rate. What sets these approaches apart is that a simulation utilizes one or more programs, which, after inputting data, use scientific formulas to produce conclusions based on that data

regarding issues material to the trial. The results produced by a simulation's programming are equivalent to the opinions reached by an expert witness.

Figure 2 illustrates how a fire pattern analysis of an existing fire scene can use image pattern recognition and a generic first-order algorithm describing fire dynamics (fuel package, virtual origin, fire plume, ceiling jet) complemented with an actual FDS fire model simulation showing heat flux exposure to interior surfaces.

Subsequently, when computer-generated simulations are offered into evidence, it is admissible if both its reliability and general acceptance into the scientific community are established. The reliability of fire modeling software is generally of high quality.

Evidence law is in flux with regard to foundational evidentiary issues associated with computer-generated animations and simulations. The initial inquiry involves distinguishing between animations and simulations.

Simulations are substantive evidence based upon scientific and physical principles rather than merely illustrative testimonial aids[87]. Data input and analysis supplants eyewitness testimony in an attempt to recreate an event to arrive at factual determinations that have independent evidentiary value. When simulations are used, fact finders are asked to rely upon mathematical calculations, computer processes, and expert scientific assumptions; in essence, the computer becomes a second witness[87].

When computer-generated evidence supplies missing information to prove a disputed material fact, assist an expert in forming an opinion, or test an expert's hypothesis, more rigorous assessments of reliability and validity are necessary before the authentication and admissibility of the proposed computer fire model can take place[85].

Admissibility of Computer Fire Models

Authentication of the Computer Fire Model

When considering the introduction of a computer fire model in ligation, authentication of evidence is a prerequisite to its admissibility. The Rule of Evidence 901 deals with this issue, stating:

(a) In General. To satisfy the requirement of authenticating or identifying an item of evidence, the proponent must produce evidence sufficient to support a finding that the item is what the proponent claims it is.

(b) Examples

(1) Testimony of a Witness with Knowledge. Testimony that an item is what it is claimed

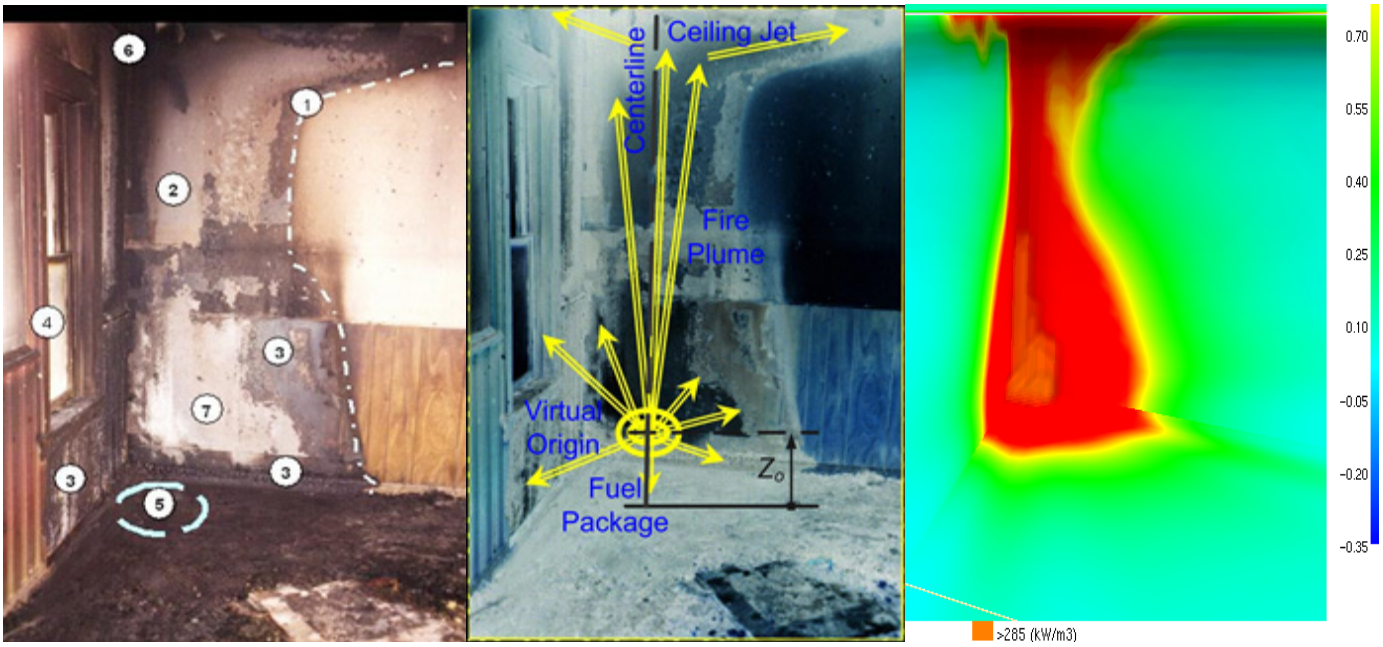

Figure 2
Example fire pattern analysis using (a) fire pattern indicators, (b) image pattern recognition and a generic algorithm describing fire dynamics (fuel package, virtual origin, fire plume, ceiling jet), and (c) an actual FDS fire model simulation showing heat flux exposure to interior surfaces. Courtesy: DJ Icove, University of Tennessee.

to be * * *.

(2) Evidence About a Process or System. Evidence describing a process or system and showing that it produces an accurate result.

Whether or not a result can be verified by another means can affect the ability to authenticate it. "Fire modeling can normally be considered as the prediction of fire characteristics by the use of a mathematical method which is expressed as a computer program[11]."

Admissibility of Evidence

There exists as a general rule, for evidence to be admissible in a court of law, the proposed exhibit:

(a) must be relevant (e.g., tend to prove or disprove a fact that is of consequence in the case);

(b) must have probative value that is not substantially outweighed by unfair prejudice, must not mislead or confuse the jury, be a waste of time or needlessly cumulative;

(c) must be authenticated (e.g., proven to be genuine and what it is purported to be);

(d) must not be hearsay or fall within an exception to hearsay;

(e) must constitute the "best evidence";

(f) if offered as an opinion, must conform to the attendant lay or expert rules;

(g) if offered as scientific evidence, then must meet the standards for admission;

(h) if offered as demonstrative evidence, must be relevant, material, and competent; and

(i) must not violate any other rule of evidence[86].

In a nutshell, evidentiary rules require a judge to determine if the expert is qualified, if their opinion is relevant and reliable, and if the proposed testimony will assist the factf inder.

Laying a Foundation for the Admission of Computer-Generated Evidence

The proponent of a computer fire model must clear two legal hurdles before the computer-generated exhibit is admitted into evidence: A foundation must be laid that is based upon what the advocate is attempting to prove (e.g., simulation or animation), and the model must negotiate a balancing test (Rule 403) to demonstrate that the evidence is more probative than prejudicial.

The testifying expert's qualifications must demonstrate that she: is qualified in the specific field of computer fire modeling and is qualified in the technique of generating a computer simulation or animation based on specific input data[89].

Computer fire models must satisfy the Daubert factors (testing, peer review, error rates, acceptability in the relevant scientific community) or any other applicable test in the jurisdiction[85]. In addition, the underlying mathematical model will be scrutinized to ensure that: (a) the chosen factors are correctly measured; (b) the selected factors are relevant and inclusive; (c) the underlying mathematical formulae and simplification procedures are appropriate; (d) the numerical tools were accurately applied; and (e) the problem was adequately translated into the model[1].

After this, foundation testimony will be required to confirm: (a) the reliability of the data underlying the computer-generated evidence; (b) the authentication of the computer equipment and the principles used in the software program; (c) the integrity and security of the computer system; and (d) the security of the output[1,83,85,89].

A computer fire modeling expert should expect questions in reference to:

- Details about how the animation/simulation was generated,
- What information was used in creating the computer-generated evidence,
- How the information used was collected,
- The appropriateness of the mathematical model,
- How the computer fire modeling program accurately processes the input information,
- The specific methodology employed,
- The facts and evidence on which their opinion is based and relied upon in reaching conclusions,

- How their expert judgment relates to the available physical evidence, and
- Any technical or scientific assumptions that have been made[80,85,89,90].

Admissibility of Demonstrative Vs. Substantive Evidence

Computer fire models may be admitted into a court of law as demonstrative or substantive evidence. Demonstrative evidence has no probative value standing alone, but merely serves as a visual aid to help the fact finder (e.g., jury) in comprehending the verbal testimony of a witness. This type of evidence is tethered to other material testimony in order to be relevant and is admissible to the same extent as the associated testimony[86].

Demonstrative evidence, such as graphics, charts, diagrams, and models, are generally admissible if the item constitutes a "fair representation" of the evidence it purports to represent[91]. In general, if a computer-generated presentation meets the requirements of the rules of evidence — and does not exceed the scope of the evidence it is intended to explain or clarify — it can be admitted at trial as a demonstrative exhibit.

Conversely, substantive evidence is defined as "that which is offered to establish the truth of a matter to be determined by the trier of fact[92]." This type of evidence has independent evidentiary value and is offered to prove a crucial fact at issue in the litigation. "Computer-generated simulations used as substantive evidence or as the basis for expert testimony regarding matters of substantive proof must have been generated from computer programs that are generally accepted by the appropriate community of scientists to be valid for the purposes at issue in the case[92]."

A note of interest: Even though a computer fire model could be inadmissible as substantive evidence due to not being properly authenticated, a jury may be allowed to view the simulation during the course of expert witnesses' testimony at trial, solely as a demonstrative exhibit.

Rule 403 and the Exclusion of Relevant Evidence

Rule 403 is sometimes utilized to exclude relevant evidence that may nevertheless pose a danger of diverting jurors with inequitable considerations that could impair the reaching of a rational decision based solely on relevant facts. In most legal settings, however, the Rule favors the admission and not the exclusion of evidence.

Rule 403. Excluding Relevant Evidence for Prejudice, Confusion, Waste of Time, or Other Reasons

The court may exclude relevant evidence if its probative value is *substantially* outweighed by a danger of one or more of the following: unfair prejudice, confusing the issues, misleading the jury, undue delay, wasting time, or needlessly presenting cumulative evidence (*emphasis added*).

Reasons for excluding computer fire models include:

- Susceptibility to and ease of manipulation,
- Convincing impact (e.g., seeing is believing, CSI effect),
- Confusion of the jury,
- A disadvantage to opponents who cannot afford to create computer fire models, unjustifiable reliance of jurors due to familiarity with computers, and/or
- A belief that the animation/simulation is an actual recreation of the event[92].

Admissibility of Expert Testimony

Admissibility and Rule of Evidence 702

The admission of computer fire models into evidence requires the testimony of an expert and is therefore governed by Daubert and Rule of Evidence 702 — Testimony by Expert Witnesses:

A witness who is qualified as an expert by knowledge, skill, experience, training, or education may testify in the form of an opinion or otherwise if:

(a) the expert's scientific, technical, or other specialized knowledge will help the trier of fact to understand the evidence or to determine a fact in issue;

(b) the testimony is based on sufficient facts or data;

(c) the testimony is the product of reliable principles and methods; and

(d) the expert has reliably applied the principles and methods to the facts of the case.

The Frye Standard and Admissibility

The Frye standard is a "general acceptance" test that

is utilized to determine the admissibility of scientific evidence[93]. Expert opinions that are based on a scientific technique are only admissible when the technique is widely used and generally accepted as reliable in the relevant scientific community. The reliability of the conclusion is not at issue with Frye — only the reliability of the methodology[93]. In a nutshell, head counting in the relevant scientific community is utilized to determine if the methods or principles used to produce the conclusion is generally accepted. In its tally, courts often consider scholarly articles, journals, and affidavits to gauge the state of knowledge in the appropriate community of scientific experts[94].

The Frye test was conceived to keep unproven junk science out of the courtroom. However, the test also prevented the introduction of novel and innovative scientific techniques and inhibited courts from receiving beneficial cutting-edge scientific evidence[87]. In 1993, many courts replaced the Frye test with the Daubert factors test, a more flexible standard entailing the contemplation of a variety of factors[95].

Daubert Factors and Admissibility

Daubert utilizes the Frye "general acceptance" test as only one factor in consideration of the reliability and admissibility of scientific evidence. While Frye offers some protection by ensuring that scientific theories are generally accepted in the scientific community, Daubert offers added protection because it applies more criteria to determine whether the proffered evidence is the consequence of reliable methodology. In fact, scientific evidence can be validated in court even before it has generally been accepted in the scientific community.

The four (core) non-exhaustive Daubert criteria[96] for evaluating the admissibility of expert testimony are:

1. Whether the methods upon which the testimony is based are centered upon a testable hypothesis;

2. The known or potential rate of error associated with the method;

3. Whether the method has been subject to peer review; and

4. Whether the method is generally accepted in the relevant scientific community.

Expert witnesses should prepare to address with specificity the above criteria explicitly mentioned in Daubert and discuss how the criterion is satisfied and, when appropriate, why the factor is not relevant or does not apply.

The understanding, explanation, or application of Daubert factors to scientific evidence is evolving and, as a result, erroneous explanations and applications (e.g., methodology, peer review) routinely appear in published and unpublished opinions. As a result, admissibility analyses are not a predictable endeavor.

Daubert challenges usually arise soon after an expert submits a report and a deposition has been taken. However, if an in limine motion challenging an expert's qualifications and/or proposed testimony is denied during the pretrial phase, an expert has been afforded a window into opposing counsel's likely approach to cross-examination at trial. Beware: Challenges may also be raised in the first instance on voir dire or during cross-examination.

Historical Legal Cases on Computer Fire Modeling

Two prevailing historical court cases help define and illustrate how expert weathers the acceptance and rejection of computer fire modeling. In both cases, experienced expert witnesses professionally presented their findings, yet the courts came to separate conclusions regarding the admissibility of their fire modeling. One overriding premise in these cases was how effectively peer-reviewed findings and reliance on V&V studies were introduced, along with documentation on the general acceptance of fire modeling in the field of fire investigation.

The following are brief summaries of the two cases[97]:

Turner v. Liberty Mutual Fire Insurance Company. Turner v. Liberty Mut. Fire Ins. Co., 2007 WL 2428035 (N.D. Ohio)]. In this case, a trial court held that the National Institute of Standards and Technology (NIST) Fire Dynamics Simulator (FDS, Version 4.0) computer simulation proffered by the defendant's expert satisfied the Daubert reliability test[98] governing expert testimony.

In the analysis of the Turner case, the plaintiff allegedly left his home to run errands, and shortly thereafter, the structure was "fully engulfed in flames." Photos taken by a passerby captured the progression of the fire at the incipient stage until total destruction had occurred. Public as well as private fire investigators classified the fire as undetermined. After this, an expert was employed by the defendant to conduct an "evaluation involving an analysis of the progression of the fire." The expert utilized

computer fire modeling to reach the conclusion that the fire was "incendiary and accelerated."

The plaintiff filed suit for breach of contract and bad faith after his insurance claim was denied, and subsequently moved to exclude the testimony of the computer fire modeling expert.

In its analysis, the court ruled that the computer simulation was reliable and admitted it into evidence because:

(a) the software had been tested ("a number of small- and large-scale experiments [had been conducted to validate FDS" e.g. "S*eptember 2005 Computer Simulation of the Fires in the World Trade Center Towers Abstract*");

(b) "[t]he software has been adequately subject to peer review and publication" ("NIST Special Publication 1018's acknowledgment section includes three pages of peer reviews and contributions while its bibliography lists 152 sources from which the technical data has been drawn");

(c) known software error rates could appropriately be addressed during cross-examination ("NIST FDS cautions that two components of its calculations — flow velocities and temperatures — have error rates of 5% to 20%. However, plaintiff notes the 5% to 20% figure does not represent an overall error rate");

(d) "computer simulation methodology is 'generally accepted' by the 'relevant scientific community'" (citing NFPA 921 and "its use in three recent nationally recognized fires: the World Trade Center collapse, the Rhode Island nightclub fire, and the South Carolina sofa store fire").

In *Santos v. State Farm Fire & Cas. Co.*, 28 Misc. 3d 1078, 905 N.Y.S.2d 497 (Sup. Ct. 2010), the general acceptance of computer fire modeling for use in determining fire origin and causation was at issue in New York, a Frye state.

The plaintiff contended that the engineering expert's proposed computer fire model was unsuited for and not generally utilized to determine fire origin and causation. The plaintiff's fire investigation expert opined that computer fire modeling is not generally accepted as an investigative tool in the fire investigation community due to speculation related to building construction and materials used — and also that the computer fire model could not be used to determine fire causation.

The opposing expert, a professor with a PhD in chemistry, testified that: (a) "the underlying equations and laws of physics [related to computer fire modeling] have been generally accepted in the fire science community;" (b) "fire modeling of fire dynamics is not a new science;" (c) his testimony was not to "state the cause and origin of the fire but rather to apply the computer dynamics to see how the fire would spread;" (d) "the results of the fire modeling established that there was a timeline that matched a particular origin of the fire, that the damage in the building corresponded to the results of the modeling, and that the determination of fire dynamics in that particular theory [the timeline] is generally accepted for that purpose;" (e) and"[t]he computer fire modeling essentially verified the hypothesis as to the ignition source or cause of the fire [and is] "never * * * accepted for determining the origin of the fire [but can help in determining the cause]."

The court's analysis led to exclusion of the computer fire model because:

(a) "[w]hile computer fire modeling may be generally accepted in the scientific community for predicting the course of fires given a particular set of circumstances and, therefore, useful in fire prevention and safety, [the expert] has not demonstrated its general acceptance in fire investigation;"

(b) [f]ire modeling carries with it a 15% to 20% margin for error assuming all conditions are correct but could be as high as 80 percent depending upon the real conditions [and the expert] acknowledged that there could be a difference between the material represented in a table and the actual material at the fire scene;"

(c) the regulatory agencies that utilize computer fire modeling (the Department of Energy and Nuclear Regulation Commission, the Department of Defense, the Department of Agriculture and ATF) "are involved in risk assessment as opposed to fire investigation based on scientific standards;"

(d) "[t]hese models in general are designed to start with the ignition of a fire under preset conditions and predict the time factors and conditions of growth and sometimes decay. They are not

designed to recreate a particular fire by working backward from a set of final observations to determine what the starting or even intermediate conditions were."

Preparing for Challenges to Your Use of Computer Fire Models in Forensic Fire Investigations

Rule 26 Expert Witness Reports

In court cases, the best method to reduce the successful challenge of your use of computer fire modeling in forensic investigations is in the preparation of a comprehensive written report.

A "written report prepared and signed by the witness" is a prerequisite to expert witness testimony[99]. Courts will utilize the report, in part, to consider Rule 702 and Daubert issues to determine relevancy, reliability, and qualifications. In theory, an expert witness is only allowed to testify to the facts and opinions contained in the expert witnesses' report[100].

An expert report must contain:

(a) A complete statement of all opinions the witness will express and the basis and reasons for them;

(b) The facts or data considered by the witness in forming them;

(c) Any exhibits that will be used to summarize or support them;

(d) The witness's qualifications, including a list of all publications authored in the previous 10 years;

(e) A list of all other cases in which, during the previous 4 years, the witness testified as an expert at trial or by deposition; and

(f) A statement of the compensation to be paid for the study and testimony in the case[101].

Failure to provide all of the information required by Rule can lead to preclusion as an expert. Conformity with Rule 26 facilitates Rule 702 admissibility if the expert witness report contains, at a minimum: (a) facts and data utilized to reach opinions held; (b) a thorough explanation of methodologies used; and (c) authoritative bases relied upon. Rule 26 also requires post-report disclosures of information in the report that is unfinished or requires supplementation. Changes that should have been included in the initial report are prohibited[102]. Beware: Opposing counsel's cross-examination may pose hypothetical questions based upon the facts not contained within the expert witness report.

Summary and Conclusions

Computer fire modeling can be a valuable tool in forensic fire engineering investigations. The forensic engineer or knowledgeable investigator must implement professional standards of care within their expert reports and testimony to ensure that the model exhaustively examines multiple hypotheses for a fire or explosion as well as address error rates. Based upon the current acceptable uses of computer fire models, experts must be prepared to contemplate the underpinnings of historical and pending legal case law, as well as methods to impart the results of modeling into expert reports and testimony. Experts should also be aware of the particular issues regarding the use of animations versus simulations, evidentiary guidelines, and authentication using verification and validation studies.

References

1. Icove DJ, Haynes GA: Kirk's Fire Investigation, Eighth edn. Ny, Ny: Pearson; 2018.

2. Mitler HE, Rockett JA: Users' Guide to FIRST, a Comprehensive Single-Room Fire Model. In. Gaithersburg, MD: National Bureau of Standards; 1987: 138.

3. Salley MH, Kassawar RP: Verification and Validation of Selected Fire Models for Nuclear Power Plant Applications: Main Report. In., vol. 1, NUREG-1824 edn. Washington, DC: U.S. Nuclear Regulatory Commission; 2007.

4. Salley MH, Kassawar RP: Verification and Validation of Selected Fire Models for Nuclear Power Plant Applications: Experimental Uncertainty In., vol. 2, NUREG-1824 edn. Washington, DC: U.S. Nuclear Regulatory Commission; 2007.

5. Salley MH, Kassawar RP: Verification and Validation of Selected Fire Models for Nuclear Power Plant Applications: Fire Dynamics Tools (FDTS). In., vol. 3, NUREG-1824 edn. Washington, DC: U.S. Nuclear Regulatory Commission; 2007.

6. Salley MH, Kassawar RP: Verification and Validation of Selected Fire Models for Nuclear Power Plant Applications: Fire-Induced

Vulnerability Evaluation (FIVE-Rev1). In., vol. 4, NUREG-1824 edn. Washington, DC: U.S. Nuclear Regulatory Commission; 2007.

7. Salley MH, Kassawar RP: Verification and Validation of Selected Fire Models for Nuclear Power Plant Applications: Consolidated Fire Growth and Smoke Transport Model (CFAST). In., vol. 5, NUREG-1824 edn. Washington, DC: U.S. Nuclear Regulatory Commission; 2007.

8. Salley MH, Kassawar RP: Verification and Validation of Selected Fire Models for Nuclear Power Plant Applications: MAGIC In., vol. 6, NUREG-1824 edn. Washington, DC: U.S. Nuclear Regulatory Commission; 2007.

9. Salley MH, Kassawar RP: Verification and Validation of Selected Fire Models for Nuclear Power Plant Applications: Fire Dynamics Simulator (FDS) In., vol. 7, NUREG-1824 edn. Washington, DC: U.S. Nuclear Regulatory Commission; 2007.

10. Bukowski RW, Spetzler RC: Analysis of the Happyland social club fire with HAZARD I. Journal of Fire Protection Engineering 1992, 4(4):117-130.

11. Babrauskas V: Fire Modeling Tools for FSE: Are They Good Enough? Journal of Fire Protection Engineering 1996, 8(2):87-96.

12. DeWitt WE, Goff DW: Forensic Engineering Assessment of FAST and FASTLite Fire Modeling Software. National Academy of Forensic Engineers 2000:9-19.

13. Emmons HW: Why fire model? The MGM fire and toxicity testing. Fire Safety Journal 1988, 13(2–3):77-85.

14. Christensen AM, Icove DJ: The application of NIST's fire dynamics simulator to the investigation of carbon monoxide exposure in the deaths of three Pittsburgh fire fighters. Journal of Forensic Sciences 2004, 49(1):104-107.

15. Mowrer FW: The Right Tool for the Job. SFPE Fire Protection Engineering Magazine 2002, 13(Winter):39-45.

16. Mitler HE: Mathematical modeling of enclosure fires. In. Gaithersburg, MD: National Institute of Standards and Technology; 1991.

17. Nelson HE, Tu K-M: Engineering analysis of the fire development in the Hillhaven Nursing Home fire, October 5, 1989: National Institute of Standards and Technology, Building and Fire Research Laboratory; 1991.

18. Mowrer FW: Spreadsheet Templates for Fire Dynamics Calculations. In. College Park, MD: University of Maryland; 2003: 91.

19. Iqbal N, Salley MH: Fire Dynamics Tools (FDTs): Quantitative Fire Hazard Analysis Methods for the U.S. Nuclear Regulatory Commission Fire Protection Inspection Program. Washington, DC; 2004.

20. Peacock RD, Reneke PA, Bukowski RW, Babrauskas V: Defining Flashover for Fire Hazard Calculations. Fire Safety Journal 1999, 32(4):331-345.

21. Bailey JL, Forney GP, Tatem PA, Jones WW: Development and Validation of Corridor Flow Submodel for CFAST. Journal of Fire Protection Engineering 2002, 12(3):139-161.

22. Hoover JB: Application of the CFAST Zone Model to Ships — Fire Specification Parameters. Journal of Fire Protection Engineering 2008, 18(3):199-222.

23. Jones WW, Peacock RD, Forney GP, Reneke PA: CFAST – Consolidated Model of Fire Growth and Smoke Transport (Version 6) Technical Reference Guide. In. Edited by Fire Research Division BaFRL, NIST Special Publication 1026 edn. Gaithersburg, Maryland: National Institute of Standards and Technology; 2009.

24. Lee Y-H, Kim J-H, Yang J-E: Application of the CFAST zone model to the Fire PSA. Nuclear Engineering and Design 2010, 240(10):3571-3576.

25. Peacock RD, McGrattan K, Klein B, Jones WW, Reneke PA: CFAST – Consolidated Model of Fire Growth and Smoke Transport (Version 6) Software Development and Model Evaluation Guide. In. Edited by Fire Research Division BaFRL.

Gaithersburg, Maryland: National Institute of Standards and Technology; 2008.

26. Chen CJ, Hsieh WD, Hu WC, Lai CM, Lin TH: Experimental investigation and numerical simulation of a furnished office fire. Building and Environment 2010, 45(12):2735-2742.

27. Cheong MK, Spearpoint MJ, Fleischmann CM: Calibrating an FDS Simulation of Goods-vehicle Fire Growth in a Tunnel Using the Runehamar Experiment. Journal of Fire Protection Engineering 2009, 19(3):177-196.

28. Rinne T, Hietaniemi J, Hostikka S: Experimental validation of the FDS simulations of smoke and toxic gas concentrations. VTT, Finland 2007.

29. Jahn W, Rein G, Torero JL: A posteriori modelling of the growth phase of Dalmarnock Fire Test One. Building and Environment 2011, 46(5):1065-1073.

30. Lan X, Liang P, Long XF: Experimental Investigation and Numerical Simulation of Road Tunnel Fire. Prog Safety Sci Tech 2008, 7:673-678.

31. Lock A, Bundy M, Johnsson EL, Hamins A, Ko GH, Hwang C, Fuss P, Harris Jr RH: Experimental Study of the Effects of Fuel Type, Fuel Distribution and Vent Size on Full-Scale Underventilated Compartment Fires in an ISO 9705 Room. In. Gaithersburg, MD: National Institute of Standards and Technology; 2008: 168.

32. Ma TG, Quintiere JG: Numerical simulation of axi-symmetric fire plumes: accuracy and limitations. Fire Safety Journal 2003, 38(5):467-492.

33. Madrzykowski D, Vettori RL: Simulation of the Dynamics of the Fire at 3146 Cherry Road NE, Washington, DC, May 30, 1999. In: NISTIR 6510. Gaithersburg, MD: National Institute of Standards and Technology, Center for Fire Research; 2000.

34. Madrzykowski D, Walton WD: Cook County Administration Building Fire, October 17, 2003. In: NIST SP 1021. Gaithersburg, MD: National Institute of Standards and Technology; 2004.

35. McGill D: Fire Dynamics Simulator, FDS 683, Participants' Handbook. . In. Edited by School of Fire Protection SC. Toronto, Ontario, Canada; 2003.

36. McGrattan K, Hostikka S, McDermott R, Floyd J, Weinschenk C, Overholt K: Fire Dynamics Simulator User's Guide. In. Gaithersburg, MD: National Institute of Standards and Technology; 2014: 268.

37. Babrauskas V: COMPF: A Program for Calculating Post-Flashover Fire Temperatures. In. Berkeley, CA: Fire Research Group, University of California, Berkeley; 1975.

38. Babrauskas V, Peacock RD, Reneke PA: Defining Flashover for Fire Hazard Calculations: Part II. Fire Safety Journal 2003, 38:613-622.

39. Nelson HE: Fire Growth Analysis of the Fire of March 20, 1990, Pulaski Building, 20 Massachusetts Avenue, NW, Washington, D.C. In: NISTIR 4489. Gaithersburg, MD: National Institute of Standards and Technology, Center for Fire Research; 1994: 51.

40. Evans DD: Sprinkler fire suppression algorithm for HAZARD: U.S. Department of Commerce, National Institute of Standards and Technology; 1993.

41. Grosshandler WL, Bryner NP, Madrzykowski D, Kuntz KJ: Report of the Technical Investigation of the Station Nightclub Fire. In: NIST NCSTAR 2. vol. 1. Gaithersburg, MD: National Institute of Standards and Technology; 2005.

42. Alpert R: Calculation of Response Time of Ceiling-Mounted Fire Detectors. Fire Technology 1972, 8(3):181-195.

43. Evans D, Stroup D: Methods to Calculate the Response Time of Heat and Smoke Detectors Installed Below Large Unobstructed Ceilings. Fire Technology 1986, 22(1):54-65.

44. Milke JA, Hulcher ME, Worrell CL, Gottuk DT, Williams FW: Investigation of multi-sensor algorithms for fire detection. Fire Technology 2003, 39(4):363-382.

45. Babrauskas V: Charring Rate of Wood as a Tool for Fire Investigations. Fire Safety Journal 2005, 40(6):528-554.

46. Bai Y, Hugi E, Ludwig C, Keller T: Fire Performance of Water-Cooled GFRP Columns. I: Fire Endurance Investigation. J Compos Constr 2011, 15(3):404-412.

47. Chowdhury EU, Bisby LA, Green MF, Kodur VKR: Investigation of insulated FRP-wrapped reinforced concrete columns in fire. Fire Safety Journal 2007, 42(6-7):452-460.

48. Malanga R: Fire endurance of lightweight wood trusses in building construction. Fire Technology 1995, 31(1):44-61.

49. Palmieri A, Matthys S, Taerwe L: Experimental investigation on fire endurance of insulated concrete beams strengthened with near surface mounted FRP bar reinforcement. Composites Part B: Engineering 2012, 43(3):885-895.

50. Richardson LR: Thoughts and observations on fire-endurance tests of wood-frame assemblies protected by gypsum board. Fire and Materials 2001, 25(6):223-239.

51. Vytenis B: Charring rate of wood as a tool for fire investigations. Fire Safety Journal 2005, 40(6):528-554.

52. Ali F, Nadjai A, Choi S: Numerical and experimental investigation of the behavior of high strength concrete columns in fire. Eng Struct 2010, 32(5):1236-1243.

53. Ariyanayagam A, Mahendran M: Development of realistic design fire time-temperature curves for the testing of cold-formed steel wall systems. Front Struct Civ Eng 2014:1-21.

54. Buchanan AH: Structural Design for Fire Safety. Chichester, England; New York: Wiley; 2001.

55. Cyriax GR: An Investigation of Structural Damage by Fire - Reply. Concrete 1970, 4(5):174-&.

56. Izydorek MS, Zeeveld PA, Samuels MD, Smyser JP: Structural Stability of Engineered Lumber in Fire Conditions. In. Edited by Gandhi PD, Backstrom B. Northbrook, IL: Underwriters Laboratories; 2009: 95.

57. Perricone J, Wang M, Quintiere J: Scale Modeling of the Transient Thermal Response of Insulated Structural Frames Exposed to Fire. Fire Technology 2007, 44(2):113-136.

58. Baker R: Smoke generation inside a burning cigarette: Modifying combustion to develop cigarettes that may be less hazardous to health. Progress in Energy and Combustion Science 2006, 32(4):373-385.

59. Baker RR, Robinson DP: Semi-theoretical model for the prediction of smoke deliveries. In: Harare, Zimbabwe: Proceedings of CORESTA Congress. Smoke and Technology Groups; 1994: 63-72.

60. Barillo DJ, Brigham PA, Kayden DA, Heck RT, McManus AT: The fire-safe cigarette: a burn prevention tool. J Burn Care Rehabil 2000, 21(2):162-164; discussion 164-170.

61. Delichatsios M: Tenability conditions and filling times for fires in large spaces. Fire Safety Journal 2004, 39(8):643-662.

62. Fu Z, Hadjisophocleous G: A two-zone fire growth and smoke movement model for multi-compartment buildings. Fire Safety Journal 2000, 34(3):257-285.

63. Levin BC, Kuligowski ED: Toxicology of Fire and Smoke. In: Inhalation Toxicology. Edited by Salem H, Katz SA. Boca Raton, FL: CRC Press (Taylor and Francis Group); 2005: 205-228.

64. Lin C-C, Wang L: Forecasting smoke transport during compartment fires using a data assimilation model. Journal of Fire Sciences 2015, 33(1):3-21.

65. Lin CS, Yu CC, Wang SC: Numerical Investigation of Fire Dynamic Behavior for a Commercial Building Basement. Advanced Materials Research 2012, 594-597:2213-2218.

66. Jones WW, Quintiere JG: Prediction of Corridor Smoke Filling by Zone Models. Combustion Science and Technology 1984, 35(5-6):239-253.

67. Muhasilovic M, Duhovnik J: CFD-Based Investigation of the Response of Mechanical Ventilation in the Case of Tunnel-Fire. Stroj Vestn-J Mech E 2012, 58(3):183-190.

68. Mulholland GW: Smoke Production and Properties. In: SFPE Handbook of Fire Protection Engineering, 4th Edition. Edited by DiNenno PJ. Quincy, MA: National Fire Protection Association; 2008: Part 2, Chapter 13, 12-297.

69. NAS: Smoke and Toxicity, vol. 3. Washington, DC: The National Academies Press; 1978.

70. NAS: Flammability, Smoke, Toxicity, and Corrosive Gases of Electric Cable Materials. Washington, DC: The National Academies Press; 1978.

71. Jensen G: Wayfinding in heavy smoke: Decisive factors and safety products: Findings related to full-scale tests. IGPAS, . In.: InterConsult Group ICG; 1998.

72. Stewart RD, Newton PE, Hosko MJ, Peterson JE: Effect of Carbon Monoxide on Time Perception. Archives of Environmental Health: An International Journal 1973, 27(3):155-160.

73. Till RC: Timed egress requirements for transit and passenger rail station evacuation as described in NFPA 130. Ashrae Tran 2006, 112:246-250.

74. Yakush SE: Uncertainty of Tenability Times in Multiroom Building Fires. Combustion Science and Technology 2012, 184(7-8):1080-1092.

75. Jin T: Visibility Through Fire Smoke--Part 5, Allowable Smoke Density for Escape from Fire. In: Report No 42. Fire Research Institute of Japan; 1976: p. 12.

76. Jin T, Yamada T: Irritating Effects of Fire Smoke on Visibility. Fire Science and Technology 1985, 5(1):79-90.

77. Rein G, Bar-Ilan A, Fernandez-Pello AC, Alvares N: A Comparison of Three Models for the Simulation of Accidental Fires Journal of Fire Protection Engineering 2006, 16(3):183-209.

78. SFPE: Fires-T3: A Guide for Practicing Engineers. In. Edited by Models STGoDoC. Bethesda, MD: Society of Fire Protection Engineers; 1995.

79. SFPE: SFPE engineering guide—The Evaluation of the Computer Model DETECT-QS. Bethesda, MD: Society of Fire Protection Engineers; 2002.

80. SFPE: Guidelines for Substantiating a Fire Model for a Given Application. Society of Fire Protection Engineers, Bethesda, Maryland 2011.

81. ASTM-E1355: ASTM E1355 - 12 Standard Guide for Evaluating the Predictive Capability of Deterministic Fire Models. In: ASTM International Subcommittee E0533 on Fire Safety Engineering. 2012.

82. ASTM-E1472: ASTM E1472-07 Standard Guide for Documenting Computer Software for Fire Models (Withdrawn 2011). In: ASTM International Subcommittee E0533 on Fire Safety Engineering. 2007.

83. ASTM-E1591: ASTM E1591 - 20 Standard Guide for Obtaining Data for Deterministic Fire Models. In: ASTM International Subcommittee E0533 on Fire Safety Engineering. 2020.

84. ASTM-E1895: ASTM E1895 - 07 Standard Guide for Determining Uses and Limitations of Deterministic Fire Models (Withdrawn 2011). In: ASTM International Subcommittee E0533 on Fire Safety Engineering. 2007.

85. NFPA-921: NFPA 921 - Guide for Fire and Explosion Investigations, 2014 edn. Quincy, MA: National Fire Protection Association; 2017.

86. Lipson AS: Is it Admissible?: LexisNexis; 2017.

87. Morande DA: A Class of Their Own: Model Procedural Rules and Evidentiary Evaluation of Computer-Generated “Animations”. University of Miami Law Review 2007, 61:1069-1135.

88. Forney GP: Smokeview (Version 5) - A Tool for Visualizing Fire Dynamics Simulation Data: Volume I: User’s Guide. In. Gaithersburg, MD: National Institute of Standards and Technology; 2010.

89. NFPA-1033: NFPA 1033--Standard for Professional Qualifications for Fire Investigator. In. Quincy, MA: National Fire Protection Association; 2014.

90. Icove DJ, Crisman HJ: Application of pattern recognition in arson investigation. Fire technology 1975, 11(1):35-41.

91. Morales LI, Canales DA: Discoverability and Admissibility of Electronic Evidence. Advocate 2017, 79.

92. Webster V, Bourn III FE: The Use of Computer-Generated Animations and Simulations at Trial. Def Counsel J 2016, 83:439.

93. Imwinkelried EJ: The Best Insurance Against Miscarriages of Justice Caused by Junk Science: An Admissibility Test That Is Scientifically and Legally Sound. 2017.

94. Easton SD: Yer Outta Here-A Framework for Analyzing the Potential Exclusion of Expert Testimony under the Federal Rules of Evidence. U Rich L Rev 1998, 32:1.

95. Beyea J, Berger D: Scientific Misconceptions among "Daubert" Gatekeepers: The Need for Reform of Expert Review Procedures. Law and Contemporary Problems 2001, 64(2/3):327-372.

96. Daubert v. Merrell Dow Pharmaceuticals, Inc. In: F 3d. vol. 43: Court of Appeals, 9th Circuit; 1995: 1311.

97. See cases: Turner v. Liberty Mutual Fire Insurance Co. In.: Dist. Court, ND Ohio; 2007 and Santos v. State Farm Fire & Cas. Co., 28 Misc. 3d 1078, 905 N.Y.S.2d 497 (Sup. Ct. 2010) .

98. Kesan JP: Critical Examination of the Post-Daubert Scientific Evidence Landscape. Food and Drug Law Journal 1997, 52:225-251.

99. Mickus L: Discovery of Work Product Disclosed to a Testifying Expert Under the 1993 Amendments to the Federal Rules of Civil Procedure. Creighton L Rev 1993, 27:773.

100. Krafka C, Dunn MA, Johnson MT, Cecil JS, Miletich D: Judge and attorney experiences, practices, and concerns regarding expert testimony in federal civil trials. Psychology, Public Policy, and Law 2002, 8(3):309.

101. Zeigler JH, Geer JD: Recent Decisions on the FRCP Rule 26 Amendments Pertaining to Experts in Products Liability Cases. Defense Counsel Journal 2013, 80(1):59.

102. Wells D: In brief: Law 101: Legal guide for the forensic expert. NIJ Journal 2012(269):24-25.

Forensic Issues from the Investigation of a Marine Shaft Failure

By Stephen R. Jenkins, CPEng (NAFE 11)

Abstract

The starboard propeller shaft of a twin-screw diesel electric rail ferry in New Zealand failed just after the ferry left port. Weather was not a factor. The ship was on a regular schedule of three sailings a day. The starboard propeller was found in 120 meters of water approximately two nautical miles from the channel — some distance from the point where power was observed to reduce to zero on the shaft. The fracture surface of the shaft showed a classic fatigue failure pattern. However, there were questions to be answered, including what initiated the failure, and why a tension failure occurred in a shaft that was primarily under compression from the reaction forces of the propeller. This paper will look at some interesting factors in the investigation, the techniques used to limit the investigation (and its cost) to relevant areas, a few of the false trails that were followed, and the processes eventually used that were the most convincing.

Keywords

Marine shaft failure, fatigue, fretting, precision scanning, digital shape comparison, digital modeling

Introduction

On November 5, 2013 on a trip from Picton to Wellington the starboard shaft of a ferry failed shortly after the ship left the Tory Channel. Once on-board tests had established that the propeller had been lost, the ship proceeded on one shaft to Wellington harbor — where it berthed successfully, unloaded, and was then shifted alongside for investigations to commence.

An underwater survey revealed no hull damage and provided good high-resolution photographs of the fracture face, which was protected from corrosion by the cathodic protection systems on the ship. The fracture face was subsequently protected by a grease-filled cap, which was removed once the vessel was docked for repair to allow metallurgical examination.

The starboard propeller was found in 120 meters of water approximately two nautical miles from Tory Channel, standing upright, with one of the four blades embedded in the ocean floor. It was recovered on December 10, 2013 and returned to Wellington.

The propeller and the stub of the shaft, which was still retained in the propeller hub, were examined by the investigating team. It was noted at this time on the recovered starboard propeller that there was a small bend at the tip of the C blade — and that the suction faces of all blades showed varying degrees of surface cavitation damage (with the C blade showing the most severe damage). A review of recent underwater surveys showed that the bent tip was not present in the 2012 survey, but was noted as present (but not requiring any remedial action) in the 2013 survey by the Marine Class Surveyors and the owner's technical staff.

Background Information

The outline specification of the ship is as follows:

Ship type:	Passenger/ RORO cargo ferry
Built	1988
Service speed:	19.5 knots
Gross tons:	17,816
Deadweight:	5,464 tons
Number of propellers:	Two, 3.95 m diameter, four blade, fixed pitch inward rotating (currently fitted)
Total kW:	2 x 5,200 kW (6973 hp) at 160 rpm normal operating speed.
Drive system	Variable-frequency electric propulsion from LFO Generators through ABB SAMI Megastar system
Length B.P. (m):	183.5 (as modified by a midships extension in 2011)

The ship was lengthened by insertion of a 30-meter mid-section and fitted with new high-efficiency propellers in 2011. The extension did not affect any of the propulsion

Stephen Jenkins, CPEng, P.O. Box 1591, Wellington, New Zealand, 6140, +64 4 439 0282, jenkins@aurecongroup.com

Figure 1
Arrangement of shaft, propeller, and rudder. The exposed shaft end is where the starboard propeller was mounted before it was lost.

Figure 2
The port side arrangement is similar. In this photo, the new high-efficiency propeller is in place and rudder is inclined toward the camera.

equipment except for the fitting of the new propellers. There was no evidence of cracking or shaft damage when the old propellers were removed.

The general arrangement (**Figures 1** and **2**) of the stern equipment was symmetrical with each propeller followed by an in-line rudder. This close up (**Figure 3**) shows the area between the aft end of the stern tube and the hub of the propeller. **Figure 3** is the port side, which was undamaged; the starboard side was similar.

Initial Observations

The high-resolution underwater photographs (**Figure 4**) showed a distinctive pattern on the fracture face, which clearly indicated that the failure was a uni axial fatigue failure[1,2]. This type of failure is caused by a fluctuating force that increases and decreases stress on one side of the shaft and generates a fatigue fracture with a single origination point that progresses across the shaft from the side where the force is being applied and results in the final overload failure occurring on the opposite side from the fluctuating force.

Because fatigue failure is a cyclic process — and requires a tensile stress to drive crack growth — an early check was made to determine if the failure originated in the use of the astern mode (propeller reversal to reverse thrust) during docking that would generate tensile stresses in the main propulsion shaft. As the rotational speed of the propellers is fixed at 160 rpm and the operating schedule is regular, annual cycle calculations showed 4.6 million revolutions on full ahead versus 80,000 on full astern. The ship is also equipped with a 2 MW bow thruster that minimizes the use of asymmetric shaft rotation. The influence of astern operation was not significant in terms of fatigue life over the two years that the new propellers had been installed and was discounted.

Figure 3
The fracture in the starboard shaft occurred just inside the propeller hub.

It was noted that the fracture face was approximately 20 millimeters inside the propeller hub, and that a certain amount of damage to the propeller hub could clearly be attributed to relative movement between the two halves of the shaft as the failure progressed.

When the shaft stub was removed from the propeller hub, there were marks on both the shaft and the bore of the propeller that indicated there may have been fretting occurring at the shaft to propeller hub interface

(**Figures 5** and **6**). Fretting is a form of surface damage that occurs when there are very small relative movements between two surfaces in very close contact. Fretting is known to reduce the ability of steel shafts to resist fatigue loading. While it can facilitate the initiation of a fatigue crack, the full development of the crack into a fracture still requires a significant fluctuating force capable of driving the fracture through the body of the shaft[3].

Detailed measurements were undertaken of both components to eliminate the possibility that the propeller was off center. Within the tolerances of the measuring equipment, it was confirmed that the hub and shaft were both constructed in accordance with the original drawings.

Specialist examination by international ship repairers and marine surveyors established that the damage and the bent tip were repairable but noted there was evidence that cavitation had been originating at small defects on the leading edge and depressions on the propeller surface (**Figure 7**). Measurements also showed that there were some significant unexpected depressions on the propeller blades. The specialist expressed the opinion that the bent tip was typical of normal operational damage and was unlikely to have any significant effect on propeller performance — and did not represent a threat to the integrity of the propulsion system. Examination showed that the cavitation damage on the starboard propeller was most

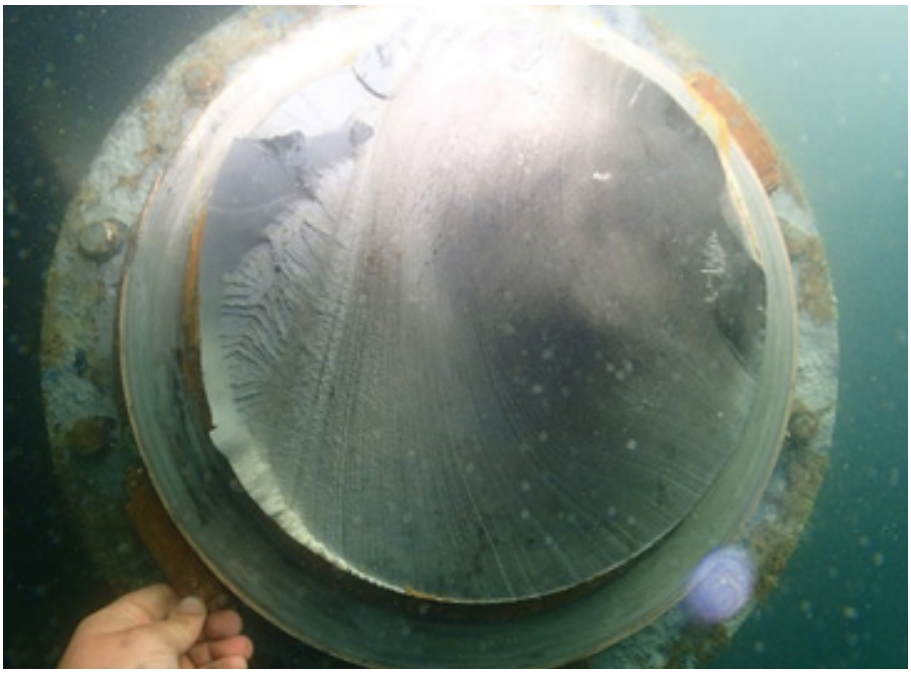

Figure 4
This fracture is distinctive and cannot be generated by any other loading pattern.

Figure 5
Fretting marks on the shaft stub.

Figure 6
Fretting marks and failure damage on the propeller hub.

Figure 7
Cavitation erosion caused by small indentations and poor edge form to the leading edge.

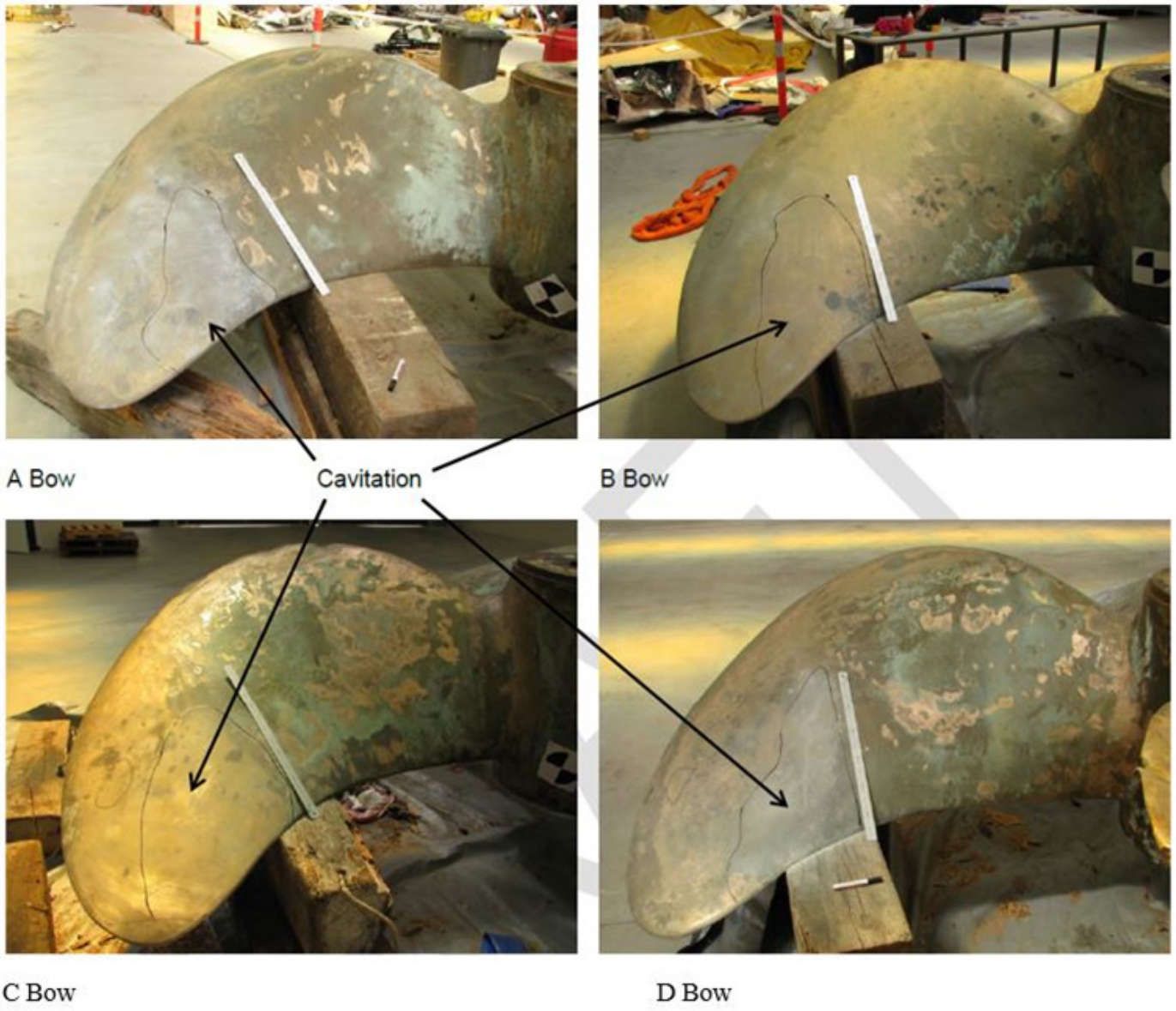

Figure 8
Cavitation patterns were observed on the suction (bow) side of the starboard propeller varying in depth and area. The C blade was the worst.

severe on the C blade (**Figure 8**).

To record the propeller shape for future analysis, the propeller was scanned using laser digital technology. Analysis of these scans showed possibly significant differences in shape between blades — particularly, the C blade (the blade with the most severe cavitation damage) appeared to be the most significantly different in terms of propeller form.

The bent tip of the C blade was measured, and an elastic/plastic analysis of the bend was done to determine the load that the creation of this bend would place on the shaft. The estimate of the instantaneous stress at 80 MPA was not sufficient to fracture the shaft or deform the propeller and was considered unlikely to have played a part in the initiation of the fatigue failure.

Some rough order finite element calculations were carried out to establish stress levels in the shaft at the plane where the fracture occurred but were inconclusive because of the many assumptions required to allow the model to be resolved, which the investigation team considered rendered the results of indicative value only. However, they did show that combined stresses, taking into account gravity loading, stresses from the interference fit, and torsion, could resolve into tensile principal stresses in the shaft in the area of the failure.

Figure 9
The fracture face on the tail shaft after removal of the protective cap.

Figure 10
Starboard rudder outboard side leading edge to right.
Arrow is at center line of propeller shaft.

Investigation in Singapore

Because of limitations of local dry docks in Australasia, the vessel sailed to Singapore on one shaft after modifications to allow all generators and drive systems to be applied to that shaft — and analysis and testing to ensure the remaining shaft was sound. Singapore was chosen because the dock was available, and there was extensive large marine repair experience there.

In the dry dock in Singapore, the fracture face on the starboard shaft was uncovered (**Figure 9**) and examined metallurgically in place. It was also noted that there was an unusual pattern of paint removal on the starboard rudder that was consistent with cavitation damage (**Figures 10** and **11**). This paint damage was not present on the port rudder.

Figure 11
Starboard rudder inboard side leading edge to left.
Arrow is at center line of propeller shaft.

It was noted that the paint damage on the inboard side of the rudder was significantly more than on the outboard side. It is known that there is a wide boundary layer called a wake field along the vessel hull and that hydrodynamic conditions in this boundary layer are different from the free field flows over most of the propeller operating volume. These facts were both relevant when evaluating the effects of the cavitation damage observed on the starboard propeller later.

The port propeller was examined in place and then removed. The end of the port tail shaft was also subjected

to magnetic particle inspection and detailed metallurgical inspection in place to see if there was any sign of distress or incipient failure — and to examine in detail the fretting damage that was also found under the port propeller hub. The surface of the propeller was closely examined for any evidence of cavitation damage. None was found.

Following in place examination, the tail shaft was removed, and a small section of shaft (which included the fracture face) was cut off and taken to a local independent metallurgical laboratory with marine equipment experience for detailed examination. The independent metallurgical laboratory in Singapore also examined the propeller seating area on the port shaft and reached the following conclusions:

1. There was no metallurgical defect at the origin of the fatigue failure on the starboard shaft.

2. There was no surface damage from fretting at the origin of the fatigue failure on the starboard shaft.

3. Fretting damage on the port shaft was more severe than on the starboard shaft.

4. There was no sign of cracking or incipient failure on the port tail shaft.

5. In their opinion, the fracture was caused by a significant uniaxial fluctuating bending forces.

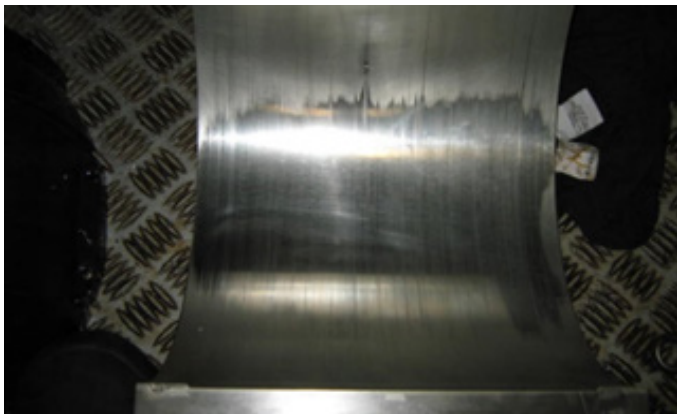

Figure 12
Starboard aft bearing.

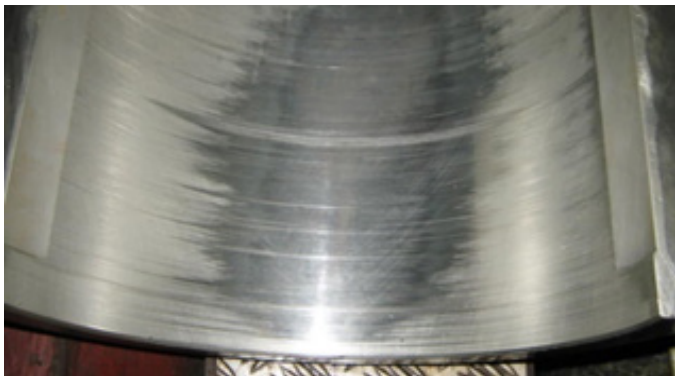

Figure 13
Port aft bearing.

While in Singapore, the alignment of the shafts was thoroughly checked and the bearings examined for signs of vibration damage. While the alignment was found to be less than satisfactory, there was no damage to the bearings that could be attributed to vibration. There was a small area of fatigue failure on both aft stern tube bearings, which was consistent with normal loading (**Figures 12** and **13**). There was no wiping of the bearing material, and no unusual wear patterns when assessed against ISO 7146-1:2008 *Plain Bearings Appearance and Characterisation of Damage to Metallic Hydrodynamic Bearings Part One General*.

Given that bearing position and condition is a significant element in the onset of vibration, it was considered unlikely that vibration had been a problem with the original drive configuration.

Late in the repair process, it was discovered that the rudder stocks were cracked and that the starboard rudder stock had growing fatigue fractures on the port and starboard sides, indicating that some force had been bending the rudder stock from side to side. This is consistent with the expected loading that fractured the shaft and with the variation in paint damage on opposite sides of the rudder. Both rudder stocks were replaced.

Investigation Plan

Given the wide range of potential causes — and the somewhat random pattern of acquisition of information during a long investigation — a key strategy was the comparison of the port and starboard propulsion systems, since they were identical when constructed, yet the port system showed no signs of distress or incipient failure even under detailed metallurgical examination during the dry docking in Singapore.

From this, the investigation team was able to include or eliminate factors by comparison between the two systems. If something was the same on both systems — and it had not initiated a failure on the port shaft — it was assessed as being unlikely to be a root cause of the failure. If a significant difference existed between the two systems, this difference was assessed as requiring further

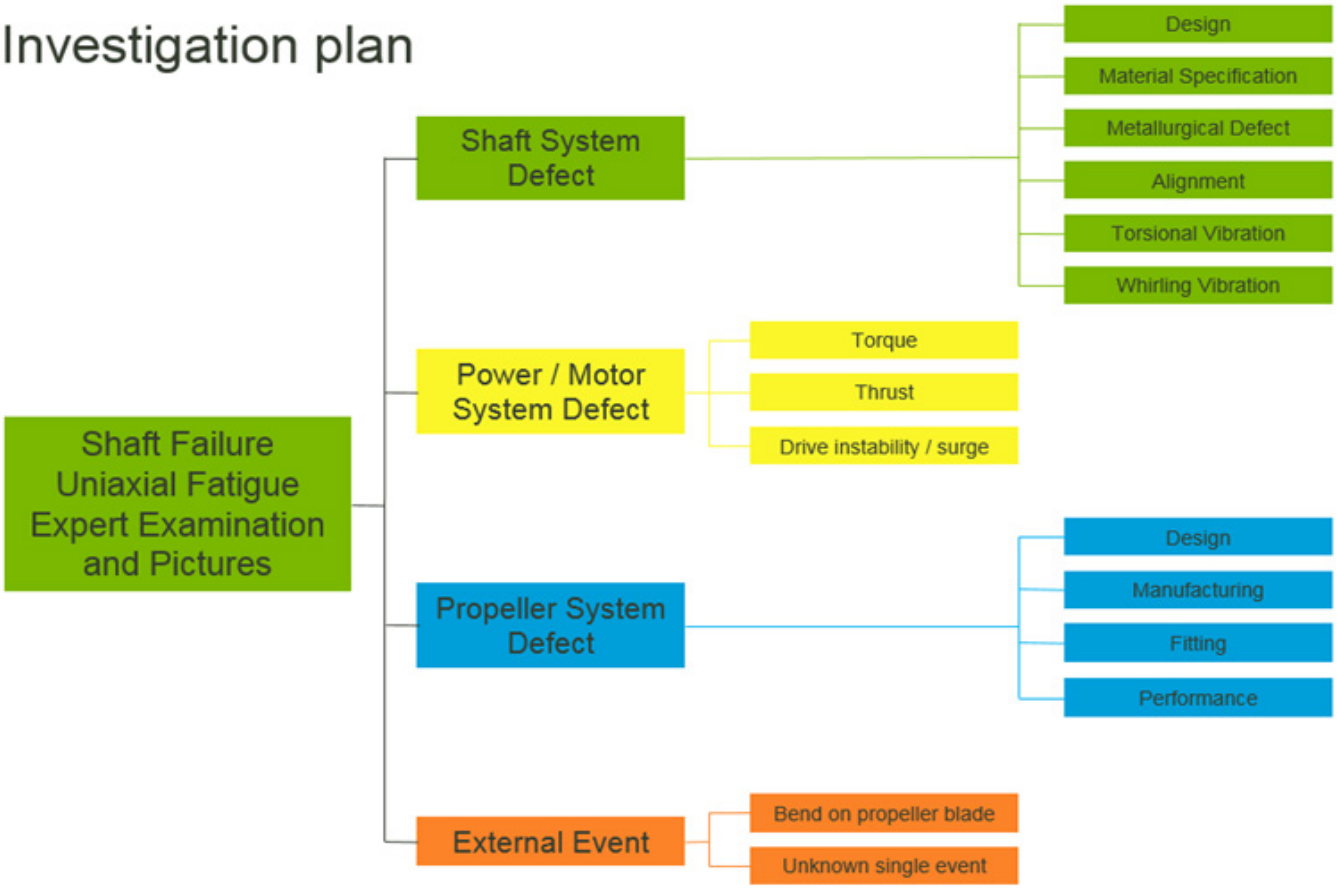

Figure 14
Detailed investigation plan.

detailed examination as a possible root cause.

To provide some structure, the system was analyzed and divided into four primary systems based on operational elements of the propulsion system. These were the propeller, shaft, power and motor system, and an external event (**Figure 14**). Observations were accumulated under each heading and potential causes evaluated with a view to confirming or eliminating their possible contribution.

External Event

There was always a possibility that the fracture had been initiated by some external event, such as an impact with a floating object. However, the nature of a fatigue fracture is that it occurs over time, so the single event does not remove the need for a uniaxial fluctuating force.

There were no reports in the ship's log of any significant impact incidents.

Power and Motor System Defect

The nature of forces in the drive system allow the defects to be considered in three areas: the torque or twisting forces in the shaft that turn the propeller; the thrust in the shaft that pushes the ship through the water; and some instability in the electrically controlled drive motor system.

Torque

The first important fact is that the motor and drive system of the ship had not changed specification since the original build so the possibility of an overload in the shaft from the system was remote.

In addition, a torque failure produces a characteristic fracture that runs at 45° to the main axis of the shaft (**Figure 15**), and is completely different from the uniaxial

Figure 15
A typical torque failure.

fatigue failure observed on the starboard shaft. On this basis, a failure related to torque can be positively ruled out.

Thrust

The new high-efficiency propellers produced 7% more thrust than the original propellers fitted to the ship. This is well within the design safety factors. If it had been a problem, we would expect to see evidence of this on both systems as they are identical. In addition, a uniaxial fatigue failure requires tensile stresses while the thrust of the propellers should only generate symmetrical compressive stresses in the shaft. Compression stress from thrust increase can therefore be ruled out.

Drive instability or a power surge

There was no record of any drive instability during the entire service life of the ship. Should this have been the cause of the failure, the nature of the fracture would have been significantly different — either being a characteristic torque failure or a fatigue failure with multiple points of origin. The team concluded that the failure did not have a root cause in the power or motor system.

Shaft System Defect

Shaft design

The port shaft, which showed no signs of distress or failure, was identical to the starboard shaft. On that basis, a design fault of the shaft can be eliminated as a root cause.

Shaft material specification

The shaft material from both shafts was tested and met the required specification in the design document and class design rules for shafting HS LC 2011-01 DET Norske Veritas Rules for Classification of High-Speed Light Craft and Naval Surface Craft January 2011.

Metallurgical defect

It is often the case that a small metallurgical defect is found at the origin of a fatigue failure. The origin area of the fracture face was examined by three independent metallurgists, all of whom could not find any defect under microscopic examination. Therefore, it is reasonable to conclude that there was no metallurgical defect present.

Alignment

Although the alignment of the shaft was less than ideal at the time of the failure, both shafts were in a similar condition, and the port shaft did not fail. Consideration of the effects of misalignment — and the constraints imposed by the bearings in the stern tube where the shaft is held in by forward and aft bearings and two intermediate bearings — makes it extremely unlikely that misalignment could have created a uniaxial force at the location of the fatigue fracture.

Torsional vibration

As discussed previously, torsional failures have a distinctive characteristic and are aligned at 45° to the axis of the shaft. The uniaxial nature of the fatigue failure rules out torsional vibration as a root cause.

Whirling vibration

Whirling vibration can usually be detected by examining the wear pattern of the bearing lining materials. There was no evidence of whirling seen in the bearings of either shaft. Machine condition vibration monitoring was inconclusive at expected whirling frequencies, but showed no evidence of any shaft vibration — although it did record blade pass frequencies.

Whirling vibration would create symmetric forces on the shaft that would result in at least two fracture origination points, which is not consistent with the evidence of the fracture surface.

Propeller System Defect

Considering the previous analysis — and the fact that clearly a significant force was required to fracture a 352 millimeter (13.8-inch) diameter shaft — the propeller system was likely to have some influence in the failure process. Not only were many of the other potential causes ruled out, but the propeller is a large mechanical element generating forces capable of pushing the ship through the water. And if there was any problem in the propeller system, it has the potential to generate effects that could have significant consequences.

To assist in the analysis of the propeller system, this was divided into four sub areas: the design of the propeller, the manufacturing process of the propeller, the fitting of the propeller, and the performance of the propeller in service.

Propeller design

The new propellers were designed to improve fuel performance and provide some increased thrust that would assist in keeping timetables in a difficult passage

The new propellers were significantly lighter than the original propellers, and analysis by the designers showed there was a possibility that the new shaft/propeller combination may vibrate in service. To overcome this, the rear

bonnet of the propeller was extended — adding weight behind the main propeller to recreate the original propeller system characteristics that had operated successfully for 23 years. This change was assessed by calculation as having a minimal effect on the stresses in the shaft.

The new propellers had a slightly higher power density in kilowatts per square meter of blade area than ships of similar design and service. The propeller improvement report noted that the new high-efficiency propellers would be slightly closer to cavitating in service. A diagram included in that report showed that, as designed, the propellers were within accepted service parameters (**Figure 16**), although the sensitivity to cavitation had increased. Therefore, damage or surface defects became more likely to initiate cavitation.

We understand that the propellers were designed using digital techniques, which calculated the geometry of the propeller to a high level of accuracy — much less than 1 millimeter. They were specified to be built to the ISO 484/1, the International Standard for Propellers of Diameter Greater Than 2.5 m, which has a base construction tolerance band of plus 2 millimeters minus 1.5 millimeters.

Manufacture

It was noted by several marine equipment experts that the thickness of the propeller blades varied quite significantly, although such physical measurements as could be taken indicated that these fell just inside the tolerance band as allowed by ISO 484-1 2015-Shipbuilding-Ship Screw Propellers Manufacturing Tolerances – Part 1: Propellers of Diameter Greater Than 2.5 m. The propellers were cast and not machined and had non-critical casting surface artefacts. The form of the blades was typical of cast components and of a shape and evenness that could not be generated by overload damage.

These observations led to the decision to digitally scan both propellers and carry out a shape comparison.

Once the two propellers were returned to New Zealand, they were digitally scanned at the same time using the same equipment in the same environment with digital and survey control measures to allow the accuracy of the scan to be assessed as plus or minus 2 millimeters for the surfaces. (This was at the limit of the technology at the time. Current equipment with proper survey control can now exceed this accuracy.) Because both propellers are inward rotating, one propeller was then digitally reflected so that the two digital images could be placed together and any differences in shape highlighted by subtraction.

The propellers were aligned using the machined

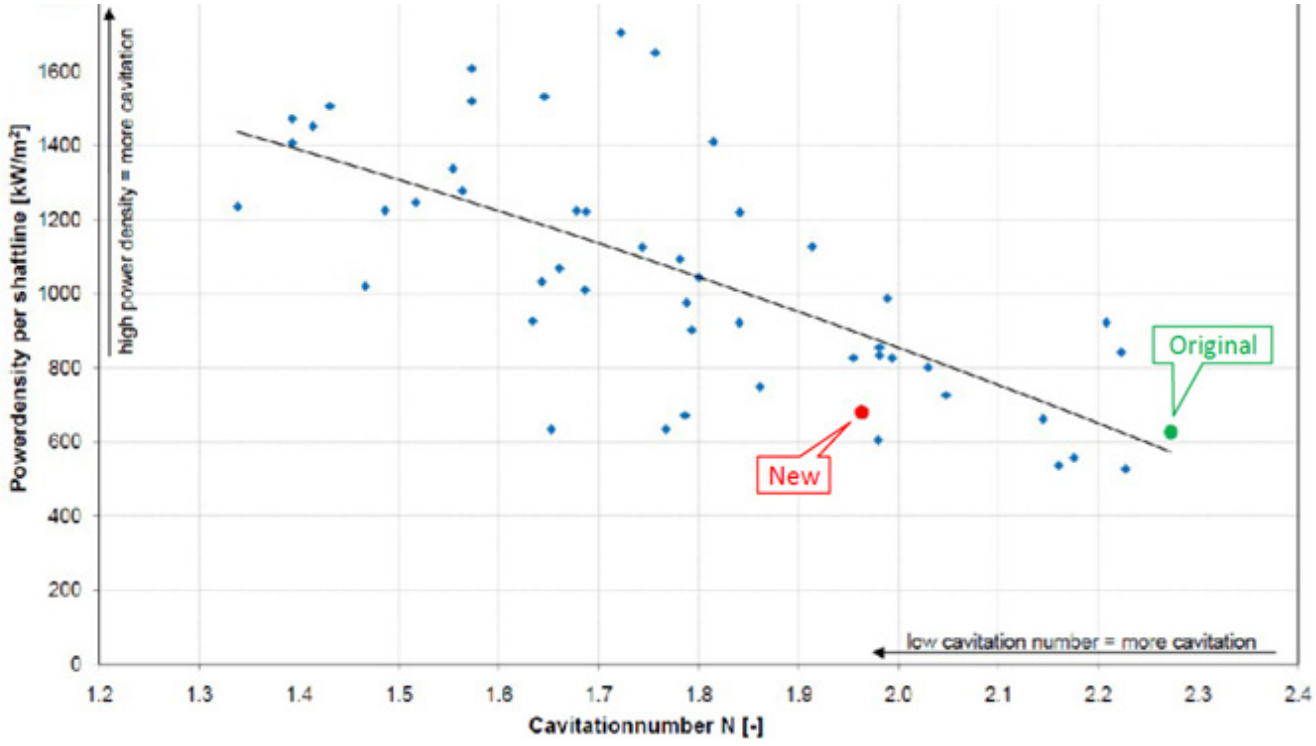

Figure 16
Power density and cavitation number for the design and the ferry reference set.

front face of the hub, and rotated until the A, B, C, and D blades were in matching positions (there is a standard naming convention for blade position). Then the difference between the two blade surfaces could be assessed. The differences were mapped, and any differences greater than plus or minus 2 millimeters (a zone that contained the acceptable manufacturing tolerances) were color-coded. **Figure 17** shows the suction face, which is where cavitation occurs. (The black spots are noise from the scan, and analysis can be ignored.)

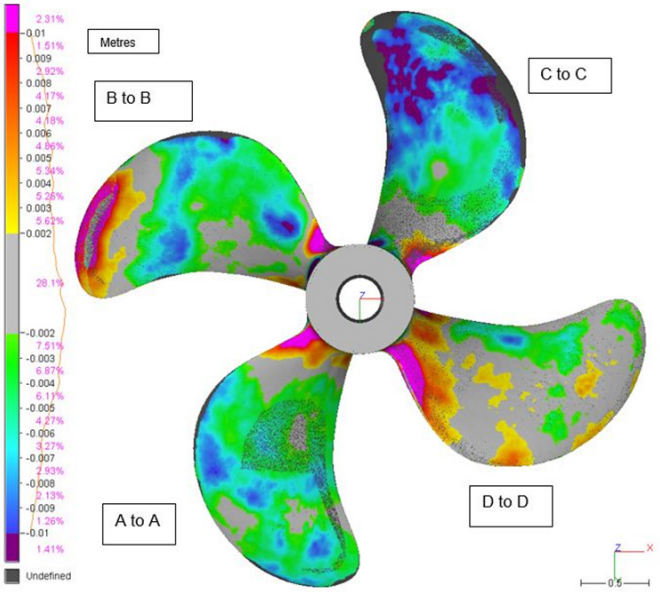

Figure 17
Digitally calculated differences between the suction faces of the two propellers.

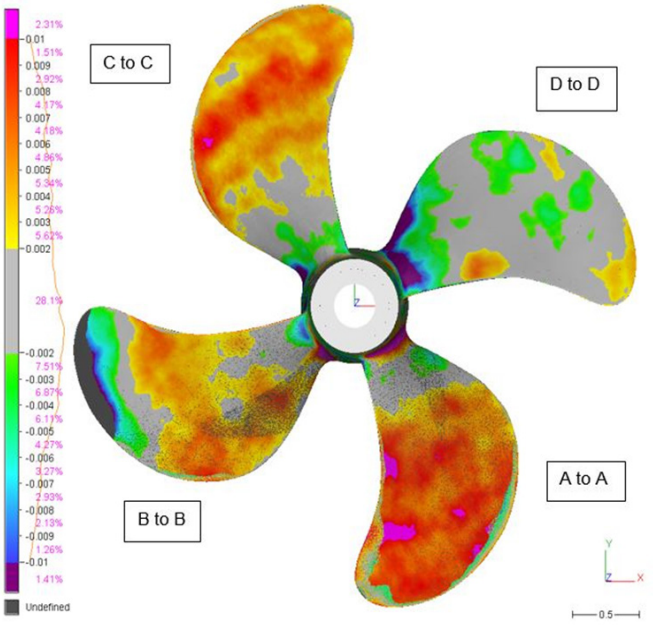

Figure 18
Digitally calculated differences between the pressure faces of the two propellers

It was clear from this comparison that there were significant differences between the A, B, and C blades of the port and starboard propellers, while the D blades fell largely within the base tolerance zone. **Figure 18** compares the pressure faces of the two propellers. The C blades were significantly different, and the C blade of the starboard propeller was also displaced rotationally around its main axis (**Figure 19**). Comparison between the mapped differences in shape (colors), and the observed cavitation (inside line) showed a close correlation in location when the two images were overlaid (**Figure 20**).

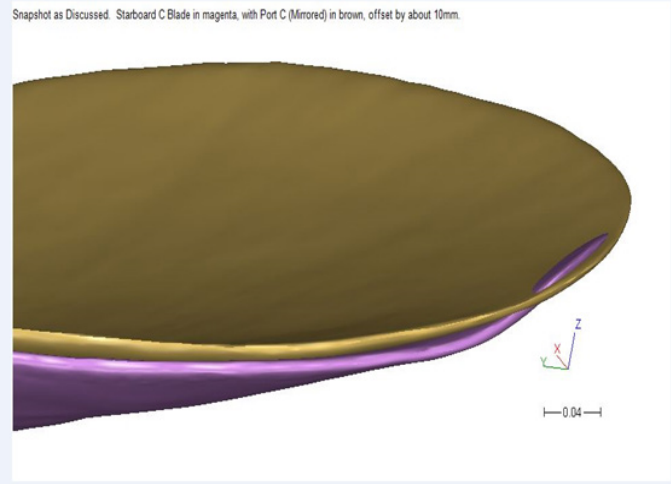

Figure 19
View of the digital model showing that the C blade of the starboard propeller is displaced rotationally around its main axis.

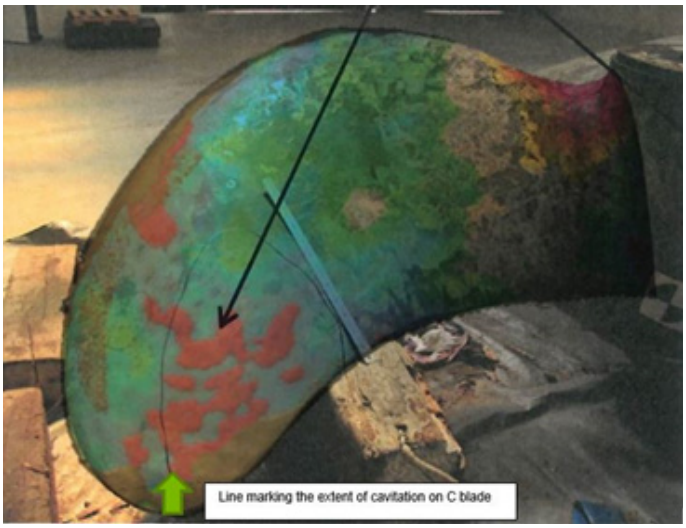

Figure 20
By overlaying the photograph of blade C in Figure 8 and blade C in Figure 17, it can be seen there is good correlation between the largest shape deviations and the observed areas of cavitation.

Propeller fitting

Because of the historical regularity of shaft failures (where propellers were secured to the tail shaft by a keyway), recent shipbuilding practice is to secure the propeller and transfer the driving torque by means of an interference fit between the tapered end of the tail shaft and the tapered bore of the propeller hub.

This interference fit is defined by the distance that the propeller is forced up the tapered end of the tail shaft. This is a controlled procedure generally monitored by the class surveyor and documented in the shipyard records. The design of the interference is intended to hold the propeller firmly on the shaft without movement. There is significant pressure at the interface between the shaft and the propeller hub and the contact area required before final push up as defined was reported, although not recorded, as complying.

If the interference fit is inadequate fretting can occur. However, fretting can only promote the initiation of a crack, and no fretting was found at the origin of the fracture face and the starboard shaft. Fretting by itself cannot drive the crack through the shaft. An external fluctuating stress must exist that is great enough to do this.

The metallurgical evidence referred to above confirmed that there had been fretting between the shaft and the propeller hub on both the port and starboard shafts. It also confirmed that there was no fretting damage at the site of the origin of the uniaxial fatigue failure. On this basis, fretting arising from any possibility that the interference was inadequate was ruled out as a root cause, leaving a fluctuating force as the remaining cause.

Propeller performance

A key factor in the performance of a propeller is a phenomenon known as cavitation. A propeller generates the thrust that pushes the ship through the water in two ways: by the back face of the propeller that pushes on the water as the propeller turns and by the suction on the front face of the propeller created as it drags the water in front of the propeller toward it. While the pushing force is generally stable, the suction force depends on the water sticking to the propeller face. If the suction becomes too strong, the water in front of the propeller cavitates, and the force generated by the blade, which is cavitating, is significantly reduced. This is a situation that propeller designers can control by design and is to be avoided. Sensitivity to cavitation is measured by the cavitation number. Cavitation occurs when the number is less than -2.

The design performance of propellers is often checked in free flow fields prior to manufacture by using hydrodynamic modeling techniques and to check and assess any improvement in performance if propellers are being changed. A hydrodynamic modeling company was commissioned to carry out this check on the scanned propeller forms. Hydrodynamic modelers were also commissioned to determine, if possible, the effect of the bent tip on the C blade to see whether this was affecting the performance of the starboard propeller in some way. These analyses were limited to free field flow for financial reasons.

The comparison between the propellers by modeling proved to be somewhat inconclusive, as the scanned forms had to be smoothed to allow the computations to run. The modelers concluded that any difference between the two propellers in terms of forces generated (with or without the bend on the tip of the C blade of the starboard propeller) fell within the uncertainty band of plus or minus 5% associated with their calculations. More accurate calculations were not possible.

While it was disappointing that the modeling did not generate results that matched the cavitation patterns on the propeller surfaces, this was explained by the limits of the software and in computational capacity. (Note: This was in 2015, and both have developed significantly since then.) They were, however, able to provide maps of the propensity of the propellers to cavitate through the calculation of a standard measure called the cavitation number. This showed that, according to their calculations, the scanned shape of the propellers operated at a cavitation number much closer to the critical level than the number proposed in the original investigation reports to determine the benefits of the new propellers. White areas in **Figure 21** are cavitating.

These results supported cavitation as a significant factor for consideration, but the uncertainty in the results meant that the physical evidence became the most reliable indicator of any performance problems with the propellers.

The investigation team was able to show from underwater dive surveys that the paint damage to the starboard rudder (**Figure 22**) was present after one year of service and prior to the appearance of the bent tip on the starboard propeller C blade. The presence of cavitation damage to the paint before the bend appeared on the propellers was accepted as evidence that the bend was not significant as suggested by other experts early in the investigation.

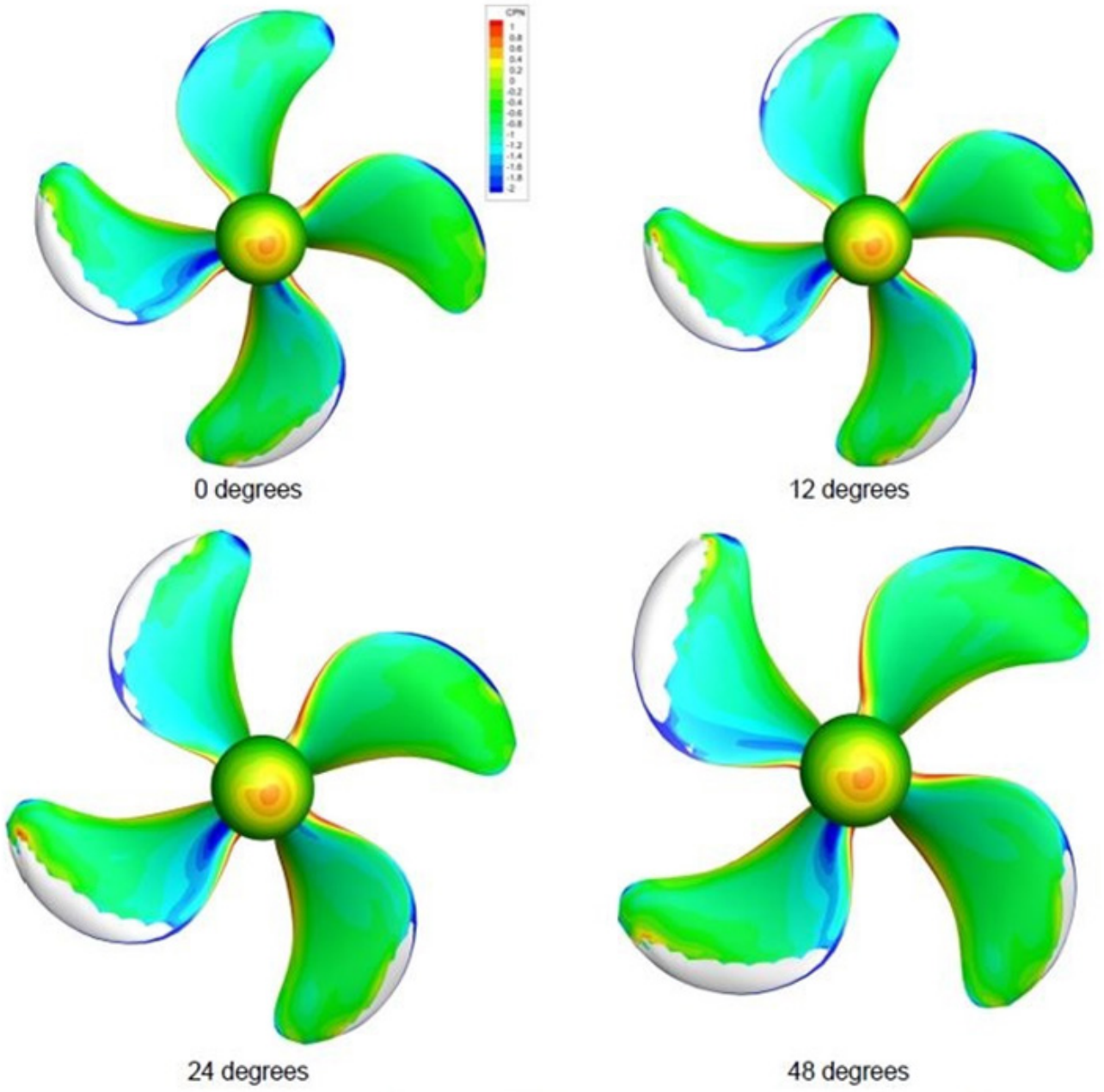

Figure 21
Pressure distribution (CPN) and sheet cavitation pattern for starboard propeller (shown mirrored, overloaded condition, 150 RPM, PD = 5,148 kW). Edge effects only, surface deformities could not be modeled.

The investigation team considered that the paint damage on the inboard side of the rudder was due to cavitation bubbles being shed as the propeller passed through the boundary layer along the hull. Physical observation of the starboard propeller showed one blade with significantly more surface damage from cavitation than the other three blades. It was considered likely by the investigation team that the blade showing the surface damage cavitated as it passed through the boundary layer.

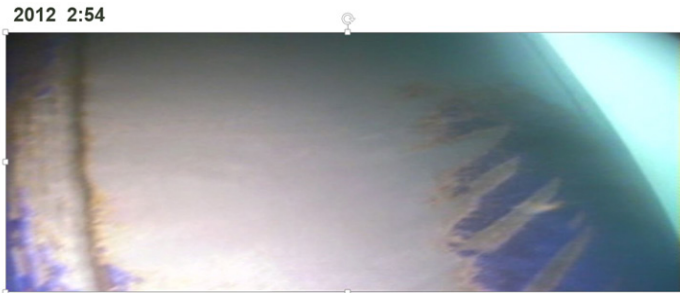

Figure 22
2012 dive inspection shows paint loss on starboard rudder.

The other better formed blades with less surface

damage were not cavitating significantly when passing through the boundary layer. When the poorly formed blade was passing through the boundary layer and cavitating three of the four blades would be operating at 100% thrust, while the inboard blade would be generating significantly less thrust. This asymmetry in the forces would generate a repeating uniaxial bending couple that could initiate tensile principal stresses in the shaft surface, and once a crack had initiated could drive the fatigue failure through the shaft. This opinion was drawn from observations and experience as modeling, and calculations failed to provide conclusive numerical proof — although the generalized results supported the reasoning.

Conclusion

The investigation team set out a plan that would allow analysis of all possible credible failure paths, and commissioned independent testing where this could contribute value to the investigation process. Some of the failure paths led rapidly to technical conclusions, which ruled them out as credible causes, and no further investigation in those areas was carried out.

The availability of a similar drive system on the port side of the vessel provided a valuable benchmark to assess the significance of observed differences and similarities, allowing more weight to be given to the differences as potential contributors to the failure.

In some areas, particularly in the hydrodynamic modeling and theoretical stress analysis areas, the number of assumptions that had to be made to allow numerical processes to be used led the team to give less weight to the outcome of those analyses and to limit these as the associated cost of more extensive calculation was assessed as contributing little value to the investigation.

Historical evidence allowed a timeline to be established where the team could see the sequence in which some of the physical evidence appeared in the record. This provided valuable information as to circumstances when that evidence appeared and allowed certain issues (such as the bend on the tip of the C blade of the starboard propeller) to be discounted as causative of the cavitation evidence as the cavitation damage preceded the appearance of the bent tip.

The team also concluded that the shape differences measured on the starboard propeller, when compared to the port propeller, were significant and consistent with the physical evidence of the fatigue fracture and the cavitation damage. Considering the physical evidence available — and by comparison between the port and starboard propeller and shaft systems — the author generated the following summary of observations and investigation:

Observations:

1. Fretting on the port shaft was worse than fretting on the starboard shaft, indicating that fretting was unlikely to be a root cause.

2. The naturally fluctuating forces of the port propeller were not able to initiate or drive a fatigue failure on the port shaft despite the higher level of fretting present.

3. There was no fretting damage present on the surface of the starboard shaft where the fracture originated suggesting that an additional force above the natural fluctuations of a rotating propeller initiated and drove the fatigue crack.

4. There was clear evidence of abnormal performance of the starboard propeller by way of cavitation damage to the suction surfaces of the propeller and paint erosion on the rudder caused by the shedding of cavitation bubbles.

5. The failure was a uniaxial fatigue failure that originated close to the C blade.

Investigations:

1. Finite element analysis, while uncertain as to the actual stresses, showed the principle stresses from torsion, interference fit, weight and bending summed to tension in one direction at the surface.

2. By comparison, between the scanned shapes of the port and starboard propellers, the C blade of the starboard propeller was most significantly different from other blades on the starboard propeller and from matching blades on the port propeller.

3. The surface damage from cavitation was most pronounced on the suction face of the C blade of the starboard propeller.

4. It is known that cavitation affects the capability of a propeller blade to generate thrust.

5. One non-performing blade on a propeller would generate a uniaxial force that fluctuated once per rotation in a consistent transverse direction across the shaft as it passed through the boundary layer.

6. That fluctuating force would generate a couple on the propeller that would act to maximum effect at the plane where the fracture occurred on the starboard shaft.

7. The intermittent couple generated by the starboard propeller initiated and drove a fatigue failure.

8. The bent tip on the C blade appeared after the evidence of cavitation on the rudder; therefore, it was not a contributing cause to the cavitation.

Based on the physical evidence, it is reasonable to conclude that a malformed C blade on the starboard propeller was the primary cause of the failure. If this blade had been well formed — and the propeller had performed symmetrically — the uniaxial driving force required to initiate and drive the fracture would not have been present.

References

1. Wulpi, D.J., Understanding How Components Fail. 1985, Metals Park, Ohio: American Society for Metals. 262.

2. Matthews, C., A Practical Guide to Engineering Failure Investigation. 1998, Great Britain: Bookcraft (Uk) Ltd. 260.

3. Szolwinski, M.P. and T.N. Farris, Mechanics of fretting fatigue crack formation. Wear, 1996. 198.

Computational Fluid Dynamics Modeling of a Commercial Diving Incident

By Bart Kemper, PE (NAFE 965S) and Linda Cross, PE

Abstract

A commercial diver using surface-supplied air was "jetting" a trench, which was using high-pressure water via an industrial "jetting hose" connected to a pressure-compensated tool to cut trenches in silty sea bottoms. This tool used high-pressure water pumped from the tender boat down to the diver. It was reported that man-made objects in the area cut the jetting hose, resulting in uncontrolled diver movement and subsequent injury. There were no direct witnesses available. The subsequent forensic engineering investigation used traditional calculations, laboratory testing, ergonomics, biomechanics, and computational fluid dynamics (CFDs) to determine the limits of the physics involved in order to assess the feasibility of the reported scenario. Specifically, CFD modeled the mass flow exiting the tool's two ends and the cut in the hose as well as modeled the diver's flow resistance while propelled through the water. The results indicated the applicable physics precluded the events as described.

Keywords

Diving, computational fluid dynamics, CFD, flow resistance, friction loss, jetting, forensic engineering, biomechanics

Introduction

One effective approach in dealing with a forensic case is to examine the chain of events required to go from a safe or neutral state to a damaged state, which is typically the crux of litigation. Sometimes, the chain of events is simple: A distracted driver speeds through an active cross walk, striking and killing a pedestrian in full view of witnesses and multiple cameras. A forensic engineer is unlikely to be called upon unless it is to establish whether a potential defect or condition significantly contributed to the event.

Some cases have no witnesses, no cameras, and no direct data to corroborate or impeach the statements of an injured party. Experimentation can be difficult or impossible due to the on-site conditions or risks associated with the events. In such instances, engineering work can be the key to establishing the conditions needed for each link in the chain to be feasible in order to assess whether the chain of events could link from the issue or state being litigated to a known state or condition[1]. Determining whether the required chain of events is physically feasible can be a decisive tool for ending the litigation. This confirmation of the chain of events also lays the foundation for follow-on work to evaluate a more nuanced scenario of "how did this happen" rather than "did this happen," as appropriate.

Diving Incident

This case study involved a commercial diver using supplied air working from a diving barge. This is different than the diving with air tanks many are more familiar with. The diver's primary air supply is via a hose provided from the surface, connected to a diving helmet encompassing the entire head and allowing the diver to speak to support crew on the surface. The diver typically is walking on the bottom instead of swimming. An example of what this work environment is like is shown in **Figure 1**.

Figure 1
An example of a commercial diver performing work on the bottom of a sea or lake. Cutting trenches using jetting nozzles is done in zero visibility due to the dense clouds of silt the process creates. (Photo credit: Dive Safe International, released for public use)

Bart Kemper, PE, 4520 Jamestown Ave., #3 Baton Rouge, LA 70808, (225) 923-2945, bkemper@kempereng.com

Federal occupational safety rules apply to commercial diving[2], which, in turn, (per OSHA Directive Number CPL 02-00-151) incorporate "International Consensus Standards For Commercial Diving And Underwater Operations," which is published by the Association of Diving Contractors International, Inc. (ADCI)[3]. This standard is often simply referred to as "ADCI."

In this instance, the diver was part of a team using water pumped through an underwater hose to dig a trench in the silty sea floor. This is defined in ADCI, Section 5.35 as "high pressure water blasting." The construction of the trench itself is addressed in Section 5.34, "underwater excavation operations guidelines[3]." With divers working in shifts (in less than 30 feet of water), the trenching operations had been going on for several days at the time of the incident. Units are in U.S. customary units to be consistent with the original work and provided data.

The tool used to dig the trench is a pressure-compensated "jetting nozzle," which receives pressurized water fed by a pump on the barge (as shown in **Figure 2**). The water travels from the pump through a flexible hose through a few swivel fittings to the nozzle. The nozzle is a "tee," where the flow is effectively split into two equal and opposite directions. One end is aimed at the silty bottom to "jet out" the desired trench. The tee is handled so the other end is behind the diver, jetting at the same flow rate as the trenching end — so there is no net force on the assembly. Therefore, there is no force on the diver from the trenching operation.

Figure 3 illustrates the concept of operations prior to the accident. The trench depth reported varied from 36 inches (shown) to 60 inches when completed. The trench section being worked at the time of the incident was reported as being a little past halfway completed. The red oval on the hose shows approximately where the cut is with relation to the diver and equipment. The cut is shown in **Figure 4**.

Figure 2
The jetting nozzle used in the incident. The 90-degree elbow has swivel fittings at both ends. The flow comes from an industrial hose, supplied from the dive boat, and splits at the tee, creating two equal and opposing flows so the jetting force is counterbalanced. The length of flexible hose taped to one end is used to enhance the diver's grip on the forward (or "jetting") end and has no bearing on the flow.

Based on the provided data, the diver was approximately the same dimensions for the 50th Percentile Male as defined by ASTM Standard F1166, "Standard Practice for Human Engineering Design for Marine Systems, Equipment, and Facilities[4]." The previous diver had left the nozzle on the sea bed when he finished his shift and returned to the boat. The incident's diver reported he had followed the jetting hose to the tool, picked it up, and asked the people on the diving boat to turn on the pump. The

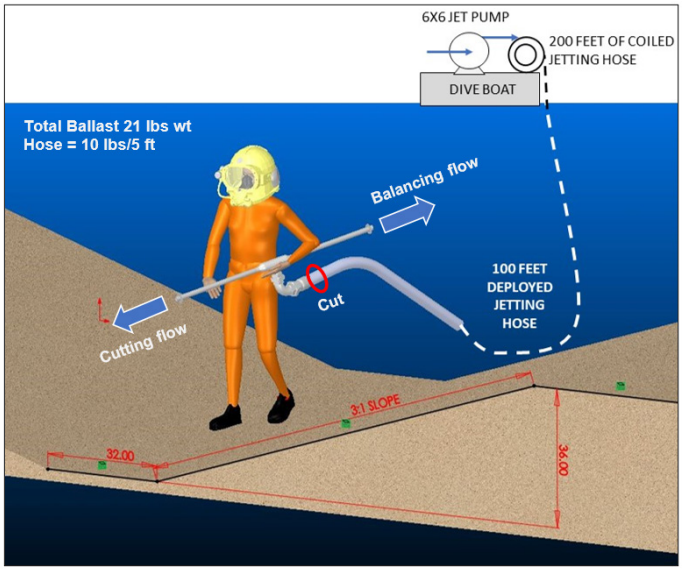

Figure 3
An approximation of the diver typical of a jetting operation. The 3D model is using an ASTM F1166 "50th Percentile Male" in Solidworks Professional. The jetting tool assembly is generally held at the hip and aimed downward in a varying angle to create the trench. The trench dimensions (in inches) are typical for the trenching in this region, and are consistent with ADCI guidance.

Figure 4
Photograph of the end of the jetting hose where it attaches to the coupling. The cut in question is about 9 inches from the coupling once it is screwed into place. In reviewing Figure 3, this places the cut approximately at hip level (location circled in red). The Parker jetting hose is constructed using layers of rubber, plastic, and tire yarn (the same reinforcement used in tires) and is intended to be resistant to cuts and abrasions in an industrial setting.

diver walked along the bottom, maintaining a negative buoyancy by using a diving weight belt. Picking up the hose and jetting nozzle would increase the total weight, acting to hold the diver downward in the soft mud bottom.

The diver picked up the nozzle, held it to his hip, and requested the hose be turned on. He put the nozzle into operation without any issue. This indicated there were no imbalanced forces acting on the nozzle or hose at the time, which, in turn, indicated there was no additional opening in the hose at that time. Suddenly, without any chance to tender on the boat, the diver reported being "thrown around like a rag doll," which included multiple impacts with the silty mud bottom.

The diver reported holding onto the nozzle assembly out of fear and began yelling. The topside crew turned off the jetting pump and was in the process of sending the stand-by diver when the deployed diver reported that was not needed. The diver returned to the boat on his own. The diving team recovered the hose and tool. The diver reported injuries and stated there was some sharp object in the work area that caused the cut in the hose, which, in turn, was the cause for the injuries. The diving team, which was in the dive boat, was not able to observe the work site to confirm the diver's testimony.

The Job Hazard Analysis (per Section 5.9, ADCI)[3] noted this was a natural littoral shallow sea water environment, with associated flora and fauna typical of the region. There had been previous marine operations in the area to include pipe lay for pipelines. Some man-made objects would be expected in these operations. There were no ship wrecks, abandoned structures, or other large hazards known to be in the work site, nor had any sharp objects been reported during previous operations. Other than the cut hose, there is no contention that the previous days of operations failed to conform to ADCI standards or the diving company's safety manual and dive plan.

Chain of Events

The diver had refused medical treatment immediately after the event but later sought medical care for back injuries. The point in contention was whether the back injuries were from the diving incident in question. In order to connect the injury to the incident, a chain of events was developed to specify elements that had to occur in order to establish causality. If the chain of events is proven, then there is direct employment-related causation. It will also justify more detailed work. For example, if the chain of events is not supported, then there is no need to conduct a detailed biomechanical review of the medical files to assess whether the medical documentation is consistent with the physics of the event. If there is no chain of events that connect the employment to the injuries, then the injuries are not due to employment.

The chain of events reviewed is as follows:

- To create the back injuries from the work-related conditions, the diver testified it was due to being repeatedly slammed into the silty seabed.
- To slam the diver multiple times, the diver had to be propelled at impact speeds into the silty sea bed with resulting shock-loading consistent with the reported injuries.
- To be propelled at speeds consistent with injury, sufficient force had to be applied to the diver.
- To develop sufficient force to be consistent with the injury, a corresponding non-compensated mass flow rate was required.
- To create that mass flow rate, a hole in the hose was needed with a corresponding pump-supplied pressure.
- For the diving company to be at fault, the creation of the hole in the hose had to be through no fault of the diver — and in a manner consistent with an argument the diving company failed to provide a workplace free of unacceptable hazards.

Equipment

The pump was a 6×6 jet pump skid using a horizontal split case multi-stage pump. The hose connecting the pump to the jetting tool was a 2.5-inch jet hose. This equipment package can be rented from a number of sources, demonstrating the equipment was typical to the field and could be considered within the normal practice in the field.

The fittings for the nozzle were standard 2.5-inch Schedule 40 90-degree-long radius elbow with swivel fixtures on both ends. One swivel fitting mated to the jetting hose. The other mated to a 2-inch to 1-inch reducing tee. About 24 inches of straight 1-inch Schedule 40 pipe was welded to both ends.

The diver was estimated to weigh 200 pounds. Fourteen pounds of belt weight was necessary to weigh

down the diver enough to work. The total nonbuoyant weight was determined to be 21 pounds, which is the force that had to be countered in order to lift the diver from the bottom. Any change in momentum engages the total mass, but the thrust only has to overcome the nonbuoyant weight to create lift. This neglects the suction force on the feet, which is typical of the environment — a conservative assumption favoring the diver's perspective by assuming "lift off" only has to overcome weight and no resistance due to mud.

The bottom conditions were silty mud into which the divers routinely sank 6 inches to 12 inches. Based on this, it is estimated a torso, with its greater cross-sectional area, would slow over 4 inches before stopping. This was a conservative value as the other divers estimated a person would sink 6 to 8 inches if landing on their back, side, or buttocks based on their kneeling and sitting in that terrain. The hose with water weighed 11 pounds per 60 inches, which means it would take an additional 11 pounds of thrust to lift the diver 5 feet upward before the hose would act as a tether to the ground.

The cut in the hose creates a variable with respect to flow. While the dimensions and location of the cut can be measured, as shown in **Figure 4**, it is unknown whether the cut was extended during the incident. It is also unclear how the various forces on the hose interacted to pull the hole wider. It was noted the location of the cut was relatively close to the coupling. Ergonomically, the operation of the jetting nozzle and carrying the jetting nozzle places this upper section well above the knees of the diver. This is not consistent with the statement that the cut was created by some unspecified man-made object that the company had failed to remove from the area or warn the divers about.

Initial Assessment

The initial question was whether the incident was feasible based on the pump's maximum flow rate. At this phase of the case, details were still being gathered. A "worst-case" method was used to evaluate the potential thrust by water flow based on the jet pump specifications and the hose dimensions.

The length of the hose used and the details of the nozzle were not made available at this point of the inquiry, but the pump specification was provided. The top end of the pump's capacity was 1,400 gal/min, or 5,390 cubic inches per second. If the pump alone, without friction losses and other factors included, could not produce sufficient flow to create significant acceleration, the inquiry could end at that point. Literature associated with evaluating human response to accelerations and impulse (shock) are often presented in term of "G-forces" or multiples of gravity. The calculations and assumptions for this initial assessment are as follows:

Calculate flow for hose without nozzle (assumed 2.5-inch diameter)

$$\boldsymbol{v = (V)/(A)}$$
$$= (5390\ in^3/sec) / (4.91\ in^2) = 1097\ inch/sec$$

Calculate force and impact acceleration (assume fresh water)

$$\mathbf{F\ (thrust) = (V)(\rho)(\mathit{v})/(g_c)} \quad \textbf{[Ref 5]}$$
$$= (5390\ in^3/sec)(0.0361\ lbm/in^3)(1097\ in/sec)/(386\ lbm\text{-}in/lbf\text{-}sec^2)$$
$$= 552\ lb\text{-}f$$

$$\mathbf{F = m*a \rightarrow a\ (thrust) = F(thrust)/m}$$

Taking advantage of U.S. Customary units allows it to be written as in terms of Gs:

$$\mathbf{a\ (thrust) = F(thrust)\ (lb\text{-}f)\ /\ weight\ (lbs)}$$
$$= 552\ (lb\text{-}f)\ /200\ (lbs) = 2.76 \times body\ weight$$
$$= 2.76\ Gs$$

F	=	force (lb-f)
ρ	=	density of salt water -= 0.0381 lbs/in^3
v	=	velocity
m	=	mass
a	=	acceleration
V	=	volumetric flow rate
C_D	=	drag coefficient
A	=	cross sectional area with respect to the flow
g_c	=	gravity constant = 386 lbm-in/lbf-sec^2
G	=	G-force, or multiples of 386 in/sec^2

Given the maximum thrust acceleration has been determined, use the diver's transcripts and other information to make an initial assessment.

- Assume the calculated acceleration of 2.76 Gs was in effect for 3 seconds before hitting the bottom. The 3 seconds is based on the 30-foot depth, the fact the diver never came close to the surface, and statements by the diver.

- Assume the silty mud bottom stops the diver in 2 inches. This was an initial conservative

assumption that was later revised to 4 inches based on better data.

- As an estimate, use a literature value for a SCUBA diver swimming of $C_D = 0.40$[6]. This is a conservative assumption as the diver in this case was propelled at the waist with a larger cross-section area with respect to the flow rather than a diver propelled forward by his fins. This allows the use of fundamental kinematic relations:

velocity = time * acceleration
(final velocity)^2 = (initial velocity)^2
+ 2(acceleration)(distance)

Given the (final velocity = 0) due to coming to a stop, this can be re-written for calculating the stopping rate as the body contacts the bottom and comes to a stop:

Acceleration$_{(impact)}$ = (velocity at contact)^2 / (stopping distance)

Now applying the previous literature:
speed$_{water}$ = speed$_{air}$/36 [Ref 6]
Velocity = [(3 sec)(2.76 Gs)(386 in/sec)] / 36
= 88.81 in/sec

Acceleration$_{(impact)}$ = (velocity^2)/(2*distance)
= (88.8 in/sec)^2/(2*2 inches)= 1971 in/sec^2
= (a)/386 = 5.1 Gs

Typical literature for correlating accelerations to injury involve ground vehicles or airframes[7-10]. An example of this is shown in **Figure 5**. This generally assumes the person is in some sort of seat with restraints. This incident has no such constraint on the body, which increases the likelihood of injury[9]. An acceleration of 5 Gs is generally below conventional thresholds for injury[7, 9, 10], but 5Gs is consistent with injuries of lateral vehicle impacts[8]. The initial conclusion pump's flow rate does not preclude a diver being injured by being propelled by the maximum flow rate. This initial estimate indicated more detailed analysis was needed.

Verification and Validation

Animations and 3D renderings are treated as an illustration of the expert. Engineering simulations, including computational fluid dynamics, can be seen as a "black box," producing results independent of the expert[11]. This is a potential hazard to the expert witness's testimony. This can be addressed by demonstrating underlying assumptions and data used are appropriate for science-based evidence, "based upon sufficient facts or data," which "are of a type reasonably relied upon by experts in the particular field." The expert also should be prepared to demonstrate the given simulation is "the product of reliable principles and methods" and how the expert "applied principles and methods reliably[12]."

This is also known as "Verification and Validation" (V&V) for simulations. "Verification" is a measure of whether the simulation code can reliably produce accurate and consistent results with sufficient precision. "Validation" is checking the results of simulation by some other means, such as experiments, classical calculations, independently developed simulations, or some combination of techniques. ASME has published V&V20, a guideline specifically for CFD[13].

Solid models of the diver, nozzle assembly and a section of attached hose were developed in Solidworks Professional, a computer-aided design package by Dassault Systemes that also has robust computational fluid dynamic modeling capabilities. Solidworks documents that its CFD package is consistent with the norms for the CFD[14]. Verification is subject to the specific application. CFD is an accepted tool for examining flow through nozzles, including using CFD to validate medical nozzles for the Federal Food and Drug Administration[15], which requires more detail and precision than an industrial jetting nozzle for underwater trenching.

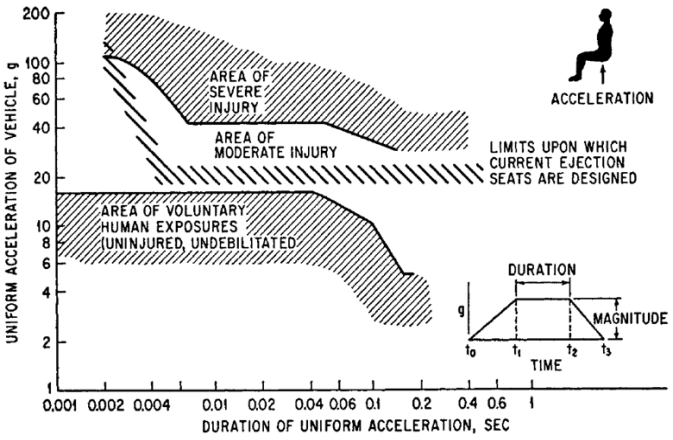

Figure 5

Example of the literature regarding impact acceleration, expressed in "Gs" versus time in terms of injury threshold[10]. This is one of the charts used to assess whether the reported injuries are consistent with the physics. This chart correlated to the diver being driven "butt-first" into the bottom. (U.S. Government report, in public domain)

The resolution of the CFD results was controlled by setting the flow characteristics (mass flow, volumetric flow) to be less than 0.01% of the nominal inputs. The model meshes were refined until the decrease in mesh did not change the results more than 10% from the previous result, consistent with Section 7 of V&V 20[13]. The models were verified by comparing the results to conventional D'Arcy friction flow calculations for the undamaged model as well general agreement with literature, which will be discussed later in this paper.

Developing a More Detailed Analysis

The solid models of nozzle assembly and a section of attached hose are shown in **Figure 6**. The nozzle, fittings, and 60-inch section of hose is one model. The length allows for 10 times the 2.5-inch diameter (25 inches) as an inlet in order to reduce any inlet effects in the model.

A model consistent with the ASTM F1166[4] standard's 50th percentile male figure was developed. The subject was roughly the same height and dimensions as a 50th percentile male, allowing the model to be used without modification other than to have the "clothes" offset 0.25 inches from the body to approximate the wet suit. While the diving hat is shown in **Figure 3**, it is omitted from the CFD models. Omitting the diving hat as well as the weight belt, reserve air tank, and other equipment is a conservative assumption, given the cited study of a SCUBA diver shows a significant increase in drag by adding a larger breathing apparatus, dive knife, and other items less bulky than a diver using surface-supplied air[6]. If the results using the simplified models show the induced drag slows the diver sufficiently to preclude the described events, then a more detailed model with greater drag is not needed.

Additional information was gathered to provide a more detailed analysis. Friction losses in the fittings and hose will decrease pump performance and lower flow rates. Per **Figure 3**, it was determined there was 100 feet of jetting hose deployed and another 200 still aboard the boat. The pump's model and associated performance curve was determined. The fittings and bends of the jet nozzle assembly were tallied up using conventional K-factors to apply the Darcy friction loss method[5].

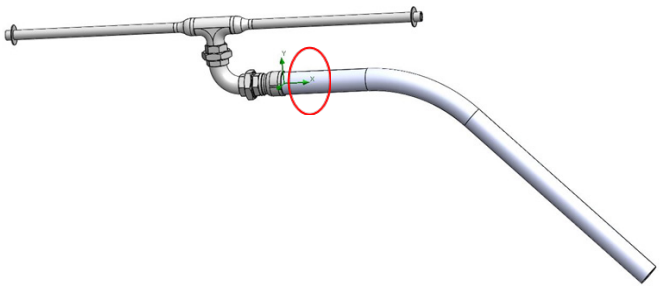

Figure 6
Solid model of the jetting nozzle assembly and 60 inches of jetting hose. This model is used for internal flow of the pressurized water flowing through the nozzle or the nozzle and cut. The red oval shows where the cut is located.

Hoses have different friction factors than pipes. Hoses absorb energy in their side walls, they flex in response to internal as well as external loads, and they vary in construction[16]. Based on the construction of the jetting hose[17], it is assumed the losses can be approximated by the losses associated with a fire hose. The losses for a 2.5-inch fire hose are available in literature[18]. This data allows the fittings to be totaled up and the head loss approximated. The nozzle's symmetrical geometry allows Darcy's equation to be used by adding the two 1-inch pipe flow areas into an equivalent pipe diameter.

$$\textbf{Friction Losses} = (\Sigma K)(v)^2 / (2*g_c) \qquad \textbf{[Ref 5]}$$

K is the friction coefficient factor. For the jetting assembly and hose intact, the total value for K is 18.4, of which 3.6 is what is shown in **Figure 6**: the last bend of the hose, coupling, elbow, tee, and run to sharp exits. The majority of the friction losses are due to flow through the hose.

The effect of the cut in the hose (**Figure 4**) is not well defined. Flow resistance is a function of velocity squared, so as the mass flow into the nozzle is reduced to the cut, the flow rate is reduced along with resistance. The flow through the cut would be the source of thrust while the flow through the nozzle is assumed to remain in balance.

It is possible the hole continued to tear and enlarge during the event. It's also unknown how the forces on the hose shaped the opening. In order to address this, two different sizes of openings are used as well as assuming the hose no longer has a coupling as if all of the flow emptied out through the cut, fully bypassing the nozzle.

The smaller cut is less than the measured cut to address the cut opening further during the incident. The larger cut is larger than the measure opening to address the "yawning" or opening being extended during jetting (**Figure 7**). The smaller effective opening would have a higher velocity, which increases thrust, but a lower mass flow rate, which reduces thrust. The intent is to use a high/low approach that should bracket the effective geometry of

the hole while the hose was pressurized.

The friction losses due to water depth are plotted against the pump curve. Their intersection determines the upstream pressure and flow rate. The losses due to the fittings and opening (or lack of one) changes the effective combined K factor.

A value of 10.8 pounds per 60 inches of jetting hose is used to represent the weight of the hose and water. This is based on the weight per unit length of the hose[17] plus the weight of water within the hose based on wall thickness. This 10.8 pounds per 60 inches (or 0.18 pounds per linear inch of filled hose) is the increased mass the thrust must counter as the diver is lifted away from the bottom. The potential thrust developed is calculated along with the drag and mass currently supported by the thrust. Drag was estimated using conventional drag calculations and the previously cited studies on a swimming diver.

$$\mathbf{F_D = r v^2 C_D A / (2 * g_c)}$$
$$\mathbf{C_D = 2 F_D g_c / r v^2 A} \quad \textbf{[Ref 5, 6]}$$

F_D = drag force, lb-f
r = density in lbm/in^3, which is why g_c is needed
v = velocity
C_D = drag coefficient
A = cross sectional area with respect to the flow (in^2)
g_c = gravity

The first CFD model is the nozzle assembly and hose, shown previously in **Figure 6** and **Figure 7**. The models all had the same outlet conditions for the nozzle as well as the opening in the hose, as applicable. Flow through piping is a classic application of CFD in industry[19]. It is a typical example problem in the mainstream CFD packages, including FLUENT and Solidworks.

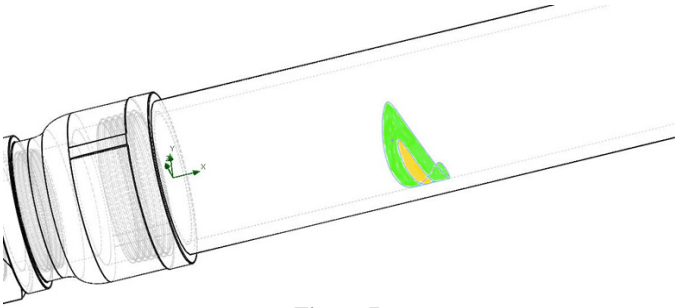

Figure 7
Detailed view of the model of the hose as it transitions into the coupling. The interior of the hose is inscribed with split-lines that can be set as outlets in CFD. The yellow shows the smaller opening with 0.375 square inches. This represents a possible small initial cut. The green shows the outline of the larger hole, which represents the length of the cut. The two colored regions total 2.00 square inches.

The input conditions are based on the flow rate determined by the intersection of pressure losses to the pump curve. The mass flow rate and volumetric flow rate remain linearly proportional for water for the conditions considered. Volumetric flow rate is an input at the open end of the hose, then the analysis reaches equilibrium with the openings, whether it is the nozzle ends, an open end (no nozzle assembly), or the two "cuts" in the hose wall. After the model converged based on output criteria, the model was run again with additional mesh refinement to confirm there was less than a 10% change to the results to ensure the mesh was sufficient. The meshing schemes for the two CFD models are shown in **Figures 8** through **10**.

The regular nozzle model is sufficiently within established literature that the conventional friction loss method should be close to the CFD results. The velocity results of the two are compared to check the CFD assumptions and boundary conditions. If the two are within 10%, the CFD model has converged on a flow rate that agrees with the conventional methods. It is expected the CFD will have a higher velocity due to the CFD model including laminar boundary layers, or "wall effects," which act to constrict the flow channel, whereas the conventional method neglects these details and assumes flow is uniform through the full cross-sectional area. If these two methods are in sufficient agreement, there is sufficient confidence in the other models. The open hose (no nozzle assembly) was calculated as a worst-case condition (maximum thrust), given the nozzle assembly remained on the jetting hose.

The other model was an external flow of water

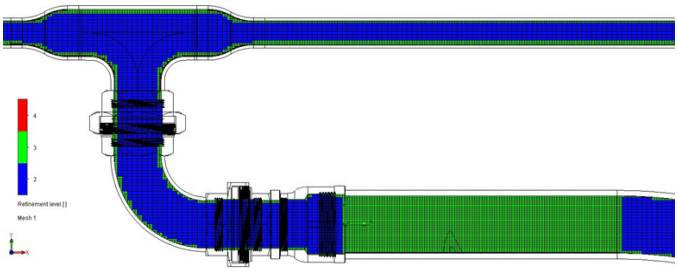

Figure 8
A 2-D projection of the 3-D mesh for the CFD model of the nozzle assembly and hose section. The blue regions represent the nominal mesh. Green areas are subdivided by one step, quadrupling the mesh density. Red is yet another subdivision. Typically, these subdivisions are used to locally refine the mesh to address changes in geometry, such as corners or channels. This is seen along the outside edges of the assembly. The region of the hose around the cut has been assigned a subdomain to control the mesh locally in a uniform manner, as illustrated with the large section of green.

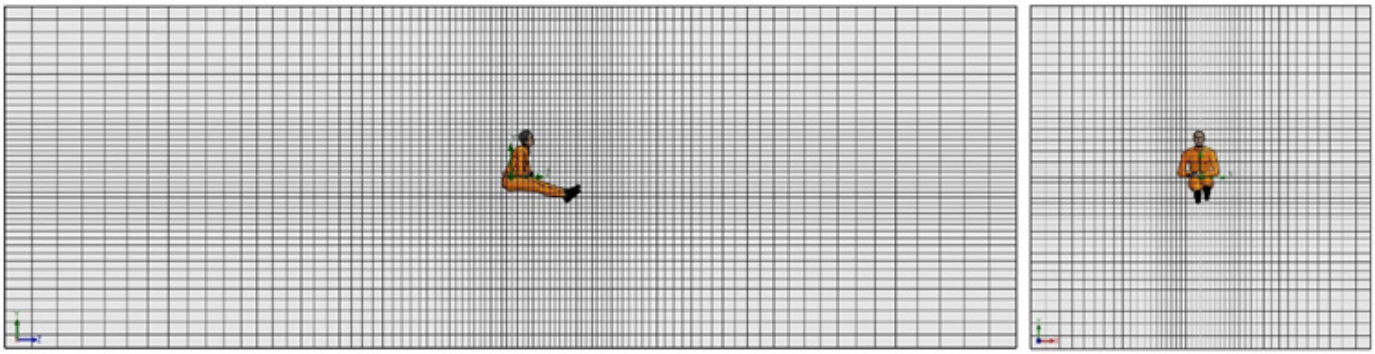

Figure 9

Macro mesh of the external flow around the diver. CFD meshes allow for larger aspect ratios than other computational applications such as Finite Element Analysis. The mesh is more refined and square around the model of the diver. A uniform, fully turbulent flow is assumed with a macro velocity of 20, 60, 100, 200, and 300 inches/second. The cross-sectional area of the diver with respect to the flow is about 530 square inches.

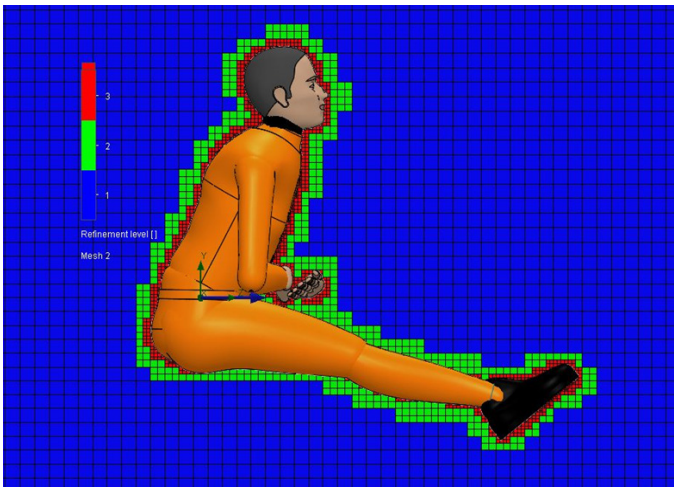

Figure 10

Detailed view of the mesh projected along the centerline of the computational domain. The 3D figure is also centered along the centerline. Diving hat, reserve air, umbilicals, and other equipment are omitted, which significantly reduces drag[6]. Similar to Figure 7, the color code shows the amount of mesh refinement, which is part of the Verification and Validation (V&V) process.

flowing around the diver as if being propelled backward. This is similar to other applications, such as CFD analysis of torpedoes[20,21]. Modeling the flow on the object returns the reaction force. The reaction force, in turn, is the force needed to propel the object at that speed. With a torpedo, it indicates the thrust the motor needs to produce. In this scenario, it's the thrust generated by the mass flow through the hole in the hose. The selected flow rates were 20, 60, 100, 200, and 300 inches/second. The upper limit is about 17 mph, which is consistent with a low-speed impact by a vehicle that is likely to cause injury. The other values are progressively less.

It is recognized that the diver did not maintain a rigid body posture during the reported event. The intent is to approximate the force needed to propel a body through the water in the manner described. It would also serve as a visual exemplar of the fluid dynamics in play — something that is challenging to communicate to a lay audience.

The nature of the hose cut is one of the primary issues related to liability. The hose was sent to an independent laboratory for measurements and an additional professional opinion regarding the characterization of the cut shown in **Figure 4**. The nature and origin of the cut was addressed as part of the overall forensic engineering analysis, but is not central to the topic of this paper.

Results

The bulk of the friction losses occur prior to the cut. The Darcy Friction Loss method is well suited for well-defined geometry, such as the majority of the hose, but it is not well suited for the irregular geometry of a cut in the side of a hose. Assuming the conditions before the cut provides the baseline flow rate, shown in **Figure 11** and **12**, the effects of the cut are shown in **Figures 13** through **16**.

The results are summarized in **Figure 17**. The significance is as follows:

- The "no cut" CFD model is consistent with the Darcy friction loss results, which validates the models.
- The force of the nozzle (F nozzle) is provided as part of the checks but does not contribute to the motion of the diver as the listed force is two such forces in opposite directions.
- The flow rate increased with more outlets or larger outlets but not by more than a few percent. This is

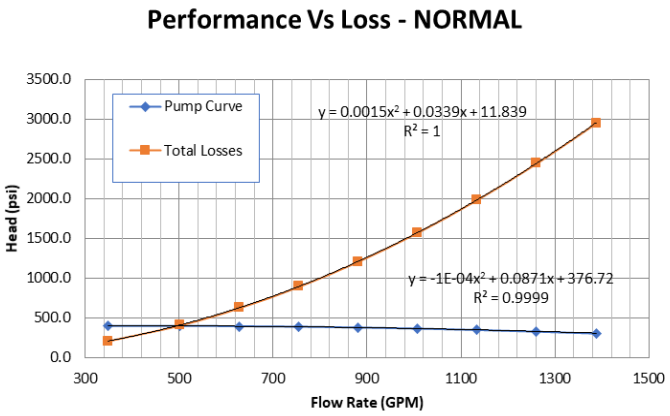

Figure 11

The friction losses and pump curve for the tee installed and no cut in the hose intersects at 494 gpm, or 1903 cubic inches/second. The small changes in total losses ("K") creates a minor change in each model's "total losses." The two equations from curve fitting are solved to determine the volumetric flow rate in GPM.

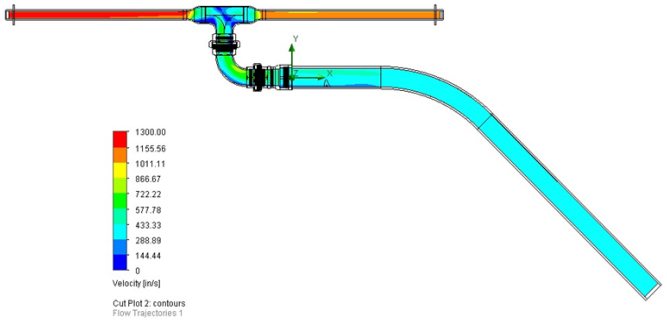

Figure 12

CFD velocity plot of the nozzle assembly and hose section plotted along the centerline. It illustrates how flow velocity increases as the pipe reduces in area. This is the baseline for velocity. While there is a slight bias of higher velocity to the left branch, the forces generated at each exit are approximately equal.

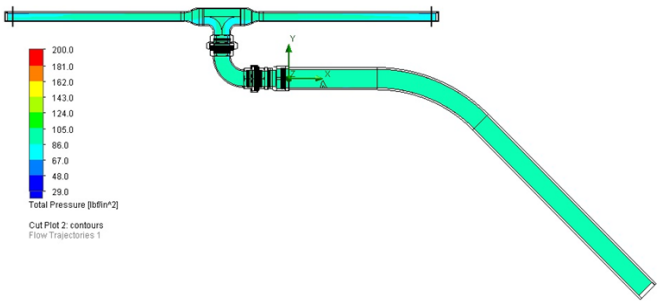

Figure 13

CFD pressure plot for large cut model plotted along the centerline. There is not a great pressure deviation over this relatively small model. This confirms the pressures indicated using friction loss methods.

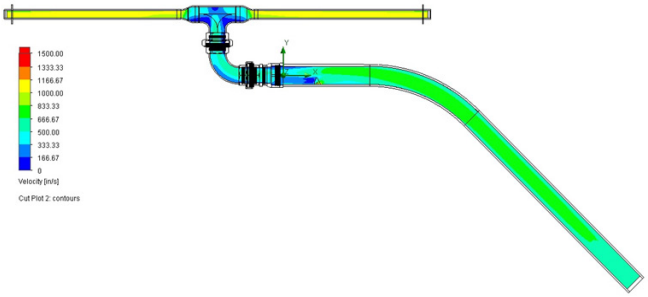

Figure 14

CFD velocity plot of the large cut model plotted along the centerline. This shows a significantly different trend from Figure 12. More detailed views will follow.

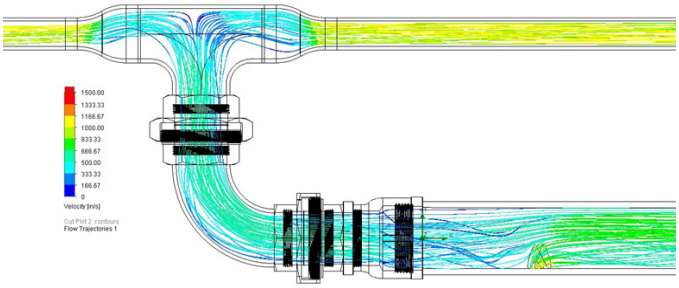

Figure 15

CFD velocity plot using particle tracing of the large cut model. This is one of the visualization methods that makes CFD a useful tool to illustrate complex flow conditions. The flow lines started on the hose inlet with 40 equally spaced start points, which followed the flow line from that position. This illustrates how flow pushes into the tee, then splits into two paths. The colors in this case correspond to velocity, but the same flow lines could be plotted with pressure, temperature, viscosity, and other properties. Other options are iso-contours, such as a curved plane of all the same pressure or velocity, as well as plotting on the surface of models or using multiple flat planes. The region highlighted with the dashed lines is the region of the cut and is shown in more detail in the next figure.

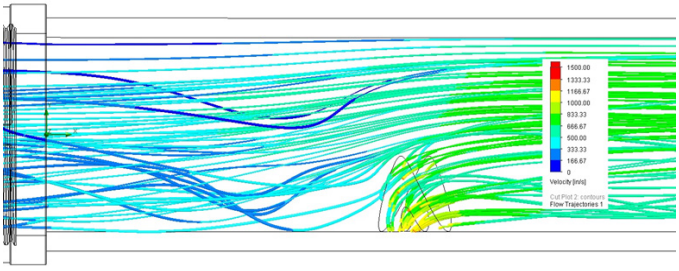

Figure 16

CFD velocity plot using particle tracing of the large cut model showing a detail of the cut area. This shows many of the flow lines terminating in the cut, illustrating how a portion of the flow is diverting out of the cut but the rest flows around the cut. It also illustrates how the flow is accelerating at the cut but has a velocity is reduced immediately downstream of the cut.

Summary of Results										
Condition	Flow (GPM)	K total	Vnoz	Mass flow rate (lbm/sec)			F Nozzle (lbf)	F Open (lbf)	Net Thrust (lbf)	Initial Gs
				Total	Nozzle	Opening				
No Cut (Darcy)	494.4	18.4	1057.5	72.5	72.5	n/a	94.0	n/a	n/a	n/a
No Cut (CFD)	494.4	18.4	1120.0	72.5	72.5	n/a	105.4	n/a	n/a	n/a
Small (CFD)	505.0	17.5	830.0	74.1	64.8	9.3	57.9	19.8	none	none
Large (CFD)	511.3	15.9	609.7	75.0	23.4	33.6	31.2	51.6	30.6	0.2

Figure 17

While the plots help illustrate complex flow, the detailed numerical results are often done by selecting model faces and querying the conditions at that location. This table represents a summary of key results.

consistent with the fact the majority of the losses are due to the friction losses prior to reaching the cut and nozzle assembly, so the variations in this model are not driving the flow conditions.

- The small cut's force is less than the 21 pounds of ballast, so it is insufficient to lift the diver. While it could push the diver sideways, it would not conform to the statements of "being picked up and slammed down repeatedly."

- The G forces are calculated using the net total force applied to the total mass of the diver. The G forces indicate the statements of "being picked up and slammed down repeatedly" is not consistent with the physical limitations of the system.

The drag was determined by using the program to sum the forces on the diver's model and breaking it out into the x, y, and z directions. The drag forces are the z-direction. The values for C_D are determined by using Eqn. 4 and the projected area of 530 square inches of the diver with respect to the flow. The G forces are calculated assuming the baseline speed (Z velocity) is achieved, and then the diver impacts into the muddy bottom, stopping in 4 inches.

The drag coefficient is somewhere between the literature value for a sphere (0.47) and a cone (0.52), which appears to be consistent with the torso being generally perpendicular to the flow and the legs trailing. By comparison, a streamlined body has a C_D of 0.04 to 0.09. Comparing it to literature, the value for C_D of a diver in a prone, head-first attitude to the flow is between 0.38 and 0.42[6]. Since the results of the upright diver (without equipment) has a higher value for C_D than the literature for a prone diver, the results for this study are generally consistent with the physics regarding flow and drag. Drag is fairly simple to visualize on simple bodies like a cube or sphere, but explaining how drag works on a complex shape is more challenging. **Figure 18** and **Figure 19** show how some of these complex flows can be visualized, including how the drag builds up as a pressure resistance.

The significance of the table shown in **Figure 20** is the force on the diver at a given flow rate. This, in turn, would be the jetting force needed to propel the diver at that speed. The maximum rate of 300 inches/second (about 17 mph) corresponds to a speed consistent with a person being struck in a low-speed vehicle impact[7-10]. This would require 1,123 pounds of thrust. The resultant G-forces in **Figure 20** are based on assuming 4 inches of stopping distance.

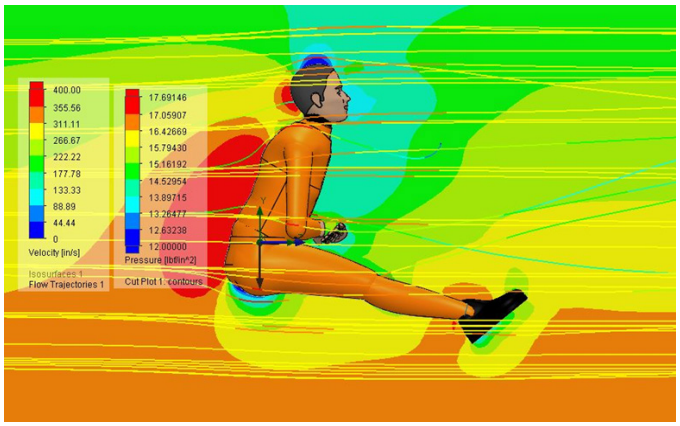

Figure 18

CFD plot of diver in a 300 inches/second flow. This is the maximum rate analyzed. While the simulation is holding the person stationary and producing a flow from left to right, this would produce the same reaction forces and flow effects of the diver being propelled from right to left in still water. This is a more complex plot to illustrate more of the potential for producing exemplars and technical illustrations. The centerline plot is a pressure plot, illustrating a higher pressure region on the diver's back and a low pressure area consistent with lift on the head. The streaks are a particle plot showing the velocity with yellow being the baseline velocity and other colors showing increases or decreases. This could be used to explain the relationship of higher velocity to lower pressure to a specific situation to a lay audience.

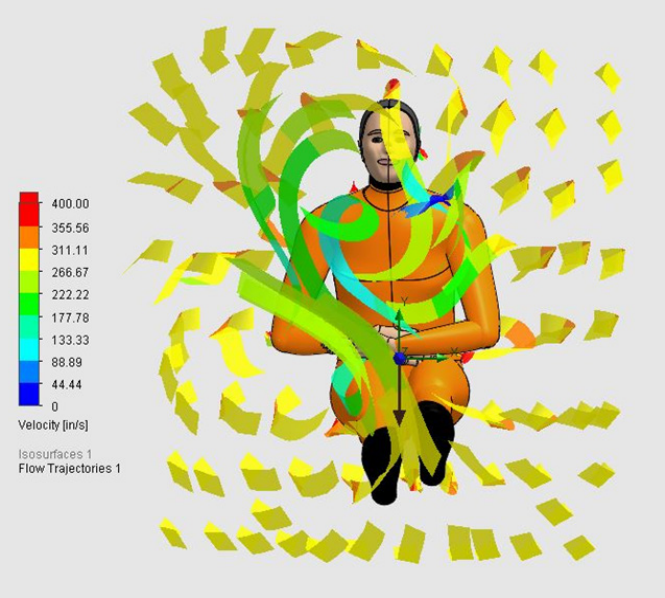

Figure 19

CFD particle plot of the diver in 300 inches/second flow. This particle plot using "ribbons" instead of "lines." The ribbons provide more visual discrimination. This is used to show the swirling around the diver as the flow goes past. One use would of this could be to illustrate how being propelled in this manner would further disturb the silty bottom and obscure the diver's vision as well as anyone observing.

The speed values neglect the time and distance needed to accelerate to maximum speed as well as neglecting the increasing weight due to lifting the jetting hose filled with water. The increasing weight would counter the thrust and slow the diver's speed. Once the total thrust equaled the total weight suspended by the jet, the jetting hose would act as a tether, constraining motion within that length.

Indexing the net thrust from (**Figure 17**) to the force needed to sustain the speeds in (**Figure 20**):

Small Cut: Cannot lift due to the force is less than the 22 pounds net ballast at start.

Large Cut: Net thrust is 30.6 lbf
Speed between 20 in/sec and 60 in/sec
Estimate impact less than 1.2 Gs
Max. distance = 13.9 ft with increasing loss of net thrust due to hose weight

The estimated impact is using very conservative values that favor the diver's perspective. Adding a tank significantly increases the drag[6], let alone the rest of the diving equipment that was not modeled. This summary was presented to appropriate medical professionals in order to assess whether the injuries are consistent with the physics after the report was submitted.

3D CFD on Diver Body			
Z vel (in/s)	*F(drag) (lbf)*	*C(drag)*	*G's @4in*
20	5.5	0.526	0.1
60	45.8	0.486	1.2
100	128	0.489	3.2
200	513	0.490	13.0
300	1123	0.477	29.1

Figure 20

This shows the result of five CFD runs of different flow speeds. The drag the diver experiences being stationary to the z-direction flow is the same force needed to propel the diver at that speed through still water. In order to propel the diver 300 inches/second (about 17 mph) as depicted, the water jet would have to produce 1,123 lb-f of thrust. This table is used to assess the diver's potential speed based on the results for the force due to mass flow through the hole in the hose.

Separate from the CFD studies, a third-party independent laboratory concluded the cutting of the reinforced wall of the Parker jetting hose was done by a sharp tool in a deliberate sawing motion and was not consistent ergonomically or mechanically with the hose contacting something sharp on the bottom of the trenching area. Its proximity to the jetting tool was assessed by the author and the laboratory to be consistent with a person holding the tool for leverage and using a utility knife, such as those commonly worn by commercial divers. The diver in question had a diving utility knife with a serrated blade consistent with the tool marks on the jetting hose.

Conclusions

- There is no evidence to support the diving company failed to maintain a safe work area in a manner consistent with the work required, profession, and training of the people.
- The location of the cut and third-party laboratory reports indicate the hose cut was consistent with a deliberate sawing action while being held and was not consistent with being dragged along the ground and cut by an unidentified object.
- The propulsive force of the pumped water would be limited by the weight of the jetting hose and water, reducing acceleration significantly the more the diver lifted or was pushed around the bottom.
- The pumped water exiting the cut in the house could not provide sufficient water flow to propel the diver in the manner described, both in terms of lifting the person violently as well as forcing violent contact with the bottom.

- The velocities calculated using the simplified conservative models are not consistent with the literature values associated with injury. Final determination of the relationship of available velocity and acceleration to the injuries was done by an appropriate medical professional qualified in evaluating these types of injuries.

- In summary, the diver's report of the underwater events is not consistent with the physics associated with the equipment in use in the reported configuration and operating conditions.

References

1. L. L. Liptai, "Forensic Engineering And The Scientific Method," Journal of the National Academy of Forensic Engineers, vol. 26, no. 1, 01/01 2009, doi: 10.51501/jotnafe.v26i1.711.

2. OSHA Laws & Regulations, O. S. H. Administration 29 CFR 1910 Subpart T "Commercial Diving", 2011.

3. International Consensus Standards For Commercial Diving And Underwater Operations, ADCI, Houston, Texas, 2011. [Online]. Available: https://www.adc-int.org/content.asp?contentid=173.

4. F1166-07 Standard Practice for Human Engineering Design for Marine Systems, Equipment, and Facilities, ASTM, West Conshohocken, PA, 2013. [Online]. Available: https://www.astm.org/Standards/F1166.htm.

5. *Flow of fluids through valves, fittings and pipe:* Technical Paper 410. Stamford, CT: Crane Valves, 2011.

6. M. A. Passmore and G. Rickers, "Drag levels and energy requirements on a SCUBA diver," Sports Engineering, vol. 5, no. 4, pp. 173-182, 2002, doi: 10.1046/j.1460-2687.2002.00107.x.

7. C. Harris and A. G. Piersol, *Harris' Shock and Vibration Handbook*, 2009, New York, NY: McGraw-Hill, 6th ed., 2009, p. 1168.

8. M. M. Panjabi, P. C. Ivancic, Y. Tominaga, and J.-L. Wang, "Intervertebral Neck Injury Criterion for Prediction of Multiplanar Cervical Spine Injury Due to Side Impacts," Traffic Injury Prevention, vol. 6, no. 4, pp. 387-397, 2005/12/01 2005, doi: 10.1080/15389580500257100.

9. "Test methodology for protection of vehicle occupants against anti-vehicular landmine effects : final report of HFM-090 Task Group 25," in "RTO technical report," NATO Research & Technology Organisation;, Neuilly-sur-Seine, 9789283700685, 2007, vol. 90. [Online]. Available: https://www.tib.eu/de/suchen/id/TIBKAT%3A578708116.

10. A. M. Eiband, "Human tolerance to rapidly applied accelerations: a summary of the literature," NASA, June 1959. [Online]. Available: https://ntrs.nasa.gov/citations/19980228043.

11. C. D. Walker. "Using Computer-Generated Animation and Simulation Evidence at Trial: What You Should Know." American Bar Assocation. https://www.americanbar.org/groups/litigation/committees/products-liability/practice/2018/using-computer-generated-animation-simulation-evidence-at-trial/ (accessed October 17, 2019).

12. V. Webster and F. Bourn, "The Use of Computer-Generated Animations and Simulations at Trial," Defense Counsel Journal, vol. 83, pp. 439-459, 10/01 2016, doi: 10.12690/0895-0016-83.4.439.

13. V&V 20 Guide For Verification And Validation In Computational Fluid Dynaics and Heat Transfer, ISBN 9780791873168, ANSI/ASME, New York, 2009.

14. A. V. Ivanov, T. V. Trebunskikh, and V. V. Platonovich. "Validation Methodology for Modern CAD-Embedded CFD Code." Dassault Systemes. https://www.solidworks.com/sw/docs/Flow_Validation_Methodology-Whitepaper.pdf (accessed 18 December, 2019).

15. P. Hariharan, G. A. D'Souza, M. Horner, T. M. Morrison, R. A. Malinauskas, and M. R. Myers, "Use of the FDA nozzle model to illustrate validation techniques in computational fluid dynamics (CFD) simulations," PLOS ONE, vol. 12, no. 6, p. e0178749, 2017, doi: 10.1371/journal.pone.0178749.

16. Neutrium. "Pressure Losses in Hoses." https://neutrium.net/fluid_flow/pressure-loss-in-hoses/

(accessed 12 Sept., 2017).

17. “Series SS122 Lightweight Water Jetting Hose.” Parker Hoses. https://ph.parker.com/us/15551/en/lightweight-water-jetting-hose (accessed 12 Sept., 2017).

18. Firedepartment.net. “2.5" Fire Hose Friction Loss Calculator.” https://www.firedepartment.net/fire-dept-tools/printable-friction-loss-calculator/two-and-a-half-inch (accessed 21 Sept., 2017).

19. A. Pasha, A. Mushtaq, and K. Juhany, “Numerical Study of Heat Transfer of Water Flow through Pipe with Property Variations,” Athens Journal of Technology and Engineering, vol. 4, pp. 359-385, 12/01 2017, doi: 10.30958/ajte.4-4-4.

20. J. V. N. Sousa, A. R. L. Macêdo, W. Amorim Jr, and A. G. B. Lima, “Numerical Analysis of Turbulent Fluid Flow and Drag Coefficient for Optimizing the AUV Hull Design,” Open Journal of Fluid Dynamics, vol. 4, pp. 263-277, 09/01 2014, doi: 10.4236/ojfd.2014.43020.

21. G. M. Wilcox, “Drag Studies in Water Entry of the MK 13-6 Torpedo,” California Institute of Technology, Pasadena, CA, July 1951 1951. [Online]. Available: https://authors.library.caltech.edu/57351/1/E-12.1.pdf.

Lessons Learned from a Forensic Engineering Investigation of a Scaffold Support Failure

By John N. Schwartzberg, PE (NAFE 639F)

Abstract

During use, a scaffold support allegedly failed, causing injuries to the user when he fell. The plaintiff's expert identified a defective weld as the cause of failure and opined that the product was improperly designed. This paper examines methods used to evaluate the circumstances of and claims made regarding the incident. A combination of engineering methodologies, including metallurgical evaluation, stress analysis, and physical testing, was used to examine the plaintiff's claims of deficiencies in the design and fabrication of the product. The engineering methodologies refute claims made about the structural capacity of the product by the plaintiff's expert and the fundamental cause of failure. This paper examines themes related to the presence of apparent defects/failure and the necessity of verifying postulated hypotheses. It also examines the efficacy of analysis and testing as part of implementation of the "forensic engineering method" in verifying or rejecting hypotheses en route to offering expert opinions in forensic engineering investigations.

Keywords

Product liability, the forensic engineering method, scaffold, failure analysis, finite element analysis, empirical stress analysis, load testing

Introduction

In forensic engineering investigations of product failures, the mere presence of a defect is insufficient to conclusively determine the cause of an incident. Rather, it must be shown by credible and reliable engineering methods that the product is defective, the defect renders the product unreasonably dangerous, and the defect is the primary cause of the incident in which harm is incurred. This paper uses a scaffold collapse incident to examine the necessity of providing engineering analysis, calculation, and/or testing to show the link between the defect and the incident. Furthermore, the ramifications of presenting preliminary findings and opinions formulated prior to litigation are examined. Use of the forensic engineering method as a road map for ensuring the validity of opinions is considered, and the relationship between the forensic engineering method and the legal doctrine of strict liability is investigated.

Background

The incident upon which this case study is based involves the failure of a tripod-style scaffold support. The product features a ladder-style fixed frame with extendable legs. An extendable third leg is attached to the upper crossmember of the frame via a hinged connection. A graphical representation of a scaffold support is shown in **Figure 1**. The scaffold frames are used in pairs to support a scaffold plank. The advantage of the independent scaffold supports with adjustable legs, according to the manufacturer, is that they can be used on uneven ground while maintaining a level and stable working surface.

The tripod leg is attached to the top horizontal member (cross-brace) of the frame via a hinge mechanism, as shown in **Figure 2**. Two aluminum alloy 6061-T6 lugs are welded to the aluminum alloy 6005-T6 extruded member. The top of the tripod leg is secured between the lugs by a cap screw. Each lug is welded to the top cross-brace with a 0.25-inch fillet weld on the outside of the lug.

Incident

The scaffold user in the present case was a homeowner who claimed to have extensive commercial construction experience, including considerable knowledge of scaffolding and its use. He purchased the pair of scaffold supports

John N. Schwartzberg, 925 West Kenyon Ave., Unit 1, Englewood, CO 80110, (303) 306-0990, john@rmemtec.com

new and claimed to have used them four times prior to the day of the incident — each time without incident. On the day of the incident, he was using the scaffold system at his house to install new siding.

In his deposition, he testified that he set up one of the supports on a concrete pad adjacent to the wall of the house on which he was working. The other support had one leg on the same concrete surface. The user testified that he had cut boards on which the other two legs were placed because they were located on gravel or dirt. On the day of the incident, he claimed that he was using an extendable aluminum plank (scaffold platform). Contrary to his statement that he had used the scaffold supports four times prior to the day of the incident without incident, he also testified that he had used a wooden board on a previous day, but had fallen off the wooden plank, citing instability of the scaffold supports as the reason for the fall.

Figure 1
Graphical representation of tripod scaffold support.

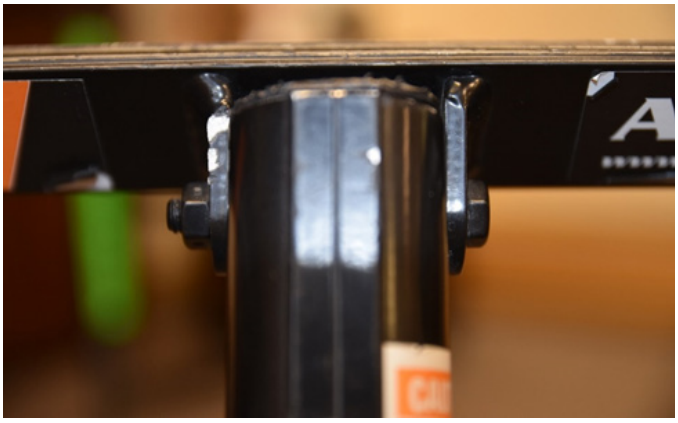

Figure 2
Arrangement of lugs and attachment of top of tripod leg to upper cross-brace.

His testimony varied as to the height of the plank on the day of the incident, but the totality of his statements suggested that the scaffold supports were up with the legs at maximum extension.

The user employed a ladder leaning against the house to ascend to the plank. When he walked to one end of the scaffold, the support at that end failed (he claimed) suddenly and without warning, causing him to fall and strike his head. He testified that after he regained consciousness, he went into the house, and then returned to the location of the scaffolding — whereupon he threw the planking and the support that reportedly had not failed into a neighbor's yard in frustration. He testified that he did not throw the collapsed scaffold support.

Applicable Standards and Load Rating

ANSI/ASSE A10.8, *Safety Requirements for Scaffolding — American National Standard for Construction and Demolition Operations*, is the specification that prescribes certain performance criteria and usage requirements for scaffolding and is applicable to the scaffold that is the subject of this investigation[1]. Furthermore, a warning label attached to the product states that it meets or exceeds the requirements of ANSI A10.8-2001.

Among other performance criteria, ANSI A10.8 states, "Scaffolds shall be capable of supporting, without failure, their own weight and at least four times the maximum intended load." The standard defines failure as: "The condition in which a component or assembly can no longer support the load (also known as load refusal)."

The manufacturer's stated load rating is 300-lbf per support or 600-lbf per pair. The manufacturer also claims that each support weighs 16-lbm, which was confirmed during the investigation. As such, the proof test load specified by ANSI A10.8 would be 1,216-lb per support.

At the time of the incident, the user claimed that his

weight (and the weight of the hand tools he carried) were less than 200 lbm.

Plaintiff's Expert Opinions

The attorney for the user retained an engineering expert to examine both the failed and unfailed scaffold supports — and to offer preliminary opinions as to the cause of the failure and the incident. The expert's pre-litigation report letter (on behalf of the plaintiff) claimed that the scaffold support failed because welded lugs at the top of the tripod had separated from the frame, resulting in the collapse of the structure. The report claimed that the failed weld did not bond properly to the aluminum frame, the lack of penetration made the weld the weakest link in the connection, and "relatively little force was required to separate this lug from the frame."

In support of these findings, the plaintiff's expert performed optical microscopy, radiography, and scanning electron microscopy (SEM)* on one or both fractured lugs from the failed support. The radiography and SEM examination (coupled with optical microscopy), it was claimed, confirmed that the weld was defective. Examples are shown in **Figure 3** and **Figure 4**, which contain a photomicrograph of one of the lugs and X-ray of both lug locations.

Figure 3
Photomicrograph from the plaintiff's expert's preliminary report, highlighting lack of root penetration.

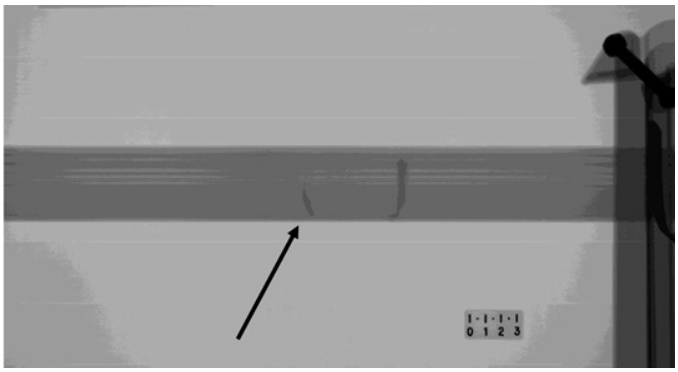

Figure 4
Photograph of radiograph from the plaintiff's preliminary report, indicating "very little weld penetration" on one of two failed lugs.

This expert's pre-litigation report offered the following:

- The scaffold support failed due to inadequate weld penetration of the lug that attaches the top of the tripod leg to the support frame.
- The failure of the scaffold support was due to defective manufacture and not due to improper use.
- The lug, which was welded on one side only, was substantially weaker than subsequent designs in which the lug was welded on both sides; as such, it was inferred, the single weld design detail was inadequate and, thus, related to the failure.

In a subsequent report prepared during litigation, the plaintiff's expert reiterated the preliminary opinions, providing specific focus on weld quality. The second report cataloged a long list of what the plaintiff's expert described as weld defects, and it was further alleged that all scaffold supports welded in the same manner were defective. In neither report did the plaintiff's expert offer any analysis, calculation, or testing to relate the observed weld condition to the failure.

Examination of the physical evidence and review of this expert's documentation showed that the failed weld exhibited (at best) modest penetration at the root of the weld. However, the lugs exhibited evidence of a small amount of ductile deformation or permanent bending. This indicated that the weld was able to withstand sufficient load to allow the lugs to bend prior to fracture, which is inconsistent with the plaintiff's expert's claim that the weld failed at low loads and in a brittle manner. Two views of the failed support are presented in **Figure 5**.

Engineering Analysis and Testing

To evaluate the significance of the observed deformation — and to evaluate the plaintiff's claims that the design of the support was defective because the lugs were welded on one side only — a stress analysis was performed. The analysis consisted of simplified hand calculations, finite

* The examination required disassembly of the parts to remove the fractured lug from the cap screw joining the lugs and the top of the tripod leg. This was done without notice to other potential parties; as such, representatives for the manufacturer and its experts were precluded from participating in this examination.

Figure 5
Two overall views of failed scaffold support with legs collapsed. Note the fractured lug welds at top of left image and deformation of spreader bar assembly visible in both views.

element analysis (FEA), and empirical stress analysis (testing).

Hand Calculations

Initially, simplified hand calculations were performed to determine the load-bearing capacity of the fillet welds that join the lugs to the frame. These calculations included several simplifying assumptions, including an assumption that the welds were without defect, the welds were oriented vertically (not at an angle with respect to vertical, as they are on the frame), and the weld was loaded only in shear. The allowable stress in the weld was calculated by determining the effective area of the weld as the effective throat multiplied by the length of the weld, as prescribed by AWS D1.2, *Structural Welding Code – Aluminum*. This code defines the effective throat as the minimum distance between the root of the weld and the face of the weld, which would be the leg length multiplied by 0.707 (the cosine of 45°) for an ideal symmetrical fillet weld[2].

Aluminum alloy 4043 is commonly used as a weld filler wire for 6000-series aluminum alloys and is the filler wire specified by the scaffold manufacturer. Product information for 4043 weld wire gives typical as-welded strength values of approximately 18 ksi for yield strength and an approximate tensile strength in the range of 27 to 33 ksi. Using the typical yield strength value of 18 ksi as an allowable stress before safety factors, the allowable load on each lug weld was calculated to be approximately 5400 lbf — or 18 times the rated load for the entire support[+].

Finite Element Analysis

Finite element analysis (FEA) was then employed to further interrogate the adequacy of the structure and the role of the claimed weld defect in the failure. For the purposes of the analysis, a conservative failure criterion was considered to be any stress in excess of the yield strength of the component. The ANSI A10.8 standard defines failure as the inability to support load, which is possible even after materials yield. Thus, the ANSI standard offers a more lenient approach to material failure than the more conservative criterion employed in the present analysis.

Autodesk Fusion 360 was used for the FEA, which was performed using linear elastic methods. Linear elastic analysis is limited to stresses in members up to their proportional limit (the stress at which permanent deformation sets in, similar to the yield strength of the material), while non-linear analysis utilizes full range stress-strain curves for each material to accommodate post-yield plastic (permanent) deformation. However, for the purposes of the present analysis, linear analysis was sufficient to evaluate the adequacy of the design; stresses beyond the yield strength of any component material would not be consistent with the criterion stated above.

A basic model for the FEA is shown in **Figure 6**. The front two feet are constrained against translation and rotation (as they would be on a flat, level surface with

+Although simplified in approach by considering only shear loading, even if combined loading were considered (i.e., shear and tension or transverse tension), it is unlikely that the effects of combined loading would be sufficient to reduce the joint strength enough to exceed the significant safety factor in pure shear.

adequate friction.) The tripod leg foot (rear) is constrained to preclude moving or deflecting in the direction normal to the surface (vertically). The leg is free to rotate, move, or deform in the direction tangential to the surface. In addition, the pinned joints are free to rotate. The rubber feet were omitted from the analytical model, as they do not perform a structural role and the constraints applied to the analysis fulfill the same function as the rubber feet in preventing the legs from sliding on the surface.

The load is applied as a distributed load on the scaffold top brace, as would be encountered in service with the use of a scaffold plank. For this analysis, the load was distributed over a 15-inch distance to match the width of the plank described by the user in his deposition. For the basic analysis, the load was applied in only the downward vertical direction (parallel to the gravity vector) in the same manner as the loading test prescribed in the ANSI standard.

A linear analysis was performed to verify the load rating (300 lbf) of the scaffold support. The loading for this load case consisted of a purely vertical 300-lbf uniform load distributed over the central 15-inch length of the scaffold top brace, as shown in **Figure 7**. This is consistent with the manner of loading that would be expected if the scaffold were used in the manner described by the manufacturer in its instructions and product information.

Results of this analysis showed that the scaffold easily bore the rated load applied in the manner shown in **Figure 7**, with Factors of Safety (against the yield strength of the materials) in excess of 4.8 and maximum (Von Mises) stress of 6.95 ksi. The maximum stress occurred in the tripod leg near hinge pin hole. The maximum stress in the scaffold frame was approximately 4 ksi and occurred in the scaffold top brace adjacent to (but not in) the weld. Results of the analysis are shown in various views in **Figure 8**.

The analysis was repeated using the same model, but with an applied load of 1200 lbf, which is approximately the load specified as the proof load in ANSI A10.8-2001. The same constraints were used as in the previous analysis. Results of this analysis, which are presented graphically in **Figure 9**, showed that the peak stress occurred in the tripod leg near the hinge hole. The maximum stress in the scaffold frame structure occurred in the top brace adjacent to the weld at a magnitude of between 15 and 18 ksi, which is less than half the minimum expected yield strength for the aluminum alloy 6005-T6 member.

Based on the foregoing analyses, the design of the structure appeared to be adequate for the rated load of 300 lbf and the specified proof test load of approximately 1200 lbf, with peak stresses less than half of the yield strength at the higher load. Thus, the safety factor as determined by FEA was more than 2:1 against yielding at the proof test

Figure 6
Overall view of basic model used for finite element analysis.

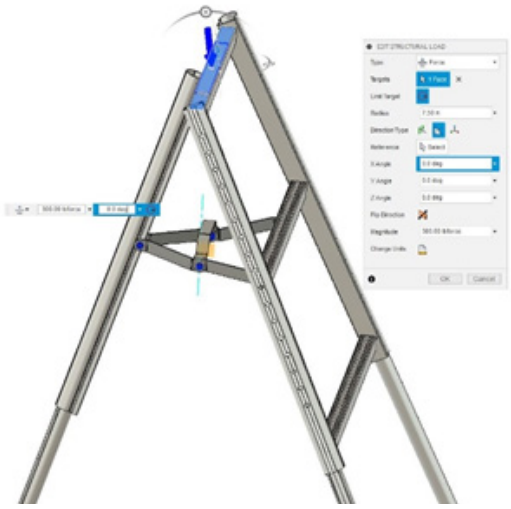

Figure 7
Applied load for 300-lbf rated load analysis.

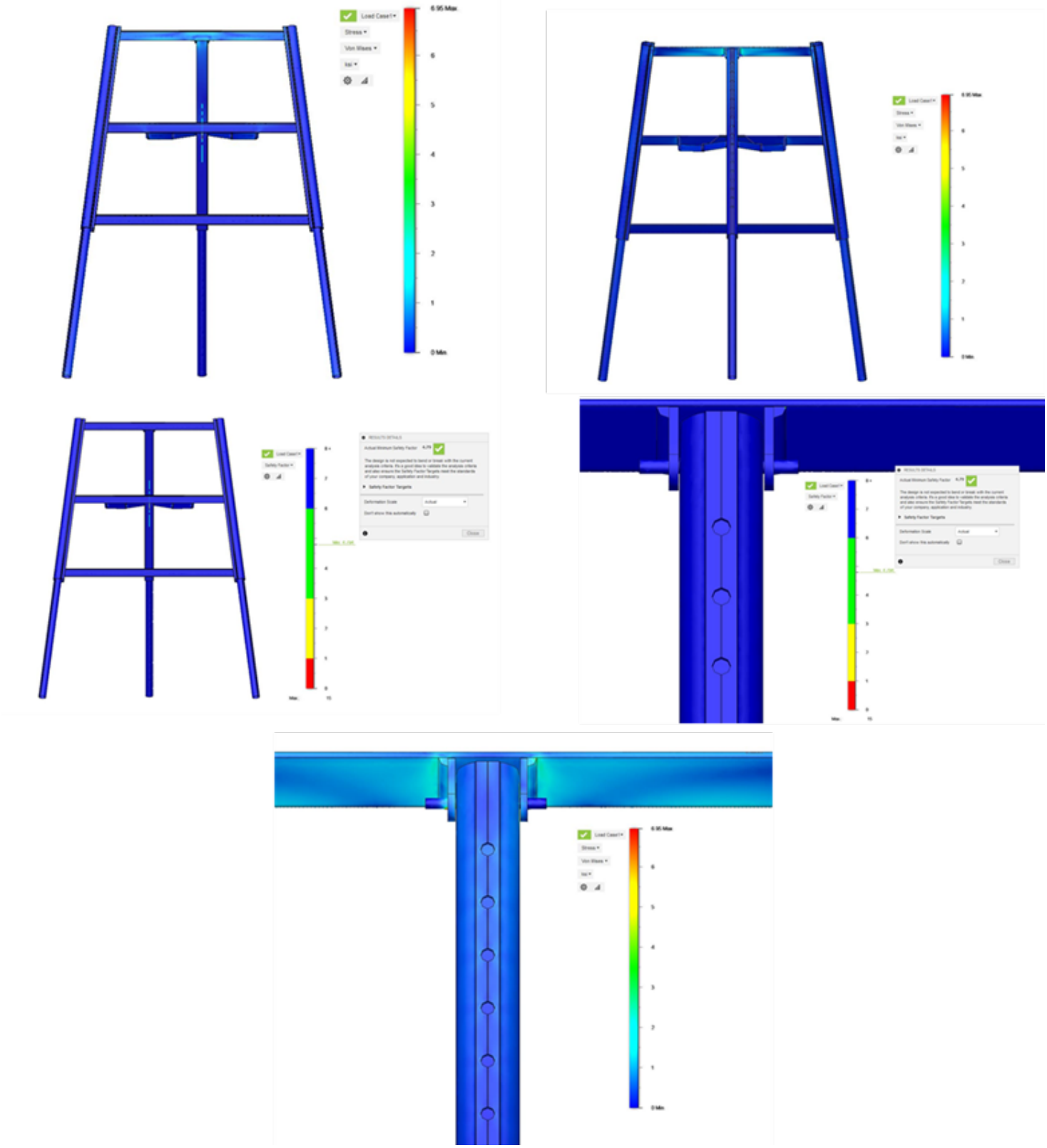

Figure 8

Graphical representations of results of FEA of rated load analysis (300 lbf). Upper left shows front view Von Mises stress (ksi). Upper right shows rear view Von Mises stress (ksi). Middle left view shows front view factor of safety (against yield). Middle right view shows factor of safety in area of top brace lug welds. Bottom view shows Von Mises stress (ksi) in area of top brace welds.

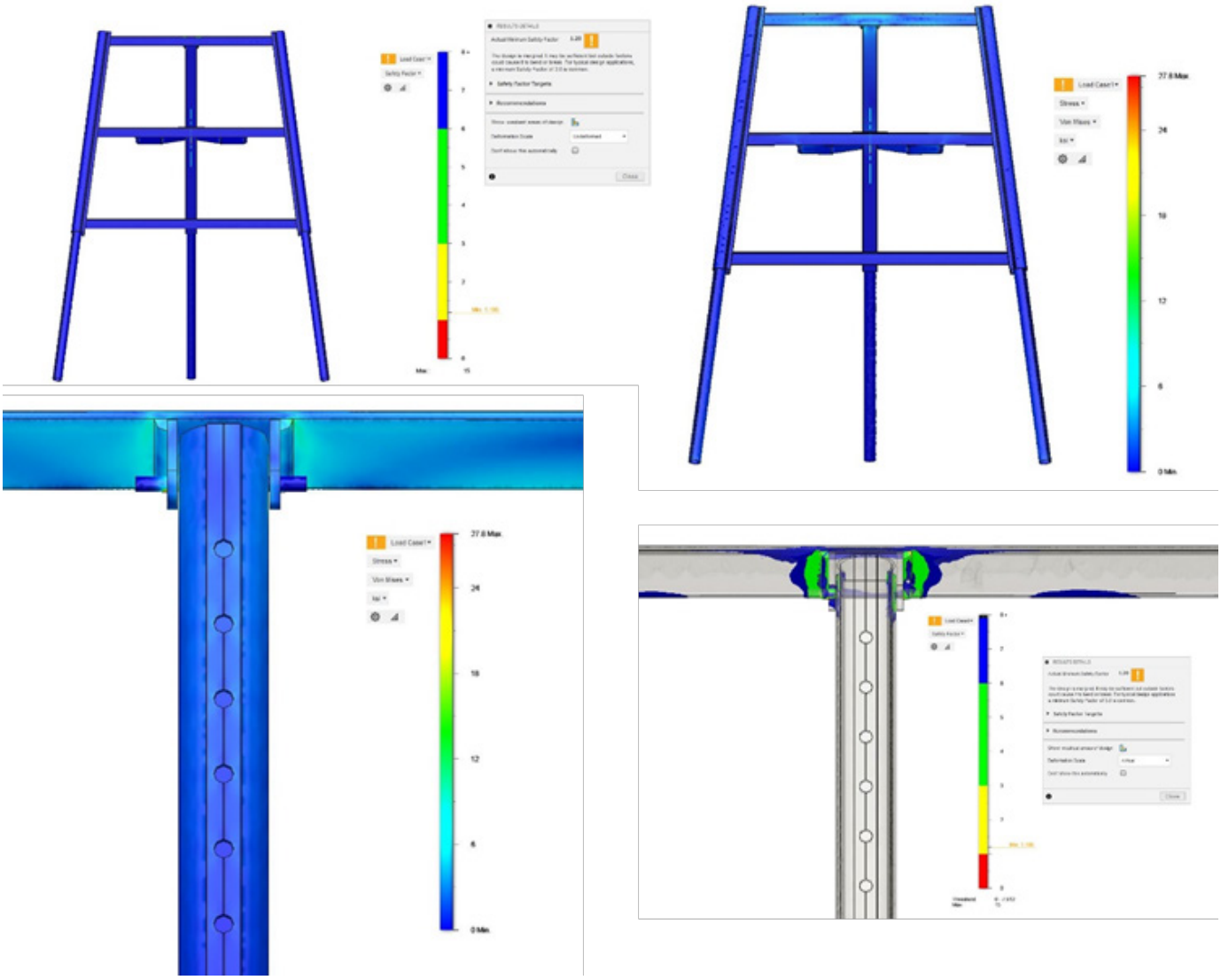

Figure 9
Graphical representations of results of 1200 lbf proof load FEA. Upper left: front view factor of safety. Upper right: front view Von Mises stress (ksi). Lower right: Close-up of Von Mises stress (ksi) in weld area. Lower right: close-up of weld area showing factor of safety.

load, and more than 8:1 against yielding at the rated load. The FEA also revealed that peak stresses did not appear in the lug welds.

The 300-lbf rated load study was repeated, but with the model modified to remove the bond between the lug-to-top brace weld on one side of the hinge (effectively removing the weld from the structure). This case, shown schematically in **Figure 10**, is the worst-case scenario of the plaintiff expert's theory of a defective weld — one that is so compromised as to bear no load at all. This condition represents complete lack of fusion/lack of penetration so that the weld is completely detached from the frame. The analysis was performed with the same loading and constraints as in the first rated load case. Results of this analysis showed that the maximum stress in the scaffold

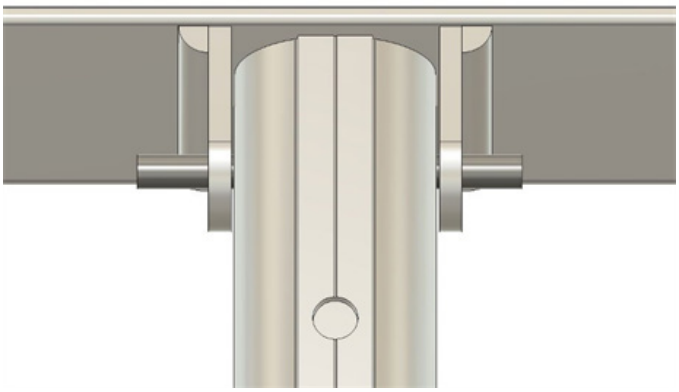

Figure 10
Close-up of lug-to-top brace weld area showing details of model for analyses with one weld detached from top brace. This condition represents complete lack of fusion/lack of penetration of the left-hand weld.

frame occurred in the tripod leg around the hinge hole at a magnitude of approximately 15.2 ksi. The highest stress in the weld area was approximately 4 to 5 ksi in the weld that remained fully bonded. This represented a safety factor between 3.6 and 4.5 against yielding at the rated load — even with one lug weld completely detached.

Load Testing

Two exemplar scaffold supports exhibiting the same weld configuration as the subject evidence were procured as part of the investigation The exemplars were in like-new condition, represented by the seller to have never been used. Examination confirmed that there was no evidence of prior use.

Load tests were performed on exemplar scaffold supports. The scaffold support was set up on cinder blocks, which were resting on a smooth concrete floor. Legs were extended to full length for testing. A piece of aluminum extrusion stock was used to distribute the applied load over a 15-inch length of the top scaffold brace. An electric winch with wire rope was used to apply a tensile load, which was measured using a 2500-lbf capacity load cell. The force value from the load cell was displayed on an indicator paired with the load cell. Smaller ($^1/_8$-inch) diameter wire rope was used to suspend a spreader bar from the loading bar, to which the primary loading line was attached. A representative photograph of the test set-up is shown in **Figure 11**.

During testing, it was observed that the application of the load produced a short-duration peak load that diminished quickly to the nominal starting static load. This peak load was detected by the load cell and indicator — and was recorded with the test record. Once the peak load reduced to the nominal static load, it was observed that the static load reduced during the load hold duration (typically four to five minutes) due to relaxation of the structure. Thus, the nominal static load was reported herein as a range (initial load to final load at the end of the load duration).

Several tests were run on an exemplar scaffold. In the first test, the scaffold support design was tested by applying a load in excess of the rated load of the scaffold. A peak load of 414 lbf was observed at the outset of the sustained loading as the load was applied. A sustained load ranging from 330 to 360 lbf was applied to the test article over a period of approximately 4 minutes. No permanent deformation, damage, or compromise in operation was observed to the scaffold support after the load was released.

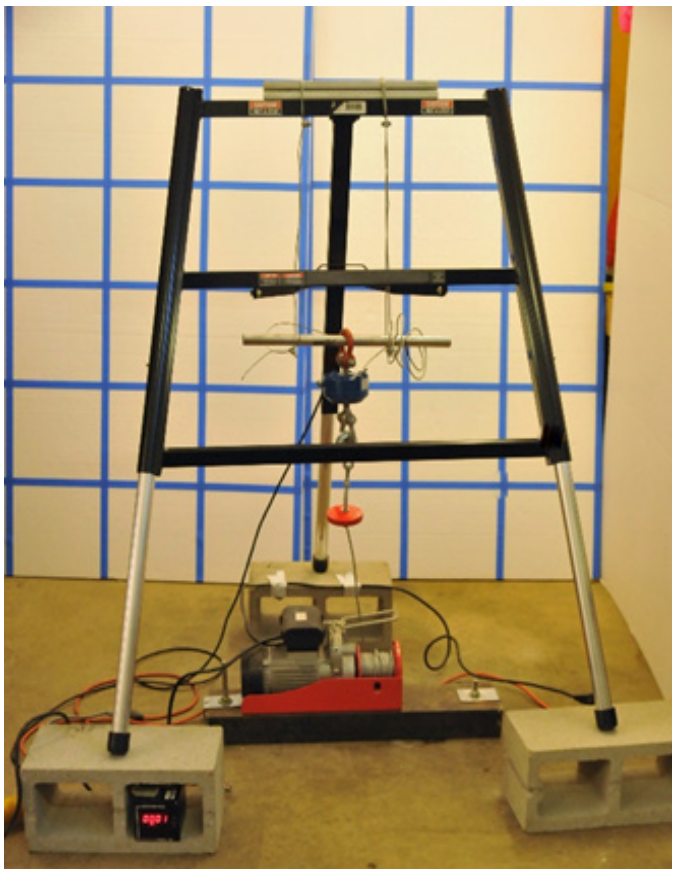

Figure 11
Load test set-up. Load is applied through wire rope (with load cell) to spreader bar, then to loading bar strapped to top scaffold brace.

In a second test, a load in excess of the proof test load specified in ANSI A10.8-2001 (four times the rated load plus the weight of the scaffold, or 1216 lbf) was applied in the same manner as the previous test. A peak load of 2387 lbf was measured before the sustained load settled in at about 1791 lbf, decreasing to 1250 lbf over a 5 minute period. The test article was loaded and unloaded several times prior to establishing the sustained load magnitude. After the test, there was no observable permanent deformation, damage, or compromise in operation.

Following the second load test, one of the upper hinge brackets (lug) was removed from the top scaffold brace by cutting the weld attaching the lug to the brace. This was equivalent to the FEA analysis performed with one weld not bonded to the frame. The load was applied in a manner similar to the previous tests using the same configuration. A peak load of 1098 lbf was measured before the sustained load of approximately 700 lbf was applied over a duration of approximately 5 minutes. As before, there were several load/unload cycles before the load was established at the sustained load magnitude. After the load was released,

there was no visible evidence of deformation, damage (other than the removed weld), or compromise in operation of the scaffold.

Two additional tests were run on the exemplar with the removed lug weld. In these tests, the loading bar was moved to each end of the top scaffold brace. Otherwise, the configuration and loading manner were essentially the same as the previous tests (except that the slight misalignment of the loading cable was adjusted to further minimize lateral loading).

With the loading bar to the right (the same side of the scaffold with the removed lug weld), a peak load of 1683 lbf was measured, with a sustained load of 1526 to 1475 lbf applied over a 5-minute period. After the sustained load period, the load was cycled six times before unloading to impart dynamic loading to the scaffold. During loading under these conditions, the scaffold exhibited a tendency to deform by rotating counter-clockwise when viewed from above (or, stated a different way, the end of the top scaffold brace with the loading bar tended to rotate toward the tripod leg). After this test, there was no visible evidence of deformation, damage (other than the removed weld), or compromise in operation of the scaffold.

With the load applied to the left end of the scaffold top brace, the peak load was 1399 lbf, with a sustained load of 1244 to 1117 lbf applied over a 5-minute duration. Following the sustained load, four load/unload cycles were applied, with the highest applied load measured at 2209 lbf. The intention was to load the scaffold to failure; the test set-up was unable to generate sufficient sustained load to bring the test article to failure. Under this offset load configuration, the scaffold tended to translate to the opposite direction, with significant bending observed in the left leg. The left end of the top brace dipped slightly. At the highest load of 2209 lbf, significant bending of the left leg was observed, along with a general translation of the upper part of the scaffold support translating to the right (approximately 3.75 inches at the highest load). As with the first offset load test, no permanent deformation or damage was observed in the test article when the load was removed.

Discussion

The analysis and testing presented above demonstrates that the design of the scaffold support was sufficient for the rated load of 300 lbf per support and the proof test load of 1200 lbf required by the ANSI standard. Maximum stresses predicted by the finite element analyses were significantly below the yield strength of the component materials, and the analyses did not predict failure at the lug welds (nor do the analyses identify the lug welds as the locations of highest stress). With one lug weld absent, FEA did not predict failure at the rated load. The empirical testing also demonstrated the adequacy of the design. Even with one weld completely removed — and with a combination of static and dynamic forces applied — the scaffold sustained a load of more than twice the rated load without deformation, damage, instability, or a compromise in operation of the scaffold.

In the present case study, the fact that test loads of more than 2000 lbf were applied without failure not only showed that the design was sufficient for the rated load, but that extreme circumstances also seemed to be required to cause failure — even when the weld in question played no part in the load-bearing capacity of the structure. Thus, although weld defects like the incomplete root penetration observed in the lug weld were undesirable, their presence may be more aesthetic than detrimental to the structural integrity of the article.

Ostensibly, in the plaintiff's expert's theory (although not specifically elucidated), the collapse of the scaffold and the related deformation of the locking spreader bar components were the result of the collapse of the scaffold after the supposedly defective weld "suddenly and without warning" failed. However, analysis — both theoretical (FEA) and empirical (testing) — were not consistent with the claims. Only under extreme circumstances was catastrophic failure of the weld and collapse of the entire structure likely — even more extreme than completely removing one weld.

The asymmetric load tests (loaded to edge of upper cross-brace) may provide some indication of the potential cause of failure. Although loading to approximately 2000 lbf did not cause failure, examination of the tendency of deformation under this loading revealed that the support began to deform (not permanently) in a manner similar to the deformation observed in the failed support. This suggested that the failure may have been caused by an extreme asymmetric loading condition, one that included a large lateral component (to the side of the support) as well as a large vertical load.

A significant lateral load component could be caused by instability of one or more feet and legs. Recall that the plaintiff had testified in his deposition that he had fallen from the scaffold on a previous day because of instability, which he attributed to the support. After that, he had cut

boards to place on the rock or gravel earth surface, upon which he placed the two feet (and legs) of the support not located on the concrete pad. Instability of one of the frame legs and/or the tripod leg would cause lateral displacement of the legs, resulting in deformation of the spreader bar assembly to the side and rotation of the tripod leg, as observed on the subject evidence. Thus, the theory that failure was due to the plaintiff's use of the product cannot be excluded. This is further compounded by the fact that he acknowledged prior instability, causing him to fall. The physical evidence did not allow a conclusive determination as to whether or not this prior incident caused damage to the support; however, it must be considered when arriving at conclusions as to the cause of the incident.

In his deposition, the plaintiff also acknowledged (perhaps unknowingly) other aspects of improper use of the supports and inconsistencies. For example, the user claimed to have used the supports only four times (days) prior to the incident, including one or two days immediately before the day on which the scaffold support failed. Examination of both the failed and unfailed supports showed characteristics not consistent with four days of use, including significant wear on the rubber feet.

The wear was also consistent with expectation if the feet slid on a hard surface. He also claimed to have stored the supports in a garage, out of the elements. However, steel components of the spreader bar assembly exhibited notable corrosion, which was not consistent with his testimony. His testimony also showed that despite his claim that he was an experienced user of scaffolding from his career as a contractor, he failed to comply with the manufacturer's instructions for use and with aspects of usage prescribed by the ANSI standard.

Both the plaintiff's expert and defendant's experts agreed that at least one of the lug welds exhibited evidence of incomplete root penetration. Root penetration is generally considered necessary for fillet welds, such as those attaching the lugs to the upper cross-brace, to meet criteria for quality welds in welding codes such as AWS D1.2. However, there is a difference between complying with welding codes and standards and conclusively determining the cause of failure. The mere presence of an indication of defect in a weld does not necessarily constitute the cause of failure, even if the indication would render the weld rejectable by certain codes, specifications, or standards. The role of the indication or defect in the chain of proximate cause of a failure must be interrogated and proven.

The foregoing information calls into question the competency of expert opinions that are offered without adequate support. The plaintiff's expert disclosure, which included two different reports, conveyed no basis for the link between the observed weld quality and the failure. There were no calculations, analysis, or testing in support of the theory; rather, the expert claimed ipse dixit that there was a weld defect and, ergo, it must have been the cause of failure, without further investigation or interrogation. The disclosure was also critical of the weld detail, claiming that the lug with the single weld was notably weaker than a subsequently manufactured exemplar that featured a lug welded on both sides. The implicit argument, propounded by the plaintiff's counsel, was that the single weld design was inadequate. This assertion was unfounded and irrelevant. Without engineering analysis or testing, the design claim failed to be credible. The fact that a part of the structure can be made stronger is irrelevant, especially when, as defense expert's analysis and testing prove, it is more than sufficient in the first place.

In their paper "Forensic Engineering and the Scientific Method,"[3] authors Liptai and Cecil provide a comprehensive comparison of the Scientific Method, the Forensic Engineering Method, and the similarities and differences between them. Science, they state, "can be defined most succinctly as a department of systemized knowledge," while engineering is "the application of science." The Scientific Method entails observation, formulation of a hypothesis, testing of the hypothesis, data analysis, and confirmation or rejection of the hypothesis in what is often an iterative process. As forensic engineering, which is most often based on the application of existing scientific principles, rarely involves formulation of true hypotheses, Liptai and Cecil outline a modification of that method appropriate for forensic engineering investigations, as shown in **Figure 12**.

This methodology involves observation (of the precedent event or, as in this case, failure), definition of the engineering problem, data collection and analysis, and the development and evaluation of findings. This, like the Scientific Method, is an iterative method. Like the necessity to validate or reject the hypothesis in the Scientific Method, the Forensic Method demands that the practitioner evaluate the findings that emerge from the investigation in the same manner that primary researchers utilizing the Scientific Method fairly gauge the validity of their own hypotheses. To do so, write Liptai and Cecil, the practitioner must engage in some manner of reasonable and credible data collection, which may consist of observation, research,

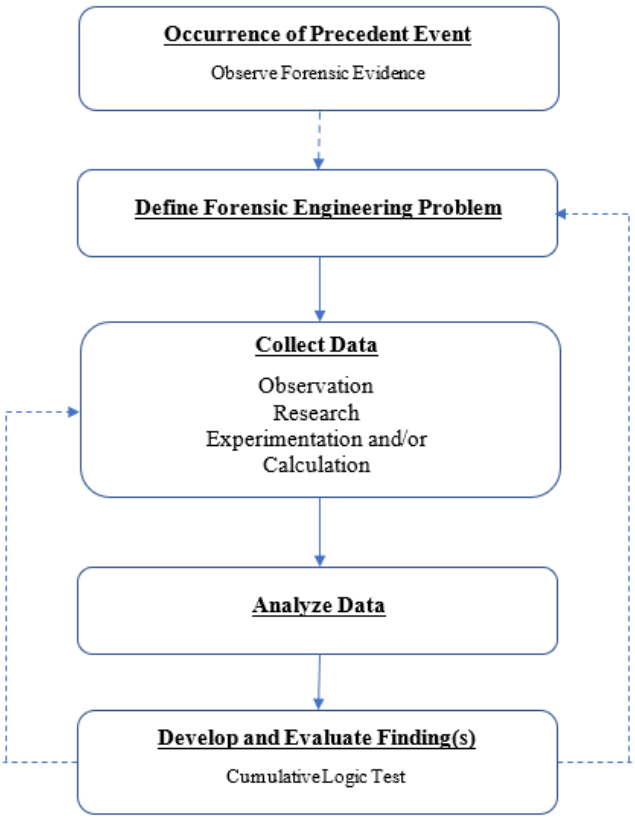

Figure 12
Schematic representation of forensic engineering method (after Liptai and Cecil).

experimentation and/or calculation, followed by reliable analysis of the data. To forward findings, opinions, and/or conclusions without benefit of these two critical steps may yield results that are flawed. More importantly, as with Daubert and Frye challenges, the results may be deemed unreliable because the methodology is flawed.

In the present case, the plaintiff's expert failed to properly collect and analyze relevant data. The plaintiff's expert's second report included a dissertation on aspects of welding practice, but stopped short of tying the perceived deficiencies to the actual failure. Furthermore, relevant evidence (plaintiff's manner of use of the product) was either ignored or was not recognized as a relevant and necessary component of the Forensic Engineering Method.

This concept is also captured by the legal doctrine of strict liability for products. This doctrine places liability on a manufacturer of a product if, as described by Thorpe and Middendorf in "What Every Engineer Should Know About Product Liability,"[4] the plaintiff can prove "that the product is defective, unreasonably dangerous, and the proximate cause of the harm." This is a three-step process. To prevail, the plaintiff must show: 1) that the product is defective; 2) that the defect renders the product unreasonably dangerous; and 3) that the defect is the primary cause of the incident in which the plaintiff suffers some injury or damage. The parallel to the forensic engineering method becomes clear: The forensic engineering method requires the practitioner to directly link the observations and data (i.e., the defect) to the outcome through proper analysis, while the legal doctrine of strict liability requires that the defect be the primary cause of the damage. Thus, good engineering practice and legal theory, although distinct and separate, coincide on the need prove that a specific condition actually caused a specific outcome.

In his pre-litigation report, the plaintiff's expert offered a number of factors associated with the failure, including that the weld defect was the cause of failure, the design of the support was inadequate, an improper filler wire was used for welding, and failure was not due to improper use. It is not unusual for attorneys to retain forensic engineering experts to help them evaluate the merits of a case prior to filing of suit. However, it is imperative that forensic engineers approach their pre-litigation reports in the same manner as those prepared as predicates for expert disclosures within litigation, understanding that the pre-litigation works may become admissible and part of their body of work in the case. Thus, even with the inclusion of conventional boiler-plate language reserving the expert's right to modify or amend opinions later, offering pre-litigation opinions without benefit of the forensic engineering method may be fraught with peril. Potential opinions or conclusions may be better posited in other terms, such as areas for additional investigation. Better yet, such potential opinions might be best reserved until proper data collection and analysis can be executed, even when such activities entail providing notice to other parties. In short, preliminary opinions, even when couched as such, may live on to become issues as the case progresses to and through the litigation process.

Conclusions

The included case study highlights the necessity to complete the chain of proximate cause in forensic engineering investigations. The mere presence of a defect is insufficient to prove that the incident or failure was caused by the defect; rather, there must credible and reliable analysis, calculation, or testing to show that the incident or failure is the direct result of the condition. The Forensic Engineering Method provides a meaningful and accepted route to formulating and affirming reliable opinions.

Furthermore, the case study illustrates the potential adverse consequences of speculative findings and opinions formulated without benefit of analysis, calculation, or testing conveyed in a pre-litigation report. Experts should expect those findings and opinions to become part of their body of work in the matter once litigation is ensued and should treat pre-litigation findings and opinions with the same weight and care as those generated once suit has been filed. In the case study presented herein, a combination of engineering analysis and testing showed claims that the design of the scaffold support was improper were unfounded and cast significant doubt that the weld defect was the primary cause of the failure.

References

1. Safety Requirements for Scaffolding — American National Standard for Construction and Demolition Operations. ANSI/ASSE Standard A10.8, 2001.

2. Structural Welding Code — Aluminum. AWS Standard D1.2, 2014.

3. L. Liptai and L. Cecil, "Forensic Engineering the Scientific Method," Journal of the National Academy of Forensic Engineers, vol. XXVI, no. 1, pp. 147-155, June 2009.

4. J. F. Thorpe and W. H. Middendorf, What Every Engineer Should Know About Product Liability, New York: Marcel Dekker, Inc, 1979.

Forensic Engineering Analysis of a Swimming Pool Electric Shock Injury

By Robert O. Peruzzi, PhD, PE, DFE (NAFE 954M)

Abstract

This case involves a minor who received an electric shock while swimming in a membership swimming pool. Her family sued the pool association, its president, the electric utility, and others. At some time, tree trimmers had accidentally severed the service drop's neutral return wire. The electric utility made a temporary splice repair, but did not permanently replace the wire until several years later (after the incident). The forensic engineer (FE) was retained by counsel for the pool and its president to opine on electrical aspects of the plaintiff's complaints. The FE inspected the pool premises, reviewed documents, and examined the spliced service wires in storage. The FE opined that the pool association and its president were not negligent or careless — and that the electric utility failed its responsibility to maintain the service drop. This report discusses three-phase electric power, current flow, and how a severed neutral can cause a shock.

Keywords

Electric shock drowning, ESD, three-phase power, stray voltage, stray current, forensic engineering

Introduction

On the opening day of swimming pool season, a young woman was shocked while swimming in a pool owned by a paid-membership community recreation association (referred to as "Association" in this paper). Others in the pool at the same time did not receive shocks or feel tingling. The victim was taken to the hospital, examined, and released the same day. Shortly thereafter, her parents filed suit. The examining physician diagnosed electric shock based upon his visual examination. There were no debilitating physical injuries.

The plaintiffs in the case were the injured minor and her parents. The defendants were the Association, its affiliated Swim Club, the president of the Association, the supplying electric utility, the Association's electrical contractor, and an unnamed tree trimming company. (The tree trimmer was never identified.)

Discovery documents revealed that several years prior to the incident, an unnamed tree trimmer had accidentally severed the neutral wire of the four-wire, three-phase service drop from the utility pole to the pool facility. The power company made a "temporary" splice repair to that wire the following day, telling the Association representative that a permanent repair would be made "soon." The power company never returned to make the permanent repair, and the splice failed several years later. The utility did replace the entire service drop after the shock incident.

The FE was retained by counsel for the Association and its president to investigate, research, and opine on the electrical aspects of the plaintiff's complaints, which alleged that the Association and president:

1. Had exclusive control of the swimming pool.
2. Were careless in the pool's electrical maintenance.
3. Failed to provide a safe swimming pool for guests of the Swim Club.

The FE inspected the swimming pool premises and reviewed discovery documents as well as examined the failed splices on the service wires that had been removed and placed into evidence storage.

Case Timeline

In April 2014, municipal inspectors issued a bonding and grounding certificate to the Association that was valid for five years.

Robert O. Peruzzi, PhD, PE, DFE, 719 Fourth Ave., Bethlehem, PA 18018, (610) 462-3939; peruzzi@rperuzzi.com

In June 2014, a private tree trimmer hired by the pool association inadvertently struck the bundle of four electric power wires (service drop) between the utility pole and the electric service entrance to the swimming pool utility shed. The service drop was the property of the power utility.

The chain saw severed the bare neutral wire, apparently leaving the three hot wires and their insulation intact. The power utility's repair crew arrived within a day and spliced an approximately 4-foot bare wire across the damaged neutral bare wire, using crimp sleeves at each end. The repair crew chief reported to the power utility and the Association that this was a temporary repair — and that the team would return and replace the entire service drop between the pool and the utility pole. The power utility did not return to make the permanent repair. Over the next few years, time, temperature fluctuations, humidity, and precipitation took their toll on the equipment, degrading the electrical integrity of the splices.

In April 2015, municipal inspectors issued an electrical compliance certificate to the pool association that was valid for one year. (Note: Municipal inspectors do not inspect the service drop; the service drop is the property of the power utility.) Unlike the grounding and bonding certificate, electrical compliance must be certified every year. The requirement for yearly inspection was not passed along to the newly volunteered chairman of the pool association, and nobody thought to act when certification expired before the 2016 pool season without notice.

Sometime between autumn 2015 and early spring 2016, unobserved and unreported, the splices failed. The neutral return wire, which was temporarily patched in 2014, became an open circuit.

In May 29, 2016, which was opening day of the pool season, a 14-year-old member was shocked while swimming at the association pool. There were dozens of other swimmers in the pool; however, she was the only person to sense a strong tingling. Climbing partially out of the pool and lying on the concrete pool deck, she contacted the pool ladder with one foot while the other was still in the water. While she began convulsing, the girl remained conscious (although she indicated she did not know this was in fact an electric shock). After bystanders pulled her away from the pool ladder and water, she was transported to the emergency room and later released from the hospital. The association officers closed the pool until the fault was found and corrected.

On May 31, 2016, the pool's electrical contractor investigated and immediately observed the severed neutral wire in the service drop. He reported his observation to the power utility, since only the utility may repair a service drop. Later that day, the power utility repair crew replaced the entire service drop. A pool association officer observed a "section of wire that looks like it was repaired at some point with some clamps of some sort and then the middle part is damaged and no longer connected to each other."

Later in 2016, the plaintiffs filed their suit against the Association and its president. A major accusation in their complaint was that by not accomplishing the annual inspection, the parties were careless in the pool's electrical maintenance — and that they failed to provide a safe swimming pool for guests of the Swim Club.

The FE investigated and submitted his report in 2019. Soon thereafter, the plaintiffs dropped the electrical aspects of their complaints against the Association and its president.

Electric Shock Drownings

AC current can "escape" its intended path when there is faulty power distribution. It can flow through land and water, including swimming pools as well as open salt and fresh water. A low-level current can shock swimmers so that they feel a tingling sensation. Current of enough magnitude can paralyze swimmers so they cannot swim or call out for help. Known as "electric shock drowning or ESD," this happens more commonly in fresh water because conductivity is higher through the human body than through fresh water[1].

Drowning caused by electric shock is a "silent killer," according to The Electric Shock Drowning Prevention Association[2], because:

- There is no visible clue as to the charged state of the water.
- The sensation of shock may not be immediately felt by the victim.
- The victim may become paralyzed and unable to call out for help.

Unless there's a witness, the swimmer's death may be reported as a common drowning. "In the vast majority of electric shock drownings, the victim's autopsy shows

no signs of electrical injury, and investigators often never learn that electricity was the cause of the drowning[2]."

Of the 60 electrocutions and 50 serious electric shocks in and around swimming pools between 1990 and 2002, the causes were about equally split between end-user carelessness with radios, power tools, extension cords, and faulty pool equipment, including pool lights, pumps and vacuums[3].

Three-Phase Electrical System Overview

See "Elements of Power System Analysis"[4] for a thorough study of power generation, transmission and distribution. For a quick overview, one may turn to Wikipedia[5].

Figure 1 shows the major parts of a typical 208Y/120-volt service electrical system. The service drop wires under the "power company" label consist of three hot wires and a neutral wire. The figure will be reused for indicating current flow through an intact system, how safety grounding operates, and how stray current may escape when the system is not intact.

The neutral wire from the transformer to the meter is bare (not insulated). In **Figure 1**, neutral is indicated by the yellow color. The hot wires are insulated. The nominal voltage between any hot wire and neutral is 120V. The hot wires are colored red, black, and blue. The nominal voltage between any two hot wires is 208 volts, and there is a 60-degree phase angle between the sinusoidal waveform of each hot wire.

The transformer's neutral terminal is held at zero volts by a grounding wire connected from the terminal to ground rods driven into the earth at the foot of the utility pole, as indicated by a green line and arrow. On the customer's side, beneath "Your Equipment," the neutral terminal of the service panel is held at zero volts by a grounding wire connected from the terminal to metal rods driven into the earth on the customer's side of the meter, as indicated by a green line and arrow.

The power utility owns and is responsible for the items under the "Power Company" label — that is, high-voltage wires coming into the transformer from the substation (not shown), the transformer, the utility pole and its grounding wire and rods, the service drop wires, and the meter. The customer owns and is responsible for the items under the "Your Equipment" label — that is, the wires from the meter to the panel, the panel, the grounding wire from the panel to the earth, and the wires from the panel to all the lights, appliances, etc., within the buildings and on the property.

Current flows from the hot terminals of the transformer, through the service drop wires, through the meter, and into the building to the input side of circuit breakers on the panel. Thence, current flows from the output sides of the breakers through household wiring to light switches, permanently connected appliances, and the contact openings of electrical outlets throughout the building and property

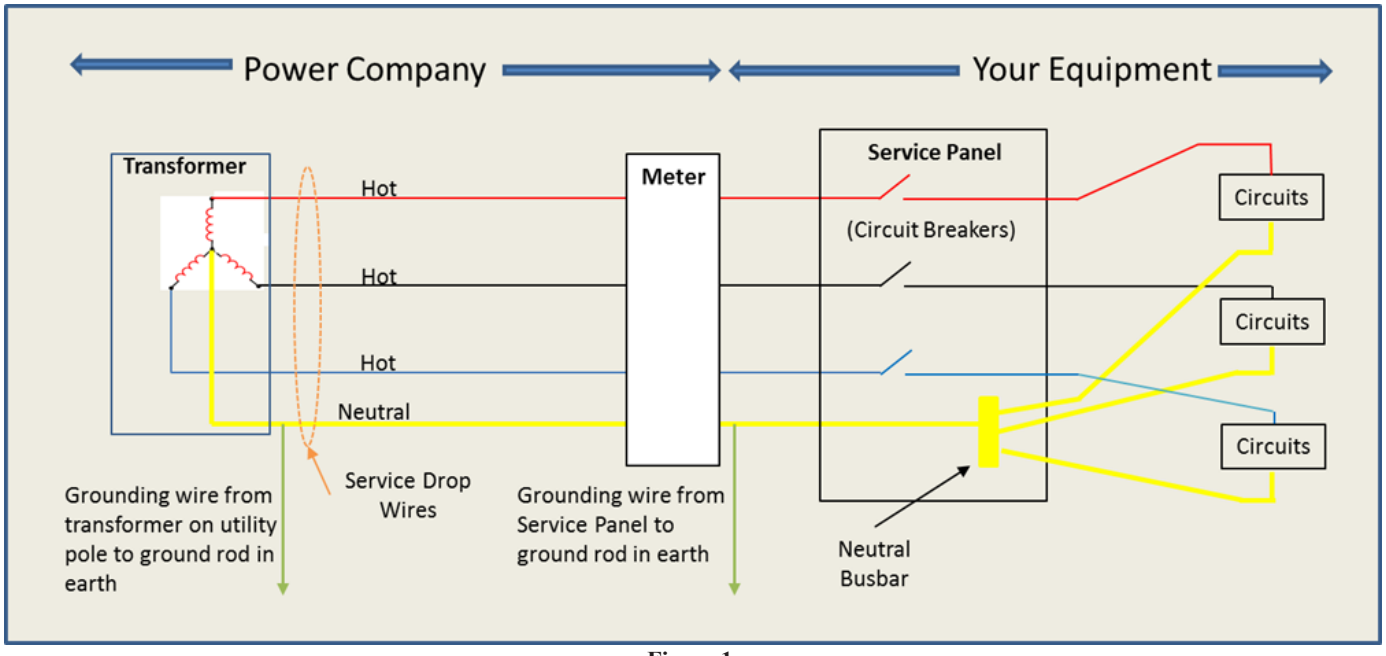

Figure 1
Typical 208Y/120V electrical system diagram.

(indicated by "Circuits").

The electric current path continues through the prongs of appliance plugs, through the wires of the appliance power cords to the hot terminals of each plugged-in 120-volt appliance.

When everything is turned off in the entire premises, no current flows to the hot terminals. The hot wires remain at 120 volts throughout the path, but no current flows.

When an appliance is plugged in and turned on, current flows through the path from the transformer into the hot terminal of the appliance and through the appliance. The current does its work inside the electric appliance and then flows out of the appliance to the return path.

Current flows through the return path from the appliance neutral terminal through the neutral wire of the building, to the neutral busbar of the service panel, through the meter, service drop wire, and into the neutral terminal of the transformer. **Figure 2** shows the current path for a single light bulb. (Ground wires are not shown for readability.)

In **Figure 2**, current flows clockwise from the upper hot terminal of the transformer, through the red service drop wire, through the meter and into the building's service panel, through the circuit breaker, and (red) building wiring ending at the hot terminal of the light bulb. The current does its work in the light bulb converting electrical energy to light and heat.

Current then flows through the return path from the light bulb's neutral contact, through the lamp fixture, neutral wiring (yellow) of the building to the neutral busbar of the service panel (yellow rectangle). From there, the return current flows back through the meter and the neutral service-drop wire (yellow), ending at the neutral terminal of the transformer.

What if there were three identical light bulbs — one each on the red, black, and blue hot wires with their neutral terminals all connected to the neutral busbar? As explained concisely in Wikipedia[5] and completely in *Elements of Power System Analysis*[4], three currents of equal magnitude, but with 60 degrees phase difference, will return from the three light bulbs and flow into the neutral busbar. The vector sum of three equal magnitude currents separated by 60 degrees is zero. The currents cancel each other out, and no current returns through the neutral wire to the transformer. What occurs is the three currents push/pull each other through the hot wires returning to the transformer.

This would be true for any three identical electrical loads on the hot wires, such as three perfect three-phase coils of an electric motor or any three identical appliance loads. This is called a balanced load and is only theoretically possible.

Some effort at load balancing is strived for and usually

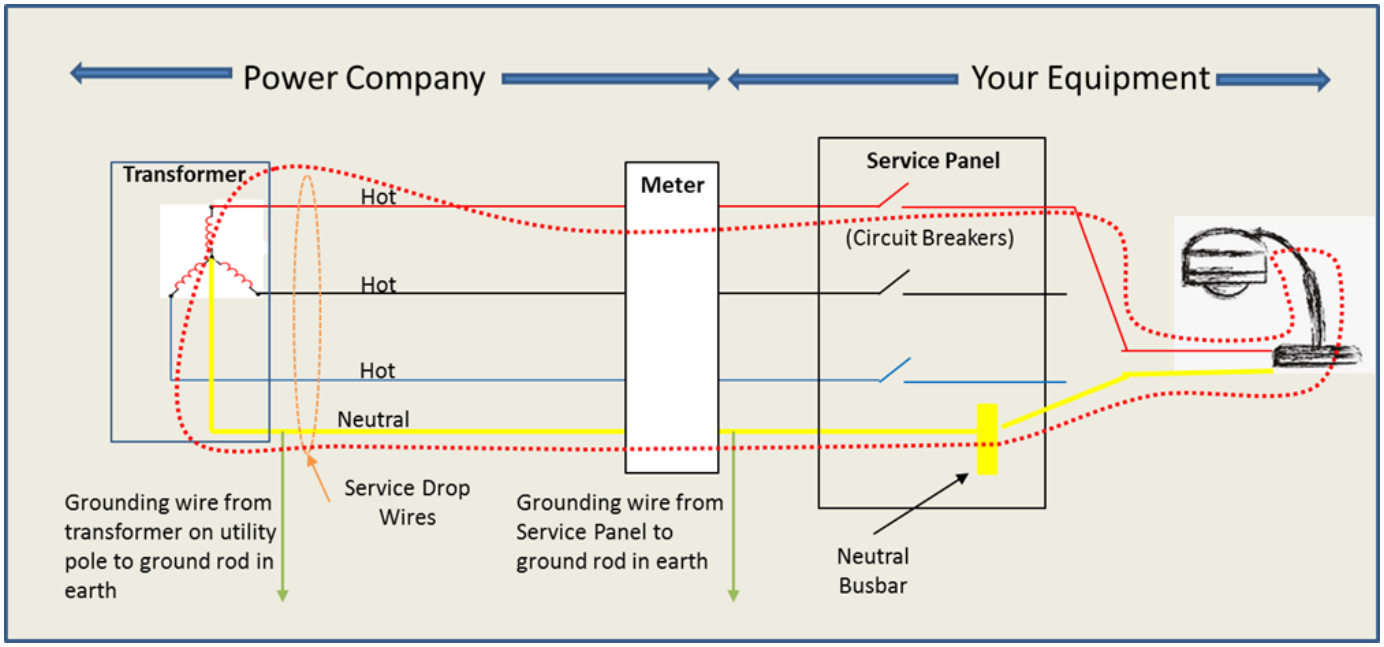

Figure 2
Current path for one light bulb.

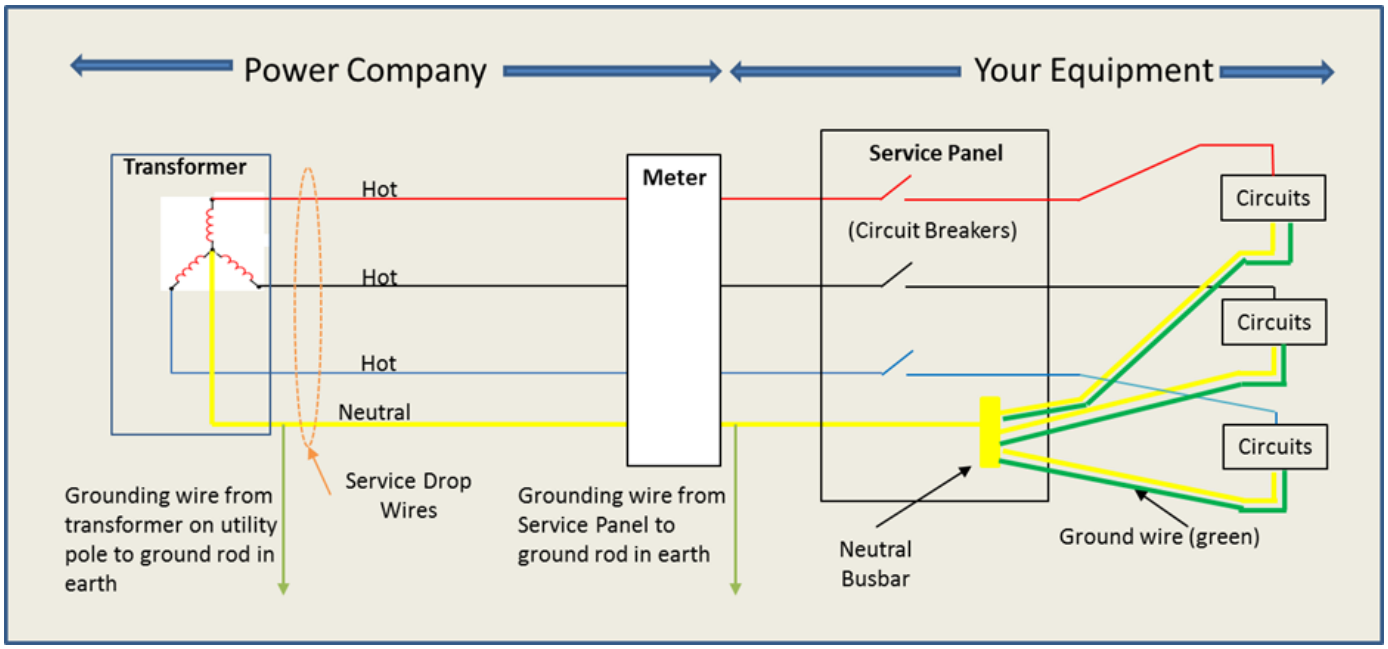

Figure 3
Electrical service diagram showing safety ground wires.

met to some extent. The current returning through the neutral wire is larger or smaller, according to the imbalance of the loads on each phase.

Figure 3 is the same as **Figure 1** but shows safety-ground wires, the "third prong" of electrical outlets, which are routed from the outlets to the neutral busbar (yellow rectangle) in the service panel separately from the neutral wires.

The purpose of ground terminals and wires is illustrated in **Figure 4**. For this example, a loose hot wire is contacting the exterior of a defective lamp fixture.

Current flows as usual from the transformer to the lamp fixture. Within the lamp fixture, current splits between the hot terminal of the light bulb and the loose wire contacting the lamp fixture's external surface. The loose wire electrically connecting the hot wire to the lamp's

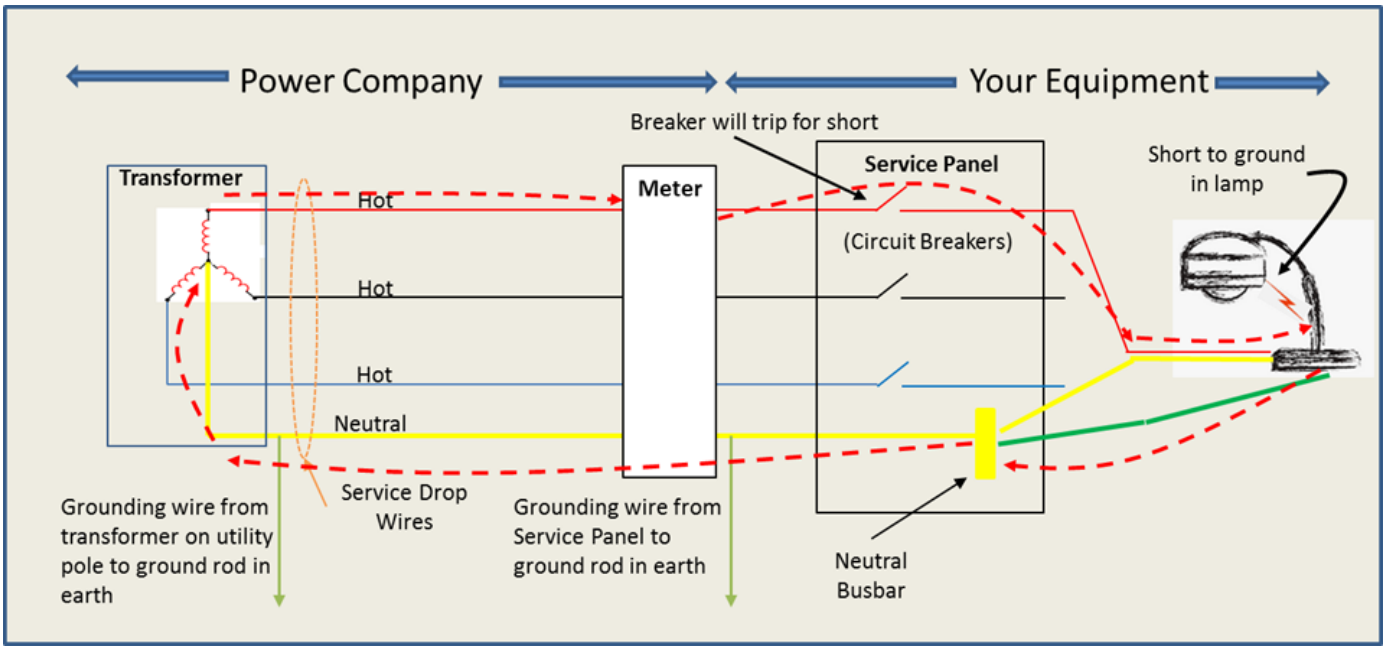

Figure 4
Current flow for one light bulb with a short to ground.

surface creates a short circuit, where, "A short circuit is a connection between two parts of an electrical circuit that you don't want to be there.[6]" The lamp's surface is energized because of the short circuit. If the lamp's surface were not grounded, the lamp would be dangerous to touch. A person touching both the lamp's surface and a conducting surface to ground could be a conducting path for current to flow, resulting in shock or electrocution.

Thanks to the proper grounding shown in **Figure 4**, the short-circuit current flows from the energized exterior lamp surface to the ground terminal of the lamp, through the ground wire of the power cord to the ground terminal of the receptacle. From the receptacle, the path flows through the building's ground wiring (green), terminating at the neutral busbar within the service panel (yellow rectangle). From the neutral busbar, the return current continues back to the neutral terminal of the transformer, as usual. If the short-circuit current is large enough, it will trip a circuit breaker in the service panel.

The low resistance of hot and neutral service-drop wires/building wires and all ground wires minimize the energy consumption that would be wasted (as heat) by current flowing through higher resistances. From the transformer to appliances, the hot voltage remains close to 120 volts with allowable current flow.

The concept of balanced three-phase power requires identical loads on each phase, so that identical current is drawn from each phase. This is a convenient abstraction but physically impossible to achieve. In the ideally balanced model, the algebraic sum of currents is zero from phase 1, phase 2, and phase 3 hot wires (red, black, and blue in **Figure 1**). Zero current returns through the neutral wire and the neutral wire remains at exactly zero volts from end to end because of the ground connections illustrated in **Figure 1** to **Figure 4**.

In real systems, there is always some imbalance. Considering **Figure 2**, there are no loads on the black or blue phases, so all the current from the red phase through the lamp returns through the neutral wire. Because of the low resistance of the neutral return wire — and the ground connections shown in **Figure 1** to **Figure 4** — the neutral voltage remains close to zero volts. However, in some unbalanced load situations, neutral-to-ground voltage of up to 25 volts is acceptable[7].

Service Drop Neutral Wire Drop

For the case at hand, the neutral wire of the service drop was severed, resulting in a dangerous condition. If the neutral wire of the service drop is severed as shown in **Figure 5**, the return current finds a different path back to the transformer. This alternative flow is from the service panel's neutral busbar (yellow rectangle) through the grounding wire and ground rods, through the earth, through the utility pole ground rods and grounding wire, back up to the transformer's neutral terminal. This path is not low resistance and is not intended to be a useful alternative to the neutral wire. "The earth shall not be considered as an effective ground-fault current path[8]." The ground rods and wires are intended only to provide a voltage reference for the low-resistance neutral wire from the service panel to the transformer.

A severed or impaired neutral wire allows stray current flow through surface and voltage gradients across the surface. **Figure 5** illustrates an electrical system where the neutral return wire from the meter to the utility transformer has been severed or impaired (indicated by the large X). "Impaired" means the wire is partially severed or corroded and its resistance is much greater than it should be.

By Kirchhoff's current and voltage laws[4], all current from the transformer hot terminals must return to the transformer. The amount of current flowing depends on which appliances are operating.

Assume the meter, panel, and all circuitry are operating perfectly, but the neutral is severed. No current can flow through the neutral service drop wire, so the returning current finds an alternate path back to the transformer. If the neutral is only impaired, the return current will divide between the neutral return wire and alternative paths according to the resistance of each path. When earth is the only path for the ground fault current, it's called an "earth fault."[9]

Multiple earth fault paths are possible, and the current flowing through the alternative paths depends on factors including how much current is being consumed by appliances on the red versus black versus blue hot lines — and on the resistance of the earth fault paths at any given time.

One such current path is indicated by the red dashed-arrows on **Figure 5**, flowing from the hot red terminal of the transformer through the meter, panel, wiring, and appliances. Return current cannot flow through the severed neutral. As the arrows indicate, the current flows from the neutral busbar, through the grounding wires and ground rods, through the earth, through the utility pole's ground

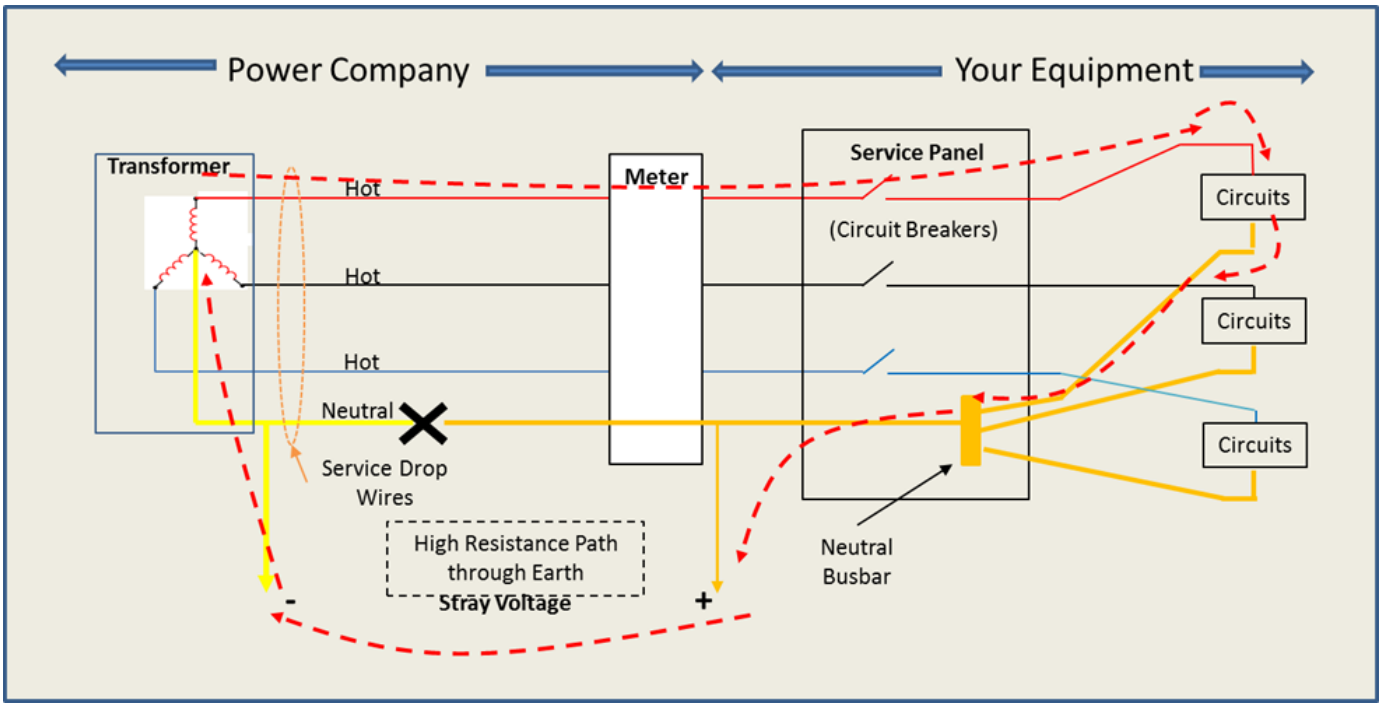

Figure 5
Current flow with severed neutral in the service drop.

rod, and back to the transformer's neutral terminal. **Figure 5** shows the wires in this path as orange.

Current flowing through the earth between the consumer and utility ground rods develops stray voltage. This magnitude of the stray voltage is determined by the magnitude of the current and resistance of the earth fault path from the pool ground rod to the utility pole ground rod.

The magnitude of the current through the earth — and thus the magnitude of the stray voltage across the surface — depends upon which appliances are operating by the balance of the load and resistance of the entire alternate path. Earth resistance is dynamic: It changes from moment to moment because of moisture, temperature, and other factors. The resistivity of soil decreases with moisture content from about 300kOhms per cubic centimeter to about 10kOhms per cubic centimeter, as moisture content increases from 10% to 20%[10].

In the theoretical case of total balance, there is no stray current or stray voltage. By elementary trigonometric identities:

$$I_{Neutral} = \sin(wt) + \sin(wt + 120^o) + \sin(wt + 240^o)$$
$$=$$
$$\sin(wt)[\cos(0)+\cos(120^o)+\cos(240^o)] + \cos(wt)[\sin(0)+\sin(120^o)+\sin(240^o)]$$
$$=$$
$$\sin(wt)[\ 1 - ½ - ½\ ] + \cos(wt)[\ 0 + \text{sqrt}(3)/2 - \text{sqrt}(3)/2]$$
$$=$$
$$\sin(wt)[\ 0] + \cos(wt)[\ 0] = 0.$$

Therefore, $I_{Neutral} = 0$ when the loads on all 3 phases are perfectly balanced, and there is no stray current to escape into the earth. But switching on an appliance results in an increasingly unbalanced load and stray current and voltage increase.

Consequences of Stray Voltage and Stray Current

"Stray voltage is the occurrence of electrical potential between two objects that ideally should not have any voltage difference between them[11]."

"Stray current refers to the electricity flow via buildings, ground or equipment due to electrical supply system imbalances or wiring flaws. It refers to an existence of electrical potential that can be found between objects that should not be subjected to voltage[12]."

Because of the severed neutral wire, the excess current that should have returned through it instead finds its way back to the transformer, as it must, as described in Kirchhoff's laws[4], choosing the path of least resistance. The stray current changes over time, as appliances are switched on and off, changing the total current drawn

from the electric utility as well as the imbalance of the three-phase system. The current passes through the various material of the earth surface in the earth fault path found because of the severed neutral. Stray voltage develops between points along these current paths.

Stray voltage is a problem everywhere — in urban, suburban, and rural settings. Consolidated Edison of New York City, N.Y., for example, reported finding 1,214 instances of stray voltage after a yearlong test of electrical equipment on city streets. The tests were ordered after several occurrences of fatal pedestrian electrocutions[13].

A young girl in the Perth (Australia) suburb of Beldon, received a massive electric shock when she touched a tap outside her house while attempting to turn off a garden hose. A damaged neutral wire was suspected of causing the tap to become electrified. Anything plugged into a wall socket (pipes and water taps) can become electrified when the neutral wire of the service drop is severed[14]. In rural areas, livestock can be electrocuted when they stand aligned with the direction of the stray electric field and current flow. The relatively long distance between front and hind hooves of cattle allows a significant stray voltage across an animal's body. Animal flesh is a better conductor than soil, so the favored current path is through the animal — sometimes electrocuting it[15,16].

Referring to **Figure 5** for the case at hand, since return current could not flow through the severed neutral, the current flowed from the neutral busbar, through the grounding wires and ground rods, through the earth. This stray current took whatever path offered the least impedance to get back to the utility pole's ground rod, and ultimately back to the transformer's neutral terminal. That path in general will change from moment to moment according to changes in impedance due to moisture, temperature, and other factors. A likely path would have included the swimming pool and its surrounding fixtures and soil. As discussed in the section on ESD, conductivity is higher through the human body than through fresh water. Persons entering the pool lower the overall impedance of the path through the pool. Depending on a person's size, depth in the pool, and orientation versus the stray electric field across the pool, they may become part of the stray current path and receive a shock.

The stray current's magnitude varies over time as well. An appliance that draws a single-phase large current from the severed-neutral system would increase the unbalance of the system. The unbalanced current, which would return through the neutral in an intact system, now increases the magnitude of the stray current. When that appliance turns off, the stray current would decrease. The dynamic nature of stray current in time (as well as position) explains why others in the pool were not shocked — and why a staff member was able to reach into the pool and say, "See, I'm not getting a shock!"

Conclusion

After reading all the provided documents, researching further into municipality, county, and state regulations, visiting the scene of the incident, and inspecting the damaged power lines that were stored as evidence, the FE submitted an expert report opining that:

1. The Association and its president did not have control over the service drop. The utility was responsible for maintaining the service drop, including the return wire, its failed splices, and the stray electric field and stray currents that resulted.

2. The Association and its president were not careless in the pool's electrical maintenance with respect to the faulty condition that led to the incident.

3. The Association and its president were not responsible for the unsafe swimming pool condition resulting from the failed service drop wires.

Furthermore, the report concluded that neither the Association's hired electrical contractor nor the municipality's electrical inspector had responsibility for the service drop wires. Only the power utility had the authority and responsibility to inspect and repair the equipment it owned. The utility was at fault for not returning to permanently repair the service drop; it was the only entity authorized to make the repair or obligated to monitor the condition of the service drop.

References

1. G. M. Dworkin and K. Doheny, "Electric Shock Drowning: A Silent Killer," Lifesaving and Rescue, 15 June 2017. [Online]. Available: https://lifesaving.com/in-the-news/electric-shock-drowning-a-silent-killer/. [Accessed 29 October 2019].

2. Electric Shock Drowning Prevention Association, "The Electric Shock Drowning Prevention Association," The Electric Shock Drowning

Prevention Association, 2019. [Online]. Available: https://www.electricshockdrowning.org/esd--faq.html. [Accessed 29 October 2019].

3. M. Dibreli, "A Review of Electric-Shock Drowning Incidents," Service Industry News, 28 November 2017. [Online]. Available: http://www.serviceindustrynews.net/featurestories/2017/11/28/h0tpjdwvvb3dr89mq16d9uaeevt179. [Accessed 29 October 2019].

4. J. William D. Stevenson, Elements of Power System Analysis, Third Edition, New York: McGraw-Hill, 1975.

5. W. Contributors, "Three-Phase Electric Power," Wikipedia, The Free Encyclopedia, 18 October 2019. [Online]. Available: https://en.wikipedia.org/w/index.php?title=Three-phase_electric_power&oldid=921812602. [Accessed 31 October 2019].

6. M. Murphy, "Ask An Engineer," MIT School of Engineering, 11 November 2017. [Online]. Available: https://engineering.mit.edu/engage/ask-an-engineer/what-is-a-short-circuit/. [Accessed 31 October 2019].

7. T. Shaughnessy, "Clearing Up Neutral-to-Ground Voltage Confusion," EC&M, 1 February 2007. [Online]. Available: https://www.ecmweb.com/power-quality/clearing-neutral-ground-voltage-confusion#close-olyticsmodal. [Accessed 31 October 2019].

8. M. W. Earley, C. D. Coache, M. Cloutier, G. Moniz and D. Vigstol, National Electrical Code Handbook, Fourteenth Edition, Quincy, MA: National Fire Protection Association, 2017.

9. P. Paul Ortmann, "Advanced Topics in Stray Voltage - Why is that voltage there?," Idaho Power Company, 2015.

10. T. M. Shoemaker and J. E. Mack, The Linemans's and Cableman's Field Manual, Second Edition, New York: McGraw Hill, 2009.

11. Definitions.net, "Definitions for stray voltage," Definitions.com, [Online]. Available: https://www.definitions.net/definition/stray+voltage. [Accessed 4 November 2019].

12. CORROSIONPEDIA, "Definition - What does Stray Current mean?," corrosionpedia.com, [Online]. Available: https://www.corrosionpedia.com/definition/1032/stray-current. [Accessed 4 November 2019].

13. S. Chan, "Con Ed Finds 1,214 Stray Voltage Sites in One Year," The New York Times, 4 March 2006. [Online]. Available: https://www.nytimes.com/2006/03/04/nyregion/con-ed-finds-1214-stray-voltage-sites-in-one-year.html. [Accessed 4 November 2019].

14. R. Trigger and G. Powell, "Warning after Denishar Woods receives near-fatal electric shock from garden tap," ABC News, 5 March 2018. [Online]. Available: https://www.abc.net.au/news/2018-03-05/what-causes-taps-to-be-electrified/9508664. [Accessed 4 November 2019].

15. D. Lanera, "Stray Voltage Facts, Straight and Simple," Stray Voltage, [Online]. Available: http://www.lanera.com/strayvoltage/strayvolt/sect1/index.html. [Accessed 4 November 2019].

16. P. Douglas J. Reinemann, "Stray Voltage Field Guide," University of Wisconsin, Madison, 2009.

Forensic Engineering Analysis of a Commercial Dry Storage Marina Reinforced Concrete Runway Slab

By David W. Stewart, PE (NAFE 301S)

Abstract

An important element of a commercial marina is the landside site work behind the bulkhead. At many dry storage marinas, boats are launched, retrieved, and handled by large forklifts with axle loads up to 100 tons. In this case, the owner of a commercial marina sued the general contractor, alleging numerous design and construction defects in the reinforced concrete "runway" between the dry storage buildings and the bulkhead. This auger cast pile supported structure served as a relieving platform carrying vertical loads below the depth of the adjacent bulkhead. Some of the observed deficiencies were random cracking, joint damage, excessive edge settlement, and readily visible live load deflections. This paper presents the methods used to investigate the design and construction of this specialized structure. A finite element model (FEM) was used to review the original design intent and help establish the cost to cure. The original design of the runway and pile foundations was found to be inadequate.

Keywords

Reinforced concrete pavement, heavy wheel loads, marina, relieving platform, auger cast piles, subgrade support, finite element model

Introduction

Ports and marinas facilitate a transition from land to water forms of transportation. Many require the use of specialized structures to create a flat area suitable for wheeled vehicles adjacent to water with adequate depth for vessel access.

The subject of this paper is a commercial "dry storage" marina constructed in 2004 to 2006. A site plan is shown in **Figure 1**. Dry storage means that boats are lifted from the water and stored on racks in a nearby enclosed building. In this case, the boat storage building is a two bay, pre-engineered steel building supported on piles. The boat storage racks are also pile supported. The floor of the building is a reinforced concrete pavement supported on a compacted subgrade.

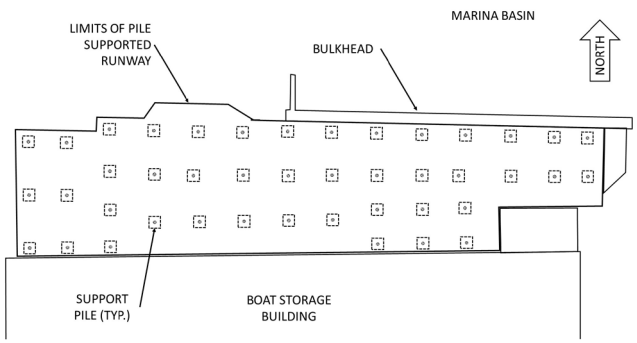

Figure 1
Site plan.

The pavement between the storage building and the marina bulkhead, referred to as the "runway," is a heavily reinforced concrete slab supported on isolated concrete piles that were cast in augered holes (hereafter "auger cast piles"). The runway slab serves as a "relieving platform," which is a structural system is used to reduce the soil pressure acting on the marina bulkhead.

The runway is used by two specialized forklifts to carry boats from the marina slips to the storage building. Each forklift has a total loaded weight of approximately 247,000 lb (123.5 tons). A section through the runway and the adjacent structures is shown in **Figure 2**. As the marina forklifts carry boats from dry storage to the marina, they cross from the slab-on-grade floor to a pile-supported grade

David W. Stewart, PE, 12060 60th St. N, West Palm Beach, FL 33411, (561) 371-9793, david.stewart@flengineer.com

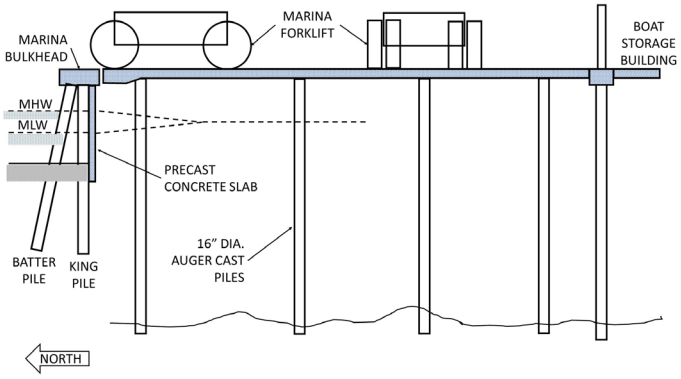

Figure 2
Section through the runway and adjacent structures.

beam to the pile-supported runway to the cap of the marina bulkhead. A smooth riding surface at these transitions is important for safe and efficient operation of the facility.

In the first eight years of use, the marina owner experienced performance issues with the concrete runway, including cracking and differential settlement of the slab. The owner claimed design and construction defects resulted in the need for substantial repairs or demolition and reconstruction of the runway. The author was retained to conduct a forensic investigation to determine the cause(s) and extent of the claimed defects.

Investigation

The investigation began with a site visit and a review of project design documents, construction plans, geotechnical studies, prior engineering studies, and other case documents obtained during discovery. This information revealed that:

- The marina bulkhead, runway, and boat storage building were each designed by a different structural engineer.
- While the runway and storage building were built by the same general contractor, the bulkhead was constructed prior to the subject work. It was shown as an existing improvement in the construction plans for the runway.
- The runway design considered the subgrade support in addition to that provided by the auger cast piles.

As stated by Bachner in *Recommended Practices for Design Professionals Engaged as Experts in the Resolution of Construction Industry Disputes*, "the expert should evaluate reasonable explanations of cause and effects"[1]. In this case, that meant looking at the structural design, construction materials and workmanship, and the owner's operation and maintenance of the marina. Critical assumptions that would need to be verified were: a) use of the runway as a relieving platform to prevent vehicle loads from impacting the marina bulkhead; and b) whether the runway slab was rigid enough to carry forklift loads to the piles.

Review of As-Constructed Conditions

The investigation began approximately eight years after construction with a general overview of the improvements. The as-constructed conditions were compared with the construction plans for significant deviations.

The plans described the runway as an "auger-cast piling supported slab." The piles consist of isolated, 16-inch diameter auger cast piles laid out in a nominal 20 ft × 20 ft rectangular grid (**Figure 1**). The actual spacing between piles varies between approximately 15 to 24 ft. Each pile was topped with a 5 ft round or 5 ft square cast-in-place concrete capital. The structural plans and details did not specify the subgrade preparation.

The runway typical section consists of a 12-inch-thick concrete slab, reinforced with two layers of $^{7}/_{8}$-inch diameter (#7) deformed steel bars. Each layer has an orthogonal grid of bars spaced at 9 inches. The bottom grid is protected from ground contact by 3 inches of concrete "cover." The top grid is protected from the salty marine environment by a cover of 4 inches. These cover dimensions reduce the effective depth of the concrete section. The concrete compressive strength was specified to be 6,000 psi.

The north perimeter of the runway is adjacent to the marina bulkhead, which was designed and built shortly before the runway but as part of the same development project. The bulkhead consists of a precast concrete "king pile-and-slab" system (**Figure 3**). The vertical concrete king piles, spaced approximately 14 ft apart, support precast concrete wall panels or slabs. There is an inclined batter pile in front of the king pile to increase the lateral load capacity of the bulkhead. The precast piles and panels are locked together with a cast-in-place reinforced concrete cap. This type of construction is also known as a "soldier-beam" retaining wall[2].

The runway is separated from the bulkhead cap by an isolation joint. The only support for the north edge of the runway is a line of individual piles spaced at 17 to 20

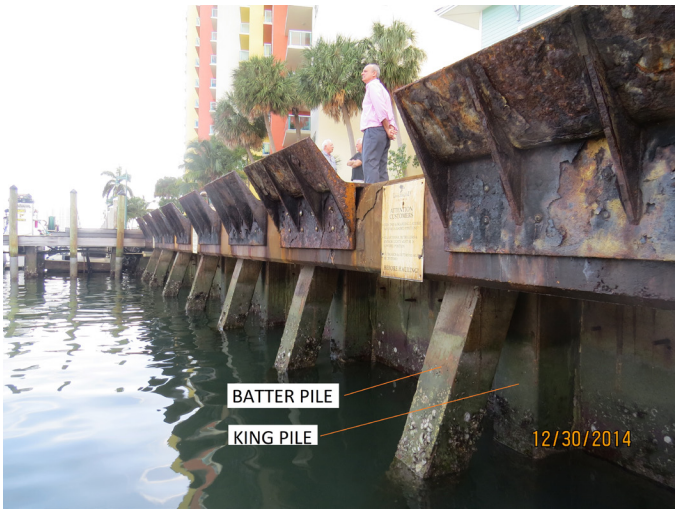

Figure 3
Marina bulkhead king pile and slab system.

feet. The runway edge cantilevers 4 ft 8 inches beyond the nearest pile centerline.

The south perimeter of the runway is adjacent to the boat storage building. The slab is pinned to the building foundation grade beam with a concrete key and steel dowels. The nearest piles are 5 ft to 14 ft 10 in. from the runway edge.

The east and west perimeters cantilever 9 ft 6 in. and 5 ft 8 in., respectively, beyond the nearest pile centerline. The east edge of the slab is separated from the adjacent slab-on-grade by an isolation joint. The west perimeter is pinned to the adjacent slab-on-grade with steel dowels.

The installation of the auger cast piles was observed by an independent testing lab. Due to a communication error, 10 piles at the east end of the runway were not observed by the testing lab. The geotechnical engineer determined that the 16-inch diameter piles should yield an allowable downward bearing capacity of 55 tons each, with a safety factor between 2 and 3.

As part of the investigation, the wheelbase and tire dimensions of one of the marina forklifts were measured and compared against the manufacturer's published data[3]. **Figure 4** shows a side view of the forklift equipment working on this site.

Observation and Testing of the Runway Surface

Additional site visits were made to make more detailed observations and coordinate material testing. The concrete runway was examined to locate the visible deficiencies described in the complaint, including differential settlement, uncontrolled cracking, and surface spalls. The general locations of these defects are shown in **Figure 5**. Where the concrete surface was spalled, no exposed reinforcing steel was observed. **Figure 6** is a representative

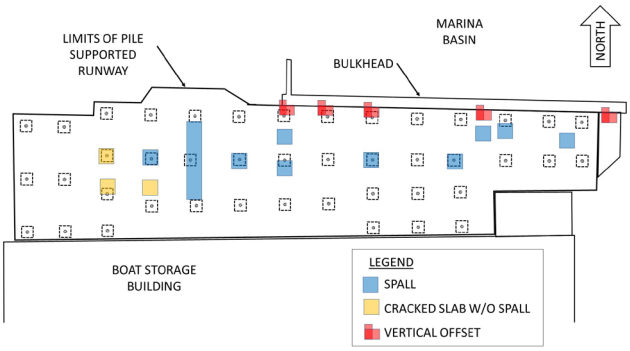

Figure 5
General location of runway deficiencies.

Figure 4
Marina forklift approaching the bulkhead.

Figure 6
Runway surface spalls and cracks.

photograph of some of the surface deficiencies. Some areas of the runway had been repaired prior to the author's first site visit. Throughout the investigation, the marina remained open, and the runway was in use.

During the original construction of the runway slab, 13 sets of concrete cylinder specimens were taken. Two specimens from each set were tested at an age of 28 days and the average reported as the compressive strength. The average strength of all tests was 7,512 psi. No test fell below the specified strength of 6,000 psi.

To further investigate the quality of the concrete, rebound hammer readings were taken at 12 locations near the observed surface defects. This is a common practice at waterfront facilities to assess the near surface uniformity of the concrete and to look for areas of poor quality or with a deteriorated condition[2]. This non-destructive test was selected because it did not require restricting the owner's use of the site. The tests were performed in accordance with the Standard Test Method for Rebound Number of Hardened Concrete (ASTM C805)[4]. The hammer readings all ranged from 43 to 51, which indicates a concrete compressive strength greater than the 6,000-psi design strength.

Visual Examination of Concrete Cores

The owner, as a remediation effort, had thirty-two 3.5-inch steel pipe micropiles installed to support the runway slab. The micropiles were installed after 24-inch-diameter access openings were cut, and the concrete "cores" were removed from the runway slab. The process disturbed the subgrade so the presence or lack of a void space below the slab could not be determined. Each pile was preloaded with a hydraulic jack to transfer a portion of the concrete slab dead load to the pile. The contractor did not measure the slab elevation before or after jacking the slab.

The oversized cores produced during installation of the micropiles were marked and stored on-site. They provided an opportunity to observe the as-constructed cross-section of the slab. Eighteen cores taken from the runway slab were measured and visually examined for mix uniformity, concrete consolidation, cracks, aggregate segregation, corrosion of the steel reinforcement, and the cover thickness to the top and bottom surfaces. See **Figure 7** for core locations and identification numbers.

Excessive flexural cracking was noted that penetrated well beyond the reinforcing steel layer. In seven of the 18 cores examined, cracks that originated at the bottom surface extended more than 6 inches up into the slab. The

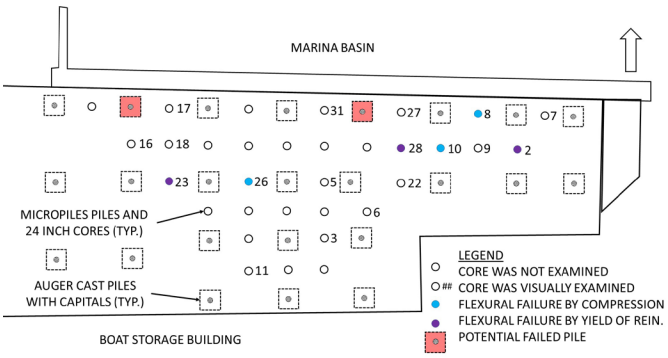

Figure 7
Select core and failure locations.

cracks in several cores (#2, #23 and #28) went further and penetrated beyond the neutral axis for balanced design. This indicates these locations failed in flexure by plastic deformation (yielding) of the steel reinforcement in tension. Core #23, shown in **Figure 8**, was taken midspan between two auger cast piles (see **Figure 7** for location). This is an area of high positive moment (i.e., tension on the bottom side of the slab). Multiple flexural cracks begin at the bottom and extend up 7.5 to 8.4 inches.

Three of the cores (#8, #10 and #26) examined had horizontal cracks at the elevation of the top reinforcing steel (**Figure 9**). This caused a delamination (spall) of the concrete cover above the top steel that indicates the concrete section failed in compression.

North Edge Deformations

Irregular settlements occurred along the north edge of the runway adjacent to the marina bulkhead cap. As forklifts cross this joint, additional live load deflections were readily visible. The owner installed steel cover plates at some

Figure 8
Concrete core with excessive flexural cracking.

Figure 9
Concrete core with horizontal cracking.

locations to ramp from the runway to the cap (**Figure 6**).

Precast concrete marina bulkheads and relieving platforms are among the types of structures commonly associated with loss of supporting soil through the retaining structure. A routine inspection of the marina bulkhead would normally include an observation of the fill behind the wall[2]. In this case, the reinforced concrete runway prevents direct observation of the fill.

As part of the investigation, vertical offsets between the north edge of the runway slab and the south edge of the bulkhead cap were measured using a straight edge and steel rule. Measurement locations were referenced to the northeast corner of the runway slab. The north edge should have been constructed flush with the top of the cap within the tolerances of the Specifications for Tolerances for Concrete Construction and Materials and Commentary (ACI 117)[5]. The measured offset is compared with the ACI 117 tolerance of 0.25 +/- inches in **Figure 10**.

Approximately 27 percent of the north edge is within 0.25 inches of the top of cap. Another 25 percent is between 0.25 and 0.5 inches. Approximately 15 percent is between 0.5 and 1.0 inches. The remaining 33 percent has deformations (settlement plus dead load deflection) between 1.0 and 2.8 inches.

Marina Forklift Design Loads

The wheel loads from the forklifts used at this marina substantially exceed those from highway trucks and general-purpose forklifts. The load from one set of dual tires on the forklift drive axle is approximately 109.4 kips (54.7 tons) based on the equipment manufacturer's data sheet used in the runway design. This is approximately equal to the 55-ton design capacity of each auger cast pile.

Regardless of the runway flexural strength, or the

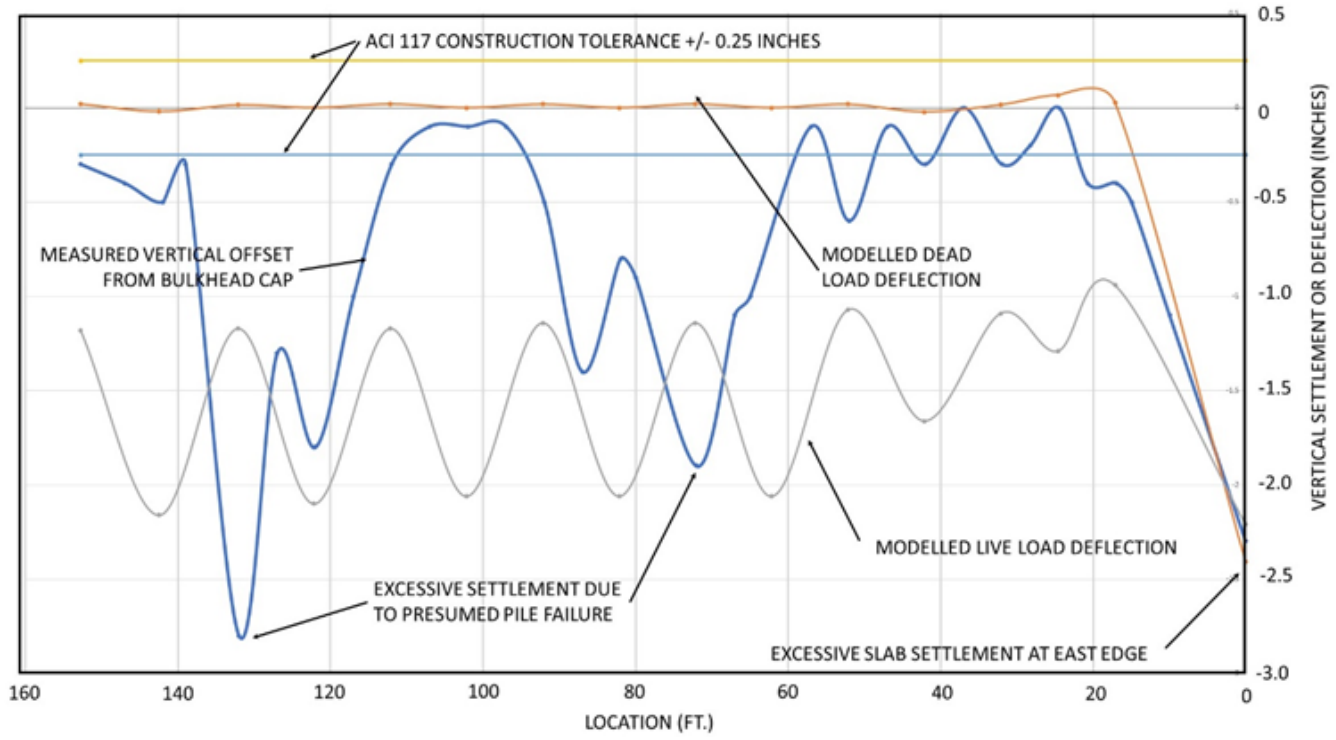

Figure 10
Measured and predicted deflections along the runway north edge.

presence of subgrade support, the auger cast piles will receive some dead load from the runway slab and the pile capital (**Figure 11**). At a minimum, each pile will support a tributary area approximately 6 ft square via shear and direct bearing. This minimum dead load is about 4.5 tons. The specified piles have a design capacity of 55 tons with a safety factor between two and three. Adding the minimum dead load of 4.5 tons to the 54.7-ton live load from one dual set of marina forklift tires yields a minimum pile load of 59.2 tons (DL + LL). This reduces the safety factor of the design, but is unlikely to trigger a pile failure.

In the worst case, with no subgrade support and a runway with adequate flexural strength, a runway area of

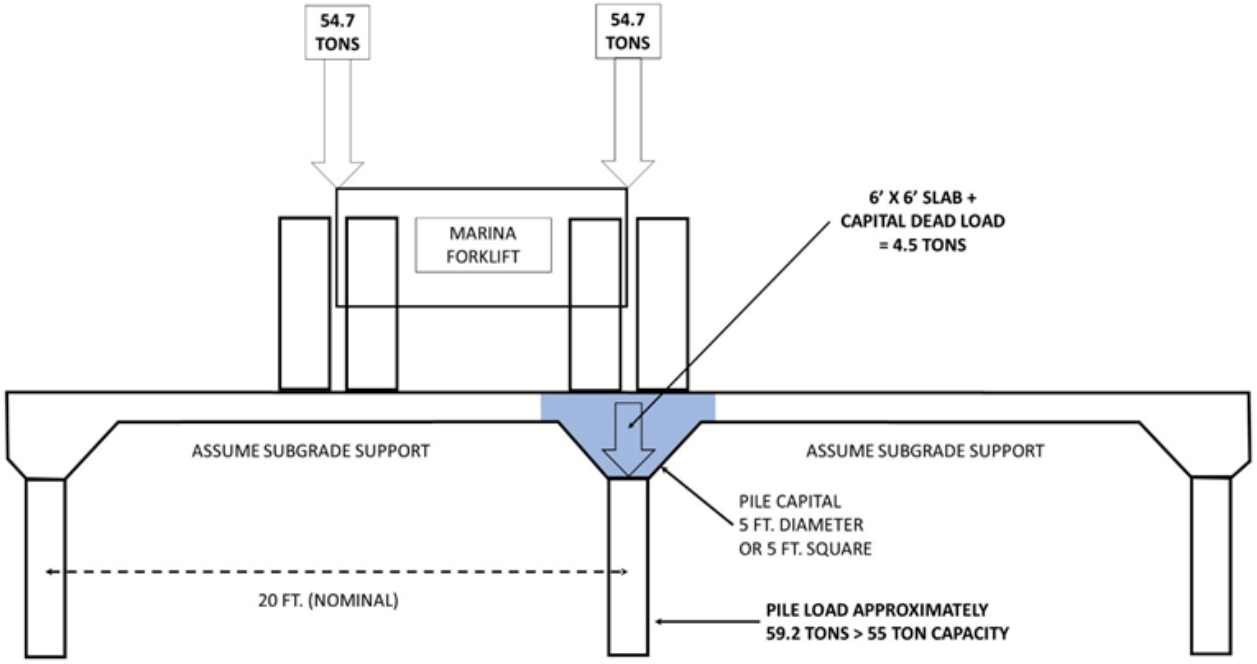

Figure 11
Minimum load on interior pile.

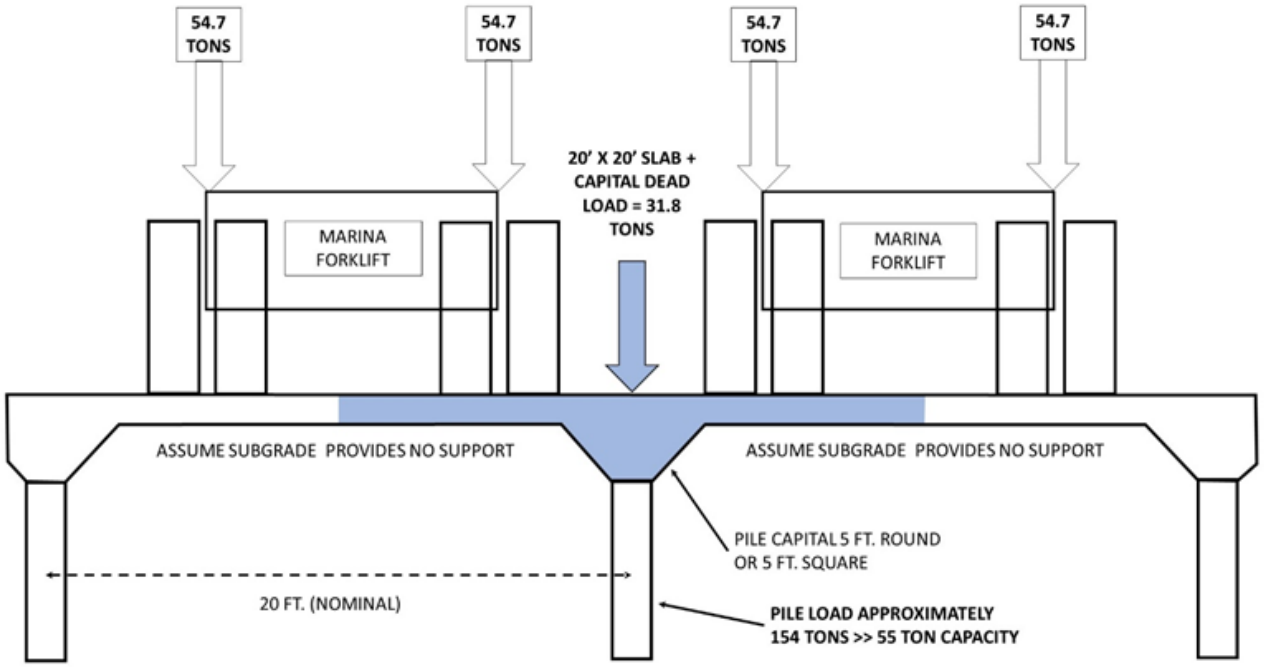

Figure 12
Maximum load on interior pile.

about 20 ft square would be tributary to the pile (**Figure 12**). This maximum dead load is about 31.8 tons. This leaves only 23.2 tons to support the forklift wheel loads.

Review of Design Intent

At the subject marina, the pile supported, reinforced concrete runway serves several primary functions. First, the supporting piles are much stiffer than a soil subgrade and should do a better job of limiting live load deflections. This is important where the runway meets and matches the elevation of other riding surfaces, such as the bulkhead cap and the floor of the storage building.

Second, the auger cast piles are founded on a deeper and stronger soil stratum. They will control the long-term settlement of the runway.

Third, the runway slab serves as a "relieving platform." This type of structural system is used to reduce the lateral pressure acting on the marina bulkhead. In essence, the heavy equipment live load and the runway slab dead load are carried as vertical loads to a deep level where they do not affect the bulkhead[6]. Without the relieving platform, the forklift wheel loads, when close to the bulkhead, would substantially increase the vertical soil pressure and thus the lateral soil pressure acting against the wall. The assumption of soil support of the runway is inconsistent with the purpose of a relieving platform.

Figure 13 illustrates the effect a relieving platform has on reducing the design loads on the bulkhead. In this example calculation, the backfill load is based on a dry unit weight of 122 lb per cu ft, an angle of internal friction of 34 degrees, and a depth to water table of 6 ft. The equipment loads on top of the backfill or "surcharge" is based on a single pair of forklift drive wheels. The normal stress was estimated from Giroud 1970 using Tables 3.14 to 3.18 as presented by Poulos and David 1974[7]. Because the bulkhead is rigidly supported by batter piles, the at-rest coefficient of earth pressure of 0.44 was used to calculate lateral pressures[8].

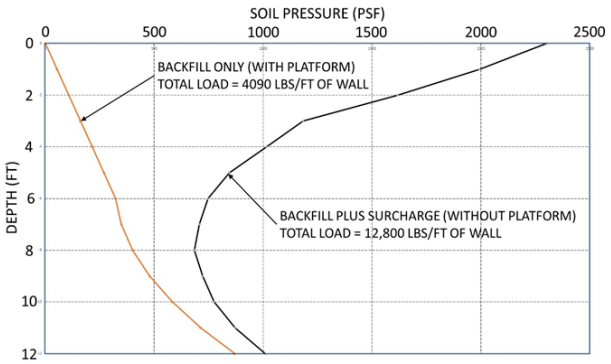

Figure 13
Effect of runway acting as a relieving platform to reduce bulkhead design load.

In this example calculation, for a condition with backfill only, the maximum lateral soil pressure is approximately 869 psf. For the backfill plus surcharge condition, the maximum lateral soil pressure is approximately 2,300 psf. Integrating over the height of the wall results in total design loads of 4,090 lb per ft of wall and 12,800 lb per ft of wall for backfill only and backfill plus surcharge, respectively. This represents an increase of more than 300% in design pressure.

To avoid this increase in design load on the bulkhead, the runway slab must be rigid enough to carry the forklift loads to the piles, and the piles must be capable of carrying the weight of the slab plus the forklifts.

During construction, the runway slab was cast against and supported by a soil subgrade. During the few weeks it took for the concrete to cure and reach design strength, the subgrade continued to carry the slab dead load. After eight years of use, the condition of the subgrade and its contribution to supporting the runway is difficult to determine.

The assumption that the subgrade would support the slab dead load throughout the service life of the structure is not well founded. The stability of the subgrade, particularly near the marina bulkhead, cannot be guaranteed. Some soil will be lost from behind the bulkhead by tide action piping through joints in the concrete panels (**Figure 14**). Additional soil can be lost from beneath the panels due to localized scour from prop wash near the bulkhead. These losses are a common occurrence for bulkheads of similar construction[2]. The previously discussed vertical deformations along the north edge of the runway are the

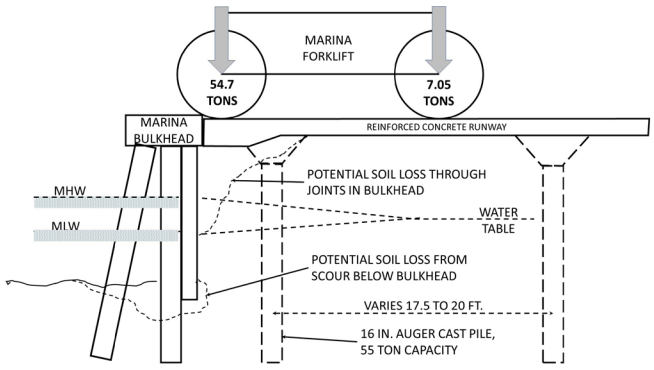

Figure 14
Runway section at marina bulkhead.

best indication that subgrade support is no longer uniform.

Finite Element Model (FEM)

Several finite element models (FEM) were created using a software application commonly used for the design of reinforced concrete slabs. An FEM permits the analysis of continuous framed concrete structures that do not meet the limitations of prescribed designs or simplified solutions. The FEM considers the elastic properties of materials and can include the elastic properties of supports. The runway slab and pile foundation were modeled as a two-way slab system. It considered the self-weight dead load of all structural elements and the live loads of two forklifts moving about the runway.

Models A and B

Multiple models were created to represent different support conditions. Model A was developed based on the runway design dimensions and typical slab section. The original design support conditions were modeled by representing the 45 ft deep auger cast piles as concrete columns and the subgrade support as a grid of spring supports. An alternate, Model B, was built using the same dimensions as Model A, but assumes no subgrade support, which is consistent with the design of a relieving platform. **Figure 15** shows the pile layout for Models A and B and the assumed edge conditions.

The wheel loads were input as area loads derived by dividing the loaded weight wheel load (109,400 lb) by the recommended tire pressure of 145 psi. The wheel loads were distributed over 755 sq. inches for each front tire, and 97 sq. inches for each rear tire. No other live loads (uniform, area, or concentrated loads) were considered in addition to the forklift loading.

Forklift wheel loads were positioned at several locations to determine the critical stresses in the runway and

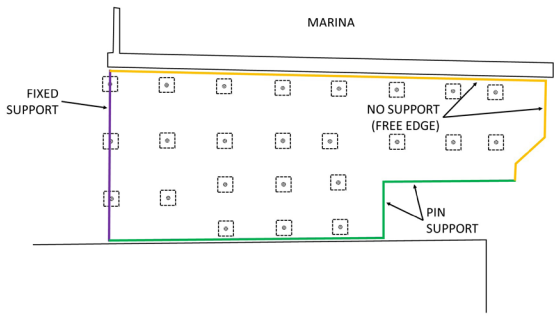

Figure 15
Models A and B pile layout and edge conditions.

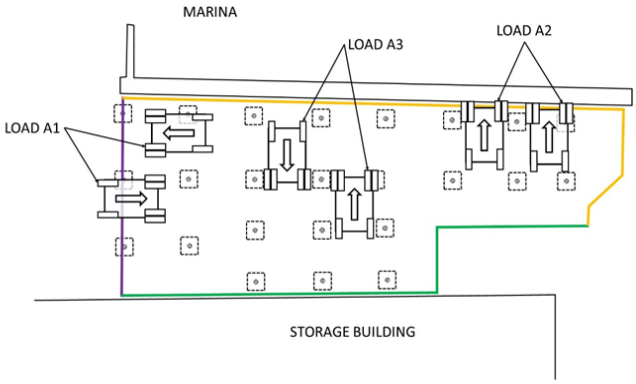

Figure 16
Partial site plan with load scenarios A1, A2, and A3.

maximum loading on the piles. Models A and B were analyzed under three load scenarios described below and illustrated in **Figure 16**.

Load A1 - Maximum positive moment: two forklifts side by side, spaced 5 feet apart, positioned with the drive (heavy) axle at the midspan between support piles.

Load A2 - Maximum negative moment over a pile: a forklift positioned with the drive axle near the north perimeter of the runway, with both wheels on the same span between two piles; and a second forklift with one drive wheel on the adjacent span.

Load A3 - Maximum pile load: two forklifts side by side, spaced 5 feet apart, positioned with the drive axles on an interior pile line, and centered on a pile.

Model C – Proposed Repair

To help estimate the cost to cure, a third finite element model, Model C, was created using a proposed reconstruction plan with closer pile spacings and a thicker slab section. It was assumed that subgrade did not contribute to the support of dead or live loads. This would result in a stiffer slab capable of distributing more load to adjacent piles. This plan was created by another party's expert but is considered by the author to be a practical (if not optimized) combination of the pile capacity, number of piles, and the slab thickness. It included a phasing plan that would have allowed partial use of the site during reconstruction.

Model C was analyzed under three load scenarios that differ slightly from Models A and B due to changes in the pile layout. They are described below and shown in **Figure 17**.

Load C1 - Maximum positive moment: two forklifts

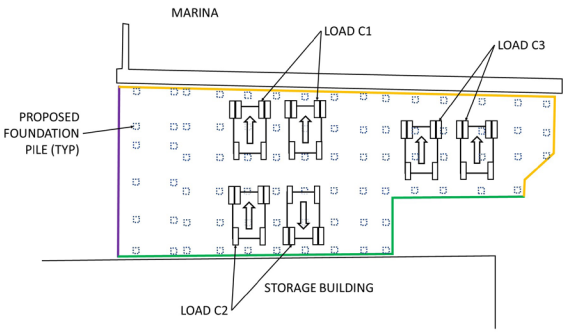

Figure 17
Proposed pile layout with load scenarios C1, C2, and C3.

side by side, spaced 5 feet apart, positioned with the drive (heavy) wheels near the midspan between support piles. The steering (light) wheels are on adjacent spans but not located near the midspan.

Load C2 - Maximum negative moment over a pile: two forklifts, side by side but facing in opposite directions, spaced 5 feet apart, positioned with the drive axle of one forklift and the steering axle of the second forklift centered on an interior pile.

Load C3 - Maximum pile load: two forklifts side by side, spaced 5 feet apart, positioned with the drive axles on an interior pile line, and over three individual piles.

FEM Results

A brief summary of the FEM results is shown in **Figure 18**. The maximum runway slab moments are presented as ultimate strength design (USD) moments based on 1.2 times dead load plus 1.6 times live load. The maximum moments for Models A and B are compared against the calculated capacity of the existing runway. Model C results are presented for information only. Since Model C is based on a proposed reconstruction plan, the capacity of the slab would be designed to meet the calculated design stresses.

The largest moments in both Model A and B are negative moments that create tension in the top of the slab over the piles. Compared with an existing capacity of (-)25.9 kip-ft per ft, Model A at (-)66.0 kip-ft per ft is under designed by a factor of 2.55. Model B at (-)90.6 kip-ft per ft is under designed by a factor of 3.50.

The pile loads shown in **Figure 18** are unfactored. The existing design capacity of 55 tons includes a safety factor of two to three. The Model A pile load of 67.5 tons is a factor of 1.23 above the capacity. Model B with a maximum load of 154 tons is a factor of 2.8 above the pile capacity.

Load Scenario	Description	Units	Existing Capacity	Model A	Model B	Model C
A1	Max positive moment	k-ft/ft	29.5	25.9	58.1	
A2	Max negative Moment	k-ft/ft	-25.9	-66.0	-90.6	
A3	Max pile load	ton	55	67.5	154	
C1	Max positive moment	k-ft/ft				50.3
C2	Max negative Moment	k-ft/ft				-11.7
C3	Max pile load	ton				68

Note:
Moments are USD based on 1.2 DL + 1.6 LL
Pile loads are unfactored
"k" = kip = 1000 lb

Figure 18
Finite element model results.

Figure 10 shows the live load deflections of the slab edge predicted by the FEM Model A. They generally oscillate between about 1.1 inches at the pile centerline and about 2.1 inches midspan between the piles.

Discussion

The runway slab appears to generally conform to the plans and specifications. The concrete compressive strength, quantity, and placement of the reinforcing steel (and overall slab thickness) were inspected and accepted during construction. Examination of concrete cores did not find aggregate segregation, cold joints, or critical deviations in the placement of the reinforcing steel. The observed surface damage, consisting of shallow spalls, chips and raveled joint lines (**Figure 6**), are not deep enough to affect the strength of the slab.

The differential settlements and dead load deflections along the north perimeter of the runway, measured as a deviation from the elevation of the bulkhead cap, are substantially larger than expected. The plans intended these surfaces to be flush. The construction tolerances of ACI 117 would allow up to 0.25 inches of deviation in the original construction[5]. There are two locations, coincident with pile centerlines, with dead load deflections approximately 1.9 and 2.8 inches below the cap. When compared with the calculated dead load deflections in **Figure 10**, these locations are shown to be deflecting too far to be within 5 ft of a pile. This indicates that two of the auger cast piles have failed in bearing or in axial compression (**Figure 7** for locations).

Ultimately, the original design of the runway slab and the supporting piles appears, based on the analysis performed as part of this investigation, inadequate for the

forklifts being used at this marina. Even when considering the subgrade's potential contribution to support the slab dead load, the negative design moments determined by the FEM analysis are as much as 2.5 times the flexural capacity of the slab (-66.0 vs. -25.9 kip-ft/ft, respectively). This is due primarily to the thin slab section and the relatively wide spacing of the piles. If the subgrade contribution to support is omitted, as is typical in designing a relieving platform, the maximum negative design moment increases to -90.6 kip-ft/ft, which is 3.5 times the slab capacity. This results in excessive cracking of the slab and increased deflections.

The north perimeter, adjacent to the marina bulkhead, is the greatest concern. The wide pile spacing, the 4 ft 8 in. slab cantilever, and the thin slab section all contribute to large live load deflections. **Figure 10** also shows the calculated live load deflections along the north edge. Depending on the location, the slab could be expected to deflect from 1 to 2 inches each time a forklift approaches the bulkhead. This discontinuous edge of the runway could have been designed with an edge beam to prevent this deflection.

Regardless of the runway flexural strength or the presence of subgrade support, the auger cast piles will be called upon to carry a minimum dead load of about 4.5 tons from the pile capital and the runway slab directly above. In the worst case — with no subgrade support and a runway with adequate flexural strength — an area of about 20 ft square will be tributary to the pile. This maximum dead load is about 31.8 tons. Based on the forensic analytical model, when two fully loaded forklifts pass each other with a pile centered between them, the maximum pile load would be as high as 154 tons (DL + LL). This event would likely fail the pile in bearing or axial compression. The pile spacing and the thin section of the runway would prevent the effective transfer of load to adjacent piles. The runway slab would subside until it was supported by the subgrade.

Conclusions

The design of the runway slab was inadequate for the support conditions and the applied loads. The slab thickness and size/spacing of steel reinforcement did not have adequate flexural capacity. Flexural failures in both tension and compression have already occurred and were observed in concrete cores taken from the reinforced concrete slab. Large dead load deflections were measured relative to the adjacent marina bulkhead.

The design of the auger cast piles was inadequate in several respects. The overall spacing between piles was too large. It allowed multiple wheel loads to be tributary to an individual pile. The design vehicle live loads, regardless of subgrade support conditions or runway flexural strength, exceed the load capacity of the piles and reduce the design safety factor. Runway edge deflections indicate that two piles may already have failed.

In addition, the pile layout did not provide adequate support for the runway at the north and east perimeters. The 4 ft 8 in. cantilever and large pile spacing along the north perimeter produces live load deflections of up to 2.1 inches below the marina bulkhead. The 9 ft 6 in. cantilever along the east perimeter increases both the flexural stress in the slab and the load on the piles.

Because of the damage that has already occurred to the runway slab, correction will require demolition and removal of the slab and substantial additions to the pile foundation. With stronger piles and a reduced pile spacing, a slab thickness of 18 inches would be adequate to support the design loads.

References

1. J. P. Bachner, "Recommended Practices for Design Professionals Engaged as Experts in the Resolution of Construction Industry Disputes," 1 October 2010. [Online]. Available: https://www.iocea.org.il/Items/03585/Recommended%20practice-experts.pdf. [Accessed 10 1 2021].

2. Waterfront Facilities Inspection Committee, Waterfront Facilities Inspection and Assessment, R. Heffron, Ed., Reston, VA: American Society of Civil Engineers, 2015, pp. 139-307.

3. Wiggins Lift Co. Inc., Model W520M2XL Equipment Data Sheet, Oxnard, California: Wiggins Lift Co. Inc., 2004, p. 1.

4. ASTM International, ASTM Standard C805, 2013, "Standard Test Method for Rebound Number of Hardened Concrete," West Conshohocken, PA: ASTM International, 2013.

5. ACI Committee 117, Specifications for Tolerances for Concrete Construction and Materials and Commentary, Farmington Hills, MI: American Concrete Institute, 2006.

6. Naval Facilities Engineering Command, Atlantic, Seawalls, Bulkheads, and Quaywalls,

MIL-HDBK 1025/4, Norfolk, VA: Department of Defense, 1988.

7. H. G. Poulos and E. H. Davis, “Elastic Solutions for Soil and Rock Mechanics,” 1974. [Online]. Available: http://research.engr.oregonstate.edu/usucger/PandD/PandD.htm. [Accessed 08 Apr. 2021].

8. U.S. Army Corps of Engineers, “Soils and Geology Procedures for Foundation Design of Buildings and Other Structures (Except Hydraulic Structures), UFC 3-220-03FA,” 2004. [Online]. Available: https://www.wbdg.org/FFC/DOD/UFC/ARCHIVES/ufc_3_220_03fa_2004.pdf. [Accessed 10 Apr. 2021].

Forensic Engineering Analysis of Video Screens for a Dispute Over Requirements and Specifications

By Robert O. Peruzzi, PhD, PE, DFE (NAFE 954M)

Abstract

This case was about LCD video screens intended to become components of medical equipment requiring an ultra-wide viewing angle. The seller was a wholesaler of various types of video screens from multiple manufacturers. The buyer was a distributor of multiple electrical components for various industries. The OEM, not involved in the case, was a manufacturer of medical instruments and equipment. Claiming that multiple units did not meet the requirements specified in the purchase agreement, the OEM refused a shipment of 1,000 LCD video screens. The buyer had already paid the seller, who refused to take back the shipment and issue a refund or credit. As a result, the buyer sued seller, and the author investigated and submitted expert opinions regarding the following questions: Did performance differ between examined samples? Did each sample meet data sheet specification for viewing angle? And was each sample adequate for its intended application as advertised in the datasheet (that is, for industrial settings requiring ultra-wide viewing angle)?

Keywords

Forensic engineering, thin film transistor liquid crystal diode, TFT-LCD, video screens, medical electronic equipment, product requirements, product specifications, video quality, video viewing angle, subjective analysis

Background

Component purchase decisions are based on the recommended applications, features, and specifications published in datasheets. This paper concentrates on one specification: viewing angle. For example, a narrow viewing angle may be desirable in laptop video screens to provide privacy to the user. On the other hand, a wide viewing is desirable for wall-mounted televisions, public information kiosks, and industrial information displays, in addition to the medical equipment product in question.

The wide viewing angle was an essential requirement for the video screens of the medical instruments and equipment manufactured and sold by the OEM. End-users of the equipment screens were typically medical professionals needing to see screen contents clearly from either side (above or below).

Thin Film Transistor (TFT) Color LCD Technology

According to a 2007 article, LCD video screen image quality at publication time was already superior to cathode-ray-tube (CRT) video screens[1]. LCD applications include PC monitors, cellular phone screens, and televisions. Their advantages (including slim size and lightweight design) made them good replacements for CRTs[2].

Figure 1 is a photo of a typical TFT LCD video screen on the author's laptop computer. **Figure 2** is a side view photo of that same computer, showing that it has a wide viewing angle. The following paragraphs and figures describe the operation and technology of TFT LCD video screens.

Figure 3 is a closeup of 16 complete pixels of a video screen. Each pixel comprises a blue, red, and green rectangular sub-pixel. Each sub-pixel is controlled by a TFT, which is controlled by data signals.

Figure 4 is a diagram showing the physical layout of a TFT LCD video screen. The diagram indicates:

1. Glass plates

Robert O. Peruzzi, PhD, PE, DFE, 719 Fourth Ave., Bethlehem, PA 18018, (610) 462-3939; peruzzi@rperuzzi.com

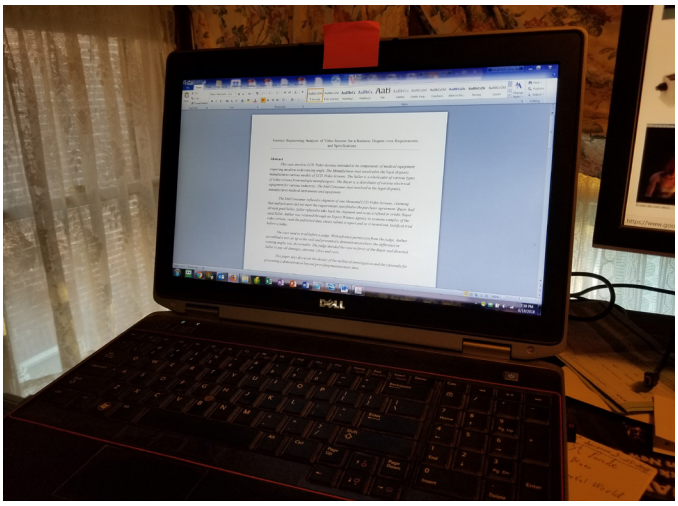

Figure 1
Typical LCD television screen.

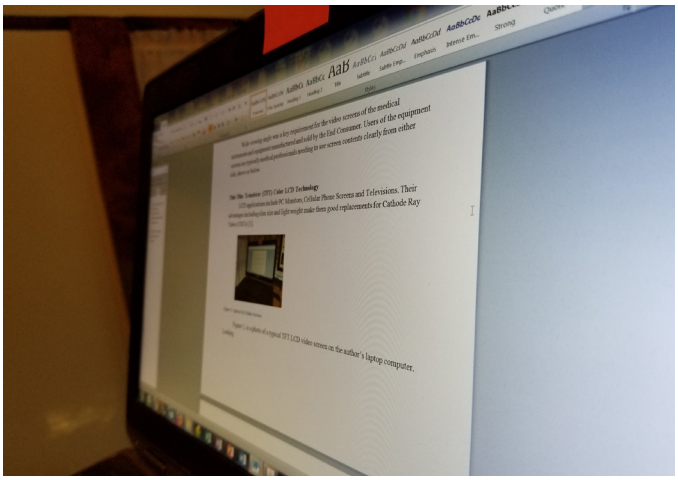

Figure 2
LCD video screen side view.

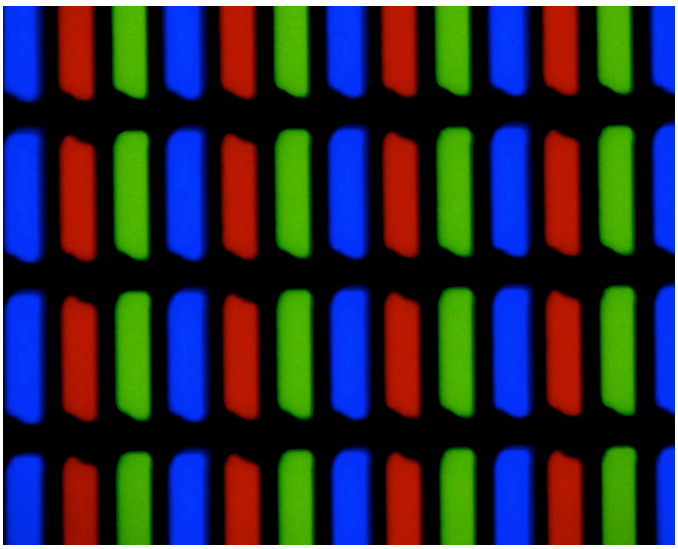

Figure 3
300X close-up of video screen[3].

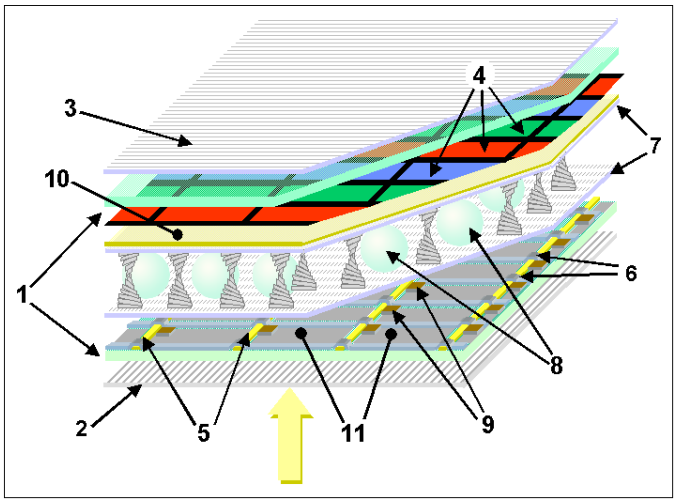

Figure 4
Color TFT LCD layout[4].

2. Vertical polarizer
3. Horizontal polarizer
4. Red, green, blue (RGB) color mask
5. Vertical command lines
6. Horizontal command lines
7. Rubbed polymer layer
8. Spacers
9. Thin-film transistors (TFTs)
10. Front electrode
11. Rear electrodes

The yellow upward-pointing arrow symbolizes light from a white backlight illuminating the video screen. First, the light passes through the vertical polarizer (2), then a lower glass plate (1). TFTs (9) control the capacitive charge deposited on the rear electrodes (11). The voltages on the rear electrodes are controlled by the voltages present on the vertical command lines (5) and the horizontal command lines (6).

Figure 5 is a partial schematic showing the electrical equivalent of two TFT pixels of an LCD display where the lower pixel is lit yellow. A yellow pixel is generated by energizing the red and green sub-pixels of the bottom pixel.

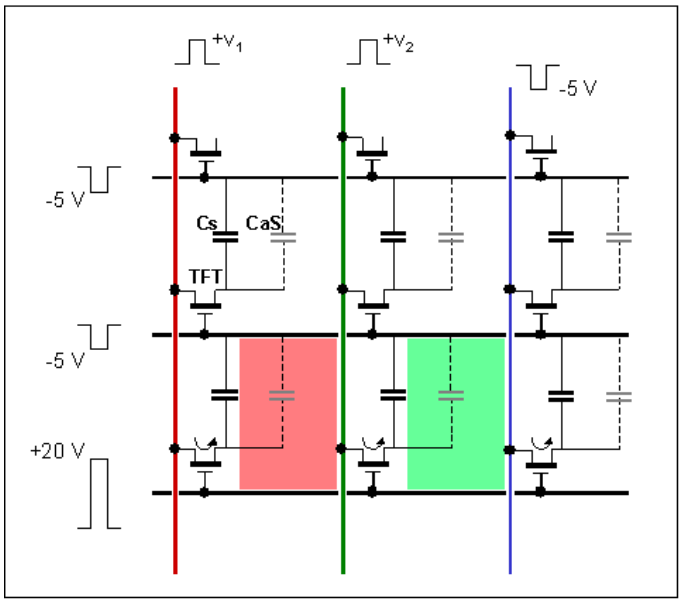

Figure 5
Color TFT-LCD cells-schematic[5].

The +20V pulse on the bottom horizontal command line turns on the bottom pixel for a time interval of the pulse duration. The -5V on the middle horizontal command-line turns off the upper pixel during that interval. A top horizontal command line turns off the next higher pixel (not shown). The +V1 vertical command line controls the brightness of the "red" sub-pixel, and +V2 vertical command line controls the brightness of the "green" sub-pixel. The -5V on the rightmost vertical command line turns off the "blue" sub-pixel during that interval.

Referring again to **Figure 4**, light passes through the rear electrodes and into the liquid crystal assembly. The thinness of the electrode dimensions makes them substantially transparent. Liquid crystal is held between the bottom and top "rubbed polymer" layers (7) and spacers (8). This substance is not numbered in the diagram but is symbolized by hourglass-shaped structures between the spacers. The property of interest of liquid crystal is that its opacity is controlled by an electric field due to the voltage present on the rear electrodes[6]. The electric field tends to polarize the orientation of amorphous silicon (A-Si) particles to block or transmit the white light. At this point, the blocked or partially transmitted light beams are shades of "grey." This modulated grey light passes through the upper rubbed polymer layer (7), and the substantially transparent front electrode (10) to the RGB color mask (4).

The light from each red, green, and blue sub-pixel passes through an upper glass plate (1) and finally the horizontal polarizer (3). The final step occurs when human perception integrates and blends the light from each sub-pixel into an image.

Video Screen General Specifications

General specifications for video screens include physical qualities, such as weight, display area monitor dimensions, drive system, number of colors, numbers and dimensions of pixels, contrast ratio, polarizer details, response time, luminance, and power consumption[7]. Readers desiring a deeper understanding of video screens and how their specifications relate to sensory quality may visit EIZO's website[8].

Viewing Angle

Subjectively, the viewing angle specification refers to the maximum angles from the sides and from the top and bottom. The screen is readable, and the colors remain consistent.

A definition and defined measurement technique for determining viewing angle might be expected to help overcome the subjectivity of judging readability and color consistency. In fact, such a standard exists. However, the Information Display Measurements Standard leaves it up to video display manufacturers to choose the measurable "optical quantity" to measure at various angles and define the allowable change in that quantity that defines the maximal viewing angle. Possible optical quantity metrics include contrast ratio, white luminance, black luminance, chromaticity coordinates, and color difference[9]. Ambiguity results in differing measurement techniques.

In 2021, Barczyk et al published their technique using contrast ratio (CR) as their defining optical quantity. They point out that the defined allowable change from CR measured at 0 degrees differs from the manufacturer and may be 5:1, 10:1, or 100:1. In addition, the manufacturer may expand the claimed viewing angle by up to 20 degrees[10].

Eunjung Lee et al, in 2010, argued that CR should no longer be used as the criterion for determining maximal viewing angle[11]. They claimed 10:1 CR is not adequate and proposed using a combination of brightness, colorfulness, and hue factors as defined in CIECAM02[12].

Not surprisingly, some manufacturers have used this ambiguity to puff their products[13]. Whatever optical quantity and degradation ratio is chosen as the measurement criterion, a 140-degree viewing angle is illustrated in **Figure 6**.

A wide viewing angle is not always desirable, and viewing angle may be deliberately designed to be narrow for screens where privacy is an issue. Typically, the LCD components are designed for wide viewing angles, and the viewing angle is precisely controlled by the dimensions of the polarizing lines in polarizers **Figure 4**.

In 2007, the manufacturer introduced LCD screens that could be set for narrow or wide viewing angle, and by 2008 it began introducing screens with switchable viewing angle[14]. The transaction for the screens in question was made in 2012.

The LCD Video Screen Module in Question

The manufacturer supplies the TFT Color LCD Module. Its datasheet[15] claims it to be applicable for industrial use and has ultra-wide viewing angles, high luminance, and high contrast. The viewing angle specification is a minimum of 70 degrees from up, down, left, and right.

The OEM ordered 1,000 units of this make and model video screen from the buyer (plaintiff). The buyer purchased these units from the seller (defendant), a licensed distributor for the manufacturer. Coincidentally, this company also manufactures another TFT Color LCD Module. Its datasheet[16] claims applicable for control system display terminals and industrial PCs and has high luminance and high contrast. The viewing angle specification is a minimum of 35 degrees from the right and left, 20 degrees from up, and 10 degrees from down. Its luminance and contrast specifications are slightly inferior to the other unit, while its other parameter specifications are nearly identical. Both were excellent video screens at the time. The "-54" version was designed for a limited viewing angle. This change, as expected, degraded its luminance and contrasted optical qualities.

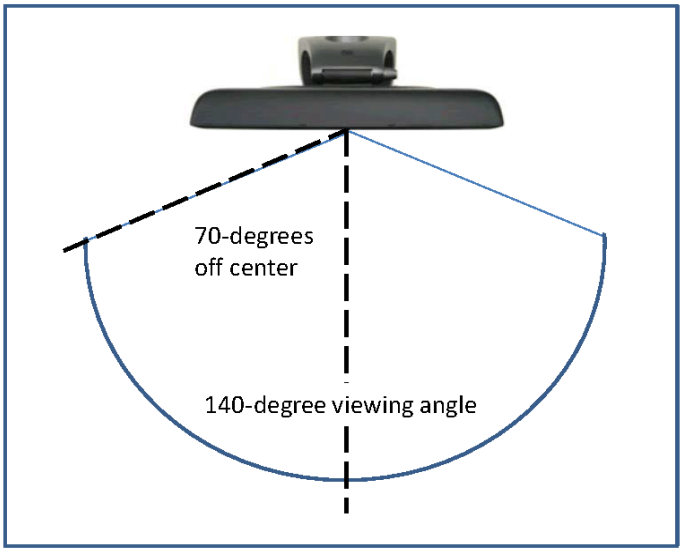

Figure 6
Viewing angle diagram.

Prior to the Investigation

An independent testing laboratory specializing in video screens was contracted by the seller to perform a list of tests, which did not include a viewing-angle test. Their test report included:

- Listed all test equipment.
- Documented calibration of test equipment.
- Described the test procedures.
- Reported the measured results.
- Interpreted the measured results, arriving at conclusions.
- Suggested corrective action.

The Author's Investigation

The author examined four samples of LCD screens after reviewing the datasheet, and submitted an expert report opining on these questions:

- Does each sample have substantially the same or different performance?
- Does each sample meet data sheet specification for viewing angle?
- Is each sample adequate for the intended application as advertised in the datasheet (that is, for industrial settings requiring ultra-wide viewing angle)?

The buyer delivered four samples for analysis. All were clearly marked TFT Color LCD Module in shipping packaging and on the modules themselves. Exhibit A was marked known-good, Exhibit B was marked "engineering sample," and Exhibits C and D were unopened as delivered from the seller to the buyer. The LCD screens were bare modules, not mounted in protective frames or including electro-static discharge (ESD) protection. All were packed in ESD-protective bags for shipment. To demonstrate and test the modules, a compatible screen tester[17] with power supply, backlight, and a wiring harness[18] were purchased.

Investigation and Report

Test Equipment:

1. Dell Vostro Laptop Computer (PC)	Video source (PC)
2. VGA Cable (monitor cable)	PC to LCD driver module
3. MS453LC-KITMS179DI TTL-DF9-31_640X480	LCD driver module
4. 2 Lamp Inverter (Backlight power)	Special power supply for LCD
5. 40W(MS112ADP) (Power supply)	Power supply for everything else
6. Viewpoint control fixture	Tool for measuring viewing angle
7. ESD wrist strap and kit	For equipment protection

Test Fixture Connections and Procedure:

An ESD safety mat covered the surface of the lab bench. An ESD protective wrist strap was worn when setting up the test fixture and throughout the test procedures. Power and signal connections between modules were made with all switches in the off position before plugging power supplies into the power mains.

Exhibit	Package Marking	Observations	Measurements
A	Known Good Panel	• Chosen as comparison standard • "Normal" appearance • No perceptible color shift as viewpoint approached 90 degrees	80 degrees in all directions measured at several points
B	Golden Sample for Engineering Evaluation	• "Normal" appearance • No perceptible color shift as viewpoint approached 90 degrees	80 degrees in all directions measured at several points
C	Panel Received from Seller	• "Normal appearance when viewed within viewing angle • Reduced viewing angle observable to naked eye • Obvious differences from exhibits A and B • As viewing angle increased, o Colors changed and quality degraded o Graphical image sharpness degraded o Both fine and large print became blurred. • As viewing angle increased further o Image blurred and "washed out" as if obscured by fog.	Top to bottom: • 40 degrees Left to right: • 60 degrees All diagonals: • 35 degrees
D	Panel Received from Seller	Substantially the same as Exhibit C	• Substantially the same as Exhibit C

Figure 7
Examination results.

PC was set to display a graphic image that included large and fine print, an intricate pattern of lines, and a wide range of subtly varying colors. For each LCD screen, the these procedures were followed:

1. Connect LCD screen to the test fixture.

2. Verify that the LCD screen shows the chosen image.

3. Allow 20 minutes for the LCD screen to warm up.

4. Observe and subjectively judge screen appearance from several positions and angles without using any equipment.

5. Using viewpoint control fixture, in all four directions (up, down, left, and right) increase the angle until one of the following occurs:

   a. Screen color and general appearance noticeably degrade.

   b. A graphical pattern of lines begins to distort.

   c. Fine print readability degrades.

Investigation Summary

The results of examining and measuring the four Exhibits are tabulated in **Figure 7**. Results show that the video screens fell into two distinct categories: wide and narrow viewing angles. Those with narrow viewing angles do not meet the published specification.

The similarity of results for Exhibits A and B and the similarity of Exhibits C and D suggest that Exhibits C and D might have been mislabeled. Destructive testing to examine the dimensions of the polarizing lines in the LCD screen polarizers was not done.

Trial

After the expert report was submitted, the case went to trial. A demonstration to compare the video screens was designed, and the components were purchased. The kit consisted of:

- A portable folding table with a non-metallic table-top surface.

- A brand-new tablet computer with a VGA output.

- An ESD protective field service kit.

- A "splitter" cable to run two video screens from one video source.

- The original and a second LCD screen test kit. (Using two LCD screen test kits, a simultaneous demonstration of two screens is possible.)

- The four previously tested video screens.

At trial, during a short recess, the author assembled the demonstration components, such that the LCD screens, the screen test kits, the tablet computer (providing several video images), onto an electro-static-discharge resistant covering over the folding table. The computer displayed identical video onto the two screens. The judge remarked on the obvious difference between the two screens.

Conclusions

- Thin-film transistor liquid crystal diode video screens can be manufactured to specifications with respect to viewing angle width.

- There was a mix of wide and narrow viewing angle screens delivered by the seller to the buyer.

- The narrow viewing angle screens did not meet published specifications and were inappropriate for the buyer's application.

- The author's demonstration and testimony effectively convinced the court of the inadequacy or the defective screens for their expected application.

References

1. A. J. De Vaan, "Competing display technologies for the best image performance," Journal of the Society for Information Display, vol. 15, no. 9, pp. 274-279, 2012.

2. Y. Takakazu and M. Tomoo, "Industrial LCD Display Modules," NEC TECHNICAL JOURNAL, vol. 2, no. 3, pp. 71 - 74, March 2007.

3. Wikimedia Commons contributors, "TN display closeup 300X," Wikimedia Commons, the free media repository., 5 April 2015. [Online]. Available: https://commons.wikimedia.org/w/index.php?title=File:TN_display_closeup_300X.jpg&oldid=155983749. [Accessed 19 June 2018].

4. Wikimedia Commons contributors, "Color TFT-LCD Layout," Wikimedia Commons, the free media repository., 9 July 2016 . [Online]. Available: https://commons.wikimedia.org/w/index.php?title=File:Color_TFT-LCD_Layout.png&oldid=201136945. [Accessed 19 June 2018].

5. Wikimedia Commons contributors, "Color TFT-LCD Cells-Schematic," Wikimedia Commons, the free media repository., 21 October 2016 . [Online]. Available: https://commons.wikimedia.org/w/index.php?title=File:Color_TFT-LCD_Cells-Schematic.png&oldid=210429248. [Accessed 20 June 2018].

6. J. Stohr and M. G. Samant, "Liquid crystal alignment by rubbed polymer surfaces: a microscopic bond orientation model," Journal of Electron Spectroscopy and Related Phenomena, Vols. 98-99, p. 189–207, 1999.

7. NEC LCD Technologies, Ltd., Data Sheet: TFT Color LCD Module, NEC LCD Technologies, Ltd., 2007.

8. EIZO Corporation, "The difference in image quality is perfectly obvious! - Let's check the LCD's display," EIZO Corporation, 2018. [Online]. Available: http://www.eizoglobal.com/library/basics/difference_in_image_quality/index.html. [Accessed 22 June 2018].

9. International Committee for Display Metrology (ICDM), "https://vesa.org/vesa-standards/," Society for Information Display, 1 June 2012. [Online]. Available: https://vesa.org/vesa-standards/. [Accessed 22 June 2018].

10. R. Barczyk, B. Kabzinski, D. Jasinska-Choromanska and A. Stienss, "Measuring of the Basic Parameters of LCD Displays," Journal of Automation, Mobile Robotics & Intelligent Systems, vol. 6, no. 1, pp. 46-48, 2012.

11. E. Lee, J. H. Chong, S. A. Yang, H. J. Lee, M. Shin, S. Y. Kim, D. W. Choi, S. B. Lee, H. Y. Lee and B. H. Berkeley, "Improved Angle-of-View Measurement Method for Display Devices," Journal of Information Display, vol. 11, no. 1, pp. 17 - 20, 2010.

12. R. M. Luo and C. Li, "CIECAM02 and Its Recent Developments," in Advanced Color Image Processing and Analysis, New York, Springer, 2013, pp. 19 - 58.

13. R. Soneira, "16 Misleading Display Specs and What They Really Mean," GIZMODO, 20 August 2012. [Online]. Available: https://gizmodo.com/5936192/[object%20Object]. [Accessed 22 June 2018].

14. S. Fallon, "New LCD Display From NEC Can Switch Between Wide and Narrow Viewing Angles," Gizmodo, 7 October 2007. [Online]. Available: https://gizmodo.com/314799/[object%20Object]. [Accessed 25 June 2018].

15. NEC LCD Technologies, Ltd., "TFT Color LCD Module NL6448BC33-53 Data Sheet," January 2007. [Online]. Available: http://www.farnell.com/datasheets/68814.pdf. [Accessed 25 June 2018].

16. NEC LCD Technologies, Ltd., "TFT Color LCD Module NL6448BC33-54 Data Sheet," March 2003. [Online]. Available: http://www.beyond-infinite.com/lcd/Library/Nec/NL6448BC33-54.pdf. [Accessed 25 June 2018].

17. LCD Parts, "LST03-V3 LCD Screen Tester," LCD Parts, 2013. [Online]. Available: http://www.lcdparts.net/LST03.aspx. [Accessed 25 June 2018].

18. LCD Parts, "LCD Screen Wire Harness," LCD Parts, 2013. [Online]. Available: http://www.lcdparts.net/WHSDetail.aspx?ProductID=3949. [Accessed 25 June 2018].

FE Analysis of Communications Systems for Drive-Thru Restaurants in a Business Dispute Over Specifications and Design Process

By Robert O. Peruzzi, PhD, PE, DFE (NAFE 954M)

Abstract

Forensic analysis in this case involves the design of a communication system intended for use in Quick Service Restaurant (QSR) drive-thru lanes. This paper provides an overview of QSR communication system components and operation and introduces communication systems and channels. This paper provides an overview of non-linear, time-varying system design as contrasted with linear, time-invariant systems and discusses best design practices. It also provides the details of how audio quality was defined and compared for two potentially competing systems. Conclusions include that one of the systems was clearly inferior to the other — mainly due to not following design techniques that were available at the time of the project.

Keywords

Forensic engineering, quick service restaurant, QSR, drive-thru, communications system, simplex, half duplex, full duplex, adaptive systems, automatic gain control, AGC, noise cancelation, linear time invariant, LTI, nonlinear time-varying

Introduction

The plaintiff's complaint refers to the system in question as a Drive-Thru System. The system is intended to provide communication between service employees at quick-service restaurants (QSRs) and their customers. Typically, a customer enters a drive-thru lane outside the QSR and approaches a structure referred to as the post, which includes a microphone and a speaker.

The system detects the customer's presence and alerts the serving employee. The serving employee, using a headset with microphone and speaker, greets the customer. The employee and customer converse through a two-way communication channel. Following the conversation, the customer proceeds to the service window where the transaction is completed.

The buyer (plaintiff) in this case had an established reputation for reselling and repairing QSR communications systems and decided to manufacture them under its own brand. It outsourced the design to the designer (defendant) who claimed expertise in radio design. Expected deliverables included assembled exemplar units, schematics, software, parts-lists, diagrams, and assembly/service instructions. The buyer and the designer agreed to specifications, schedule, and cost. Both cost and schedule were overrun. The buyer demanded contract rescission and refund. The buyer sued the designer after negotiations failed. The author was retained by the buyer's attorney to investigate and opine on:

- Measured audio quality of the system. Did it meet specifications?
- Did the designer follow best design practices?

History and Overview

Red's Giant Hamburg, on Route 66 in Springfield, Illinois, opened the first drive-thru in 1947. Since Red's closed in 1984, it is likely that In-N-Out Burgers, operating since 1948, is now the longest-running fast food restaurant offering a complete drive-thru package. At the time of its opening, In-N-Out's drive-thru system included a state-of-the-art two-way speaker box[1]. Other drive-thru early adopters were Jack-in-the-Box in 1950 and Wendy's in 1969. In the mid-1970s, McDonalds opened its first drive-thru lane[2].

A Quick Service Restaurant is the restaurant industry's term for what people usually call a fast-food restaurant[3].

Robert O. Peruzzi, PhD, PE, DFE, 719 Fourth Ave., Bethlehem, PA 18018, (610) 462-3939; peruzzi@rperuzzi.com

Most major QSR chains report that drive-thru lanes account for about 70% of sales — and that accuracy and speed of service are the two most critical drive-thru metrics[4].

The technology behind the communication is a key link to drive-thru accuracy. "The quick-service industry relies on efficient communication. A poor sound quality can lead to incorrect orders/delays and can greatly impact the quality of service and customer experience[5]." Taking the order correctly relies on technology. Poor performance of the drive-thru speaker and employee headsets can lead to inefficiencies and customer loss. Digital communication has replaced analog for the communications system for several reasons, which will be developed more fully later.

1. Digital communication systems can be designed to reduce noise and external interference.

2. Digital signal processing can be used to make speech more intelligible.

3. Digital systems can perform non-linear time varying control over voice communication.

Communications System

This section is a general overview of audio communications systems. Simplex, half duplex and full duplex are three types of communication channels[6]. See reference for a full introduction to digital communications systems[7].

Simplex

A one-way communication channel is referred to as a simplex channel. An example of a one-way communication channel is an on-stage announcer speaking into a microphone, with the announcer's voice coming through a speaker to the audience. A channel in this announcer/audience example is the electronic (or wireless) set of equipment forming a path from the announcer to the audience. Radio and television station broadcasts are other examples of simplex communication.

Half Duplex

Combining two one-way communication channels into a two-way communication channel, with which only one person may speak at time, is referred to as a half duplex channel. A pair of walkie-talkies or a pair of CB radios are examples of half duplex channels. Conversations over half duplex channels may include jargon such as a talker finishing a speech segment by saying "over." In other examples, there is a button that the talker presses and holds while speaking. It is up to channel users to cooperate and take care to share a half duplex channel appropriately.

Full Duplex

A two-way communication channel, allowing participants to speak simultaneously, is referred to as a full duplex channel. In ordinary face-to-face conversation between two or more people, any participant may speak at any time — reciting together, singing together, interrupting, or talking over a different participant. A full duplex communication channel allows for this ordinary and natural-like communication. When talker-B interrupts talker-A, talker-B continues to hear what talker-A is saying, and talker-A hears the interruption. Talkers resolve the interruption the same way they do while conversing face to face.

The telephone service we have known all our lives is an example of a full duplex system. Maintaining high-quality full duplex operation throughout the evolution from analog wired telephone service first to digital wired telephone service and then to digital wireless telephone service initially required significant effort on the part of telecommunications engineers. Full duplex functionality is now commonplace in both wired and wireless telephone service.

Earlier generations of drive-thru systems used half duplex. However, half duplex conversations may result in miscommunication, and overall they seem unnatural to some people. A customer may interrupt the employee to change an order while the employee is speaking. The employee may not realize the customer's requested order change, reducing the quality of the system's functionality and perhaps increasing costs to the QSR.

QSR System Functional Block Diagrams

Component placement throughout QSR systems may differ, but the following components are part of the communication system.

As indicated in **Figure 1**, the microphone converts the sound pressure of the employee's voice to a voice-band analog electrical signal. The amplifier increases the amplitude of the electrical signal and filters it in preparation for digitizing. The digitizer converts the voice-band analog signal to a stream of digital words (digital signal) and encodes a base-band signal in preparation for modulating an RF carrier. The radio transmitter generates a radio frequency (RF) carrier, modulates it with the base-band digital signal, and transmits it as a wide-band RF signal over the air.

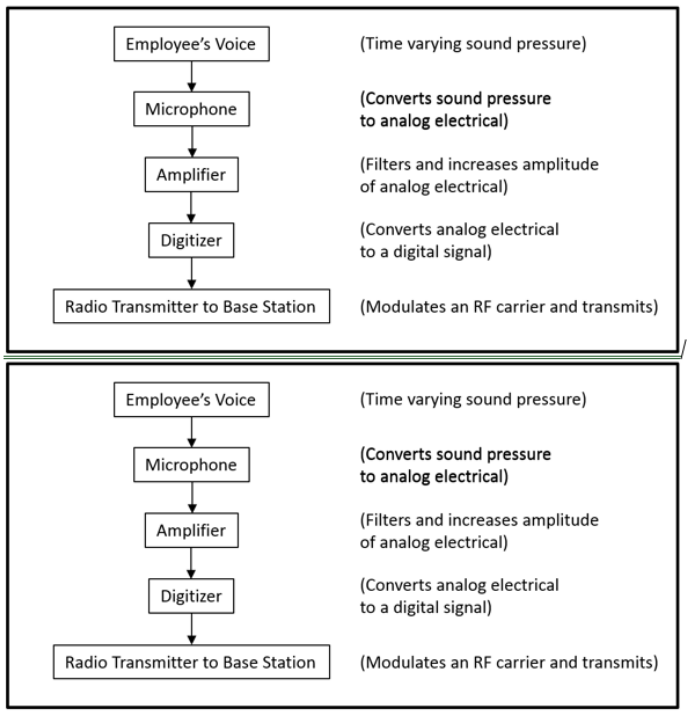

Figure 1
Outbound path – block diagram of employee's headset.

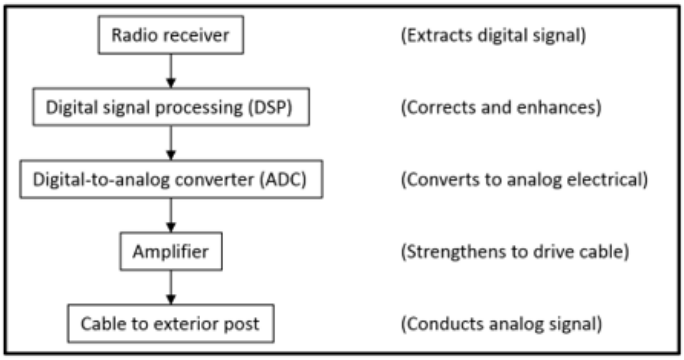

Figure 2
Outbound path – block diagram of base station.

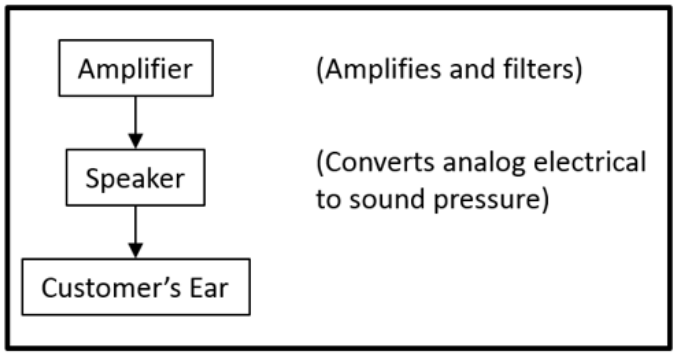

Figure 3
Outbound path — exterior post in drive-thru lane.

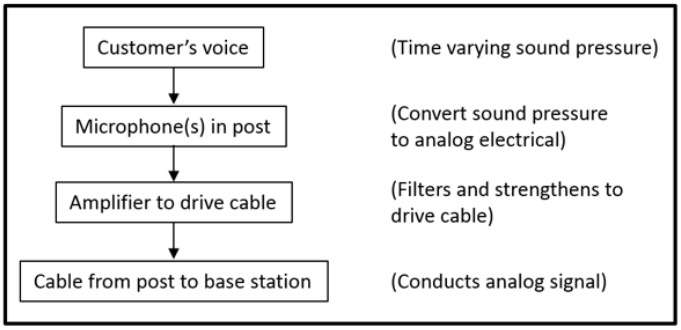

Figure 4
Inbound path — exterior post in drive-thru lane.

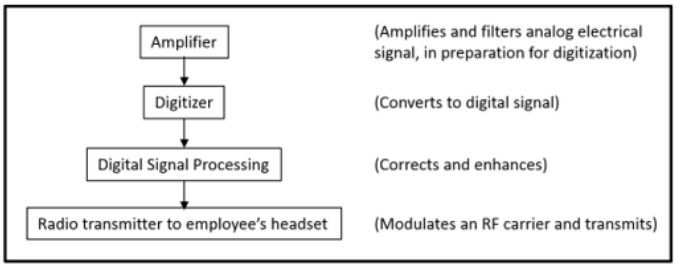

Figure 5
Inbound path — base station.

Outbound Path – Employee's Headset
Outbound Path – Base Station

Typically, the base station is mounted on a wall in the drive-thru booth, within a few meters of the employee. As indicated in **Figure 2**, the base station contains a radio receiver that demodulates the wide-band RF signal from the employee's headset, extracting the digital message signal from the base-band signal. Multi-function DSP, as described later in the paper, corrects and enhances the digital signal. The processed digital signal is then converted to an analog electrical signal, which is driven through a cable to the post.

Outbound Path – Exterior Post in Drive-Thru Lane

As shown in **Figure 3**, the exterior post in the drive-thru lane completes the path from the employee's microphone to the customer's ear, by way of the amplifier and speaker.

Inbound Path – Exterior Post in Drive-Thru Lane

As indicated in **Figure 4**, microphones in the external post convert the sound pressure of the customer's voice to a voice-band analog electrical signal. The amplifier amplifies, filters, and conditions the signal, and drives it through the cable to the base station.

Inbound Path – Base Station

As shown in **Figure 5**, the inbound amplifier in the base station receives the analog electrical signal conducted by cable from the external post. It amplifies and filters the

signal to prepare it for digitization. Multi-function DSP corrects and enhances the digital signal, converting it into a base-band signal suitable for modulating an RF carrier. The radio transmitter generates and modulates an RF carrier with the base-band signal and transmits the resulting wide-band signal over the air.

Inbound Path – Employee's Headset

As indicated in **Figure 6**, the employee's headset contains a radio receiver that demodulates the wide-band RF signal from the base station, extracting the digital message signal from the base-band signal. Multi-function DSP corrects and enhances the digital signal. The processed digital signal is then converted to an analog electrical signal, which is amplified and conditioned to match the headset's speaker. The speaker converts the analog electrical signal to sound pressure heard by the employee.

Digital Signal Processing (DSP)

From the electronics point of view, the major differentiator of product quality is its digital signal processing. DSP algorithms enhance the audio environment of the system. DSP features include automatic gain control (AGC), noise reduction, and echo suppression.

Automatic Gain Control (AGC)

AGC works to keep the speaker/headphone sound volume constant. Some customers speak louder than others. The employee needs to understand the customers to fulfill orders accurately and quickly. DSP measures the loudness of customers' conversation and compares the loudness to a desired level set by the employee. When the customer speaks softly, DSP turns up the volume automatically. DSP turns down the volume automatically when customers speak too loudly. This is the essence of AGC, which is used in both the outgoing and incoming paths.

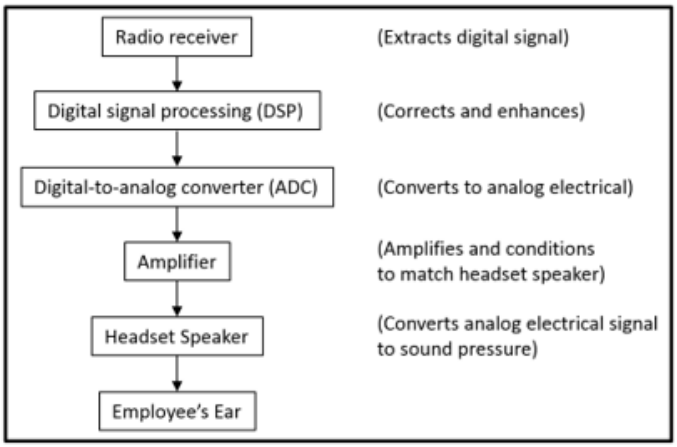

Figure 6
Inbound path — employee's headset.

AGC has been used in communication systems for a long time and was accomplished prior to DSP in totally analog systems[8]. DSP AGC procedures are well known to system designers. See reference for an example[9].

Noise Reduction (NR)

For drive-thru systems, it is convenient to define "noise" as any unwanted sound other than the talker's voice[10]. Strictly speaking from an electrical engineering and physics point of view, this usage of the term "noise" ought to be called "interference plus noise." Typical sources of interference, which the parties to this case call "noise," include smoothie blenders inside the restaurant and automobile engines in the drive-thru lanes. In physics and electronics, noise is random and unpredictable. Electronic noise refers to the thermal, shot, flicker, burst, and transit-time noise, which comprise total physical noise-power, which is compared to signal-power to derive the Signal-to-Noise Ratio (SNR)[11]. Noise reduction techniques for random, unpredictable electronic noise are different than those for interference, such as from blenders and car engines[12].

The "voice" signal from microphones includes not only the voice of the talker, but also the background sounds the microphone picks up. For the inbound path from customer to employee, unwanted noise may include sounds from the customer's car or motorcycle engine, or noise from other customers' vehicles, passing traffic, lawn mowers, machinery, etc. For the outbound path from employee to customer, noise may include sounds made by kitchen machinery, such as mixers, blenders, and others. Certain system design flaws can cause audible humming from the speaker, which is picked up by the microphone. Unwanted system sound is considered noise in this context. All these sounds (along with talker's voice) get amplified and digitized.

DSP noise reduction is relatively new, dating from the 1980s[13]. A typical DSP procedure examines the digitized signal and looks for recurring patterns that share characteristics with the noise sources described in the previous paragraph and goes on to reduce their loudness. For instance, the customer may still recognize the sound of a blender, but when DSP is operating properly, that sound is reduced enough for the customer to understand the employee.

Echo Suppression

Echo in a drive-thru system can refer to talkers hearing their words repeated through the speaker after a delay. Echo suppression in this context can be accomplished with

a DSP function called autocorrelation which examines the digitized signal and looks for repeated patterns corresponding to previously processed voice signal[14]. As in a typographical rendering of an echo "HELLO … Hello … hello …," the DSP procedure detects and removes the "Hello … hello …" from the speech signal being processed. Let us refer to this as "double-talk" echo suppression.

Echo suppression may also refer to suppressing the squealing sound (popularly called "feedback") that one hears when a microphone is placed too close to a speaker. This squealing can occur when an employee gets too close to a permanently mounted speaker inside the restaurant, or stands near a solid wall, allowing sound power to conduct from the headset speaker back to the headset microphone. Like the noise reduction function, the echo suppression DSP algorithm detects the squealing "feedback" sound within the microphone output and when detected, works to quickly change the frequency response of the amplifier to squelch the squealing sound power present in the speaker output[15].

Timeline of the Case

In 2012, the buyer engaged the designer's services to develop and design a new drive-thru system for use in the quick service restaurant industry. The top product requirement was noise reduction for both inbound and outbound paths. The second highest product requirement was that the audio quality of the system must surpass or equal the audio quality of the market-leading competitor's system. The agreed upon scope of work (SOW) included $385,000 to $475,000 cost estimate and a seven-month timeline ending in October 2013.

The design progression included obtaining and analyzing an exemplar drive-thru system from the competitor to determine how to improve upon that system's noise reduction and overall sound quality. The designer represented to the buyer that they did have the ability to meet or exceed the competitor's audio quality. The designer included this representation in their proposal of work to the buyer.

After multiple cost increases and delays, on February 10, 2016, the buyer demanded rescission of the contract. Aside from the delay and cost overrun, the major complaints voiced by the buyer were:

- Unclear and non-crisp inbound audio.
- Hum emanating through the outside speaker.
- No full duplex audio.
- Inadequate noise reduction.

In 2018, counsel for the buyer retained the author to investigate and opine on:

- Measured audio quality of the system. Did it meet specifications?
- Did the designer follow best design practices?

Author's Investigation of Audio Quality

The author visited the buyer's premises, and made subjective and objective tests, comparing the buyer's partially designed system to the exemplar system of the market-leading competitor.

Subjective Tests

Subjective tests of the partially designed system and the competitor drive-thru systems helped the author direct further objective testing. Listening to the sound quality of both systems from both the customer's (external post) and the employee's (headset) perspective, the author was able decide which audio tests would demonstrate objective, measurable differences in system performance.

For subjective tests, drive-thru posts were positioned on the back steps of the buyer's facility facing their parking lot, emulating the order-posts customers would interact with. Cables from posts were routed through the building to a base station room in the far opposite corner of the building, providing acoustic isolation.

The base station room included the buyer and the competitor base stations mounted on a wall, the buyer and the competitor wireless headsets on shelves, and test instruments on a laboratory bench.

Order Post (Outbound Path) Subjective Tests

The author first took the customer's point of view by standing outside the building and facing the order posts to interact with either the buyer or the competitor system and subjectively evaluate their outbound performance.

The buyer's representative was in the base station room, where he played the role of employee. He wore the first one, then the other system headset, without identifying which.

The test procedure for each system was as follows:

1. Half duplex evaluation

2. Full duplex evaluation

The evaluation criteria were as follows:

1. In the half duplex demonstration, one person speaks. The other listens for clarity and speech intelligibility, expecting the lack of any sounds inserted by the system that could muddle the sound.

2. In the full duplex demonstration, both persons speak over each other. The author listens for the buyer representative's voice to continue smoothly as the author and the buyer speak, without the system noticeably cutting back and forth.

Observations

1. [Half duplex] The partially designed system sounded muddled. Words were intelligible, but there were unnatural system artifacts (unexpected noise) inserted into the sound. The competitor's system sounded clear, and the buyer's words (deliberately nonsensical) were clear and intelligible in our half duplex conversation.

2. [Full duplex] With the partially designed system, chopping between our conversations was audible. The discontinuity was disconcerting. The competitor's system demonstrated proper full duplex.

Outbound Path Clarity and Intelligibility Evaluation

1. The partially designed system exhibited a constant hum. There was also clipping (system overload) when there was significant low-frequency content in the employee's speech. Clipping (resulting in harmonic distortion) and hum can be objectively measured using various instruments and measurement techniques.

2. With the competitor's system, the author could not subjectively identify any faults. To compare and confirm, the system was objectively tested with the same instruments and measurement techniques as the partially designed system.

Outbound Path Full Duplex Evaluation

1. The partially designed system full-duplex operation was flawed. This is a go/no-go test, which does not require instrumentation to prove its results.

2. The competitor's system full-duplex operation was established.

Headset (Inbound Path) Subjective Tests

The author took the employee's point of view by swapping positions. In this test, the buyer played the role of customer, and the author played the role of employee, wearing first one, then the other system headset. The buyer and the author followed the same procedure as in the order-post subjective tests and used the same evaluation criteria.

Observations

1. [Half duplex] For both the partially designed system and the competitor's systems, from the employee's perspective, words were intelligible, and there were no unnatural system artifacts present.

2. [Full duplex] With the partially designed system, chopping between our conversations was audible. The discontinuity was disconcerting. The competitor's system demonstrated proper full duplex.

Inbound Path Clarity and Intelligibility Evaluation

From the employee's perspective, the author could not subjectively identify any clarity and intelligibility faults with either the partially designed system or the competitor's system.

Inbound Path Full Duplex Evaluation

1. The partially designed system full-duplex operation was flawed. This is a go/no-go test, which does not require instrumentation to prove its results.

2. The competitor's system full-duplex operation was established.

Objective Tests of Outbound Path

The author devised objective tests confirming that low-frequency distortion was the root cause of the audible clipping and overall unpleasant sound at the customer post using the partially designed system, and to uncover any other measurable faults in either system.

Specialized audio test equipment was rented from NTI Audio[16].

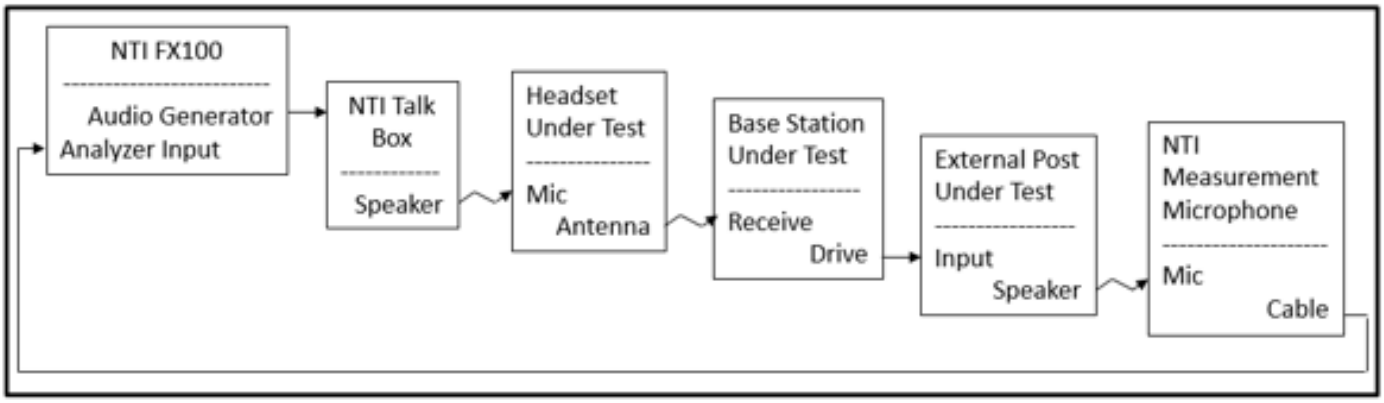

Figure 7
Test setup for outbound path.

- NTI Talk Box Speaker.
- NTI Measurement Microphones
- NTI Audio Analyzer FX100, using NTI computer software

The Talk Box can be set to present through its speaker either self-generated random audio or audio generated by the FX100 analyzer. Calibrated measurement microphones are of adequate quality to not significantly affect testing. The FX100 includes functions for signal generation, data acquisition, signal digitization, and DSP analysis. FX100 software accomplishes the control and communication of audio tests, calculation of analytical data from analyses, and generating graphical and tabular output of test results.

Tests with the NTI FX100 Analyzer confirmed objectively that the partially designed system outbound path has significant harmonic distortion in the low-frequency range. This is the root cause of the subjectively observed unpleasant audio quality from the customer post speaker.

Figure 7 shows the test setup for the outbound path. The audio generator in the NTI FX100 outputs a test signal by wire to the NTI Talk Box. The headset under test is mounted with its microphone about five centimeters in front of the speaker. The base station under test receives the wireless transmission from the headset and drives a cable to the external post under test. The NTI Measurement Microphone is positioned about one meter from the external post's speaker. The microphone cable is routed back to the NTI FX100 Analyzer Input, completing the test loop. The author performed the following tests for both the partially designed system's and competitor's headset, base station, and external post.

Glide-Sweep Tests with Audio Analyzer

For this test, the FX100 generator applies a 100 Hz sinusoid to the TalkBox for two seconds (to allow the System to settle), and then sweeps the frequency from 100 Hz to 20 kHz. The signal follows the loop indicated in **Figure 7** back to the FX100 analyzer, which records the measurement microphone's signal and performs several analyses of the recorded signal.

One such analysis is frequency response, as shown in **Figure 8**. The vertical axis of this graph is the relative sound pressure level (SPL) of the post speaker output in dBSPL. SPL is roughly equivalent to the loudness of the sound. The horizontal axis is frequency in Hertz (Hz).

The pink trace on this graph is the frequency response of the competitor's system. It shows a gradual increase from 50 dBSPL at 100 Hz to 80 dBSPL at 500 Hz. The SPL varies somewhat between 500 Hz and 3 kHz where it drops off steeply to about 30 dBSPL at about 4 kHz and remains

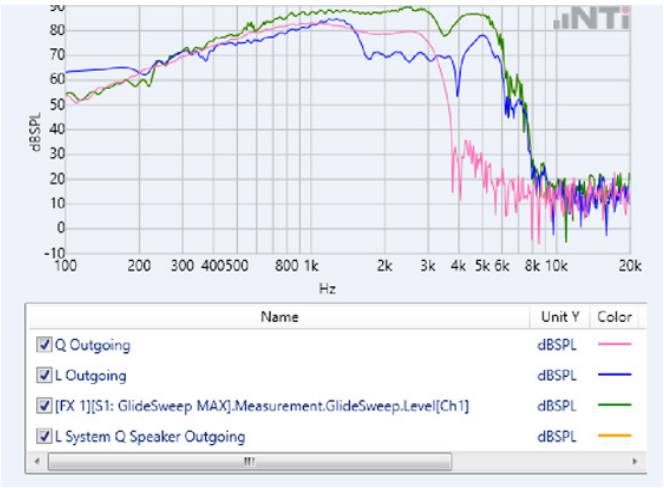

Figure 8
Frequency response test results.

substantially below 30 dBSPL from there on. One would say that the competitor's system has a 3 kHz bandwidth.

The blue and green traces are the partially designed system's frequency response. Results of two tests were saved where the green trace used a slightly higher input volume than the blue trace from the FX100 analyzer into the system. There are two apparent differences from the competitor system's performance. The SPL of the partially designed system does not drop off steeply until about 6 kHz, and more so at about 7 kHz. One would say the partially designed system has a 7 kHz bandwidth. For Hi-Fi audio, wider bandwidth is considered an advantage. But in the partially designed system, there is a wider variation in SPL between 500 Hz and 7 kHz. This approximately 30 dBSPL variation is perceptible to humans with typical hearing.

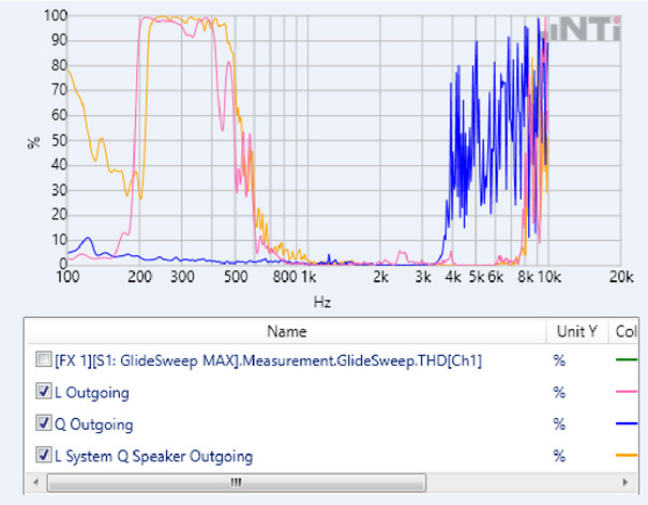

Figure 9
Distortion versus frequency test results.

The subjective observation of low-frequency distortion is objectively confirmed by measurement in **Figure 9**. It shows distortion versus frequency as calculated from the recorded glide-sweep tests. The vertical axis is total harmonic distortion in percent (%). The horizontal axis is frequency in Hz.

The blue trace is the total harmonic distortion (THD) in % for the competitor's system. It shows THD substantially less than 10% throughout its 3 kHz bandwidth. High distortion at frequencies above the bandwidth (above 3 kHz for the blue trace) is not audible. The pink trace is the THD for the partially designed system. THD is greater than 90% between about 200 and 400 Hz and does not fall to less than 10% until about 700 Hz. This shows objectively that there is significant, measurable distortion at low frequencies. The orange trace corresponds to the retest of the partially designed system using the competitor's external post, ruling out the external speaker posts as the cause of distortion.

Single-Tone Tests with Audio Analyzer

The author ran single-tone distortion tests at several frequencies to examine THD more closely in the partially designed system.

As a reference point, **Figure 10** shows the spectrum of the recorded output of the partially designed system's

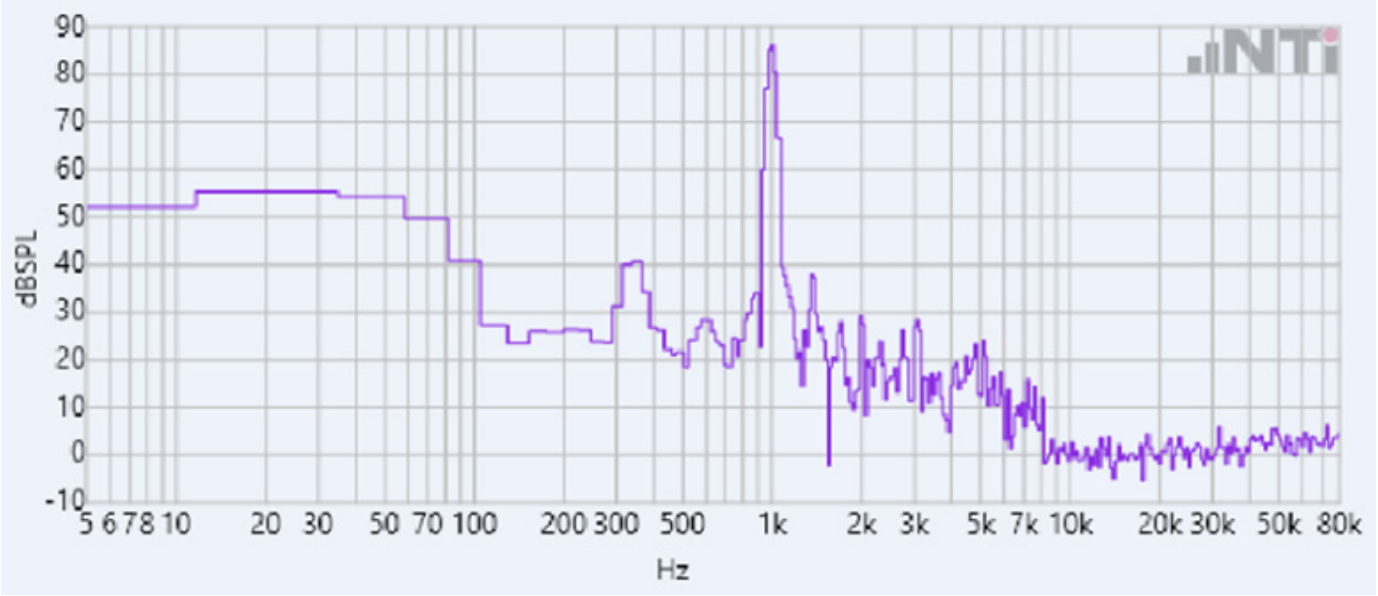

Figure 10
The partially designed system buyer's system output spectrum with 1 kHz input.

external post speaker when a 1 kHz tone is applied by the NTI Analyzer. The vertical axis is in dBSPL, and the horizontal axis is in Hz. The magenta trace is the relative loudness at each frequency. At 1 kHz, the magnitude is about 85 dBSPL. If there were significant harmonic distortion, we would see similar spikes at 2k, 3k, and higher multiples of 1 kHz. At 1 kHz, there is no significant harmonic distortion. However, notice the raised area of the trace between about 300 and 400 Hz, which reaches about 40 dBSPL. This range of frequencies corresponds to the audible hum of the partially designed system.

A 500 Hz input tone caused the worst measured distortion, as shown in **Figure 11**. At 500 Hz, the magnitude is a little more than 80 dBSPL. At that frequency, at one or more points within the partially designed system, the 500 Hz magnitude is so large that the system is overloaded. Instead of a smooth sinusoid, the signal is "clipped" so that it is flat at the top and steep at the sides.

The spectrum shown in **Figure 11** is consistent with a clipped sinusoid. In addition to the spike at 500 Hz, there are spikes at 1k, 1.5k, 2.5, etc. A signal with this spectrum will sound clipped to typical human perception, and speech through such a system will not sound as clear and crisp as speech through a system without such distortion.

Notice the **Figure 11** spectrum also shows the system-

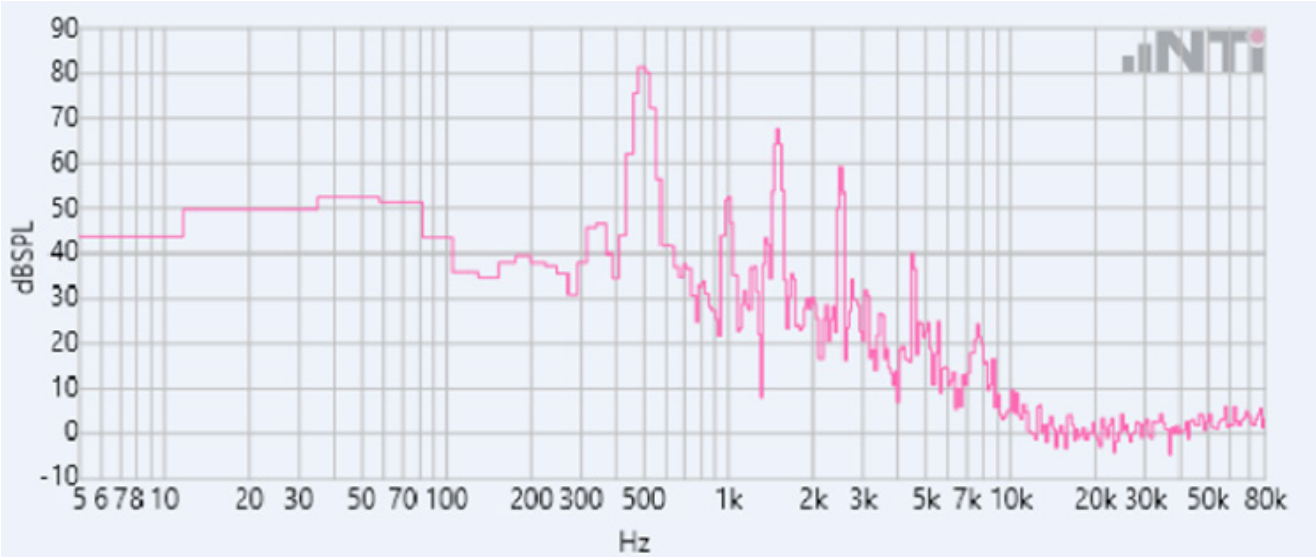

Figure 11
Partially designed system buyer's system output spectrum with 500 Hz input.

Figure 12
Partially designed system buyer's system output spectrum with 300 Hz input.

generated hum between 300 and 400 Hz. To explore that 300 Hz hum more closely, the final test applied a 300 Hz sinusoid with results shown in **Figure 12**.

The expected spike at 300 Hz is there, at about 80 dB-SPL. Distortion tones are visible at 600 and 900 Hz. Notably, the 300 Hz spike is widened by the system-generated hum.

Conclusions Regarding Audio Quality

The communication system that the designer delivered to the buyer did not meet the agreed specifications of the system requirements documents or the contract. This was shown by objective measurement/testing and confirmed by subjective listening tests.

The measured low-frequency distortion and hum of the buyer's outbound system are much worse than the same measurements for the competitor's system. The higher bandwidth of the partially designed system is not an advantage.

Best Design Practices

The author had been asked to opine on whether the designer followed best design practices.

Linear Time Invariance Non-Linear Time-Varying Systems

The audio system of a drive-thru lane is a non-linear, time-varying system. Its complexity arises from competing functions, including automatic gain control, noise reduction, echo suppression, and full-duplex operation, which involve multiple interdependent feedback control loops.

In contrast, feedback loops in linear, time invariant (LTI) systems are independent. LTI systems are easier to design than non-LTI systems using hand or spreadsheet calculations and engineering reasoning. See references for a formal mathematical article on LTI systems[17,18]. A good article about nonlinear time-varying systems can be found here[19].

To explain linearity, let' s say the input from a microphone to a linear amplifier is "x", the amplifier gain is "G", and the amplifier output to the speaker or headset is "y". Then if the amplifier is linear, "y = G*x". If the input becomes twice as loud, 2x, then the changed output (call it "z") is also twice as loud "z = G*2x", so "z = 2*y". When you wiggle the input x, the output wiggles the same way, but G times bigger.

G may be different for different frequencies in an LTI system. The relative size of G at different frequencies is called its "frequency response." In a typical audio system such as the drive-thru system, G is very small at frequencies higher than the system's bandwidth.

Time invariance means that in the equation "y = G*x", it doesn't matter when "x" is applied to the input. G remains constant over time, even if G is different for different frequencies of "x". To put it mathematically, if the value of x at time t is x(t), then y(t) = G*x(t). In a time-invariant system, for any time T, y(T) = x(T). In a time-varying system, G changes with time. For example, when a soft-spoken customer is at the post, G increases from its level for a loud customer.

An audio system with a maximum output loudness is an example of non-linearity. Let's say that its maximum output loudness is K. While "G*x" is less than K, then "y = G*x" is true, and the system is operating in its linear region. However, while "G*x" is greater than K, then "y=K". While "G*x" is greater than K, wiggling x does not change y. For this situation, the system is operating outside of its linear region and "y" is said to be clipped.

Assuming LTI and independent feedback loops, one may devise mathematical formulas for analyzing frequency response and the stability of control loops — and these formulas may serve as the basis upon which to design the system. However, the AGC, NR, full-duplex operation, and echo suppression functions that were to be present in the buyer's drive-thru system are all non-linear and time-varying functions. Designing a system with all these functions is not straightforward.

As described previously, the AGC function works to keep the speaker/headphone sound volume "y" constant. If the microphone output "x" is small, the AGC increases "G". If "x" is large, the AGC decreases "G". Thus, "G" is not constant over time, and the system is "time-varying."

The noise reduction function of the processing algorithm detects noise sound within the microphone signal "x." When interference is detected, the algorithm works to quickly change the frequency response of the system to decrease the noise power present in the speaker output "y" In one sense of echo suppression, the DSP echo suppression function works in a similar manner, detecting the squealing echo pattern and squelching it. In both noise reduction and echo suppression (both squelching and double-talk) functions, the system is time varying.

The full-duplex operation of the system is also non-linear and time-varying. In this duplex system, both the customer's and the employee's microphones and speakers are always on. Duplex operation requires a non-linear control loop algorithm to create a natural sounding conversation such as in telephone conversations.

Because these four control loops are interdependent, they get in each other's way. For one example, a large interference sound from the microphone "x" may incorrectly cause the AGC loop to decrease the system gain "G" to keep speaker output "y" constant. This was indeed the case, as communicated by the buyer in July 2015: "As the background noise gets louder, the inbound microphone volume decreases."

Designing a non-linear, time-varying system is more difficult than designing a linear, time-invariant system. Modern design methodologies for non-linear, time-varying systems use model-based design and functional simulation early in the design process to help the designer understand and anticipate design challenges before designing or buying hardware or writing or buying software code. Model-based design entails simulating the functionality of a system comprised of behavioral models. Functional simulation, behavioral simulation, and model-based simulation are synonymous.

Functional simulation entails the creation or purchase of functional behavioral models for each subsystem. The models mathematically describe how each subsystem's outputs change over time as its inputs change over time. Models are written to reflect the subsystem's non-linearities and time dependencies. Subsystems represented by models are interconnected to form the top-level system. A simulation testbench interconnects the top-level system with models that provide stimulus signals to system inputs and models that examine and analyze system outputs. Tests are written to exercise the system inputs in ways that verify the system reacts properly to the inputs.

Model-based design and simulation of complex electronic systems has been the design flow best-practice since the mid-1990s. Based on the documents and emails provided, the designer did not use a model-based design methodology.

The following is a partial list of electronic design automation (EDA) tools capable of model-based design that were available to the designers before 2012. Since then, some of the vendors have consolidated, and new vendors have joined the market. The list is not intended to be all-inclusive, only to show that there were multiple options for incorporating model-based design:

- The Mentor Graphics "PADS" EDA platform[20] (which was available to the designer). The PADS EDA platform is capable of model-based design using its VHDL-AMS simulator. VHDL-AMS behavioral models could have been purchased from component vendors or written in-house for circuitry and algorithms that were to be designed by the designer.

- A similar EDA platform sold by Cadence Design Systems[21] uses either Verilog-AMS or VHDL-AMS.

- The Advanced Design System (ADS) sold by Keysight (formerly Agilent Systems, formerly Hewlett Packard) is an EDA platform for RF, analog, and digital system design, which includes signal generator models which correspond directly to Keysight's laboratory instruments[22].

- Several companies produce prototyping systems that incorporate MATLAB with Simulink and HDL-Coder to drive electrical signals into hardware and receive electrical systems from hardware. This is known as "Hardware in the Loop" verification[23].

The drive-thru system is a non-linear, time-varying system that was to include at least four interdependent control loops of automatic gain control, noise reduction, echo suppression, and full-duplex operation. Integrating these competing functions was complex because a change to one component may cause its function to interfere with the function of another component.

Best practice is to design and verify the noise reduction, automatic gain control, and echo suppression functions in tandem. The designer's assumption that third-party algorithms can be plugged into the overall DSP program was simplistic. A reasonable approach is to use models of third-party components in the system simulator of choice, discover where they interfere with each other, and modify the software components accordingly.

Given the difficulties of designing a complex, non-linear, time-varying, multi-feedback-loop system such as the drive-thru system, it was an unreasonable decision by the

designer to attempt the project without taking advantage of best practices for modern design methodology. The designer had a choice of EDA platforms, modeling styles, or simulation engines to use and present to the buyer; choosing "no system simulation" was an unreasonable choice that deviated from best practices in the field, was a major contributor to the project being late, over budget, and incomplete, and ultimately resulted in the designer's inability to provide a system with the required feedback loops after working on the project for nearly three years.

Conclusions Regarding Design Practice

a. Solving the complexity of the required system was beyond the designers' capability using Linear Time-Invariant design techniques. The limitation of Linear Time Invariant design approach is taught at the undergraduate level to electrical engineering majors.

b. The designers should have realized upon reviewing the requirements document that the well-known difficulty of stabilizing a control system comprising multiple non-linear, time-varying feedback loops without the use of system simulation software programs was impractical using linear time-invariant design methodology.

c. When outsourcing software design of individual system components, the designers should have provided a top-level framework for simulating and verifying the software with hardware.

Resolution

The author submitted an expert report late in 2018. The designer and the buyer reached an agreement soon thereafter. The author was not privy to the terms of the agreement, but presumably the expert report was convincing to both parties.

References

1. B. Tuttle, "10 Things You Didn't Know About the Fast Food Drive-Thru," Money, 8 October 2014. [Online]. Available: http://money.com/money/3478752/drive-thru-fast-food-fast-casual/. [Accessed 15 May 2019].

2. N. Barksdale, "Fries With That? A Brief History of Drive-Thru Dining," A&E Television Networks, 22 August 2018. [Online]. Available: https://www.history.com/news/fries-with-that-a-brief-history-of-drive-thru-dining. [Accessed 15 May 2019].

3. I. Lord, "What is a Quick Service Restaurant?," Study.com, 2019. [Online]. Available: https://study.com/academy/lesson/what-is-a-quick-service-restaurant.html. [Accessed 19 June 2019].

4. S. Oches, "The 2018 QSR Drive-Thru Study," QSR Magazine, October 2018. [Online]. Available: https://www.qsrmagazine.com/reports/2018-qsr-drive-thru-study. [Accessed 19 June 2019].

5. J. Ciampi, "Tech Solutions to Combat Drive-Thru Challenges," QSR Magazine, December 2018. [Online]. Available: https://www.qsrmagazine.com/outside-insights/tech-solutions-combat-drive-thru-challenges. [Accessed 19 June 2019].

6. Orenda, "Introduction to Simplex, Half Duplex and Full Duplex," Medium, 1 July 2016. [Online]. Available: https://medium.com/@fiberstoreorenda/introduction-to-simplex-half-duplex-and-full-duplex-fbda8d591e3a. [Accessed 19 June 2019].

7. A. Grami, Introduction to Digital Communications, Waltham, MA: Elsevier, Inc., 2016.

8. J. Staley, Application note AN-934 "60 dB Wide Dynamic Range, Low Frequency AGC Circuit Using a Single VGA," 2007. [Online]. Available: https://www.analog.com/media/en/technical-documentation/application-notes/AN_934.pdf. [Accessed 20 June 2019].

9. T. Youngblood, "Adaptive Gain Control with the Least Mean Squares Algorithm," All About Circuits, 30 November 2015. [Online]. Available: https://www.allaboutcircuits.com/technical-articles/adaptive-gain-control-with-the-least-mean-squares-algorithm/. [Accessed 20 June 2019].

10. R. Nordquist, "Noise and Interference in Various Types of Communication," Thought Co., 3 January 2019. [Online]. Available: https://www.thoughtco.com/noise-communication-term-1691349. [Accessed 20 June 2019].

11. R. Keim, "What Is Electrical Noise and Where Does It Come From?," All About Circuits, 21 June 2018. [Online]. Available: https://www.allaboutcircuits.com/technical-articles/electrical-noise-what-causes-noise-in-electrical-circuits/.

[Accessed 20 June 2019].

12. J. W. MARSHALL LEACH, "Fundamentals of Low-Noise Analog Circuit Design," PROCEEDINGS OF THE IEEE, vol. 82, no. 10, pp. 1515 - 1538, 1994.

13. S. M. Kuo and D. R. Morgan, "Review of DSP Algorithms for Active Noise Control," in Proceedings of the 2000 IEEE International Conference on Control Applications, Anchorage, AK, 2000.

14. UCLA, "Auto-Correlation and Echo Cancellation Overview," [Online]. Available: http://www.seas.ucla.edu/dsplab/aec/over.html. [Accessed 21 June 2019].

15. D. Troxel, "Understanding Acoustic Feedback & Suppressors," Rane Commercial Audio Products, October 2005. [Online]. Available: https://www.rane.com/note158.html. [Accessed 21 June 2019].

16. NTI Audio, "NTI Audio," NTI Audio, 2019. [Online]. Available: https://www.nti-audio.com/en/. [Accessed 25 June 2019].

17. R. Wang, "Linear Time-Invariant (LTI) Systems,"12 December 2012. [Online]. Available: http://fourier.eng.hmc.edu/e59/lectures/e59/node7.html. [Accessed 21 June 2019].

18. A. Chumbley, J. Areias and C. Williams, "Linear Time Invariant Systems," Brilliant, [Online]. Available: https://brilliant.org/wiki/linear-time-invariant-systems/. [Accessed 21 June 2019].

19. L. R. Hunt and R. Su, "Control of nonlinear time-varying systems," in 20th IEEE Conference on Decision and Control including the Symposium on Adaptive Processes, San Diego, CA, 1981.

20. Mentor Graphics, "PADS," Mentor Graphics, [Online]. Available: https://www.mentor.com/training/course_categories/pads. [Accessed 21 June 2019].

21. Cadence Design Systems, "Virtuoso AMS Designer," Cadence Design Systems, 2019. [Online]. Available: https://www.cadence.com/content/cadence-www/global/zh_TW/home/training/all-courses/84468.html. [Accessed 21 June 2019].

22. Keysight Technologies, "Advanced Design System (ADS)," Keysight Technologies, 2019. [Online]. Available: https://www.keysight.com/en/pc-1297113/advanced-design-system-ads?&cc=US&lc=eng. [Accessed 21 June 2019].

23. National Instruments, "Hardware-in-the-Loop (HIL) Simulation," National Instruments, 2019. [Online]. Available: https://www.ni.com/en-us/innovations/automotive/hardware-in-the-loop.html. [Accessed 21 June 2019].